

**Semimetal-functionalized Polyoxovanadates**

Journal:	<i>Chemical Society Reviews</i>
Manuscript ID:	CS-REV-07-2015-000531.R1
Article Type:	Review Article
Date Submitted by the Author:	12-Aug-2015
Complete List of Authors:	Monakhov, Kirill; RWTH Aachen University, Institut für Anorganische Chemie Bensch, Wolfgang; der Universitate Kiel, Institut für Anorganische Chemie Kögerler, Paul; Aachen, Chemistry

# Semimetal-Functionalised Polyoxovanadates

Kirill Yu. Monakhov,<sup>\*a</sup> Wolfgang Bensch<sup>\*b</sup> and Paul Kögerler<sup>\*ac</sup>

<sup>a</sup> Institut für Anorganische Chemie, RWTH Aachen University, Landoltweg 1, 52074 Aachen (Germany)

<sup>b</sup> Institut für Anorganische Chemie, Christian-Albrechts-Universität zu Kiel, Max-Eyth-Str. 2, 24118 Kiel (Germany)

<sup>c</sup> Jülich-Aachen Research Alliance (JARA-FIT) and Peter Grünberg Institute (PGI-6), Forschungszentrum Jülich, 52425 Jülich (Germany)

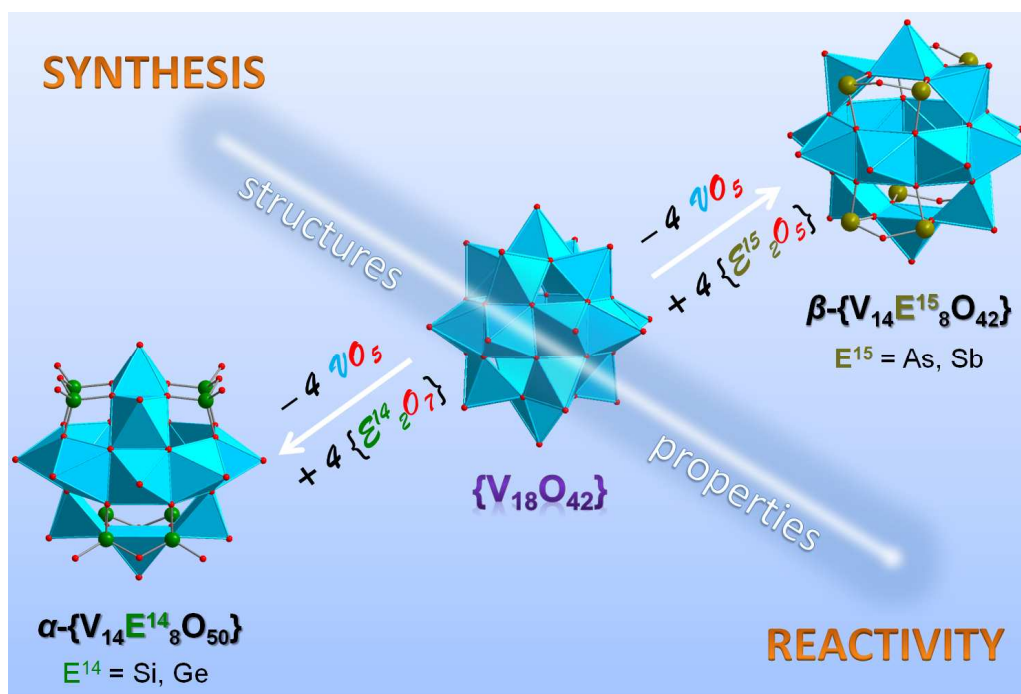
\* Corresponding authors (Emails):

kirill.monakhov@ac.rwth-aachen.de, wbensch@ac.uni-kiel.de, paul.koegerler@ac.rwth-aachen.de

**Abstract:** Polyoxovanadates (POVs), known for their wide applicability and relevance in chemical, physical and biological sciences, are a subclass of polyoxometalates and usually self-assemble in aqueous-phase, pH-controlled condensation reactions. Archetypical POVs such as the robust  $[V^{IV}_{18}O_{42}]^{12-}$  polyoxoanion can be structurally, electronically and magnetically altered by heavier group 14 and 15 elements to afford Si-, Ge-, As- or Sb-decorated POV structures (*hetero*POVs). These main-group semimetals introduce specific chemically engineered functionalities which cause the generally hydrophilic *hetero*POV compounds to exhibit interesting reactivity towards organic molecules, late transition metal and lanthanoid ions. The fully-oxidised ( $V^V$ ), mixed-valent ( $V^V/V^{IV}$  and  $V^{IV}/V^{III}$ ), “fully-reduced” ( $V^{IV}$ ) and “highly-reduced” ( $V^{III}$ ) *hetero*POVs possess a number of intriguing properties, ranging from catalytic to molecular magnet characteristics. Herein, we review key developments in the synthetic and structural chemistry as well as the reactivity of POVs functionalised with Si-, Ge-, As- or Sb-based heterogroups.

**Keywords:** Polyoxovanadates · Silicon · Germanium · Arsenic · Antimony

## TOC Synopsis



## Author information

*Kirill Monakhov received his Dr. rer. nat. degree in 2010 with Prof. Gerald Linti (Heidelberg University, Germany). After two years as a postdoctoral fellow of the German Research Foundation and the Cercle Gutenberg with Prof. Pierre Braunstein (University of Strasbourg, France), and after being awarded the Academia Europaea Burgen Scholarship in 2011, he returned to Germany in 2013 with a DFG postdoctoral reintegration fellowship to join the group of Paul Kögerler at RWTH Aachen University. In 2015 he received a DFG Emmy Noether fellowship and now leads a junior research group at the Institute of Inorganic Chemistry at RWTH Aachen.*

*Wolfgang Bensch received his Dr. rer. nat. with Prof. Eberhard Amberger at the Ludwig-Maximilians-University of Munich (Germany) in 1983. He was a postdoctoral fellow at the University of Zurich (Switzerland) and joined Siemens Company (Munich) in 1986. In 1990 he started his habilitation at the Johann Wolfgang Goethe University Frankfurt (Germany) which was finished in 1993. He was appointed as full professor for Inorganic Solid State Chemistry at the Christian-Albrechts-University Kiel in 1997.*

*Paul Kögerler graduated with a Dr. rer. nat. degree with Prof. Achim Müller at the University of Bielefeld (Germany) in 2000, followed by a postdoctoral research stay at the Department of Physics and Astronomy at Iowa State University (USA). In 2003, he was appointed as a tenured Associate Scientist at the U.S. DOE Ames Laboratory, before returning to Germany in 2006 as Professor of Chemistry at the Institute of Inorganic Chemistry at RWTH Aachen University and Group Leader for Molecular Magnetism at the Peter Grünberg Institute, Research Centre Jülich.*

## 1. Introduction

**1.1 General remarks.** Although vanadium is best known for its use in the large-scale industrial production of alloys and steels, this group 5 transition metal also plays a significant role in biological systems and bioinorganic chemistry.<sup>1,2</sup> Vanadium shows common oxidation states between +2 and +5 revealed by characteristic colours such as lilac/purple ( $V^{2+}$ ), green ( $V^{3+}$ ), blue ( $\{V^{IV}O\}^{2+}$ ), and yellow ( $\{V^VO_2\}^+$  and  $\{V^VO_3\}^-$ ) and exhibits

a particularly rich coordination chemistry in aqueous solutions.<sup>3,4</sup> It has a high tendency to form oxovanadium ions whose nuclearity, structural motifs and net charge are strongly influenced by the specific reaction conditions such as stoichiometries and concentration of the reactants, pH (alkaline vs acidic aqueous solutions), temperature, pressure, and reaction time. In general, vanadium oxide compounds find a wide range of applications in catalysis,<sup>5</sup> biochemistry,<sup>1,2,6</sup> sol-gel chemistry,<sup>7</sup> gas sensing,<sup>8</sup> geochemistry<sup>9</sup>, sorption<sup>10</sup> and intercalated layered material,<sup>11</sup> surface and nano sciences<sup>12</sup> and perform their role as secondary electrode materials for advanced lithium ion batteries and vanadium redox-flow batteries.<sup>13</sup> Even in photosynthesis the role of vanadate and vanadyl citrate compounds was investigated.<sup>14</sup> The chemistry of polyoxovanadates (POVs),<sup>15</sup> the latter being a subclass of polynuclear molecular early transition metal oxides known as polyoxometalates (POMs),<sup>16</sup> is a very fast growing area of research, mainly due to the versatile redox activities of POVs,<sup>17</sup> their current application and further perspectives in various branches of chemical, physical and biological sciences.

**1.2 Structure and characterisation of conventional POVs.** In aqueous and organic<sup>18</sup> solutions, POVs are formed in pH-dependent condensation reactions in which small  $[\text{VO}_n]^{Q-}$  fragments aggregate to form a large variety of high- and low-nuclearity cluster structures with diverse coordination geometries of the vanadium cations. POVs usually exhibit cage-, sphere-, hollow-, basket-, belt-, and barrel-like structural motifs,<sup>19</sup> which are constructed of a number of polyhedra fused and/or linked through a common vertex (corner) and/or polyhedral edges and faces. These polyhedra consist of the homo- or heterovalent V atoms showing e.g. square-pyramidal<sup>20</sup>  $[\text{V}^{\text{V}}\text{O}_5]^{5-}$  and  $[\text{V}^{\text{IV}}\text{O}_5]^{6-}$ , octahedral  $[\text{V}^{\text{V}}\text{O}_6]^{7-}$  and  $[\text{V}^{\text{IV}}\text{O}_6]^{8-}$  and tetrahedral  $[\text{V}^{\text{V}}\text{O}_4]^{3-}$  coordination geometries. Thus, the adjustable coordination behaviour of V in POVs contrasts with the predominantly octahedral coordination environments of Mo and W ions in their POM structures. One of the most studied and structurally characterised POVs is the orange-coloured decavanadate ion,<sup>21</sup>  $[\text{V}_{10}\text{O}_{28}]^{6-}$  (Figure 1), that demonstrates the ability to build supramolecular assemblies<sup>22</sup> and shows fascinating biological activity.<sup>23</sup> This polyanion, reported for the first time in 1956, has also been found in minerals (see, e.g. lasalite,  $\text{Na}_2\text{Mg}_2[\text{V}_{10}\text{O}_{28}] \cdot 20\text{H}_2\text{O}$ ).<sup>24</sup>

POVs can be divided into four general families: fully-oxidised ( $\text{V}^{\text{V}}$ ), mixed-valent ( $\text{V}^{\text{V}}/\text{V}^{\text{IV}}$  or  $\text{V}^{\text{IV}}/\text{V}^{\text{III}}$ ), “fully-reduced” ( $\text{V}^{\text{IV}}$ ) and “highly-reduced” ( $\text{V}^{\text{III}}$ ) species. The following crystallographically characterised POVs  $[\text{V}_2\text{O}_7]^{4-}$ ,<sup>25</sup>  $[\text{V}_3\text{O}_9]^{3-}$ ,<sup>26</sup>  $[\text{V}_4\text{O}_{12}]^{4-}$ ,<sup>27</sup>  $[\text{V}_5\text{O}_{14}]^{3-}$ ,<sup>28</sup>  $[\text{V}_{10}\text{O}_{28}]^{6-}$ ,<sup>29</sup>  $[\text{V}_{12}\text{O}_{32}]^{4-}$ ,<sup>30</sup>  $[\text{V}_{13}\text{O}_{34}]^{3-}$ ,<sup>31</sup>  $[\text{V}_{15}\text{O}_{42}]^{9-}$ ,<sup>32</sup>  $[\text{V}_{16}\text{O}_{42}]^{4-}$ <sup>33</sup> constitute the class of fully-oxidised vanadium species (Figure 1). X-ray single-crystal structures have been determined for  $[\text{V}^{\text{IV}}_2\text{V}^{\text{V}}_8\text{O}_{26}]^{4-}$ ,<sup>34</sup>  $[\text{V}^{\text{IV}}_8\text{V}^{\text{V}}_7\text{O}_{36}]^{5-}$ ,<sup>35</sup>  $[\text{V}^{\text{IV}}_{11}\text{V}^{\text{V}}_5\text{O}_{38}]^{7-}$ ,<sup>36</sup>  $[\text{V}^{\text{IV}}_3\text{V}^{\text{V}}_{13}\text{O}_{42}]^{7-}$ ,<sup>37</sup>  $[\text{V}^{\text{IV}}_5\text{V}^{\text{V}}_{12}\text{O}_{42}]^{4-}$ ,<sup>38</sup>

$[V^{IV}_6V^{V}_2O_{42}]^{10-}$ ,<sup>39</sup>  $[V^{IV}_{10}V^V_8O_{42}]^{4-}$ ,<sup>39</sup>  $[V^{IV}_8V^V_{10}O_{44}]^{6-}$ ,<sup>40</sup>  $[V^{IV}_6V^V_{13}O_{49}]^{9-}$ ,<sup>41</sup>  $[V^{IV}_8V^V_{14}O_{54}]^{6-}$ ,<sup>40</sup>  $[V^{IV}_{16}V^V_{18}O_{82}]^{10-}$ <sup>42</sup> (disregarding encapsulated supramolecular guest species) from the class of the mixed-valent  $V^V/V^{IV}$  species (Figure 2). The mixed-valent  $V^V/V^{IV}$ -POVs and the “highly-reduced”  $V^{III}$ -POVs consist mostly of a variety of vanadium alkoxide structures.<sup>43,44</sup> The most renowned representative in the class of the “fully-reduced” POVs is the  $[V^{IV}_{18}O_{42}]^{12-}$  polyoxoanion whose chemical and structural characterisation were reported for the first time by Johnson and Schlemper in 1978 (Figure 3).<sup>45</sup> The  $\{V_{18}O_{42}\}$  architecture constructed from the edge-sharing square-pyramidal  $\{O=VO_4\}$  units represents an archetypal structure with a diameter of *ca.* 11 Å which may adopt idealised  $T_d$  and  $D_{4d}$  symmetries. The strong infrared stretching frequencies of terminal V=O groups characteristically appear in the range 940 – 1000  $cm^{-1}$ .

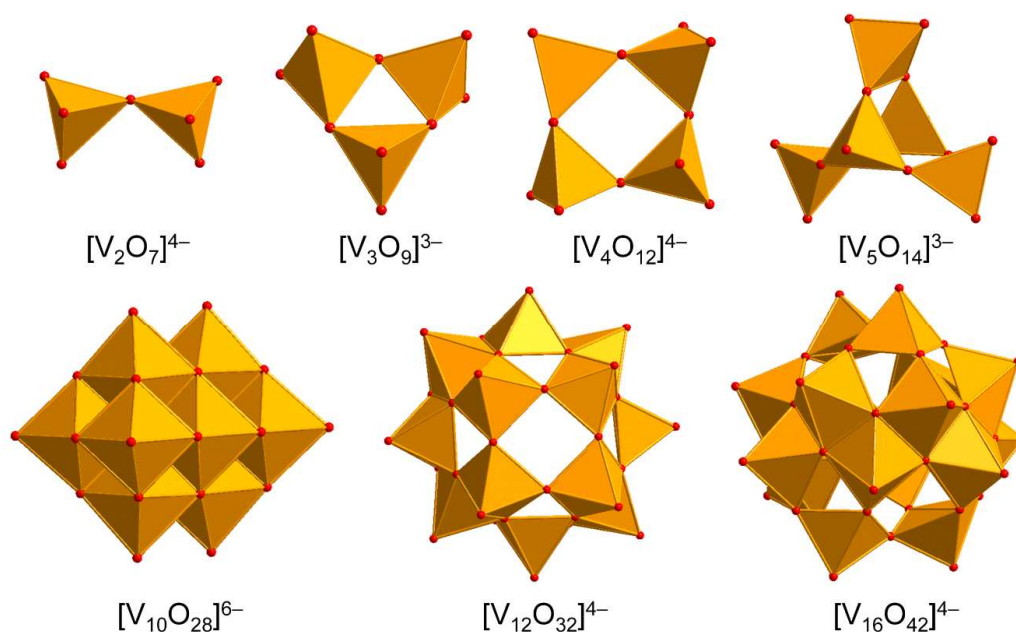


**Figure 1.** Polyhedral representation of structurally characterised fully-oxidised POVs with different topologies involving V ions in the formal oxidation states of +5. Oxygen positions are shown as small red spheres, the  $V^VO_x$  coordination polyhedra in orange colour.

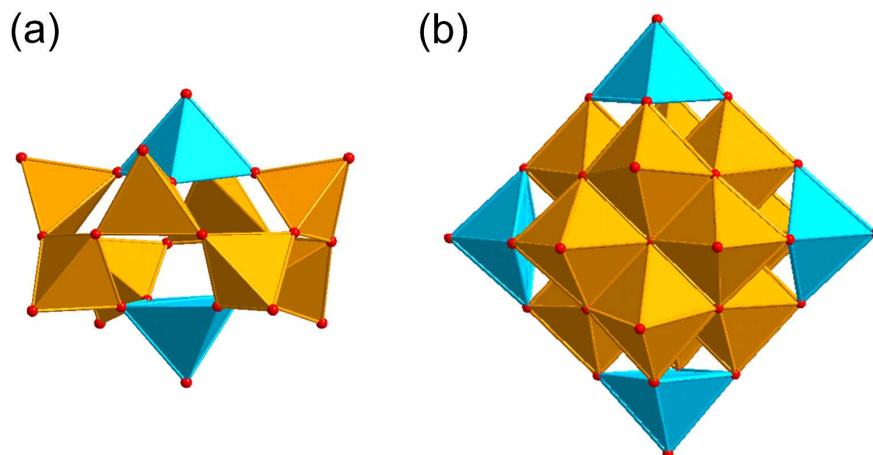


**Figure 2.** (a)  $[V_{10}O_{26}]^{4-}$  with two  $V^{IV}$  (caps) and eight  $V^V$  atoms. (b)  $[V_{17}O_{42}]^{4-}$  with five  $V^{IV}$  (four peripheral and one central) and twelve  $V^V$  atoms. Colour code: O, red;  $V^{IV}O_x$ , sky-blue polyhedra;  $V^VO_x$ , light-orange polyhedra.

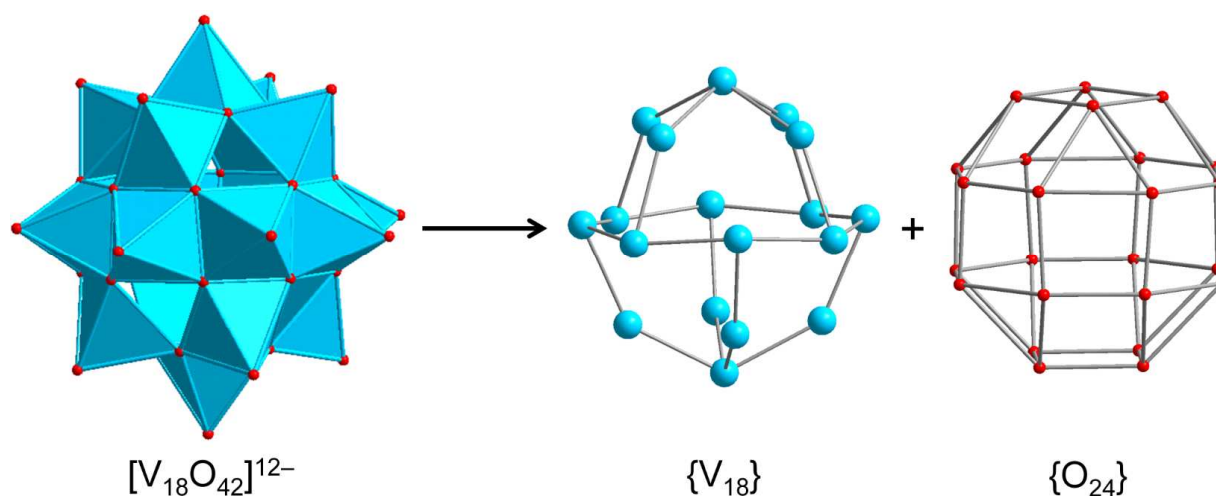


**Figure 3.** Schematic decomposition of the “fully-reduced”  $[V_{18}O_{42}]^{12-}$  POV into the  $\{V_{18}^{IV}\}$  skeleton and the  $\{O_{24}\}$  polyhedron of bridging oxygen sites (rhombicuboctahedron). Colour code: O, red;  $V^{IV}$ , sky blue;  $V^{VO}_x$ , sky-blue polyhedra.

The presence of heterovalent vanadium atoms in some POVs occasionally complicates the assignment of the positions of the individual V atoms. This is due to the multifaceted nature of the POV structures, which often afford similar coordination geometries (e.g. square-pyramidal) around the  $V^V/V^{IV}$  ions and feature charges which are delocalised over the vanadium centres. Generally, there are several approaches to assign the oxidation states of V atoms in the entire POV structure: (i) overall charge balance, (ii) calculation of bond valence sums from determined bond lengths,<sup>46</sup> (iii) redox titration and (iv) X-ray photoelectron spectroscopy (XPS). Elemental, thermal (TG-DTA),<sup>47</sup> X-ray powder diffraction and electron microprobe (EMP) analyses, infrared (IR) spectroscopy, electron paramagnetic resonance spectroscopy (EPR),  $^1H$ ,  $^{17}O$  and  $^{51}V$  nuclear magnetic resonance spectroscopy

(NMR),<sup>48</sup> energy-dispersive X-ray spectroscopy (EDXS), ultraviolet-visible (UV-vis) spectroscopy, electrospray ionisation mass spectrometry (ESI-MS),<sup>49</sup> cyclic voltammetry (CV), and inelastic neutron scattering (INS) have been used for the chemical and structural characterisation of POVs. Temperature- and field-dependent magnetic susceptibility measurements were routinely applied to evaluate the magnetic characteristics of reduced POVs. A study combining density functional theory (DFT) calculations and <sup>51</sup>V NMR experiments for [V<sub>10</sub>O<sub>28</sub>]<sup>6-</sup> was published some time ago.<sup>50</sup> More recently, joint experimental and computational studies have been performed on positively-charged vanadium oxide clusters in the gas phase and in solution. These involved e.g. the combination of laser desorption time-of-flight mass spectrometry, UV-vis and IR spectroscopy, and DFT calculations,<sup>51</sup> or analysis by ESI-MS, collision-induced dissociation experiments and DFT.<sup>52</sup>

**1.3 Relation of POVs to classical POMs.** The POV structures are usually derived or deduced from transferable vanadium oxoanion building blocks and host-guest aggregates, but also from small stable POM archetypes. Although the redox behaviour of the POVs differs from that of POMs comprised of group 6 transition metals (M = Mo, W), some of the construction principles of the metal-oxide core frameworks are very similar between these two classes of compounds. The POVs have thus been shown to adopt the structures of the classical Lindqvist-type [M<sub>6</sub>O<sub>19</sub>]<sup>Q-</sup> polyanions,<sup>53</sup> as exemplified by the mixed-valent [V<sub>6</sub>O<sub>19</sub>]<sup>Q-</sup> polyoxoanions,<sup>54</sup> and to exhibit expanded Keggin-type [YM<sub>12</sub>O<sub>40</sub>]<sup>Q-</sup> structures (Y: heteroatom).<sup>55</sup> A first representative in the latter family, a fully-oxidised [PV<sub>14</sub>O<sub>42</sub>]<sup>9-</sup> POV, which is composed of an  $\alpha$ -Keggin [PV<sub>12</sub>O<sub>40</sub>]<sup>15-</sup> polyoxoanion capped by two VO<sup>3+</sup> moieties, was reported in 1980.<sup>56</sup> A mixed-valent bicapped polyoxomolybdate Keggin-type polyoxoanion with two {VO}<sup>2+</sup> caps,<sup>57</sup> [PMo<sup>V</sup><sub>6</sub>Mo<sup>VI</sup><sub>6</sub>O<sub>40</sub>(V<sup>IV</sup>O)<sub>2</sub>]<sup>5-</sup>, is of interest due to its isostructural relations with the fully-oxidised [V<sub>15</sub>O<sub>42</sub>]<sup>9-</sup> isopolyoxovanadate. So-called superkeggin structures based on the {V<sub>18</sub>O<sub>42</sub>} constituents have been found for the mixed-valent complexes [V<sup>IV</sup><sub>12</sub>V<sup>V</sup><sub>6</sub>O<sub>42</sub>(SO<sub>4</sub>)]<sup>8-</sup>,<sup>58</sup> [V<sup>IV</sup><sub>18</sub>O<sub>42</sub>H<sub>9</sub>(V<sup>V</sup>O<sub>4</sub>)]<sup>6-</sup>,<sup>58</sup> and [V<sup>IV</sup><sub>14</sub>V<sup>V</sup><sub>4</sub>O<sub>42</sub>(PO<sub>4</sub>)]<sup>11-</sup>.<sup>59</sup> Note that the structure of the archetypal “fully-reduced” [V<sup>IV</sup><sub>18</sub>O<sub>42</sub>]<sup>12-</sup> polyoxoanion with *D*<sub>4d</sub> symmetry can formally be derived stepwise from the fully-oxidised  $\alpha$ -Keggin-type framework [V<sup>V</sup><sub>12</sub>O<sub>36</sub>]<sup>12-</sup>, as illustrated in Figure 4.



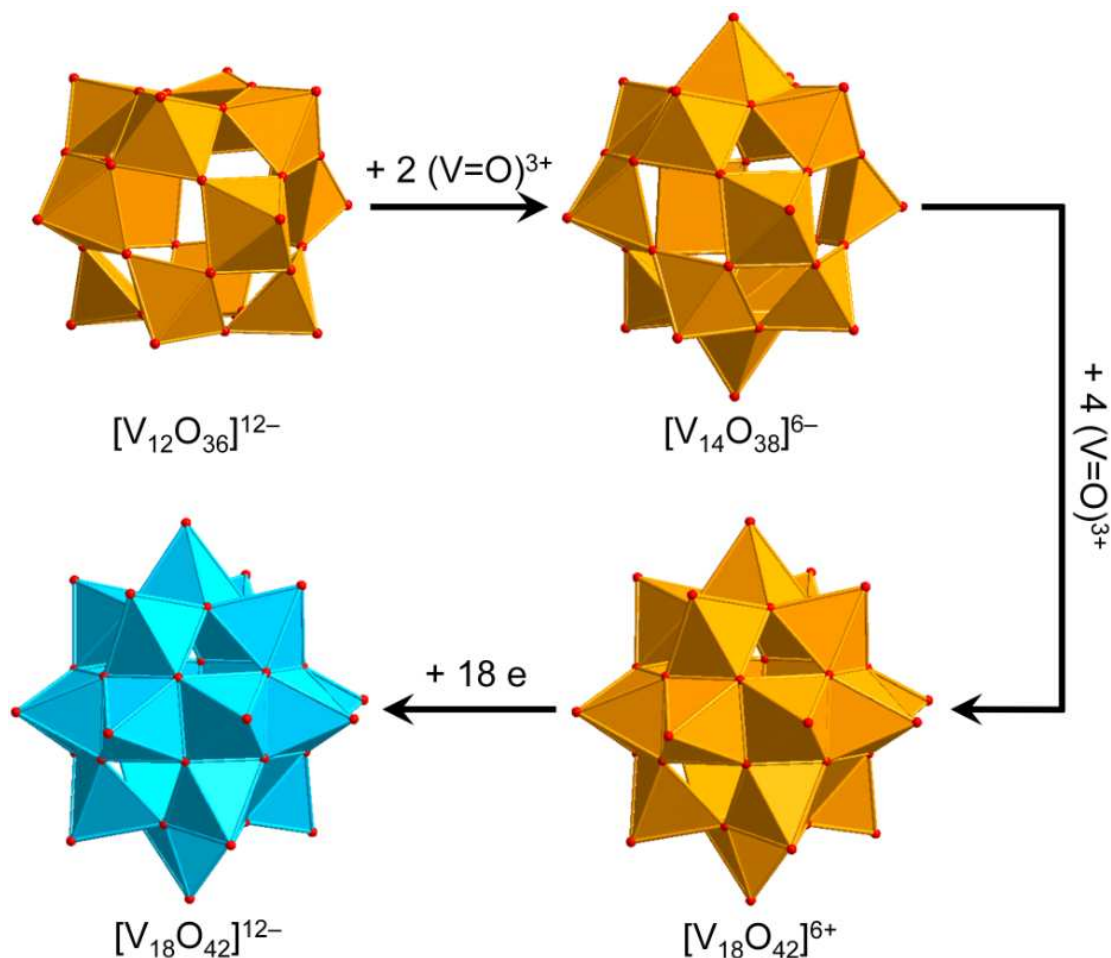


**Figure 4.** Schematic structural evolution of the fully-oxidised  $\alpha$ -Keggin-type framework  $[V_{12}O_{36}]^{12-}$  towards the “fully-reduced”  $[V_{18}O_{42}]^{12-}$  POV via formation of the bicapped Keggin structure  $[V_{14}O_{38}]^{6-}$  and the hypothetical  $[V_{18}O_{42}]^{6+}$  structure, the latter here assumed as isostructural to  $[V_{18}O_{42}]^{12-}$ . Colour code as in Fig. 2.

**1.4 'Host-guest' complexation in POV chemistry.** The cage-, basket-, barrel- and sphere-like shape of high-nuclearity POVs enables them to entrap small guest species<sup>60</sup> in their central voids, in a manner that is structurally reminiscent of the “molecular container” behaviour of e.g. fullerenes. The case of a discrete (small) number of water molecules enclosed in a molecular container generally is of great interest: Jung and coworkers e.g. emphasise that “a single water molecule within an isolated space is a hot research topic in molecular science, owing to potential applications to delicate functions such as proton transfer, tautomerism, recognition, and biological systems.”<sup>61,62</sup> Figure 5 illustrates that not only Pd(II) cage-type coordination complexes<sup>61</sup> and fullerene  $C_{60}$ ,<sup>63</sup> but also the hydrophilic POVs are able to host an individual  $H_2O$  molecule.<sup>64</sup> In the following, for reasons of clarity we indicate the supramolecular encapsulation state of a guest species by the “@” notation when specifying the composition of a discrete polyanion, whereas in full formulas for POV-based compounds the guest species is simply set in brackets.

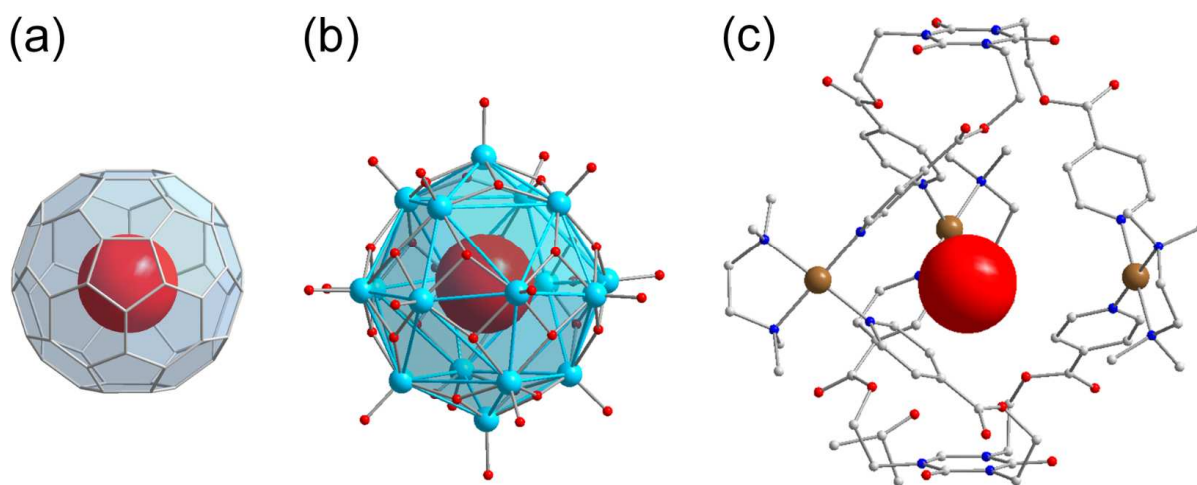


**Figure 5.** The H<sub>2</sub>O-endohedral (@) complexes of C<sub>60</sub> (a),<sup>65</sup> the “fully-reduced” [V<sub>18</sub>O<sub>42</sub>]<sup>12-</sup> POV (b),<sup>45,64</sup> and [Pd<sub>3</sub>L<sub>2</sub>]<sup>6+</sup> (c).<sup>61</sup> C, grey; N, blue; O, red; V<sup>IV</sup>, sky blue; Pd, brown.

The prototypical fully-oxidised, mixed-valent and “fully-reduced” POV shells (e.g., bowl-like {V<sub>12</sub>O<sub>32</sub>}, nearly spherical *D*<sub>4d</sub> {V<sub>18</sub>O<sub>42</sub>}, ellipsoidal *D*<sub>2h</sub> {V<sub>18</sub>O<sub>44</sub>}, bulb-shaped *D*<sub>2d</sub> {V<sub>22</sub>O<sub>54</sub>}) were found to enclose not only water molecules but also anions (e.g., Cl<sup>-</sup>, Br<sup>-</sup>, I<sup>-</sup>, HCOO<sup>-</sup>, MeCOO<sup>-</sup>, CN<sup>-</sup>, CO<sub>3</sub><sup>2-</sup>, NO<sup>-</sup>, NO<sub>2</sub><sup>-</sup>, N<sub>3</sub><sup>-</sup>, PO<sub>4</sub><sup>3-</sup>, SH<sup>-</sup>, SCN<sup>-</sup>, SO<sub>3</sub><sup>2-</sup>, SO<sub>4</sub><sup>2-</sup>, ClO<sub>4</sub><sup>-</sup>, and VO<sub>4</sub><sup>3-</sup>) within the vanadium oxide shells.<sup>39,66</sup> Larger neutral guests (methanol, ethanol, ethane-1,2-diol) have furthermore been reported to exist in phosphate- and diaminopropane-capped {V<sup>III</sup><sub>3</sub>V<sup>IV</sup><sub>18</sub>}<sup>67</sup> type cluster shells.<sup>67</sup> In all of these compounds, the encapsulated halide, pseudohalide, inorganic or organic guest anion interacts with the anionic host shell solely via weak electrostatic and van der Waals forces at distances of *ca.* 3.5 – 4.0 Å. In this regard, the POV host structures<sup>68</sup> can also be regarded as vanadium oxide matrices that isolate unstable guests with short lifetimes or high reactivities. The formation of POV host shells can also be controlled by templating effects of small guest anions present in solution.<sup>40,69</sup> Interestingly, also certain cationic groups such as dimethylammonium that weakly bind to polyoxovanadate shell structures can assume the role of an interchangeable template as well, for example in the POV [Cl<sup>-</sup>@V<sup>V</sup><sub>12</sub>O<sub>32</sub>(H<sub>2</sub>NMe<sub>2</sub>)<sub>2</sub>]<sup>3-</sup> where one or both dimethylammonium groups can subsequently be exchanged by first-row transition metal cations.<sup>70</sup> Macrocyclic, highly-oxidised POV structures [PdV<sup>V</sup><sub>6</sub>O<sub>18</sub>]<sup>4-</sup>, [Cu<sub>2</sub>V<sup>V</sup><sub>8</sub>O<sub>24</sub>]<sup>4-</sup>, and [Ni<sub>4</sub>V<sup>V</sup><sub>10</sub>O<sub>30</sub>(OH)<sub>2</sub>(H<sub>2</sub>O)<sub>6</sub>]<sup>4-</sup> incorporating transition-metal cationic templates (Pd<sup>2+</sup>, Cu<sup>2+</sup>, and Ni<sup>2+</sup>) are also known.<sup>15,71</sup>

The far-reaching consequences for the properties of the host matrix are exemplified by a family of purely inorganic host-guest assemblies [X@HV<sup>IV</sup><sub>8</sub>V<sup>V</sup><sub>14</sub>O<sub>54</sub>]<sup>6-</sup> (X = VO<sub>2</sub>F<sub>2</sub><sup>-</sup>, SCN<sup>-</sup>, and ClO<sub>4</sub><sup>-</sup>).<sup>72</sup> Here the nature of the guest (X) anion defined the magnetic and

electrochemical characteristics of the virtually isostructural, mixed-valent  $V^V/V^{IV}$ -POV host matrices. Similarly, template-dependent reactivity has also been observed for the photooxidation of an organic dye by nearly isostructural  $[X@(\text{Bi}(\text{dmsO})_3)_2V_{12}O_{33}]^-$ -type POVs ( $X = \text{Cl}^-, \text{Br}^-$ ).<sup>73</sup> In general, POVs exhibiting host-guest relationships consist of transferable substructures and exist in a variety of reduction (and protonation) states. In the words of Müller *et al.*: “*The template syntheses of new cluster compounds utilizing intrinsic host-guest relationships open up new possibilities for chemists to create nanosized host or cluster structures with novel magnetic properties.*”<sup>74</sup>

**1.5 Magnetism of POVs.** The POVs can be magnetically functionalised either via their reduction towards the mixed-valent, “fully-reduced”, and “highly-reduced” structures comprising vanadyl  $\{V^{IV}O\}^{2+}$  (isotropic spin-1/2) and  $\{V^{III}O\}^+$  (spin-1) groups or via incorporation of paramagnetic transition metal or lanthanoid cations. The last few decades have shown that such POVs are ideal objects for magnetochemical studies<sup>75</sup> and the exploration of nanoscale molecular magnetism<sup>76</sup> due to their intriguing magnetic features, ranging from geometrical spin frustration to single-molecule magnet characteristics.<sup>77</sup> Most commonly, the mixed-valent ( $V^V/V^{IV}$  or  $V^{IV}/V^{III}$ ), “fully-reduced” ( $d^1$ - $V^{IV}$ ) and “highly-reduced” ( $d^2$ - $V^{III}$ ) vanadium spin-centres are coupled antiferromagnetically via bridging oxygen atoms, although ferromagnetic coupling between the vanadium ions is also possible, as has been forecasted in a quantum-chemical study of the synthetically readily accessible mixed-valent alkoxo-hexavanadates of the  $[V^{IV}_4V^V_2O_7(\text{OR})_{12}]$  type.<sup>78</sup> A comparative theoretical study of the magnetic properties of a homovalent  $[V^{IV}_{18}O_{42}]^{12-}$  POV with 18 fully localised valence electrons and its structurally identical mixed-valent derivative  $[V^{IV}_{10}V^V_8O_{42}]^{4-}$  with 10 partially delocalised electrons explored the role of electron transfer processes and magnetic exchange interactions in these structures.<sup>79</sup> The preparation of the first water-soluble salt-inclusion solid  $[\text{Cs}_{11}\text{Na}_3(\text{V}_{15}\text{O}_{36})\text{Cl}_6]$  containing the mixed-valent  $[V^{IV}_{11}V^V_4O_{36}\text{Cl}]^{9-}$  building block is an interesting result in view of the development of “*quantum magnetic solids within extended systems*”.<sup>80,81</sup> Notably, the chemical reactivity and acid-dissociation constants of fully and partly reduced POVs can in principle be influenced by the extent of charge delocalisation.

**1.6 Catalysis with POVs.** The catalytic activity of the POV-based compounds was demonstrated by a number of authors. Gao and Hua reported that  $\text{K}_7[\text{Ni}^IV\text{V}_{13}\text{O}_{38}] \cdot 16\text{H}_2\text{O}$  containing the fully-oxidised  $[V^{V}_{13}O_{38}]^{11-}$  building block catalyses oxidative mineralisation of *p*-nitrophenol and *p*-chlorophenol into  $\text{CO}_2$ ,  $\text{NO}_3^-$ , and  $\text{Cl}^-$  using 30% aqueous  $\text{H}_2\text{O}_2$  as oxidant under mild conditions.<sup>82,83</sup> Khan and coworkers investigated the selective catalytic reduction of nitrogen oxides into  $\text{N}_2$  by propylene as the reductant using the mixed-valent

heterometallic compounds  $\text{Li}_6[\text{M}_3(\text{H}_2\text{O})_{12}\text{V}_{18}\text{O}_{42}(\text{YO}_4)] \cdot 24\text{H}_2\text{O}$  ( $\text{M} = \text{Mn}^{\text{II}}, \text{Ni}^{\text{II}}; \text{Y} = \text{V}, \text{S}$ ) and  $[\text{M}_3(\text{H}_2\text{O})_{12}\text{V}_{18}\text{O}_{42}(\text{YO}_4)] \cdot 24\text{H}_2\text{O}$  ( $\text{M} = \text{Fe}^{\text{II}}, \text{Co}^{\text{II}}; \text{Y} = \text{V}, \text{S}$ ) as precursors.<sup>84</sup> The catalytic oxidative dehydrogenation of propane by the nanostructured compounds  $[\text{M}_3(\text{H}_2\text{O})_{12}\text{V}_{18}\text{O}_{42}(\text{YO}_4)] \cdot 24\text{H}_2\text{O}$  ( $\text{M} = \text{Fe}, \text{Co}, \text{Mn}; \text{Y} = \text{V}, \text{S}$ ) has also been studied.<sup>85</sup> Wu *et al.* showed that the compound  $(\text{NH}_4)_2\{[\text{Mn}(\text{salen})(\text{H}_2\text{O})]_6\text{V}_6\text{O}_{18}\}(\text{NO}_3)_2 \cdot 30\text{H}_2\text{O}$  ( $\text{salen}^{2-} = \text{N,N}'\text{-(ethylene)bis(salicylideneimine)}$ )), the structure of which comprises a cyclic POV anion decorated with six  $\text{Mn}^{\text{III}}$ -salen Schiff-base complex groups, acts as photocatalyst for organic dye degradation.<sup>86</sup> Chakrabarty and Banerjee studied the decomposition of  $\text{H}_2\text{O}_2$  into  $\text{O}_2$  and  $\text{H}_2\text{O}$ , which is catalysed by the  $[\text{Mn}^{\text{IV}}\text{V}^{\text{V}}_{13}\text{O}_{38}]^{7-}$  polyoxoanion in aqueous acetate buffer.<sup>87</sup> The compound  $(\text{NH}_4)\{[\text{Zn}_4(\text{dach})_7(\text{H}_2\text{O})_3][\text{V}_3\text{V}_{18}\text{P}_6\text{O}_{60}(\text{dach})_3]\} \cdot 19\text{H}_2\text{O}$  ( $\text{dach} = (\pm)\text{-trans-1,2-cyclohexanediamine} = \text{C}_6\text{H}_{14}\text{N}_2$ ) containing the nanoscale, highly-reduced  $[\text{V}^{\text{III}}_3\text{V}^{\text{IV}}_{18}\text{P}_6\text{O}_{60}(\text{dach})_3]^{9-}$  building block was shown to selectively catalyse styrene oxidation in the presence of  $\text{H}_2\text{O}_2$ .<sup>44</sup>  $(\text{N}_7\text{Bu}_4)_4[\text{V}_{16}\text{O}_{38}(\text{Br})]$  containing the mixed-valent  $[\text{Br}@\text{V}^{\text{IV}}_7\text{V}^{\text{V}}_9\text{O}_{38}]^{4-}$  building block exhibited catalytic activity in the oxidative bromination reactions of aromatic substrates under aerobic conditions.<sup>88</sup> The mixed-valent  $(\text{N}_7\text{Bu}_4)[\text{V}^{\text{IV}}_5\text{V}^{\text{V}}_1\text{O}_7(\text{OMe})_{12}]$  compound was demonstrated to catalyse photoinduced water oxidation.<sup>89</sup>

**1.7 Scope of the review.** Embedding heteroelements into POV structures<sup>90</sup> allows us to alter the electronic and magnetic properties, as well as the electrical conductivities<sup>91</sup> of the resultant heteropolyoxovanadate (*hetero*POV) spin structures (reminiscent of “doping” semiconducting materials) through the interplay between stoichiometries, heavy atom effects and redox potentials as well as steric and electronic environment around the terminal  $\text{V}=\text{O}$  groups. Herein, we place emphasis on the structural variety of silicato-, germanato-, arsenato-, and antimonato-derivatised polyoxovanadates and their hybrid compounds with middle and late transition metals and discuss interesting molecular features and application perspectives of these *hetero*POVs. Great interest in the polynuclear molecular vanadium oxides decorated with the heavier group 14 and 15 elements (E) is generated by the specific synthetic, structural, host-guest and vast redox chemistry and extraordinary magnetic characteristics of these compounds, involving e.g. geometrical spin-frustration.<sup>92</sup> Remarkably, the structurally, electronically and spin density-modified *hetero*POVs introduce different functionalities linked to the main-group metalloid atoms (E = Si, Ge, As, Sb) that may act as bonding mediators. The steric requirements around terminal  $\text{V}=\text{O}$  groups in the *hetero*POVs differ between the building blocks comprising E =  $\text{Si}^{\text{IV}}, \text{Ge}^{\text{IV}}$  and those with E =  $\text{As}^{\text{III}}, \text{Sb}^{\text{III}}$  due to the presence of lone electron pairs at the latter elements. The fully-oxidised ( $\text{V}^{\text{V}}$ ), mixed-valent ( $\text{V}^{\text{V}}/\text{V}^{\text{IV}}$  and  $\text{V}^{\text{IV}}/\text{V}^{\text{III}}$ ), “fully-

reduced" ( $V^{IV}$ ), and "highly-reduced" ( $V^{III}$ ) *hetero*POVs with various point-group symmetries and different isomeric structures of  $\alpha$  and  $\beta$  types show an astonishing propensity for organic and transition metal/lanthanoid functionalization. This grants access to multifunctional inorganic-organic supramolecular materials<sup>93</sup> and the closely-related chemistry of metal-organic frameworks (MOFs)<sup>94</sup> and thus offers potential for applications of *hetero*POVs in catalysis, surface science, and information technology.

## 2. Group 14 (Si, Ge) element-functionalised POVs

### 2.1 Preview.

The chemistry of *hetero*POVs incorporating the most common  $\{E_2O_7\}$  groups and more rare  $\{E_2O_5S_2\}$  ones with  $E = Si$  or  $Ge$  (SiPOVs and GePOVs) is still underdeveloped. In their molecular structures, the  $E^{IV}$  atoms usually favour four-fold coordination, thus yielding tetrahedral  $\{EO_4\}$  geometries. However, an example of a *hetero*POV with a  $Ge^{IV}$  centre adopting a six-fold  $\{GeO_6\}$  coordination was also described. Interestingly, the Si–O and Ge–O bond lengths ( $d_{E-O} = 1.56 - 1.79 \text{ \AA}$ ) are comparable to the bond lengths of terminal  $V=O$  groups ( $d_{V=O} = 1.56 - 1.64 \text{ \AA}$ ), but shorter when compared to the single  $V-O$  bonds ( $d_{V-O} = 1.88 - 2.28 \text{ \AA}$ ). The  $\{E_2O_7\}$ - or  $\{E_2O_5S_2\}$ -decorated POV structures are typically viewed as being formally derived from the  $[V^{IV}_{18}O_{42}]^{12-}$  archetype. The family of polyoxovanadatosilicates (SiPOVs) is represented by the assemblies with nuclearity  $V_{15}$ ,  $V_{17}$  and  $V_{18}$ . The polyoxovanadatogermanates (GePOVs) display a series of assemblies classified as  $V_6$ ,  $V_9$ ,  $V_{12}$ ,  $V_{14}$ ,  $V_{15}$  and  $V_{16}$ . The SiPOVs and GePOVs usually encapsulate discrete water molecules or halide ions and can exhibit negative charges up to  $12-$ . The SiPOVs (Table 1) and GePOVs (Table 2) are usually synthesised by hydrothermal or solvothermal reactions using  $V_2O_5$ ,  $VOSO_4$  and  $NH_4VO_3$  as precursors.

### 2.2 Polyoxovanadatosilicates (SiPOVs).

Only a few studies describing the isolation of SiPOVs have been performed so far. These SiPOVs constitute a series with the general formula  $\{V_{18-z}Si_{2z}O_{42+2z}\}$  and are characterised by antiferromagnetic coupling between the spin-1/2 vanadyl  $\{VO\}^{2+}$  moieties.

#### 2.2.1 SiPOVs with one-dimensional (1D) structures.

**Vanadyl(V)-extended SiPOVs.** The first report about the spherical POV chemically modified with  $Si^{IV}$  dates back to 2001 when Jacobson and coworkers described the  $[V^{IV}_{16}Si_4O_{46}]^{12-}$  polyoxoanion (Figure 6a) that is a component of the compound  $Cs_{10.5}[(V_{16}O_{40})(V_{1.5}Si_{4.5}O_{10})] \cdot 3.5H_2O$  synthesised under hydrothermal conditions (Table 1).<sup>95</sup> The crystal structure of this hybrid compound shows a 1D linear chain of the "fully-reduced"

$[V^{IV}_{16}O_{40}]^{16-}$  POVs interlinked by vanadosilicate six-membered rings with the composition  $\{V^{V}_{1.5}Si_{4.5}O_{10}\}^{5.5+}$  (Figure 7a).  $[V_{16}O_{40}]^{16-}$  is hypothetically derived from the  $\alpha$ -Keggin  $\{V_{12}O_{36}\}$  archetype or, accordingly, the  $\{V_{18}O_{42}\}$  archetype (Figure 4). Replacing two vanadyl  $\{VO\}^{2+}$  groups on two opposite sides of the  $[V_{18}O_{42}]^{12-}$  isopolyoxoanion by two silicate  $\{Si_2O_3\}$  subunits, the spherical  $[V^{IV}_{16}Si_4O_{46}]^{12-}$  dodecaanion is formed. A water molecule is located in the void of the polyoxoanion.

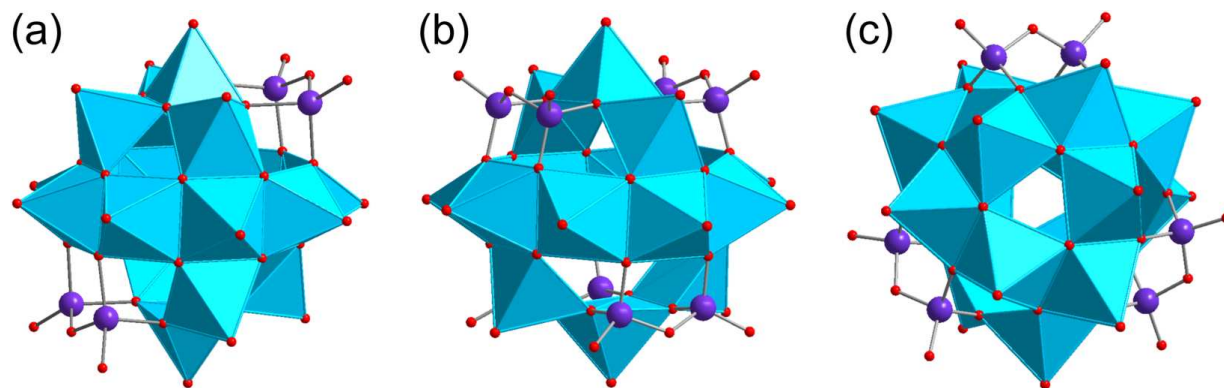


**Figure 6.** Polyhedral representations of the “fully-reduced” SiPOVs  $[V^{IV}_{16}Si_4O_{46}]^{12-}$  (a),  $\alpha$ - $[H_4V^{IV}_{14}O_{44}(SiO)_8]^{12-}$  (b), and  $[V^{IV}_{15}Si_6O_{42}(OH)_6]^{6-}$  (c). Encapsulated  $H_2O$  (a, b),  $Cl^-$  (c), and hydrogen atoms are not shown. Colour code: Si, violet; O, red spheres;  $V^{IV}O_x$ , sky-blue polyhedra.

Later on, two extended chains based on the “fully-reduced”  $\{V^{IV}_{15}Si_6O_{48}\}$  building blocks<sup>96</sup> were obtained from reactions under hydrothermal conditions where the pdn molecules (pdn = 1,3-propanediamine) acted as reductant for  $V^V$  (Table 1). These two inorganic-organic hybrid compounds can be assigned to the classes of vanadyl-extended and transition metal complex (TMC)-supported SiPOVs.

1D zig-zag chains of the SiPOVs doubly bridged by the fully-oxidised  $\{V^VO_2\}^+$  moieties through  $(Si-O)-V-O(-Si)$  bonds with  $d_{V-O} = 1.79 \text{ \AA}$  and  $1.81 \text{ \AA}$  (Figure 7b) were observed in the crystal of the compound  $(H_{1.5}pdn)_6\{[H_2V_{15}Si_6O_{48}(Cl)](VO_2)_2\} \cdot 4H_2O$ .<sup>96</sup> The partially protonated pdn molecules compensate the high negative charge of the mixed-valent  $\{[Cl@H_2V^{IV}_{15}Si_6O_{48}]\{V^VO_2\}_2\}^{9-}$  assembly and reside in the voids between the zig-zag chains, along with  $H_2O$  solvate molecules.

**TMC-supported SiPOV.** One-dimensional infinite chains of  $[H_6V^{IV}_{15}Si_6O_{48}]^{6-}$  polyoxoanions that are singly bridged by  $[Co(pdn)_2(H_2O)]^{2+}$  fragments through  $(V-O)-Co-O(-Si,V)$  linkages (Figure 7c) were found in the crystal structure of  $(H_2pdn)(Hpdn)_2[H_6V^{IV}_{15}Si_6O_{48}][Co(pdn)_2(H_2O)] \cdot 9H_2O$ .<sup>96</sup>



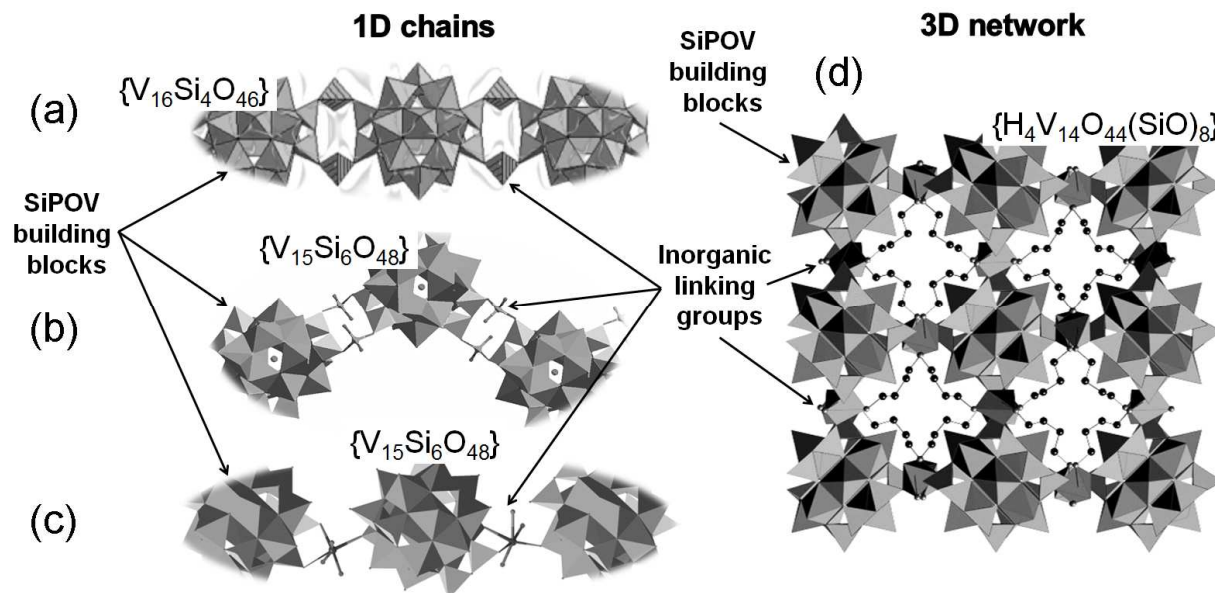


**Figure 7.** Representation of the extended structures of SiPOVs covalently linked by inorganic groups.

### 2.2.2 SiPOV with three-dimensional (3D) structures.

In 2003, Clearfield and coworkers described a 3D cross-linked structure consisting of the  $[H_4V_{14}O_{44}(SiO)_8]^{12-}$  building blocks bridged by  $\{(VO)_2N_2\}$  pyramids that are covalently interconnected by bidentate dab ligands (dab = 1,4-diaminobutane) through the  $V^{IV}$  ions (Figure 7d).<sup>97</sup> The “fully-reduced”,  $\alpha$ - $[H_4V^{IV}_{14}O_{44}(SiO)_8]^{12-}$  polyoxoanion (Figure 6b) with idealised  $D_{2d}$  symmetry is a component of the hydrothermally prepared compound  $[H_4V_{18}O_{46}(SiO)_8(dab)_4(H_2O)] \cdot 4H_2O$  (Table 1). This SiPOV shows a modified  $[V_{18}O_{42}]^{12-}$  structure where four  $\{VO_5\}$  square pyramids are substituted by four handle-like  $\{Si_2O_7\}$  silicate units. Each of these units is made up of two corner-sharing  $[SiO_4]^{4-}$  tetrahedra. The POV shell is constructed of an octagonal ring sharing two crescent-type  $\{VO_5\}$  chains fused to each side of the former and exhibits non-bonding  $V \cdots V$  distances of 2.83 – 3.09 Å.

### 2.2.3 Discrete SiPOV within hydrogen bonding networks.

The formal replacement of three  $\{VO_5\}$  square pyramids in the  $\{V_{18}O_{42}\}$  archetypal structure with three partially protonated handle-like  $\{Si_2O_5(OH)_2\}$  groups results in the  $D_3$ -symmetrical  $[V^{IV}_{15}Si_6O_{42}(OH)_6]^{6-}$  polyoxoanion (Figure 6c) found as the central building block in the hydrothermally prepared compound  $(H_2pdn)_3(Hpdn)[V_{15}Si_6O_{42}(OH)_6(Cl)] \cdot nH_2O$  ( $n = 7-10$ ) with a solid-state close-packed layer aggregate structure (Table 1).<sup>98</sup> Here, the discrete SiPOV  $[Cl@V^{IV}_{15}Si_6O_{42}(OH)_6]^{7-}$  exhibits closest intracluster  $V \cdots V$  distances of ca. 3.0 Å and hosts a  $Cl^-$  anion. In the crystal structure, extensive  $N-H \cdots O$  hydrogen bonding interactions were observed, which interlink the pdn groups and the “fully-reduced” SiPOVs. Notably,

these N–H⋯O hydrogen bonds are crucial in the formation of the supramolecular network structure.

#### 2.2.4 Corollary for SiPOVs.

All above-mentioned SiPOVs can be regarded as derivatives of the  $[V_{18}O_{42}]^{12-}$  archetype (Figure 3), as a specific number ( $n = 2 - 4$ ) of its  $[VO_5]^{6-}$  square pyramids are formally replaced with an equal number of handle-like silicate  $[Si_2O_7]^{6-}$  iso-anionic or partly protonated  $[Si_2O_5(OH)_2]^{4-}$  groups. All discussed “fully-reduced” SiPOV building blocks were shown to form diverse networks (Figure 7) in the solid state principally due to the following points: (i) the chemical composition and structures of the inorganic linkers and the nature of the metal ions, which played a crucial role in the self-assembly behaviour of the spherical SiPOVs; (ii) the presence of the silicate groups in SiPOVs which are involved in the covalent bonding to the linking groups. As it was noted, *“the interconnection of polyoxometal building blocks like polyoxovanadates by means of covalent bonds could create new porous materials with ultralow framework densities and high porosity.”*<sup>99</sup> In view of the structural arrangement and organisation of the extended solid-state structures discussed above, it appears highly desirable to explore the role of the SiPOV-based networks as microporous molecular materials resembling zeolites or molecular sieves, e.g., for catalytic performance, gas storage, and ion exchange.



**Table 1.** Selected details of synthesis and characterisation of **SiPOV**-based compounds.

Formula	Colour	Characteristics of crystal structure <sup>a</sup>	Reactants	Reaction conditions	Yield	Characterised via	Ref.
<i>SiPOV-based compounds</i>							
<b>V<sub>15</sub></b> (H <sub>2</sub> pdn) <sub>3</sub> (Hpdn)[V <sub>15</sub> Si <sub>6</sub> O <sub>42</sub> (OH) <sub>6</sub> (Cl)]· <i>n</i> H <sub>2</sub> O ( <i>n</i> = 7 – 10)	brown	close-packed layer aggregate	V <sub>2</sub> O <sub>5</sub> , H <sub>2</sub> O, pdn, tetraethyl orthosilicate (teos), HCl	180 °C, 6 d	72% based on V <sub>2</sub> O <sub>5</sub>	EA, IR, TGA, EDXS, XPS, powder X-ray, single-crystal XRD, magnetometry	98
(H <sub>2</sub> pdn)(Hpdn) <sub>2</sub> [H <sub>6</sub> V <sub>15</sub> Si <sub>6</sub> O <sub>48</sub> ][Co(pd <sub>n</sub> ) <sub>2</sub> (H <sub>2</sub> O)]·9 H <sub>2</sub> O	red brown	1D infinite chain	V <sub>2</sub> O <sub>5</sub> , pdn, H <sub>2</sub> O, teos, EtOH, Co(OAc) <sub>2</sub> ·4H <sub>2</sub> O, HCl	180 °C, 6 d	35% based on V	EA, IR, XPS, single-crystal XRD, magnetometry	96
<b>V<sub>17</sub></b> (H <sub>1.5</sub> pdn) <sub>6</sub> [(H <sub>2</sub> V <sub>15</sub> Si <sub>6</sub> O <sub>48</sub> (Cl))(VO <sub>2</sub> ) <sub>2</sub> ]·4H <sub>2</sub> O	brown	1D zig-zag chain	V <sub>2</sub> O <sub>5</sub> , pdn, H <sub>2</sub> O, teos, EtOH, HOAc, HCl	180 °C, 6 d	83% based on V	EA, IR, XPS, single-crystal XRD, magnetometry	96
<b>V<sub>17-18</sub></b> Cs <sub>10.5</sub> [(V <sub>16</sub> O <sub>40</sub> )(V <sub>1.5</sub> Si <sub>4.5</sub> O <sub>10</sub> )]·3.5H <sub>2</sub> O	dark brown	1D extended chain	VOSO <sub>4</sub> ·3H <sub>2</sub> O, SiO <sub>2</sub> , H <sub>2</sub> O, CsOH	240 °C, 3 d		EMP, IR, single-crystal XRD	95
<b>V<sub>18</sub></b> [H <sub>4</sub> V <sub>18</sub> O <sub>46</sub> (SiO) <sub>8</sub> (dab) <sub>4</sub> (H <sub>2</sub> O)]·4H <sub>2</sub> O	dark green	cross-linked 3D network	V <sub>2</sub> O <sub>5</sub> , SiO <sub>2</sub> , dab, H <sub>2</sub> O	180 °C, 5 d	61% based on SiO <sub>2</sub>	EA, IR, powder XRD, single-crystal XRD	97

<sup>a</sup> Dimensionality resulting from hydrogen bonding networks is not considered.

## 2.3 Polyoxovanadatogermanates (GePOVs).

### 2.3.1 Discrete GePOVs with $\{\text{Ge}_2\text{O}_7\}$ and partially protonated germanate groups.

The chemical and structural characterisation of the first GePOVs dates back to 2003, when Jacobson and coworkers described the compounds  $\text{Cs}_8[\text{V}_{16}\text{Ge}_4\text{O}_{42}(\text{OH})_4] \cdot 4.7\text{H}_2\text{O}$ ,  $(\text{H}_2\text{ppz})_4(\text{Hppz})_4[\text{V}_{14}\text{Ge}_8\text{O}_{50}(\text{H}_2\text{O})]$  (ppz = piperazine,  $\text{C}_4\text{H}_{10}\text{N}_2$ ) and  $\text{K}_5[\text{H}_8\text{V}_{12}\text{Ge}_8\text{O}_{48}(\text{SO}_4)] \cdot 10\text{H}_2\text{O}$ , which were synthesised under hydrothermal conditions (Table 2).<sup>100</sup> These compounds are based, respectively, on the “fully-reduced”  $[\text{V}^{\text{IV}}_{16}\text{Ge}_4\text{O}_{42}(\text{OH})_4]^{8-}$  (Figure 8a) and  $\alpha\text{-}[\text{V}^{\text{IV}}_{14}\text{Ge}_8\text{O}_{50}]^{12-}$  polyoxoanions (Figure 8b) and the mixed-valent  $[\text{H}_8\text{V}_{12}\text{Ge}_8\text{O}_{48}(\text{SO}_4)]^{5-}$  polyoxoanion that encloses a sulfate template anion in the centre of a spherical GePOV shell. The structures of  $[\text{V}_{16}\text{Ge}_4\text{O}_{42}(\text{OH})_4]^{8-}$  and  $[\text{H}_8\text{V}_{12}\text{Ge}_8\text{O}_{48}(\text{SO}_4)]^{5-}$  are derived from the “fully-reduced”  $[\text{V}^{\text{IV}}_{18}\text{O}_{42}]^{12-}$  shell (i.e., Keggin-type  $[\text{V}^{\text{IV}}_{12}\text{O}_{36}]^{24-} + 6 \{\text{V}^{\text{IV}}\text{O}\}^{2+}$  caps) on substitution of  $\{\text{VO}\}^{2+}$  caps in the latter by a certain number of  $\{\text{Ge}^{\text{IV}}_2\text{O}(\text{OH})_2\}^{4+}$  dimeric units (two and four, respectively). To get to the final composition of  $[\text{H}_8\text{V}_{12}\text{Ge}_8\text{O}_{48}(\text{SO}_4)]^{5-}$ , two further  $\{\text{VO}\}^{2+}$  caps in  $[\text{V}^{\text{IV}}_{18}\text{O}_{42}]^{12-}$  are formally omitted. Similarly, replacing four  $\{\text{VO}\}^{2+}$  caps in the archetypal structure by four  $\{\text{Ge}^{\text{IV}}_2\text{O}_3\}^{2+}$  groups affords the polyoxoanion cage of the composition  $[\text{V}_{14}\text{Ge}_8\text{O}_{50}]^{12-}$ . It is interesting to note that the  $[\text{V}_{14}\text{Ge}_8\text{O}_{50}]^{12-}$  and  $[\text{H}_8\text{V}_{12}\text{Ge}_8\text{O}_{48}(\text{SO}_4)]^{5-}$  constituents are the structural analogues to the family of the polyoxovanadoarsenates with the general formula  $[\text{V}_{18-z}\text{As}_{2z}\text{O}_{42}(\text{Y})]^{m-}$  ( $\text{Y} = \text{SO}_3, \text{SO}_4, \text{Cl}$ ;  $z = 3, 4$ ), which are discussed below. In contrast to the structures of  $[\text{V}_{14}\text{Ge}_8\text{O}_{50}]^{12-}$  and  $[\text{H}_8\text{V}_{12}\text{Ge}_8\text{O}_{48}(\text{SO}_4)]^{5-}$  displaying rhombicuboctahedral topology, the molecular structure of  $[\text{V}_{16}\text{Ge}_4\text{O}_{42}(\text{OH})_4]^{8-}$  reveals an elongated square gyrobicupola topology.

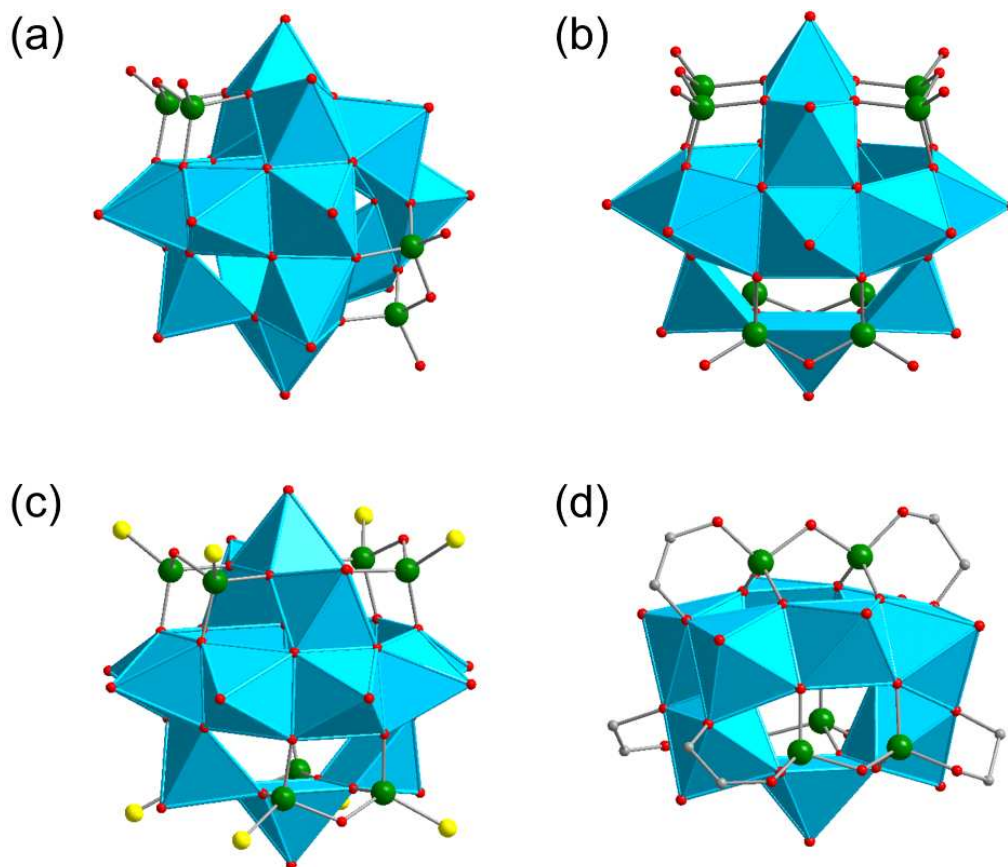


**Figure 8.** Polyhedral representations of the “fully-reduced” GePOVs  $[V^{IV}_{16}Ge_4O_{42}(OH)_4]^{8-}$  (a),  $\alpha-[V^{IV}_{14}Ge_8O_{50}]^{12-}$  (b),  $\alpha-[V^{IV}_{14}Ge_8O_{42}S_8]^{12-}$  (c), and  $[H_2V^{IV}_9Ge_6O_{26}(L)_6]^{2-}$  (d). Encapsulated water molecules and hydrogen atoms are not shown. Colour code: C, grey; Ge, green; O, red spheres;  $V^{IV}O_x$ , sky-blue polyhedra.

The compound  $(H_2dab)_4[V_{14}O_{44}(GeOH)_8] \cdot 6H_2O$  was obtained by Clearfield and coworkers from the hydrothermal reaction between  $V_2O_5$ ,  $GeO_2$  and 1,4-diaminobutane (dab) in water (Table 2).<sup>97</sup> The “fully-reduced”, protonated  $\alpha-[V^{IV}_{14}O_{44}(GeOH)_8]^{8-}$  polyoxoanion is isostructural to the aforementioned  $\alpha-[H_4V^{IV}_{14}O_{44}(SiO)_8]^{12-}$  polyoxoanion (Figure 6b). In contrast to  $[H_4V_{18}O_{46}(SiO)_8(dab)_4(H_2O)] \cdot 4H_2O$ , the Ge(IV)-containing compound contains doubly protonated  $H_2dab^{2+}$  counteranions.

A GePOV structural analogue to the  $[Cl@V^{IV}_{15}Si_6O_{42}(OH)_6]^{7-}$  polyoxoanion (Figure 6c) was also reported. The main structural difference between the two compounds containing the  $[Cl@V^{IV}_{15}E_6O_{42}(OH)_6]^{7-}$  component is the packing of the structural building blocks. The compound with  $E = Si$  shows a close-packed layer structure, whereas the one with  $E = Ge$  exhibits a 1D chain structure.<sup>98</sup> The crystal structure of the GePOV-based compound (Table 2) with the formula  $(H_2tren)_2(H_3tren)[V_{15}Ge_6O_{42}(OH)_6(Cl)] \cdot 2H_2O$  is furthermore characterised by the  $N-H \cdots O$  hydrogen bonds formed between the oxygen atoms of the “fully-reduced” polyoxoanions and the organic tris(2-aminoethyl)amine (tren) counteranions.

The compound  $(\text{H}_3\text{aep})_4[\text{V}_{14}\text{Ge}_8\text{O}_{50}] \cdot 2(\text{aep}) \cdot 13\text{H}_2\text{O}$  ( $\text{aep} = 1-(2\text{-aminoethyl})\text{piperazine} = \text{C}_6\text{H}_{15}\text{N}_3$ ) and the already described  $(\text{H}_2\text{ppz})_4(\text{Hppz})_4[\text{V}_{14}\text{Ge}_8\text{O}_{50}(\text{H}_2\text{O})]$  compound<sup>100</sup> with the “fully-reduced”  $\alpha\text{-}[\text{V}^{\text{IV}}_{14}\text{Ge}_8\text{O}_{50}]^{12-}$  components were formed in solvothermal reactions involving  $\text{Cu}(\text{NO}_3)_2 \cdot 3\text{H}_2\text{O}$  below 150 °C and above 150 °C, respectively (Table 2).<sup>101</sup> Since  $\text{Cu}^{2+}$  was reduced to metallic Cu during the syntheses, the linking of the GePOV building blocks through  $\text{Cu}^{2+}$ -centred complexes into extended structures was unsuccessful. Interestingly,  $(\text{H}_3\text{aep})_4[\text{V}_{14}\text{Ge}_8\text{O}_{50}] \cdot 2(\text{aep}) \cdot 13\text{H}_2\text{O}$  could also be produced without utilising the copper salt  $\text{Cu}(\text{NO}_3)_2 \cdot 3\text{H}_2\text{O}$ . However, the presence of copper in the reaction mixture turned out to be crucial for the crystallisation of  $(\text{H}_2\text{ppz})_4(\text{Hppz})_4[\text{V}_{14}\text{Ge}_8\text{O}_{50}(\text{H}_2\text{O})]$ . The high negative charge of  $[\text{V}^{\text{IV}}_{14}\text{Ge}_8\text{O}_{50}]^{12-}$  (Figure 8b) is compensated by the protonated amine molecules. Weak ( $> 2 \text{ \AA}$ ) and strong ( $< 2 \text{ \AA}$ ) N–H $\cdots$ O hydrogen bonds between the organic ammonium counteranions and the exposed oxygen atoms of the GePOVs in the crystals of both compounds result in 3D H-bonded networks. The preliminary analysis of the magnetic properties of  $(\text{H}_3\text{aep})_4[\text{V}_{14}\text{Ge}_8\text{O}_{50}] \cdot 2(\text{aep}) \cdot 13\text{H}_2\text{O}$  indicated strong antiferromagnetic exchange interactions between the spin-1/2 vanadyl  $\{\text{VO}\}^{2+}$  moieties through the near-linear V– $\mu$ –O–V and bent V(– $\mu$ –O–) $_2$ V bridges.

### 2.3.2 GePOVs with $\{\text{Ge}_2\text{O}_5\text{S}_2\}$ groups.

**Discrete GePOV.** The structural diversity of the GePOVs was explored towards their sulfur-functionalised analogues. Two polyoxothio compounds  $(\text{H}_3\text{dien})_4[\text{V}_{14}\text{Ge}_8\text{O}_{42}\text{S}_8] \cdot 5\text{H}_2\text{O}$  ( $\text{dien} = \text{diethylenetriamine}$ ) and  $(\text{H}_3\text{aep})_4[\text{V}_{14}\text{Ge}_8\text{O}_{42}\text{S}_8]$  consisting of the “fully-reduced”  $[\text{V}^{\text{IV}}_{14}\text{Ge}_8\text{O}_{42}\text{S}_8]^{12-}$  GePOVs and protonated amines as counteranions were synthesised hydrothermally (Table 2).<sup>99</sup> The  $\alpha\text{-}[\text{V}^{\text{IV}}_{14}\text{Ge}_8\text{O}_{42}\text{S}_8]^{12-}$  polyoxoanion (Figure 8c) with a diameter of ca. 7.4 Å shows structural, but not functional similarities to  $\alpha\text{-}[\text{V}^{\text{IV}}_{14}\text{Ge}_8\text{O}_{50}]^{12-}$  (Figure 8b). The  $\{\text{V}_{14}\}$ -nuclearity building block of the thio-modified GePOV is composed of fourteen condensed  $\{\text{VO}_5\}$  square pyramids and eight tetrahedral  $\{\text{GeO}_3\text{S}\}$  units. Thus, eight terminal oxygen sites of four  $\{\text{Ge}_2\text{O}_7\}$  groups were formally exchanged for eight sulfur atoms to form four  $\{\text{Ge}_2\text{O}_5\text{S}_2\}$  groups.

**Cobalt-GePOV hybrid.** Another example of thio-functionalised GePOV,  $[\text{H}_2\text{O}@\text{V}^{\text{IV}}_{15}\text{Ge}_6\text{O}_{42}\text{S}_6]^{12-}$ , composed of six slightly distorted  $\{\text{GeO}_3\text{S}\}$  tetrahedra ( $d_{\text{Ge-S}} = 2.09 - 2.14 \text{ \AA}$ ), fifteen  $\{\text{VO}_5\}$  square pyramids and an encapsulated central  $\text{H}_2\text{O}$  molecule was obtained under hydrothermal conditions using metavanadate as precursor and elemental Ge, Co and S (Table 2).<sup>102</sup> The spherical  $[\text{V}^{\text{IV}}_{15}\text{Ge}_6\text{O}_{42}\text{S}_6]^{12-}$  structure is constructed of three  $\{\text{V}_7\text{Ge}_2\text{O}_{24}\text{S}_2\}$  rings which are perpendicular to each other. This polyoxoanion is formally derived from the  $\{\text{V}_{18}\text{O}_{42}\}$  archetype by substituting three  $\{\text{VO}_5\}$  pyramidal units of  $[\text{V}_{18}\text{O}_{42}]^{12-}$  by three handle-like  $\{\text{Ge}_2\text{O}_5\text{S}_2\}$  groups (for comparison, see

$[\text{V}^{\text{IV}}_{15}\text{Si}_6\text{O}_{42}(\text{OH})_6]^{6-}$  in Figure 6c). This “fully-reduced” GePOV is further expanded by two  $\{\text{Co}(\text{tren})\}^{2+}$  complexes through Co–S bonds, thus featuring the Co–S=Ge–O–V connections. These two trigonal-bipyramidal Co(II) complexes are attached to the terminal sulfide sites ( $\text{S}^{2-}$ ) and, along with two  $[\text{Co}(\text{tren})(\text{H}_2\text{tren})]^{4+}$  counteranions, reduce the high negative charge of the polyoxoanion to give the compound  $[\text{Co}(\text{tren})(\text{H}_2\text{tren})]_2\{[\text{Co}(\text{tren})]_2\text{V}_{15}\text{Ge}_6\text{O}_{42}\text{S}_6(\text{H}_2\text{O})\}\cdot 9\text{H}_2\text{O}$  where tren molecules act as mono- and tetradentate ligands. The presence of the N–H $\cdots$ O hydrogen-bonding pattern in the crystal structure of this compound results in two differently oriented channels. Similar to other  $\{\text{V}^{\text{IV}}_{15}\text{E}_6\}$ -type structures (see also 3.2.5), the magnetic structure of the GePOV building block can be described as being composed of a geometrically frustrated, antiferromagnetically coupled equilateral  $\{\text{V}_3\}$  triangle that is sandwiched between the two  $\{\text{V}_6\}$  hexagons characterised by strong antiferromagnetic nearest-neighbor coupling.

### 2.3.3 Discrete GePOV with alkoxo ligands.

Wang and colleagues synthesised and characterised the first polyoxoalkoxovanadium germanate (hereafter referred to as *alkoxoGePOV*). The compound  $(\text{NH}_4)_2[\text{H}_2\text{V}_9\text{Ge}_6\text{O}_{26}(\text{L})_6]\cdot 0.65\text{H}_2\text{O}$  ( $\text{H}_2\text{L} = \text{HOCH}_2\text{CH}_2\text{OH}$ , ethylene glycol) was obtained from a solvothermal reaction<sup>103</sup> where ethylene glycol functioned as a reducing agent for  $\text{NH}_4\text{VO}_3$  that was used as the vanadium source (Table 2). The “fully-reduced”  $[\text{H}_2\text{V}^{\text{IV}}_9\text{Ge}_6\text{O}_{26}(\text{L})_6]^{2-}$  species shows the cage-like structure consisting of six edge- and corner-sharing  $\{\text{VO}_6\}$  octahedra, three edge-sharing  $\{\text{VO}_5\}$  square pyramids, and six corner-sharing  $\{\text{GeO}_4\}$  tetrahedra (Figure 8d). The six ethylene glycol oxygen-donor groups act as bridging alkoxide ligands. This *alkoxoGePOV* features the spherical  $\{\text{V}_9\text{Ge}_6\text{O}_{38}\}$  shell with approximate  $D_{3h}$  symmetry and experiences non-bonding V $\cdots$ V distances of ca. 3.07 Å. EPR studies performed on  $(\text{NH}_4)_2[\text{H}_2\text{V}_9\text{Ge}_6\text{O}_{26}(\text{L})_6]\cdot 0.65\text{H}_2\text{O}$  at room temperature revealed the presence of a partial delocalisation of nine unpaired  $3d^1$  ( $\text{V}^{\text{IV}}$ ) electrons in the *alkoxoGePOV* building block.

### 2.3.4 Discrete GePOVs with two-electron reduced structures.

**GePOV with a  $\{\text{GeO}_6\}$  group.** A mixed-valent  $[\text{V}^{\text{V}}_{12}\text{V}^{\text{IV}}_2\text{GeO}_{40}]^{8-}$  polyoxoanion with an octahedrally coordinated  $\text{Ge}^{\text{IV}}$  heteroatom occupying a central geometrical position within the GePOV structure was isolated as the compound  $\text{K}_2\text{Na}_6[\text{V}_{14}\text{GeO}_{40}]\cdot 10\text{H}_2\text{O}$ .<sup>104</sup> The compound was obtained by reaction of  $\text{GeBr}_2$  and  $\text{NaVO}_3$  in aqueous acidic solution where  $\text{GeBr}_2$  acted as a reducing agent for the  $\text{V}^{\text{V}}$  source (Table 2). This  $D_{4h}$ -symmetric GePOV consists of a central  $\{\text{Ge}^{\text{IV}}\text{O}_6\}$  octahedron and fourteen  $\{\text{VO}_6\}$  octahedra, all of which are edge-shared (Figure 9). Interestingly, this polyoxoanion is the structural analogue to the  $[\text{V}^{\text{IV}}_2\text{V}^{\text{V}}_{12}\text{Al}^{\text{III}}\text{O}_{40}]^{9-}$ <sup>105</sup> and  $[\text{V}^{\text{IV}}_2\text{V}^{\text{V}}_{12}\text{As}^{\text{V}}\text{O}_{40}]^{7-}$ <sup>106</sup> polyoxoanions; the Al-containing *heteroPOV*

is found in the mineral sherwoodite,  $\text{Ca}_{4.5}[\text{V}_{14}\text{AlO}_{40}]$ . It is worth mentioning that the  $[\text{V}^{\text{IV}}_2\text{V}^{\text{V}}_{12}\text{GeO}_{40}]^{8-}$  polyoxoanion extends the family of *heteroPOVs* where the main-group heteroatoms ( $\text{E} = \text{Al}^{\text{III}}, \text{Ge}^{\text{IV}}, \text{As}^{\text{V}}$ ) reside *within* the  $\{\text{V}_{14}\text{O}_{40}\}$  cores. The dicapped cuboctahedral topology was ascribed to the  $\{\text{V}^{\text{IV}}_2\text{V}^{\text{V}}_{12}\text{EO}_{40}\}$  building blocks. Magnetic studies of  $\text{K}_2\text{Na}_6[\text{V}_{14}\text{GeO}_{40}]\cdot 10\text{H}_2\text{O}$  showed that two apical spin-1/2  $\text{V}^{\text{IV}}$  ions, which are separated from each other by 8.52 Å via one O–Ge–O bond, are weakly antiferromagnetically coupled. X-band and Q-band EPR measurements indicated very weak spin-spin exchange coupling between these  $\text{V}^{\text{IV}}$  ions. The magnetic properties of the mixed-valent  $[\text{V}_{14}\text{GeO}_{40}]^{8-}$  were theoretically studied by Suaud, Coronado and coworkers on the basis of model Hamiltonian calculations and wave function theory as well as an electric field approach.<sup>107</sup> In particular, it was shown that an external electric field can induce a reversible transition from a paramagnetic (triplet) to an antiferromagnetic (singlet) ground state configuration of  $[\text{V}_{14}\text{GeO}_{40}]^{8-}$ , meaning that this polyoxoanion can in principle act as a molecular switch. For a discussion about the relevance of  $[\text{V}_{14}\text{GeO}_{40}]^{8-}$  to the field of molecular spintronics, see the review by Coronado and coworkers.<sup>75</sup> Moreover, the  $[\text{V}^{\text{IV}}_2\text{V}^{\text{V}}_{12}\text{GeO}_{40}]^{8-}$  polyoxoanion was reported to be a two-electron catalyst for the oxidation of the coenzyme NADH at pH = 8. Note that POMs usually act as one-electron catalysts.<sup>108</sup>

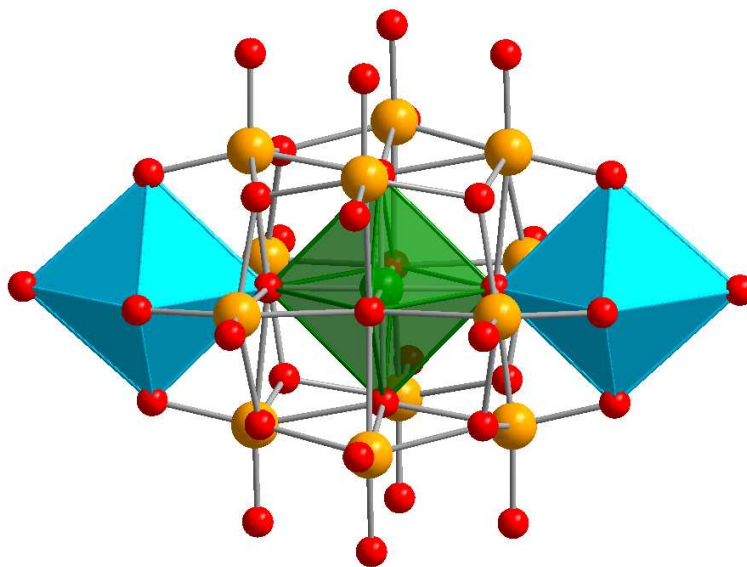


**Figure 9.** Structure of the mixed-valent  $[\text{V}^{\text{IV}}_2\text{V}^{\text{V}}_{12}\text{GeO}_{40}]^{8-}$  polyoxoanion, as present in  $\text{K}_2\text{Na}_6[\text{V}_{14}\text{GeO}_{40}]\cdot 10\text{H}_2\text{O}$ . Colour code: O, red; Ge, green;  $\text{V}^{\text{IV}}\text{O}_x$ , sky-blue polyhedra;  $\text{V}^{\text{V}}$ , light orange.

**Neutral GePOV.** Another two-electron reduced GePOV was reported by Bian, Dai and colleagues.<sup>109</sup> The mixed-valent compound  $[\text{V}^{\text{IV}}_2\text{V}^{\text{V}}_4\text{Ge}_5\text{O}_{21}(\text{heda})_6]\cdot 3\text{H}_2\text{O}$ , in which the deprotonated amine ligands [ $\text{Hheda} = N$ -(2-hydroxyethyl)ethylenediamine] coordinate covalently to the GePOV shell in three different coordination modes (monodentate and

chelating for V centres, and multi-chelating for Ge centres), was obtained by solvothermal synthesis using Hheda as a reducing agent for  $V^V$  (Table 2). The pale purple colour of this low-nuclearity compound was shown to be due to the absorption bands at 2.18 eV (568 nm) and 1.46 eV (856 nm) assigned to d–d transitions of the vanadium ions in quasi-octahedral coordination. The central fragment of  $[V_6Ge_5O_{21}(heda)_6] \cdot 3H_2O$  is a  $C_2$  symmetrical GePOV, which is not structurally related to the  $\{V_{18}O_{42}\}$  archetype like the above-mentioned “fully-reduced” *alkoxo*GePOV  $[H_2V^{IV}_9Ge_6O_{26}(L)_6]^{2-}$ <sup>103</sup> and the mixed-valent  $[V^{V}_{12}V^{IV}_2GeO_{40}]^{8-}$  polyoxoanion.<sup>104</sup> The structure of the neutral  $[V_6Ge_5O_{21}(heda)_6]$  compound is composed of two  $\{VO_5\}$  square pyramids, two  $\{VO_6\}$  octahedra and two  $\{VO_5N\}$  octahedra and involves three tetrahedral  $\{GeO_4\}$  and two octahedral  $\{GeO_4N_2\}$  moieties. According to the optical diffuse reflectance spectrum,  $[V_6Ge_5O_{21}(heda)_6] \cdot 3H_2O$  possesses an energy gap of 2.88 eV.

### 2.3.5 TMC-supported GePOVs.

**Zinc- and Cadmium-GePOV hybrids.** Yang and coworkers succeeded in the hydrothermal synthesis of a series of the inorganic-organic hybrid materials  $[Cd(en)_2]_2[Cd_2(en)_2V_{12}O_{40}(GeOH)_8(H_2O)] \cdot 6H_2O$  (*en* = ethylenediamine =  $C_2H_8N_2$ ),  $[Zn_2(enMe)_3][Zn(enMe)_2][V_{15}Ge_6O_{48}(H_2O)][Zn(enMe)_2(H_2O)]_2 \cdot 3H_2O$  (*enMe* = 1,2-diaminopropane), and  $[Cd_3(\mu-dien)_2(Hdien)_2(H_2O)_2][V_{16}Ge_4O_{42}(OH)_4(H_2O)] \cdot 2H_2O$  (Table 2).<sup>110</sup> The adjustment of the pH value to the alkaline media (pH = 8.8–12.5) was crucial for isolation of these products. Their crystal structures show the “fully-reduced” polyoxoanions  $[Cd_2(en)_2V^{IV}_{12}O_{40}(GeOH)_8(H_2O)]^{4-}$  (Figure 10),  $[H_2O@V^{IV}_{15}Ge_6O_{48}]^{12-}$  and  $[H_2O@V^{IV}_{16}Ge_4O_{42}(OH)_4]^{8-}$  (Figure 8a) which are interconnected by transition metal cations  $[Cd(en)_2]^{2+}$ ,  $[Zn(enMe)]^{2+}/[Zn_2(enMe)_3]^{4+}$  and  $[Cd_3(\mu-dien)_2(Hdien)_2(H_2O)_2]^{8+}$ , respectively. These bind to the GePOV building blocks through the O atoms of  $\{VO_5\}$  square pyramids or the apical O atoms of  $\{GeO_4\}$  tetrahedra, thus forming Cd–O<sub>term</sub>–V and Zn–O<sub>term</sub>–Ge connectivities. Interestingly, the  $[Cd_2(en)_2V^{IV}_{12}O_{40}(GeOH)_8]^{4-}$  polyoxoanion illustrated in Figure 10 incorporates two  $[Cd(en)]^{2+}$  units in the dilacunary-type  $\alpha$ - $[V^{IV}_{12}O_{40}(GeOH)_8]^{8-}$  backbones. The 1D sinusoidal chains established for  $[Cd(en)_2]_2[Cd_2(en)_2V_{12}O_{40}(GeOH)_8(H_2O)] \cdot 6H_2O$  with  $d_{V \dots V} = 2.86 - 3.03$  Å are additionally arranged through N–H⋯O and O–H⋯O hydrogen bonds to afford a 3D supramolecular framework with pseudocircular channels. The interchain distance was found to be ca. 10.65 Å. The  $\{V_{15}\}$ - and  $\{V_{16}\}$ -nuclearity GePOVs are the representatives of the class of polynuclear molecular mixed-metal oxides with the general formula  $[V_{18-z}Ge_{2z}O_{42}(O,OH)_{2z}]$  ( $z = 2, 3$ ) and show interesting structural relationships to other reported GePOVs and SiPOVs. Whereas  $[V^{IV}_{15}Ge_6O_{48}]^{12-}$  and  $[V^{IV}_{15}Si_6O_{42}(OH)_6]^{6-}$  (Figure 6c) are isostructural

analogues, the polyoxoanions  $[V^{IV}_{16}Ge_4O_{42}(OH)_4]^{8-}$  (Figure 8a) and  $[V^{IV}_{16}Si_4O_{46}]^{12-}$  (Figure 6a) are conformational isomers differing by the geometrical positions of the handle-like  $\{E_2O_7\}$  groups in the POV structure. While the  $[Cd_2(en)_2V^{IV}_{12}O_{40}(GeOH)_8(H_2O)]^{4-}$  and  $[V^{IV}_{15}Ge_6O_{48}]^{12-}$  polyoxoanions exhibit strong antiferromagnetic coupling, the magnetic behaviour of the  $[V^{IV}_{16}Ge_4O_{42}(OH)_4]^{8-}$  polyoxoanion was reported to exhibit intramolecular ferrimagnetic coupling, which is rare for such POMs.<sup>111</sup>

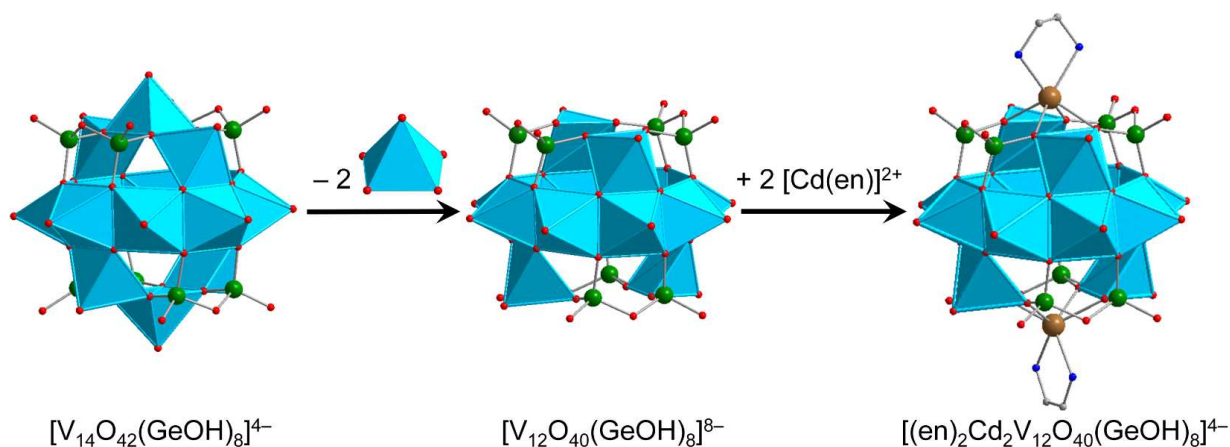


**Figure 10.** Schematic design of the TMC-supported, “fully-reduced” hybrid polyoxoanion  $[Cd_2(en)_2V^{IV}_{12}O_{40}(GeOH)_8]^{4-}$  (right). This tetraanion is formed when two  $\{VO\}^{2+}$  caps situated between the  $\{Ge_2O_7\}$  groups in  $\alpha$ - $[V^{IV}_{14}O_{42}(GeOH)_8]^{4-}$  (left) are replaced with two  $[Cd(en)]^{2+}$  fragments. Encapsulated water molecule and hydrogen atoms are not shown. Colour code: Ge, green; N, blue; O, red;  $V^{IV}O_x$ , sky-blue polyhedra; Cd, brown.

Tetra-Cd<sup>II</sup>-substituted GePOVs were also reported. Two isomorphous, mixed-valent compounds with the general formula  $\{[CdL]_4V_{10}Ge_8O_{46}(H_2O)[V(H_2O)_2]_4(GeO_2)_4\} \cdot 8H_2O$  (L = en, enMe) were synthesised under hydrothermal conditions using the weak acids  $H_3BO_3$  or  $H_2C_2O_4 \cdot 2H_2O$  and the alkaline media at pH = 9.7–10 (Table 2).<sup>112</sup> Their crystal structures exhibit 3D 10-connected, inorganic–organic frameworks (point-symbol of  $3^{12} \cdot 4^{28} \cdot 5^5$  for the *bct* topology) which are constructed from the  $D_{4h}$ -symmetric, “fully-reduced”  $\{[CdR]_4V^{IV}_{10}Ge_8O_{46}(H_2O)\}^{12-}$  hybrid polyoxoanions covalently connected to each other via the planar, “highly-reduced”  $[V^{III}_4O_2(H_2O)_8]^{8+}$  units ( $d_{V \dots V} = 2.47 \text{ \AA}$ ) and the *bridging*  $\{GeO_4\}$  tetrahedra (an unusual situation in POM chemistry, however observed for  $\{SiO_4\}$  units in  $Cs_{10.5}[(V_{16}O_{40})(V_{1.5}Si_{4.5}O_{10})] \cdot 3.5H_2O$ <sup>95</sup>). The  $Cd^{2+}$  ions are incorporated into the backbones of the tetralacunary  $\beta$ -isomeric GePOV building block composed of ten  $\{VO_5\}$  square pyramids and thus display trigonal prismatic geometries ( $CdO_4N_2$ ), similarly to the “fully-reduced”  $[Cd_2(en)_2V^{IV}_{12}O_{40}(GeOH)_8]^{4-}$  hybrid polyoxoanion (Figure 10). An attempt to replace these  $Cd^{2+}$  ions coordinated in a circular  $\{[CdR]_4Ge_8O_{28}\}^{16-}$  constituent of the



dodecaanion by  $\text{Mn}^{2+}$ ,  $\text{Fe}^{2+}$ ,  $\text{Co}^{2+}$ ,  $\text{Ni}^{2+}$  or  $\text{Zn}^{2+}$  under applied reaction conditions (Table 2) has failed. This type of  $\text{Cd}^{\text{II}}$ -substituted GePOVs exhibit antiferromagnetic properties.

**Cobalt-GePOV hybrids.** Further two  $\{\text{V}_{16}\text{Ge}_4\}$ -type polyoxoanions now supported by bridging  $\text{Co}^{\text{II}}$  complexes were described by Xu, Hu and colleagues.<sup>113</sup> The compounds  $[\text{Co}(\text{enMe})_2]_3[\text{Co}_2(\text{enMe})_4][\text{V}_{16}\text{Ge}_4\text{O}_{44}(\text{OH})_2(\text{H}_2\text{O})] \cdot 5\text{H}_2\text{O}$  and  $[\text{Co}_2(\text{en})_3][\text{Co}(\text{en})_2]_2[\text{Co}(\text{en})_2(\text{H}_2\text{O})][\text{V}_{16}\text{Ge}_4\text{O}_{44}(\text{OH})_2(\text{H}_2\text{O})] \cdot 10.5\text{H}_2\text{O}$  with extended 3D frameworks in their crystal structures were obtained hydrothermally in alkaline solutions at  $\text{pH} = 10.2\text{--}10.8$  (Table 2). The structures of these compounds consist of the “fully-reduced”  $[\text{H}_2\text{O}@V^{\text{IV}}_{16}\text{Ge}_4\text{O}_{44}(\text{OH})_2]^{10-}$  anions charge-balanced by  $\text{Co}^{2+}$  centred amine complexes and exhibit different structural topologies. Whereas  $[\text{Co}(\text{enMe})_2]_3[\text{Co}_2(\text{enMe})_4][\text{V}_{16}\text{Ge}_4\text{O}_{44}(\text{OH})_2(\text{H}_2\text{O})] \cdot 5\text{H}_2\text{O}$  adopts a NaCl-type network composed of different TMC linkers and  $[\text{H}_2\text{O}@V^{\text{IV}}_{16}\text{Ge}_4\text{O}_{44}(\text{OH})_2]^{10-}$  polyoxoanions as 6-connected nodes,  $[\text{Co}_2(\text{en})_3][\text{Co}(\text{en})_2]_2[\text{Co}(\text{en})_2(\text{H}_2\text{O})][\text{V}_{16}\text{Ge}_4\text{O}_{44}(\text{OH})_2(\text{H}_2\text{O})] \cdot 10.5\text{H}_2\text{O}$  is characterised by a (4,6)-connected network [Schläfli symbol  $(4^6 \cdot 6^7 \cdot 8^2)_2(4^2 \cdot 6^4)$ ], which was previously not known for *hetero*POVs. Two types of relatively short interatomic distances  $d_{\text{V}\dots\text{V}} = 2.80\text{--}3.07\text{ \AA}$  and  $d_{\text{Co}\dots\text{V}} = 3.38\text{--}3.60\text{ \AA}$  were observed. According to the variable temperature susceptibility measurements, these two compounds feature ferrimagnetic characteristics.

**Manganese- and Nickel-GePOV hybrids.** The solvothermally prepared  $\{[\text{Mn}(\text{tren})(\text{H}_2\text{tren})]\{[\text{Mn}(\text{tren})]_4\text{V}_{15}\text{Ge}_6\text{O}_{48}(\text{H}_2\text{O})_{0.5}\} \cdot \text{tren} \cdot 2\text{H}_2\text{O}$  and  $\{[\text{Ni}(\text{tren})]_4(\text{H}_2\text{tren})_2\text{V}_{15}\text{Ge}_6\text{O}_{48}(\text{H}_2\text{O})\} \cdot 2\text{H}_2\text{O}$  compounds are characterised by the  $\{\text{V}_{15}\text{Ge}_6\}$ -type polyoxoanions which could be expanded into the high-nuclearity GePOV networks.<sup>114</sup> The structural analysis of these charge-neutral helical 1D strands and 2D layers revealed different coordination environments of unique, *in situ*-formed  $\text{Mn}^{\text{II}}$  and  $\text{Ni}^{\text{II}}$  complexes as well as different interconnection modes of the spherical, “fully-reduced”  $[\text{V}^{\text{IV}}_{15}\text{Ge}_6\text{O}_{48}]^{12-}$  polyoxoanions with encapsulated water guest molecules. Interestingly, the reaction conditions were very similar in each case except the nature and amount of transition metal starting materials (Table 2). The central  $\{\text{V}_{15}\text{Ge}_6\text{O}_{48}(\text{H}_2\text{O})_{0.5}\}$  structural motif of  $\{[\text{Mn}(\text{tren})(\text{H}_2\text{tren})]\{[\text{Mn}(\text{tren})]_4\text{V}_{15}\text{Ge}_6\text{O}_{48}(\text{H}_2\text{O})_{0.5}\} \cdot \text{tren} \cdot 2\text{H}_2\text{O}$ , which is stable up to  $350\text{ }^\circ\text{C}$ , is coordinated by five crystallographically independent  $\text{Mn}^{\text{II}}$  complexes via  $\text{Mn}\text{--O}(\text{--V}/\text{Ge})$  bonds. The compound exhibits a three layer solid-state structure, which is composed of the following subfragments: (i) six corner- and edge-sharing square pyramidal  $\{\text{VO}_5\}$  units and a  $[\text{MnO}(\text{H}_2\text{tren})(\text{tren})]^{2+}$  complex; (ii) a  $\{\text{V}_3\text{Ge}_6\text{O}_{28}\}$  ring,  $[\text{Mn}(\text{tren})]^{2+}$  and  $[\text{Mn}_2\text{O}_2(\text{tren})_2]^{4+}$  complexes; (iii) six corner- and edge-sharing  $\{\text{VO}_5\}$  square pyramids. The crystal structure of this GePOV-based inorganic-organic hybrid displays  $[\text{Mn}(\text{tren})]^{2+}$  and  $[\text{Mn}(\text{tren})(\text{H}_2\text{tren})]^{4+}$

moieties and a rare dinuclear  $[\text{Mn}_2\text{O}_2(\text{tren})_2]^{4+}$  fragment that bridges two terminal O atoms of the handle-like  $\{\text{Ge}_2\text{O}_7\}$  groups from the adjacent GePOVs. In contrast to  $[\text{Mn}_2\text{O}_2(\text{tren})_2]^{4+}$ , the  $[\text{Mn}(\text{tren})(\text{H}_2\text{tren})]^{4+}$  complex is bound to the surface of the GePOV shell via a terminal O atom of a pyramidal  $\{\text{VO}_5\}$  unit. The crystal structure of  $[\{\text{Ni}(\text{tren})\}_4(\text{H}_2\text{tren})_2\text{V}_{15}\text{Ge}_6\text{O}_{48}(\text{H}_2\text{O})] \cdot 2\text{H}_2\text{O}$  comprises binuclear  $[\{\text{Ni}(\text{tren})\}(\text{H}_2\text{tren})\{\text{Ni}(\text{tren})\}]^{6+}$  complexes, which coordinate only to the  $\{\text{VO}_5\}$  square pyramids of the polyoxoanion and bridge the neighbouring  $\{\text{V}_{15}\text{Ge}_6\text{O}_{48}\}$  building blocks through V=O–Ni bonds in a manner to allow for the formation of “rhombic windows” in which crystal water molecules reside. The magnetochemical analysis of these two compounds indicated that neither  $\text{Mn}^{\text{II}}$  nor  $\text{Ni}^{\text{II}}$  ions affect the spin structure of the  $[\text{V}_{15}\text{Ge}_6\text{O}_{48}]^{12-}$  polyoxoanion showing the typical “ $\text{V}_6\text{--V}_3\text{--V}_6$ ” layer structure with V...V distances ranging from 2.84 to 3.10 Å. The compounds feature weak antiferromagnetic interactions between the spin-1/2 vanadyl  $\{\text{VO}\}^{2+}$  moieties of the  $\{\text{V}_{15}\text{Ge}_6\text{O}_{48}\}$  building block and the adjoined  $\text{Mn}^{\text{II}}$  or  $\text{Ni}^{\text{II}}$  complexes.

### 2.3.6 Corollary for GePOVs.

“Fully-reduced” *alkoxo*GePOV and TMC-supported GePOVs as well as a number of structurally isolated “fully-reduced” and mixed-valent GePOVs have been published so far. These polyoxoanions include tetrahedral  $\text{Ge}^{\text{IV}}$  heteroatoms, with only one example of octahedral  $\text{Ge}^{\text{IV}}$  inclusion and are characterised by a range of different (approximate) symmetries, e.g.  $D_{3h}$  for  $[\text{H}_2\text{V}^{\text{IV}}_9\text{Ge}_6\text{O}_{26}(\text{L})_6]^{2-}$ ,  $D_{2d}$  for  $[(\text{en})_2\text{Cd}_2\text{V}^{\text{IV}}_{12}\text{O}_{40}(\text{GeOH})_8]^{4-}$  and  $[\text{V}^{\text{IV}}_{14}\text{O}_{44}(\text{GeOH})_8]^{8-}$ ,  $D_{4h}$  for  $[\text{V}^{\text{IV}}_2\text{V}^{\text{V}}_{12}\text{GeO}_{40}]^{8-}$  and  $[\{\text{CdR}\}_4\text{V}^{\text{IV}}_{10}\text{Ge}_8\text{O}_{46}(\text{H}_2\text{O})]^{12-}$ ,  $S_4$  for  $\alpha\text{-}[\text{V}^{\text{IV}}_{14}\text{Ge}_8\text{O}_{50}]^{12-}$  and  $\alpha\text{-}[\text{V}^{\text{IV}}_{14}\text{Ge}_8\text{O}_{42}\text{S}_8]^{12-}$ ,  $D_3$  for  $[\text{V}^{\text{IV}}_{15}\text{Ge}_6\text{O}_{48}]^{12-}$  and  $C_2$  for  $[\text{V}^{\text{IV}}_{16}\text{Ge}_4\text{O}_{42}(\text{OH})_4]^{8-}$ . Similarly to the SiPOV building blocks, the GePOVs were connected by TMC bridging groups to afford network structures of different dimensionality. Unlike the SiPOVs, the GePOVs were found to incorporate secondary TMCs in the backbones of the polyoxoanion shells (Figure 10). Furthermore, unusual handle-like  $\{\text{Ge}_2\text{O}_5\text{S}_2\}$  groups were identified in the  $[\text{V}^{\text{IV}}_{14}\text{Ge}_8\text{O}_{42}\text{S}_8]^{12-}$ <sup>99</sup> (Figure 8c) and  $[\text{H}_2\text{O}@\text{V}^{\text{IV}}_{15}\text{Ge}_6\text{O}_{42}\text{S}_6]^{12-}$ <sup>102</sup> polyoxoanions. The  $\{\text{V}_{16}\text{Ge}_4\}$ -type GePOVs were found to exhibit ferrimagnetic properties.<sup>110,113</sup>

**Table 2.** Selected details of synthesis and characterisation of **GePOV**-based compounds.

Formula	Colour	Characteristics of crystal structure <sup>a</sup>	Reactants	Reaction conditions	Yield	Characterised via	Ref.
<b>V<sub>6</sub></b>							
[V <sub>6</sub> Ge <sub>5</sub> O <sub>21</sub> (heda) <sub>6</sub> ]·3H <sub>2</sub> O	pale purple	layer-like arrangement	NH <sub>4</sub> VO <sub>3</sub> , GeO <sub>2</sub> , Hheda, H <sub>2</sub> O	160 °C, 3 d	65% based on NH <sub>4</sub> VO <sub>3</sub>	EA, IR, EPR, TGA, powder XRD, single-crystal XRD, optical diffuse reflection	109
<b>V<sub>9</sub></b>							
(NH <sub>4</sub> ) <sub>2</sub> [H <sub>2</sub> V <sub>9</sub> Ge <sub>6</sub> O <sub>26</sub> (L) <sub>6</sub> ]·0.65H <sub>2</sub> O	blue		NH <sub>4</sub> VO <sub>3</sub> , GeO <sub>2</sub> , H <sub>2</sub> O, HF, ethylene glycol (H <sub>2</sub> L)	170 °C, 3 d	58% based on Ge	EA, IR, TGA, EPR, single- crystal XRD	103
<b>V<sub>12</sub></b>							
K <sub>5</sub> [H <sub>8</sub> V <sub>12</sub> Ge <sub>8</sub> O <sub>48</sub> (SO <sub>4</sub> )]·10H <sub>2</sub> O	brown	channels	VOSO <sub>4</sub> , GeO <sub>2</sub> , KOH	180 °C, 4 d		IR, single-crystal XRD	100
[Cd(en) <sub>2</sub> ] <sub>2</sub> [Cd <sub>2</sub> (en) <sub>2</sub> V <sub>12</sub> O <sub>40</sub> (GeOH) <sub>8</sub> (H <sub>2</sub> O)]·6H <sub>2</sub> O	black	1D sinusoidal chain	NH <sub>4</sub> VO <sub>3</sub> , GeO <sub>2</sub> , CdCl <sub>2</sub> ·2.5 H <sub>2</sub> O, H <sub>3</sub> BO <sub>3</sub> , en, H <sub>2</sub> O	170 °C, 5 d	80% based on GeO <sub>2</sub>	EA, IR, TGA, EDXS, powder XRD, single-crystal XRD, magnetometry	110
<b>V<sub>14</sub></b>							
K <sub>2</sub> Na <sub>6</sub> [V <sub>14</sub> GeO <sub>40</sub> ]·10H <sub>2</sub> O	blue black		NaVO <sub>3</sub> , GeBr <sub>2</sub> , NaOAc, KCl	50 °C (1 h) → r.t.	64%	EA, IR, UV-vis, <sup>51</sup> V-NMR, XPS, electrochemistry, EPR, single-crystal XRD, magnetometry	104
(H <sub>2</sub> ppz) <sub>4</sub> (Hppz) <sub>4</sub> [V <sub>14</sub> Ge <sub>8</sub> O <sub>50</sub> (H <sub>2</sub> O)]	olive brown		VOSO <sub>4</sub> , GeO <sub>2</sub> , ppz, H <sub>2</sub> O	170 °C, 4 d	45% based on V	EA, IR, TGA, single-crystal XRD	100
(H <sub>2</sub> ppz) <sub>4</sub> (Hppz) <sub>4</sub> [V <sub>14</sub> Ge <sub>8</sub> O <sub>50</sub> (H <sub>2</sub> O)]	black		NH <sub>4</sub> VO <sub>3</sub> , GeO <sub>2</sub> , Cu(NO <sub>3</sub> ) <sub>2</sub> ·3H <sub>2</sub> O, aep, H <sub>2</sub> O	> 150 °C, 9 d		EA, single-crystal XRD	101

$(\text{H}_3\text{aep})_4[\text{V}_{14}\text{Ge}_8\text{O}_{50}] \cdot 2(\text{aep}) \cdot 13\text{H}_2\text{O}$	dark brown	layer-like arrangement	$\text{NH}_4\text{VO}_3$ , $\text{GeO}_2$ , $\text{Cu}(\text{NO}_3)_2 \cdot 3\text{H}_2\text{O}$ , aep, $\text{H}_2\text{O}$	< 150 °C, 9 d	73% based on $\text{GeO}_2$	EA, IR, DTA-TG, single- crystal XRD, magnetometry	101
$(\text{H}_2\text{dab})_4[\text{V}_{14}\text{O}_{44}(\text{GeOH})_8] \cdot 6\text{H}_2\text{O}$	dark green		$\text{V}_2\text{O}_5$ , $\text{GeO}_2$ , dab, $\text{H}_2\text{O}$	170 °C, 5 d	69% based on $\text{GeO}_2$	EA, IR, single-crystal XRD	97
$(\text{H}_3\text{dien})_4[\text{V}_{14}\text{Ge}_8\text{O}_{42}\text{S}_8] \cdot 5\text{H}_2\text{O}$	black	layer-like arrangement	$\text{NH}_4\text{VO}_3$ , Ge, S, dien, $\text{H}_2\text{O}$	160 °C, 7 d	60% based on Ge	EA, DTA-TG-MS, powder X-ray, single-crystal XRD	99
$(\text{H}_3\text{aep})_4[\text{V}_{14}\text{Ge}_8\text{O}_{42}\text{S}_8]$	black	layer-like arrangement	$\text{NH}_4\text{VO}_3$ , Ge, S, aep, $\text{H}_2\text{O}$	170 °C, 7 d	60% based on Ge	EA, DTA-TG-MS, powder X-ray, single-crystal XRD, magnetometry	99
$\{[\text{Cd}(\text{en})_4\text{V}_{10}\text{Ge}_8\text{O}_{46}(\text{H}_2\text{O})][\text{V}(\text{H}_2\text{O})_2]_4(\text{GeO}_2)_4\} \cdot 8\text{H}_2\text{O}$	red	3D framework	$\text{NH}_4\text{VO}_3$ , $\text{GeO}_2$ , $\text{CdCl}_2 \cdot 2.5\text{H}_2\text{O}$ , $\text{H}_3\text{BO}_3$ , en, $\text{H}_2\text{O}$	170 °C, 4 d, pH = 9.7–10	36% based on $\text{GeO}_2$	EA, IR, EDXS, XPS, TGA, powder XRD, single-crystal XRD, magnetometry	112
$\{[\text{Cd}(\text{enMe})_4\text{V}_{10}\text{Ge}_8\text{O}_{46}(\text{H}_2\text{O})][\text{V}(\text{H}_2\text{O})_2]_4(\text{GeO}_2)_4\} \cdot 8\text{H}_2\text{O}$	red	3D framework	$\text{NH}_4\text{VO}_3$ , $\text{GeO}_2$ , $\text{CdCl}_2 \cdot 2.5\text{H}_2\text{O}$ , $\text{H}_2\text{C}_2\text{O}_4 \cdot 2\text{H}_2\text{O}$ , enMe, $\text{H}_2\text{O}$	170 °C, 4 d, pH = 9.7–10	52% based on $\text{GeO}_2$	EA, IR, EDXS, XPS, TGA, powder XRD, single-crystal XRD, magnetometry	112
<b>V<sub>15</sub></b>							
$(\text{H}_2\text{tren})_2(\text{H}_3\text{tren})[\text{V}_{15}\text{Ge}_6\text{O}_{42}(\text{OH})_6(\text{Cl})] \cdot 2\text{H}_2\text{O}$	brown	1D channel	$\text{NH}_4\text{VO}_3$ , $\text{GeO}_2$ , $\text{H}_2\text{O}$ , tren, HCl	170 °C, 5 d	53% based on $\text{NH}_4\text{VO}_3$	EA, IR, TGA, EDXS, XPS, powder X-ray, single-crystal XRD	98
$[\text{Zn}_2(\text{enMe})_3][\text{Zn}(\text{enMe})_2][\text{V}_{15}\text{Ge}_6\text{O}_{48}(\text{H}_2\text{O})][\text{Zn}(\text{enMe})_2(\text{H}_2\text{O})]_2 \cdot 3\text{H}_2\text{O}$	brown	2D layered network	$\text{V}_2\text{O}_5$ , $\text{GeO}_2$ , $\text{ZnSO}_4$ , enMe, $\text{H}_2\text{O}$	170 °C, 3 d	78% based on $\text{GeO}_2$	EA, IR, TGA, EDXS, powder XRD, single-crystal XRD, magnetometry	110
$\{[\text{Ni}(\text{tren})_4(\text{H}_2\text{tren})_2\text{V}_{15}\text{Ge}_6\text{O}_{48}(\text{H}_2\text{O})] \cdot 2\text{H}_2\text{O}$	dark brown	2D layer	$\text{NH}_4\text{VO}_3$ , $\text{GeO}_2$ , $\text{Ni}(\text{NO}_3)_2 \cdot 6\text{H}_2\text{O}$ , tren, $\text{H}_2\text{O}$	130 °C, 7 d	43% based on V	EA, IR, TGA, powder XRD, single-crystal XRD, magnetometry	114

[Co(tren)(H <sub>2</sub> tren)] <sub>2</sub> [[Co(tren)] <sub>2</sub> V <sub>15</sub> Ge <sub>6</sub> O <sub>42</sub> S <sub>6</sub> (H <sub>2</sub> O)] ·9H <sub>2</sub> O	dark red brown	channels	NH <sub>4</sub> VO <sub>3</sub> , Ge, Co, S, tren, H <sub>2</sub> O	140 °C, 7 d	60% based on V	EA, IR, TG-DTA-MS, single-crystal XRD, magnetometry	102
[[Mn(tren)(H <sub>2</sub> tren)] <sub>4</sub> {Mn(tren)} <sub>4</sub> V <sub>15</sub> Ge <sub>6</sub> O <sub>48</sub> (H <sub>2</sub> O) <sub>0.5</sub> ] ·(tren)·2H <sub>2</sub> O	dark brown	helical 1D strand	NH <sub>4</sub> VO <sub>3</sub> , GeO <sub>2</sub> , MnCl <sub>2</sub> ·2H <sub>2</sub> O, tren, H <sub>2</sub> O	130 °C, 7 d	41% based on V	EA, IR, TGA, powder XRD, single-crystal XRD, magnetometry	114
<b>V<sub>16</sub></b> Cs <sub>8</sub> [V <sub>16</sub> Ge <sub>4</sub> O <sub>42</sub> (OH) <sub>4</sub> ]·4.7H <sub>2</sub> O	brown	layer-like arrangement	VO <sub>2</sub> , GeO <sub>2</sub> , H <sub>2</sub> O, CsOH	170 °C, 3 d	30% based on V	IR, EMP, TGA, single- crystal XRD	100
[Cd <sub>3</sub> (dien) <sub>2</sub> (Hdien) <sub>2</sub> (H <sub>2</sub> O) <sub>2</sub> ][V <sub>16</sub> Ge <sub>4</sub> O <sub>42</sub> (OH) <sub>4</sub> (H <sub>2</sub> O)] ·2H <sub>2</sub> O	black	3D open framework	V <sub>2</sub> O <sub>5</sub> , GeO <sub>2</sub> , CdCl <sub>2</sub> ·2.5 H <sub>2</sub> O, dien, ethylene glycol, H <sub>2</sub> O	170 °C, 3 d	90% based on GeO <sub>2</sub>	EA, IR, TGA, EDXS, powder XRD, single-crystal XRD, magnetometry	110
[Co(enMe) <sub>2</sub> ] <sub>3</sub> [Co <sub>2</sub> (enMe) <sub>4</sub> ][V <sub>16</sub> Ge <sub>4</sub> O <sub>44</sub> (OH) <sub>2</sub> (H <sub>2</sub> O)] ·5H <sub>2</sub> O	brown	3D open framework	V <sub>2</sub> O <sub>5</sub> , GeO <sub>2</sub> , Co(OAc) <sub>2</sub> ·4H <sub>2</sub> O, H <sub>2</sub> O, enMe	170 °C, 5 d	86% based on V	EA, IR, XPS, TGA, powder XRD, single-crystal XRD, magnetometry	113
[Co <sub>2</sub> (en) <sub>3</sub> ][Co(en) <sub>2</sub> ] <sub>2</sub> [Co(en) <sub>2</sub> (H <sub>2</sub> O)][V <sub>16</sub> Ge <sub>4</sub> O <sub>44</sub> (O H) <sub>2</sub> (H <sub>2</sub> O)]·10.5H <sub>2</sub> O	brown	3D open framework	V <sub>2</sub> O <sub>5</sub> , GeO <sub>2</sub> , Co(OAc) <sub>2</sub> ·4H <sub>2</sub> O, H <sub>2</sub> O, en	170 °C, 5 d	63% based on V	EA, IR, XPS, TGA, powder XRD, single-crystal XRD, magnetometry	113

<sup>a</sup> Dimensionality resulting from hydrogen bonding networks is not considered.

### 3. Group 15 (As, Sb) element-functionalised POVs

#### 3.1 Preview.

One of the key differences between the SiPOVs/GePOVs and the polyoxovanadatoarsenates (AsPOVs)/polyoxovanadatoantimonates (SbPOVs) is the absence of the effective electron lone pairs at  $\text{Si}^{\text{IV}} / \text{Ge}^{\text{IV}}$  in the former and their presence at  $\text{As}^{\text{III}} / \text{Sb}^{\text{III}}$  in the latter. Note that these electron lone pairs provide different steric hindrances around the E and terminal oxygen atoms ( $\text{O}_{\text{term}}$ ) in the *hetero*POVs, thus influencing the reactivity of the E sites towards the TMC complexes and organic ligands. In comparison to SiPOVs and GePOVs, the chemistry of Sb- and, especially, As-incorporating POVs is more widely developed and resulted in a variety of discrete and multidimensional structures with interesting chemical and physical properties. The AsPOVs and SbPOVs are frequently prepared under hydrothermal or solvothermal conditions (Tables 3 and 4). The AsPOVs known thus far are characterised by both the low-nuclearity and high-nuclearity assemblies, which are classified as  $V_5$ ,  $V_6$ ,  $V_{10}$ ,  $V_{12}$ ,  $V_{13}$ ,  $V_{14}$ ,  $V_{15}$ ,  $V_{16}$ ,  $V_{20}$  and  $V_{24}$  series. SbPOVs show assemblies with nuclearity  $V_{14}$ ,  $V_{15}$ ,  $V_{16}$  and  $V_{20}$ . Some of their most common skeletons are shown in Figure 11.

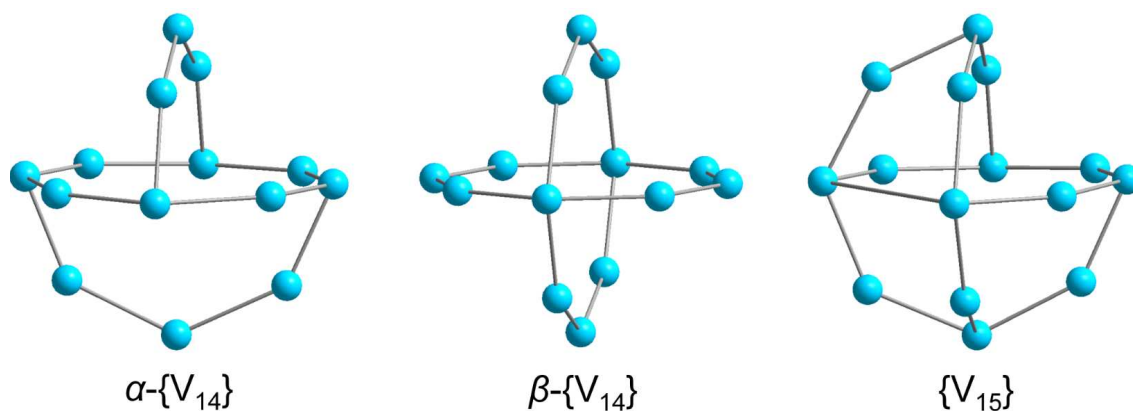


**Figure 11.** Vanadium skeletons found in some “fully-reduced” AsPOVs and SbPOVs.

As vanadium precursors for the synthesis of the AsPOVs (Table 3) and SbPOVs (Table 4),  $\text{V}_2\text{O}_5$  and  $\text{NH}_4\text{VO}_3$  were extensively used, whilst  $\text{NaVO}_3$ ,  $\text{VOSO}_4$  and vanadium halides were employed less frequently. The POV structures decorated with handle-like  $\{\text{E}_2\text{O}_5\}$  groups (E = As, Sb) are typically viewed as being derived from the  $\{\text{V}_{18}\text{O}_{42}\}$  archetype, with only some exceptions which are discussed in section 3. In contrast to the  $\text{Si}^{\text{IV}}$  and  $\text{Ge}^{\text{IV}}$  atoms displaying tetrahedral  $\{\text{EO}_4\}$  geometries in the *hetero*POV structures, the heavier group 15 elements, As and Sb, usually adopt trigonal pyramidal  $\{\text{EO}_3\}$  geometries and show the formal oxidation state +3; however, very rarely tetrahedral  $\{\text{AsO}_4\}^{3-}$  units and arsenic

atoms in the formal oxidation state +5 were also identified. The As–O bonds ( $d_{\text{As-O}} = 1.52 - 2.02 \text{ \AA}$ ) are usually longer than the terminal V=O bonds ( $d_{\text{V=O}} = 1.52 - 1.68 \text{ \AA}$ ), but shorter than the bridging V–O bonds ( $d_{\text{V-O}} = 1.72 - 2.33 \text{ \AA}$ ). The Sb–O bonds ( $d_{\text{Sb-O}} = 1.90 - 2.04 \text{ \AA}$ ) fall in the range of V–O bond lengths, but these are remarkably longer than the V=O bonds.

### 3.2. Polyoxovanadatoarsenates (AsPOVs).

#### 3.2.1 AsPOVs with a low proportion of As<sup>V</sup>.

**AsPOVs with the encapsulated AsO<sub>4</sub> units.** In the early 1990s Müller, Gatteschi and colleagues described the synthesis and magnetic properties of the compound  $\text{K}_6[\text{H}_3\text{KV}_{12}\text{As}_3\text{O}_{39}(\text{AsO}_4)] \cdot 8\text{H}_2\text{O}$  exhibiting electron delocalisation effects.<sup>115</sup> The central constituent of this compound obtained upon reduction of an aqueous solution of potassium metavanadate  $\text{KVO}_3$  is the mixed-valent  $[\text{H}_3\text{KV}^{\text{IV}}_4\text{V}^{\text{V}}_8\text{As}^{\text{V}}_3\text{O}_{39}(\text{As}^{\text{V}}\text{O}_4)]^{6-}$  polyoxoanion with approximate  $C_3$  symmetry (Table 3). The structure of this AsPOV consists of nine  $\{\text{VO}_6\}$  octahedra, three  $\{\text{VO}_4\}$  tetrahedra, and four  $\{\text{As}^{\text{V}}\text{O}_4\}$  tetrahedra. One of these arsenate units  $\{\text{AsO}_4\}^{3-}$  is covalently enclosed within the AsPOV shell (Figure 12). The terminal O atoms of three other, peripheral  $\{\text{As}^{\text{V}}\text{O}_4\}$  groups are protonated. A potassium ion caps the monolacunary  $[\text{H}_3\text{V}_{12}\text{As}_3\text{O}_{39}(\text{AsO}_4)]^{7-}$  polyoxoanion. The electron population in this AsPOV was confirmed by bond valence sum analysis and manometric titration. In the structure,  $\text{K}_6[\text{H}_3\text{KV}_{12}\text{As}_3\text{O}_{39}(\text{AsO}_4)] \cdot 8\text{H}_2\text{O}$  displays zig-zag chains in which the neighbouring  $[\text{H}_3\text{KV}^{\text{IV}}_4\text{V}^{\text{V}}_8\text{As}^{\text{V}}_3\text{O}_{39}(\text{As}^{\text{V}}\text{O}_4)]^{6-}$  polyoxoanions are linked through the  $\text{K} \cdots \text{O}_{\text{term}} - \text{V}$  interactions.

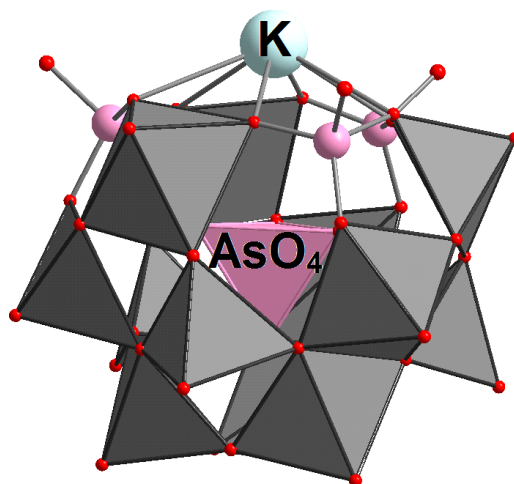


**Figure 12.** Polyhedral representation of the mixed-valent  $[\text{H}_3\text{KV}^{\text{IV}}_4\text{V}^{\text{V}}_8\text{As}^{\text{V}}_3\text{O}_{39}(\text{As}^{\text{V}}\text{O}_4)]^{6-}$  polyoxoanion resembling the  $\epsilon$ -Keggin-type POM archetype. Hydrogen atoms are not shown. Colour code: As<sup>V</sup>, rose;  $\{\text{As}^{\text{V}}\text{O}_4\}$ , rose tetrahedron in the centre; O, red; V<sup>V</sup>/V<sup>IV</sup>O<sub>x</sub>, dark-grey polyhedra; K, turquoise.

Another potassium-containing compound,  $K_3[H_{12}V_{12}O_{36}(AsO)_2(AsO_4)] \cdot 12H_2O$  (Table 3), displays a structure that can be formally viewed as  $\alpha$ -Keggin-type  $\{V^{IV}_6V^V_6O_{36}(As^VO_4)\}$  core with two of its six tetragonal  $\{V_4O_4\}$  faces additionally capped by two  $\{As^VO\}$  groups.<sup>116</sup> As in the case of  $[H_3KV^{IV}_4V^V_8As^V_3O_{39}(As^VO_4)]^{6-}$ , the tetrahedral  $\{AsO_4\}^{3-}$  unit is enclosed within the  $\{V_{12}O_{36}\}$  cage of the mixed-valent  $[H_{12}V^{IV}_6V^V_6O_{36}(AsO)_2(AsO_4)]^{3-}$  polyoxoanion. The twelve O sites of this AsPOV are protonated and three  $K^+$  cations then compensate the  $-3$  net charge of the polyoxoanion. In the crystal structure, each of these  $K^+$  cations is coordinated by four water molecules and is involved in bonding to four adjoined  $[H_{12}V_{12}O_{36}(AsO)_2(AsO_4)]^{3-}$  polyoxoanions through (weak) K–O bonds.

Another type of a bicapped Keggin structure with two capping  $\{V^VO\}$  groups instead of two  $\{As^VO\}$  ones was found for the fully-oxidised  $[H_6V^V_{12}O_{36}(V^VO)_2(AsO_4)]^{3-}$  polyoxoanion isolated as  $(NEt_4)_3[H_6V_{12}AsO_{40}(VO)_2] \cdot 20H_2O$  (Table 3).<sup>117</sup> The  $\alpha$ -Keggin core of this AsPOV consists of twelve  $\{VO_6\}$  octahedra and the covalently enclosed, central  $\{AsO_4\}$  tetrahedron whose O atoms are shared by four  $\{V_3O_{13}\}$  groups of edge-sharing octahedra.

**Neutral AsPOV with the capping  $AsO_4$  units.** The tetrahedral  $\{AsO_4\}^{3-}$  units capping tetragonal vanadium oxide faces were observed in hydrothermally synthesised  $[V^{IV}_8V^V_2As^V_2O_{26}(H_2O)] \cdot 8H_2O$  (Table 3).<sup>118</sup> Its crystal structure shows an extended 3D network in which the neutral, mixed-valent POVs are joined through  $\{AsO_4\}$  bridging groups. Notably, this compound exhibited catalytic activity for phenol hydroxylation, offering high selectivity to hydroquinone.

### 3.2.2 $\{V_{12}As_8\}$ -type polyoxoanions.

**Discrete mixed-valent AsPOVs.** The first polyoxoanions from this class of AsPOVs were presented by Müller and co-workers, in 1991.<sup>119</sup> The formate-enclosing  $\beta$ - $[HCO_2@V^{IV}_6V^V_6As_8O_{40}]^{3-}$  and  $\beta$ - $[HCO_2@V^{IV}_8V^V_4As_8O_{40}]^{5-}$  components of the mixed-valent compounds  $(NH_4)_2(NH_2Me)_2[V_{12}As_8O_{40}(HCO_2)] \cdot 2H_2O$  and  $Na_5[V_{12}As_8O_{40}(HCO_2)] \cdot 18H_2O$  (Table 3), respectively, display different electron populations and different types of spin-spin interactions, albeit their AsPOV shells with encapsulated formate ions are isostructural and possess  $D_{4h}$  symmetries. The strength of the spin-spin coupling in these polyoxoanions composed of four handle-like  $\{As_2O_5\}$  groups and twelve  $\{VO_5\}$  square pyramids was shown to be influenced by the number of  $V^{IV}$  centres: the larger number of these centres, the stronger coupling. Their magnetic properties were additionally studied by Gatteschi and colleagues.<sup>120</sup> Although the  $[HCO_2@V^{IV}_6V^V_6As_8O_{40}]^{3-}$  and  $[HCO_2@V^{IV}_8V^V_4As_8O_{40}]^{5-}$  polyoxoanions are isonuclear, they exhibit dissimilar magnetic properties due to the different AsPOV spin topologies and delocalisation effects of the  $d^1$ - $V^{IV}$  electrons. According



to the magnetic susceptibility data, the AsPOV trianion is characterised by ferromagnetic coupling between delocalised and localised  $V^{IV}$  ions and the AsPOV pentaanion features a singlet ( $S = 0$ ) ground state because of strongly coupled, delocalised  $V^{IV}$  ions. Furthermore, it was stated that field-dependent relaxation effects may influence the EPR spectra (at X-band) of these dodecanuclear species.

About 10 years later, Güdel and colleagues conducted an INS study for three new, but related dodecanuclear  $\beta$ -AsPOVs isolated as  $Na_4[V^{IV}_8V^V_4As_8O_{40}(H_2O)] \cdot 23H_2O$ , the deuterated derivative  $Na_4[V^{IV}_8V^V_4As_8O_{40}(D_2O)] \cdot 16.5D_2O$ , and  $(NH_4)_4[V^{IV}_8V^V_4As_8O_{40}(H_2O)] \cdot H_2O$  (Table 3).<sup>121</sup> The goal of the study was to gain insights into magnetic exchange interactions in these mixed-valent spin structures possessing two outer ( $d_{V \cdots V} = 3.410 - 3.450 \text{ \AA}$ ) and one inner (or central)  $V_4$  squares ( $d_{V \cdots V} = 5.26 - 5.31 \text{ \AA}$ ) bridged by  $[As_2O_5]^{4-}$  groups. The magnetic transitions (up to four) between the  $S = 0$  ground state of the  $\{V^{IV}_8V^V_4As_8\}$  building block and its excited states were identified by INS. By this study, the authors confirmed “*the essential correctness of an earlier model developed on the basis of magnetic and EPR measurements*”<sup>120</sup> that were performed for the aforementioned  $[HCO_2@V^{IV}_8V^V_4As_8O_{40}]^{5-}$  polyoxoanion.

The family of the  $\{V^{IV}_8V^V_4As_8\}$ -type compounds<sup>119-121</sup> was extended by the compound  $(NH_4)_4[V_{12}As_8O_{40}(H_2O)] \cdot 4H_2O$  obtained under solvothermal conditions using the mixtures of ethyl ether/ $H_2O$  or ethanol/ $H_2O$  as reducing agents (Table 3).<sup>122</sup> The building block of this compound is the mixed-valent  $\beta$ - $[H_2O@V^{IV}_8V^V_4As_8O_{40}]^{4-}$  polyoxoanion with the shortest interatomic  $V \cdots V$  distance of  $3.02 \text{ \AA}$  and a diameter of *ca.*  $11 \text{ \AA}$ . In the crystal of  $(NH_4)_4[V_{12}As_8O_{40}(H_2O)] \cdot 4H_2O$ , the AsPOVs are joined by weak intercluster  $As \cdots O$  interactions with the shortest  $As \cdots O$  distance of  $3.05 \text{ \AA}$ . The  $H_2O$  molecules and  $NH_4^+$  counteranions reside in the voids between the polyoxoanions. The strong hydrogen bonds formed between the  $NH_4^+$  ions and the terminal O atoms of the  $[H_2O@V^{IV}_8V^V_4As_8O_{40}]^{4-}$  polyoxoanion result in the formation of a 3D network.  $(NH_4)_4[V_{12}As_8O_{40}(H_2O)] \cdot 4H_2O$  exhibits a distinct solubility in  $H_2O$ , MeOH and DMF and shows an optical energy gap of  $2.80 \text{ eV}$ .

**Zinc-AsPOV hybrids.** A number of hydrothermally synthesised compounds based on the bis-transition metal-substituted AsPOVs of the type  $\{M_2V_{12}As_8O_{40}\}$ , which exhibit antiferromagnetic exchange interactions, were described. These hybrid polyoxoanions are formally derived from the  $\alpha$ - $\{V_{14}As_8O_{42}\}$  polyoxoanion (discussed in section 3.2.4) in which two  $\{VO\}^{2+}$  caps situated between the mutually opposite  $\{As_2O_5\}$  groups are replaced by two  $M^{2+}$  ions. This kind of incorporation of transition metal cations into the backbones of dilacunary  $\alpha$ -heteroPOV shells was also observed in the case of the aforementioned “fully-

reduced"  $[\text{Cd}_2(\text{en})_2\text{V}^{\text{IV}}_{12}\text{O}_{40}(\text{GeOH})_8]^{4-}$  polyoxoanion<sup>110</sup> (Figure 10). One of these  $\text{M}_2$ -decorated AsPOVs was found in  $\{[\text{Zn}(\text{enMe})_2]_2(\text{enMe})_2[\text{Zn}_2\text{V}_{12}\text{As}_8\text{O}_{40}(\text{H}_2\text{O})]\} \cdot 4\text{H}_2\text{O}$ <sup>123</sup> (Table 3). The main structural motif of this hybrid compound is a dilacunary  $\{\text{V}_{12}\text{As}_8\text{O}_{40}\}$  shell functionalised with two  $[\text{Zn}_2(\text{enMe})_3]^{2+}$  complexes via Zn–O bonds (Figure 13a). Each of two  $[\text{Zn}(\text{enMe})_2]^{2+}$  moieties is linked to the  $[\text{H}_2\text{O}@\text{Zn}_2\text{V}^{\text{IV}}_{12}\text{As}_8\text{O}_{40}]^{4-}$  polyoxoanion by the enMe residuals through Zn–N bonds. Strong hydrogen bonds contribute to the formation of a 3D supramolecular array. The crystal structure of another similar compound  $\{[\text{Zn}(\text{dien})]_2(\text{dien})_2[\text{Zn}_2\text{V}_{12}\text{As}_8\text{O}_{40}(0.5\text{H}_2\text{O})]\} \cdot 6\text{H}_2\text{O}$ <sup>124</sup> (Table 3) displays two crystallographically independent  $[0.5\text{H}_2\text{O}@\text{Zn}_2\text{V}^{\text{IV}}_{12}\text{As}_8\text{O}_{40}]^{4-}$  polyoxoanions each of which is decorated with two  $[\text{Zn}(\text{dien})]^{2+}$  complexes through dien connecting groups. The two resulting  $[\text{Zn}(\text{dien})]_2(\text{dien})_2[\text{Zn}_2\text{V}_{12}\text{As}_8\text{O}_{40}(0.5\text{H}_2\text{O})]$  constituents are linked to form a dimer by a weak Zn–O bond.

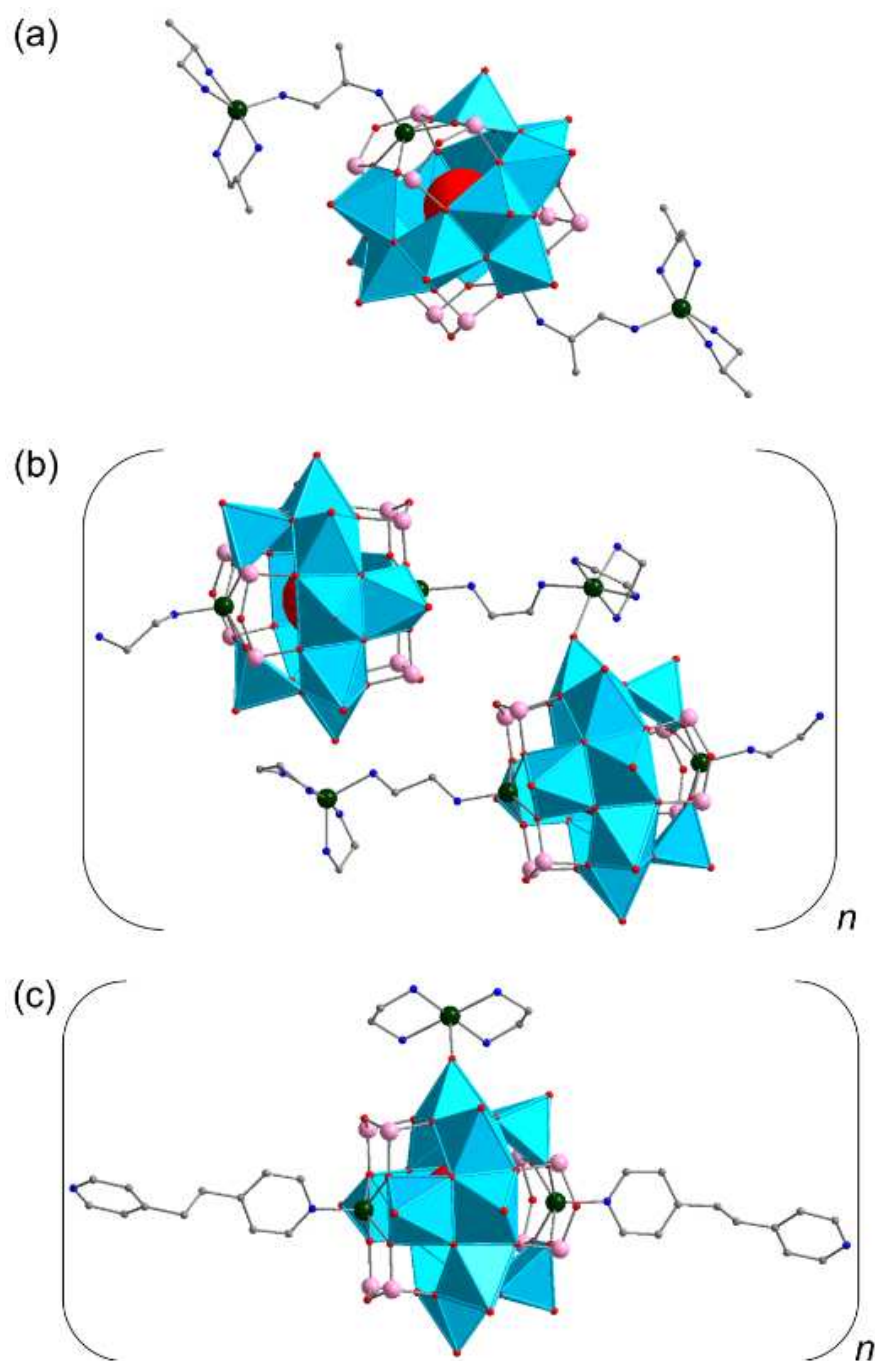


**Figure 13.** (a) Polyhedral representation of  $[\{Zn(enMe)_2(enMe)_2\}Zn_2V_{12}As_8O_{40}(H_2O)]$  containing the “fully-reduced”  $[H_2O@Zn_2V^{IV}_{12}As_8O_{40}]^{4-}$  hybrid polyoxoanion. (b) A segment of the polymeric solid-state structure of  $[\{Zn(en)_3\}_2\{Zn_2V_{12}As_8O_{40}(H_2O)\}] \cdot 4H_2O \cdot 0.25bipy$ . (c) A segment of the polymeric solid-state structure of  $[Zn_2(en)_5][\{Zn(en)_2\}\{(bpe)HZn_2V_{12}As_8O_{40}(H_2O)\}_2] \cdot 7H_2O$ . Hydrogen atoms are omitted for clarity. Colour code: C, grey; N, blue; As, rose; O, red;  $V^{IV}O_x$ , sky-blue polyhedra; Zn, dark green.

The compound  $[Zn(en)_2]_2[Zn_2(bpe)_2V_{12}As_8O_{40}(H_2O)]$  (Table 3) is composed of the  $[(bpe)_2Zn_2V^{IV}_{12}As_8O_{40}(H_2O)]^{4-}$  polyoxoanion [bpe = 1,2-bis(4-pyridyl)ethylene] and two  $[Zn(en)_2]^{2+}$  countercations.<sup>125</sup> This hybrid polyoxoanion based on the  $\alpha$ -AsPOV is

constructed from twelve  $\{VO_5\}$  square pyramids, two square-pyramidal  $\{ZnNO_4\}$  units and four handle-like  $\{As_2O_5\}$  groups. The  $Zn^{2+}$  ions introduced into the backbones of the AsPOV building block are coordinated by the bpe ligands through Zn–N bonds. The two terminal O atoms on the opposite sides of the eight-membered,  $\{VO_5\}$ -composed ring of the  $[(bpe)_2Zn_2V^{IV}_{12}As_8O_{40}(H_2O)]^{4-}$  polyoxoanion are covalently connected to the  $[Zn(en)_2]^{2+}$  complexes through Zn–O bonds. This compound with two structurally exposed pendant pyridyl rings of the bpe ligand could probably be of relevance for surface deposition studies.

The compounds  $[Zn(enMe)_2]_2[(4,4'\text{-bipy})Zn_2V_{12}As_8O_{40}(H_2O)]$ ,  $[Zn(en)_2(H_2O)][Zn(en)_2(4,4'\text{-bipy})Zn_2V_{12}As_8O_{40}(H_2O)] \cdot 3H_2O$ ,  $\{[Zn(en)_3]_2[Zn_2V_{12}As_8O_{40}(H_2O)]\} \cdot 4H_2O \cdot 0.25bipy$  and  $[Zn_2(en)_5]\{[Zn(en)_2]\{(bpe)HZn_2V_{12}As_8O_{40}(H_2O)\}_2\} \cdot 7H_2O$  composed of zinc(II) amine complexes and the “fully-reduced”, bis-zinc-substituted  $\alpha$ -isomeric AsPOVs with compositions  $[H_2O@Zn_2V^{IV}_{12}As_8O_{40}]^{4-}$  and its protonated  $[H_2O@HZn_2V^{IV}_{12}As_8O_{40}]^{3-}$  form were reported.<sup>126</sup> Crystalline samples of these inorganic-organic hybrid materials could only be obtained in alkaline solutions when the pH value was adjusted between 8 and 10, which allowed deprotonation of N-donor ligands and their easier coordination to the  $Zn^{2+}$  ions (Table 3). The different structural features of the organic ligands captured by the secondary  $Zn^{2+}$  ions were shown to have an effect on the formation and construction of the above compounds, thus resulting in the polyoxoanions that are packed in linear or staggered arrangements in the solid state. The crystal structure of  $[Zn(enMe)_2]_2[(4,4'\text{-bipy})Zn_2V_{12}As_8O_{40}(H_2O)]$  exhibits linear chains of the  $[(4,4'\text{-bipy})Zn_2V_{12}As_8O_{40}(H_2O)]^{4-}$  polyoxoanions charge-balanced by discrete  $[Zn(enMe)_2]^{2+}$  complexes occupying the interchain regions. The “fully-reduced”  $[H_2O@Zn_2V^{IV}_{12}As_8O_{40}]^{4-}$  polyoxoanions are linked by bridging 4,4'-bipy ligands through Zn–N bonds. It was also found that  $[Zn(enMe)_2]_2[(4,4'\text{-bipy})Zn_2V_{12}As_8O_{40}(H_2O)]$  is electrocatalytically active in the reduction and oxidation of  $H_2O_2$  and  $NO_2^-$  using bulk-modified carbon paste electrodes. The crystal structure of  $[Zn(en)_2(H_2O)][Zn(en)_2(4,4'\text{-bipy})Zn_2V_{12}As_8O_{40}(H_2O)] \cdot 3H_2O$  displays 1D winding chains of the  $[(4,4'\text{-bipy})Zn_2V_{12}As_8O_{40}(H_2O)]^{4-}$  hybrid clusters functionalised with the  $[Zn(en)_2]^{2+}$  complexes through Zn–O bonds;  $[Zn(en)_2(H_2O)]^{2+}$  complexes act as counterions. Similarly to the previous compound, the 4,4'-bipy ligands bridge the  $\{Zn_2V_{12}As_8O_{40}\}$  building blocks through Zn–N bonds. The  $Zn^{2+}$  cations are incorporated into the dilacunary-type AsPOV shell through Zn–O bonds. The extensive hydrogen bonding in the crystal lattice results in the formation of a 3D supramolecular architecture. The crystal structure of  $\{[Zn(en)_3]_2[Zn_2V_{12}As_8O_{40}(H_2O)]\} \cdot 4H_2O \cdot 0.25bipy$  is described as an eight-shaped chiral helical chain, where the “fully-reduced”  $[H_2O@Zn_2V^{IV}_{12}As_8O_{40}]^{4-}$  hybrid polyoxoanions are covalently bridged by the  $[Zn(en)_3]^{2+}$  complexes through Zn–N and Zn–O bonds, as shown

in Figure 13b. In contrast to the above-mentioned compounds,  $[\text{Zn}_2(\text{en})_5][\{\text{Zn}(\text{en})_2\}\{\text{(bpe)HZn}_2\text{V}_{12}\text{As}_8\text{O}_{40}(\text{H}_2\text{O})\}_2]\cdot 7\text{H}_2\text{O}$  has a 2D layer structure with nanosized inner 1D rectangular cavities of  $33.7 \times 14.7 \text{ \AA}$ . These cavities are occupied by the lattice  $\text{H}_2\text{O}$  molecules and  $[\text{Zn}_2(\text{en})_5]^{4+}$  cations. The connectivity of the “fully-reduced”  $[\text{H}_2\text{O}@\text{HZn}_2\text{V}_{12}^{\text{IV}}\text{As}_8\text{O}_{40}]^{3-}$  building blocks through the  $[\text{Zn}(\text{en})_2]^{2+}$  complexes and the bidentate bpe ligands (Figure 13c), yielding a single-stranded (right- and left-handed) helical chain, resembles that found in the crystal structure of  $[\text{Zn}(\text{en})_2]_2[\text{Zn}_2(\text{bpe})_2\text{V}_{12}\text{As}_8\text{O}_{40}(\text{H}_2\text{O})]$ .<sup>125</sup>

**Cadmium-AsPOV hybrids.**  $\text{Cd}^{2+}$ -en complexes were incorporated into the dilacunary  $\beta$ - $\{\text{V}_{12}\text{As}_8\text{O}_{40}\}$ -type structure through Cd–O bonds to form the “fully-reduced”  $[\text{Cd}_2(\text{en})_2\text{V}_{12}^{\text{IV}}\text{As}_8\text{O}_{40}]^{4-}$  polyoxoanion, which is charge-balanced by two  $[\text{Cd}(\text{en})_2]^{2+}$  complexes.<sup>127</sup> This compound with composition  $[\text{Cd}(\text{en})_2]_2[\text{Cd}_2(\text{en})_2\text{V}_{12}\text{As}_8\text{O}_{40}]$  was prepared under hydrothermal conditions (Table 3) and displays a 1D chain structure where neighbouring  $[\text{Cd}_2(\text{en})_2\text{V}_{12}^{\text{IV}}\text{As}_8\text{O}_{40}]^{4-}$  polyoxoanions are doubly bridged via  $[\text{Cd}(\text{en})_2]^{2+}$  groups. The interface between these hybrid building blocks is characterised by eight-membered rings involving  $\text{Cd}^{2+}$  ions from the TMC linkers and terminal and bridging O atoms from the connected polyoxoanions. Hydrogen bonds extend the 1D chains into a 3D supramolecular network.

Two other compounds,  $[\text{Cd}(\text{enMe})_3]_2[(\text{enMe})_2\text{Cd}_2\text{V}_{12}\text{As}_8\text{O}_{40}(0.5\text{H}_2\text{O})]\cdot 5.5\text{H}_2\text{O}$  and  $[\text{Cd}(\text{enMe})_2]_2[\text{Cd}_2(\text{enMe})_2\text{V}_{12}\text{As}_8\text{O}_{40}(0.5\text{H}_2\text{O})]$ , were found to contain  $\alpha$ - and  $\beta$ -isomeric  $[\text{Cd}_2(\text{enMe})_2\text{V}_{12}^{\text{IV}}\text{As}_8\text{O}_{40}(0.5\text{H}_2\text{O})]^{4-}$  constituents, respectively (Table 3).<sup>128</sup> Whereas the former compound can be viewed as an isolated (0D) inorganic–organic hybrid, the latter compound shows an infinite, 1D linear chain structure due to the  $[\text{Cd}(\text{enMe})_2]^{2+}$  linkages and is furthermore isomorphic with the above-mentioned example  $[\text{Cd}(\text{en})_2]_2[\text{Cd}_2(\text{en})_2\text{V}_{12}\text{As}_8\text{O}_{40}]$ ,<sup>127</sup> with the exception of organic ligands coordinated to the Cd(II) centres and a half  $\text{H}_2\text{O}$  molecule encapsulated by the polyoxoanion shell. In both compounds, the  $[\text{Cd}(\text{enMe})]^{2+}$  complexes are attached to the AsPOV building blocks through Cd–O bonds. According to the diffuse reflectance UV-vis spectra, these compounds are characterized by optical energy gaps of ca. 2 eV.

### 3.2.3 $\{\text{V}_{13}\text{As}_8\}$ -type polyoxoanions.

The structural chemistry of this class of AsPOVs is still underdeveloped. To date, only the results reported by the groups of Yang, Xu and Wang are available. When a  $\{\text{VO}\}^{2+}$  group situated inbetween the  $\{\text{As}_2\text{O}_5\}$  groups in  $\alpha$ - $[\text{V}_{14}\text{As}_8\text{O}_{42}]^{4-}$  (discussed in section 3.2.4) is substituted by a divalent transition metal ion, a polyoxoanion of general composition

$[M^{II}V^{IV}_{13}As_8O_{41}]^{4-}$  results. Thus, the cluster structure of this monosubstituted hybrid polyoxoanion is comparable to that of the aforementioned di-substituted  $[M_2V^{IV}_{12}As_8O_{40}]^{4-}$  polyoxoanion whose two  $\{VO\}^{2+}$  groups were exchanged by two divalent transition metal ions. The monolacunary  $\{V_{13}As_8\}$ -nuclearity polyoxoanion was found to incorporate  $Zn^{2+}$  or  $Cd^{2+}$  ions as well as  $Ni^{2+}$  ion in the way presented above.

**Zinc-AsPOV hybrid with a mixed  $V_{13}/V_{14}$ -structure.** The compound  $[Zn(2,2'$ -bipy) $_3]_4[(ppz)\{\{Zn(tepa)\}_2ZnV_{13}As_8O_{41}(H_2O)\}_2][V_{14}As_8O_{42}(0.5H_2O)]_2 \cdot 4H_2O$  (tepa = tetraethylenepentamine)<sup>124</sup> displays two different types of AsPOV constituents, namely the Zn-monosubstituted  $[H_2O@ZnV^{IV}_{13}As_8O_{41}]^{4-}$  hybrid and the  $[0.5H_2O@V^{IV}_{14}As_8O_{42}]^{4-}$  polyoxoanion. The latter belongs to the class of  $\{V_{14}As_8\}$ -based compounds which are discussed in the next section. The ppz and tepa organic groups in this compound were *in situ*-formed from dien molecules used in the hydrothermal reaction (Table 3) and coordinate to the  $Zn^{2+}$  cations to result in the complexes  $[Zn_2(ppz)]^{4+}$  and  $[Zn(tepa)]^{2+}$ . The  $[Zn_2(ppz)]^{4+}$  unit bridges the two neighbouring  $\alpha$ - $\{V_{13}As_8\}$ -type AsPOVs, each of which is decorated with two  $[Zn(tepa)]^{2+}$  moieties through Zn–O bonds (Figure 14a). The  $Zn^{2+}$  ions of the  $[Zn_2(ppz)]^{4+}$  complex are integrated into the backbones of the  $[\{Zn(tepa)\}_2V^{IV}_{13}As_8O_{41}(H_2O)]^{2-}$  polyoxoanions to form  $[\{Zn(tepa)\}_2ZnV^{IV}_{13}As_8O_{41}(H_2O)]$ , which are thus held together by ppz linkers via Zn–N bonds.

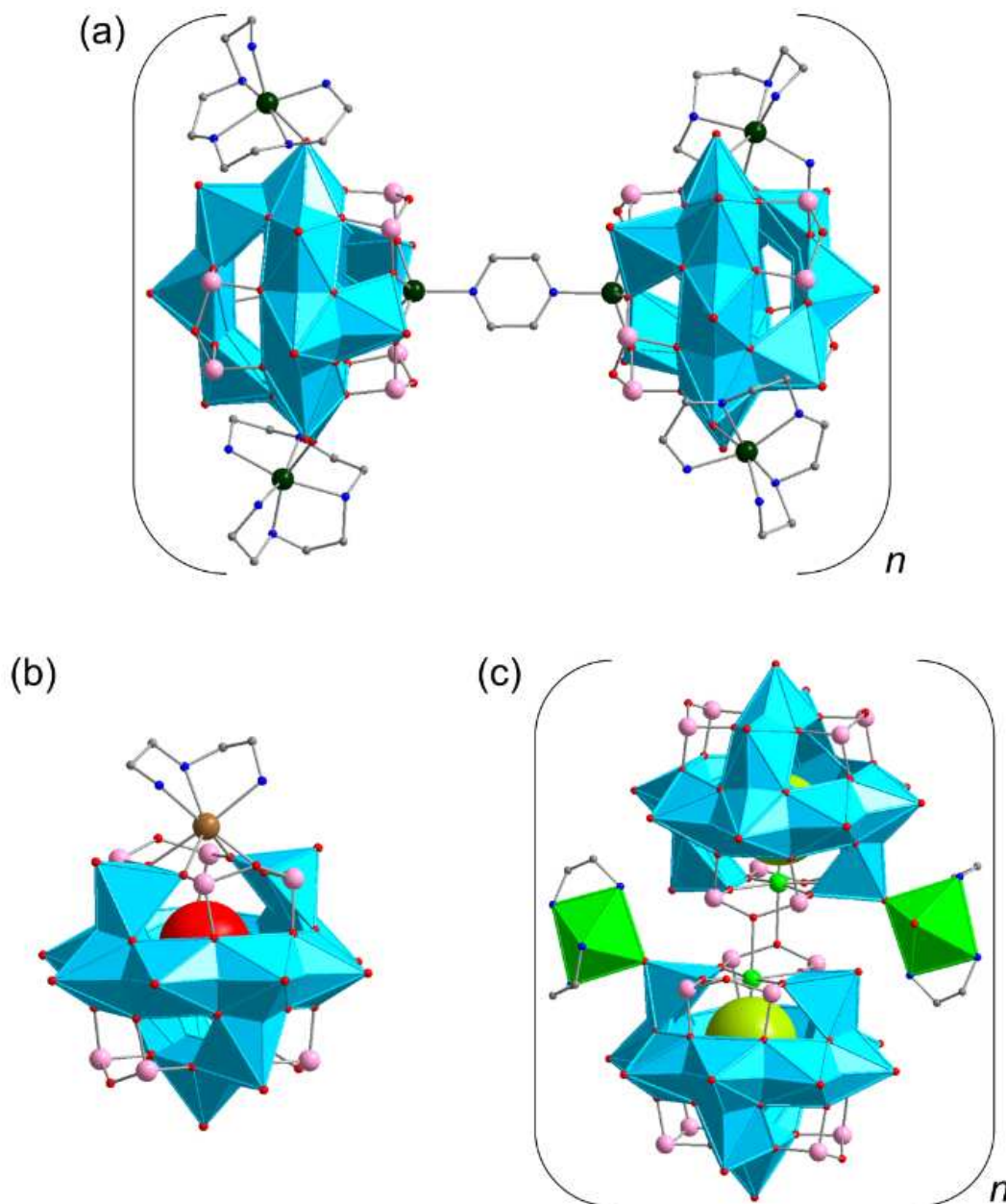


**Figure 14.** (a) The “fully-reduced”  $[\{Zn(tepa)\}_2ZnV^{IV}_{13}As_8O_{41}(H_2O)]$  building blocks connected via ppz ligand. (b) Polyhedral representation of the “fully-reduced”  $[(dien)CdV^{IV}_{13}As_8O_{41}(H_2O)]^{4-}$  hybrid polyoxoanion. (c) Polyhedral representation of the “fully-reduced” AsPOV dimer,  $\{Cl@NiV^{IV}_{13}As_8O_{41}\}_2$ , expanded by two octahedral  $[Ni(en)_2(H_2O)]$  fragments. Hydrogen atoms are omitted for clarity. Colour code: C, grey; N, blue; As, rose; O, red; Cl, lime;  $V^{IV}O_x$ , sky-blue polyhedra; Ni, bright green; Zn, dark green; Cd, brown.

**Cadmium-AsPOV hybrid.** The “fully-reduced”  $[Cd(dien)V^{IV}_{13}As_8O_{41}(H_2O)]^{4-}$  polyoxoanion (Figure 14b) with the seven-coordinate  $Cd^{2+}$  ion was hydrothermally isolated as the compound  $[Cd(dien)_2]_2[Cd(dien)V_{13}As_8O_{41}(H_2O)] \cdot 4H_2O$  (Table 3) showing strong antiferromagnetic interactions between the spin-1/2 vanadyl  $\{VO\}^{2+}$  moieties.<sup>127</sup> The other two hydrothermally prepared compounds  $[Cd(en)_3][Cd(phen)(en)(H_2O)_2][Cd(en)V_{13}As_8O_{41}(H_2O)] \cdot 1.5H_2O$  and

[Cd(phen)<sub>2</sub>(en)]<sub>2</sub>[Cd(phen)V<sub>13</sub>As<sub>8</sub>O<sub>41</sub>(H<sub>2</sub>O)]·21H<sub>2</sub>O·phen (phen = 1,10-phenanthroline) feature the [Cd(en)V<sup>IV</sup><sub>13</sub>As<sub>8</sub>O<sub>41</sub>(H<sub>2</sub>O)]<sup>4-</sup> and [Cd(phen)V<sup>IV</sup><sub>13</sub>As<sub>8</sub>O<sub>41</sub>(H<sub>2</sub>O)]<sup>4-</sup> structures, where the Cd<sup>2+</sup> ions coordinated by en and phen ligands are incorporated into the monolacunary  $\alpha$ -type *heteroPOV* shells (Table 3).<sup>125</sup> In contrast to [Cd(dien)V<sub>13</sub>As<sub>8</sub>O<sub>41</sub>(H<sub>2</sub>O)]<sup>4-</sup>, the antiferromagnetic [Cd(en)V<sup>IV</sup><sub>13</sub>As<sub>8</sub>O<sub>41</sub>(H<sub>2</sub>O)]<sup>4-</sup> and [Cd(phen)V<sup>IV</sup><sub>13</sub>As<sub>8</sub>O<sub>41</sub>(H<sub>2</sub>O)]<sup>4-</sup> hybrid polyoxoanions comprise six-coordinate Cd<sup>2+</sup> ions. In all these Cd-containing compounds, the [Cd(dien)<sub>2</sub>]<sup>2+</sup>, [Cd(en)<sub>3</sub>]<sup>2+</sup>, [Cd(phen)(en)(H<sub>2</sub>O)<sub>2</sub>]<sup>2+</sup>, and [Cd(phen)<sub>2</sub>(en)]<sup>2+</sup> complexes act as counteranions.

**Nickel-AsPOV hybrid.** The “fully-reduced” [NiV<sup>IV</sup><sub>13</sub>As<sub>8</sub>O<sub>41</sub>]<sup>4-</sup> polyoxoanion with the Ni<sup>II</sup>-filled monolacunary POV structure was isolated as the compound {[V<sub>13</sub>As<sub>8</sub>NiClO<sub>41</sub>][Ni(en)<sub>2</sub>(H<sub>2</sub>O)][Ni(en)<sub>2</sub>]}{[Ni(en)<sub>2</sub>(H<sub>2</sub>O)<sub>2</sub>]<sub>0.5</sub>}·4H<sub>2</sub>O under hydrothermal reaction conditions (Table 3).<sup>129</sup> Its crystal structure displays the host-guest [Cl@NiV<sup>IV</sup><sub>13</sub>As<sub>8</sub>O<sub>41</sub>]<sup>5-</sup> building blocks linked to each other through Ni–O–As bonds to form a dimeric assembly (Figure 14c). The latter is further connected to the neighbouring dimer via bridging [Ni(en)<sub>2</sub>]<sup>2+</sup> complexes (corner-sharing Ni–O<sub>term</sub>–V interactions) to result in an infinite 1D chain. The [Cl@NiV<sup>IV</sup><sub>13</sub>As<sub>8</sub>O<sub>41</sub>]<sup>5-</sup> structure can be described as being constituted of thirteen square-pyramidal {VO<sub>5</sub>} moieties, four handle-like {As<sub>2</sub>O<sub>5</sub>} groups, and one square-pyramidal {ClNiO<sub>4</sub>} entity with the strong Ni–Cl bonding interaction. The [Ni(en)<sub>2</sub>(H<sub>2</sub>O)]<sup>2+</sup> and [Ni(en)<sub>2</sub>]<sup>2+</sup> complexes and a half [Ni(en)<sub>2</sub>(H<sub>2</sub>O)<sub>2</sub>]<sup>2+</sup> complex compensate the negative charge of this hybrid polyoxoanion. The compound exhibits antiferromagnetic properties.

### 3.2.4 {V<sub>14</sub>As<sub>8</sub>}-type polyoxoanions.

**Discrete AsPOVs.** This class of AsPOVs offers a large number of discrete polyoxoanions. In 1991, Müller and Döring reported a series of the “fully-reduced”  $\alpha$ -AsPOVs with the general formula [Y@V<sub>18-z</sub>As<sub>2z</sub>O<sub>42</sub>]<sup>m-</sup> where Y = SO<sub>3</sub><sup>2-</sup>, SO<sub>4</sub><sup>2-</sup> or H<sub>2</sub>O and z = 4. These host-guest polyoxoanions were isolated as crystal solvent-free ammonium compounds (NH<sub>4</sub>)<sub>6</sub>[V<sub>14</sub>As<sub>8</sub>O<sub>42</sub>(SO<sub>3</sub>)], (NH<sub>4</sub>)<sub>6</sub>[V<sub>14</sub>As<sub>8</sub>O<sub>42</sub>(SO<sub>4</sub>)] and (NMe<sub>4</sub>)<sub>4</sub>[V<sub>14</sub>As<sub>8</sub>O<sub>42</sub>(H<sub>2</sub>O)].<sup>130</sup> The authors highlighted that the V/As ratio, pH, and concentration of the reducing agents such as hydrazine sulfate (N<sub>2</sub>H<sub>6</sub>SO<sub>4</sub>), hydrazine chloride (N<sub>2</sub>H<sub>5</sub>Cl) and sodium dithionite (Na<sub>2</sub>S<sub>2</sub>O<sub>4</sub>) play an important role in the formation of these {Y@V<sub>14</sub>As<sub>8</sub>O<sub>42</sub>}-based compounds (Table 3) where the inner voids of the POV shells are occupied by statistically disordered small anionic or neutral guest (Y) species. Here, the D<sub>2d</sub>-symmetrical AsPOVs are formally derived from the corresponding [Y@V<sub>18</sub>O<sub>42</sub>]<sup>m-</sup> structures by replacing four {V<sup>IV</sup>O}<sup>2+</sup> vanadyl groups in the latter with four {As<sup>III</sup><sub>2</sub>O}<sup>4+</sup> moieties.



Also in 1991, Huan *et al.* presented a spherical  $[(\text{H}_2\text{O})_{0.5}@\text{V}^{\text{IV}}_{14}\text{As}_8\text{O}_{42}]^{4-}$  polyoxoanion that formed as the compound  $(\text{NMe}_4)_4[\text{V}_{14}\text{As}_8\text{O}_{42}(\text{H}_2\text{O})_{0.5}]$  under hydrothermal conditions (Table 3).<sup>131</sup> This “fully-reduced” AsPOV consists of fourteen condensed  $\{\text{VO}_5\}$  square pyramids and four handle-like  $\{\text{As}_2\text{O}_5\}$  groups and is characterised by a  $\alpha$ - $\{\text{V}_{14}\text{As}_8\text{O}_{42}\}$  shell of rhombicuboctahedral topology (Figure 15a). This cluster shell encapsulates a disordered  $\text{H}_2\text{O}$  guest molecule. The  $\beta$ -isomer (Figure 15b) encapsulating a statistically disordered  $\text{SO}_4^{2-}$  ion was identified in the hydrothermally prepared compound  $[\text{NH}_2(\text{CH}_2)_4\text{NH}_2]_4[\text{V}_{14}\text{As}_8\text{O}_{42}(\text{SO}_4)] \cdot (\text{HSO}_4)_2$  (Table 3).<sup>132</sup> In contrast to the  $\alpha$ -isomer with  $D_{2d}$  symmetry, the “fully-reduced”  $\beta$ - $[\text{SO}_4@\text{V}^{\text{IV}}_{14}\text{As}_8\text{O}_{42}]^{6-}$  polyoxoanion exhibits  $D_{4h}$  symmetry which results from the rotation of the three-membered vanadium oxide arc and two  $\{\text{As}_2\text{O}_5\}$  groups over an eight-membered ring in  $\alpha$ - $[\text{V}^{\text{IV}}_{14}\text{As}_8\text{O}_{42}]^{4-}$  by  $90^\circ$  around the  $S_4$  axes (Figure 15a,b). In the structure crystal the  $(\text{C}_4\text{N}_2\text{H}_{12})^{2+}$  piperazine cations, two  $\text{HSO}_4^-$  anions and terminal O atoms of the  $\beta$ -AsPOV building blocks are involved in strong hydrogen bonding interactions, thus generating a 3D network structure.

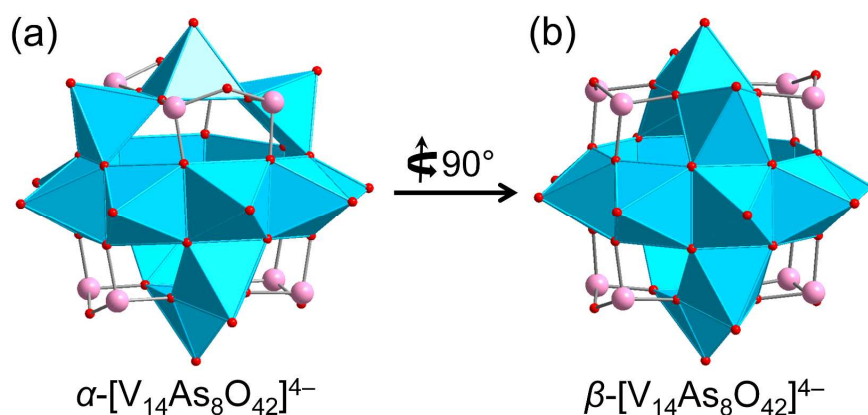


**Figure 15.** Polyhedral representation of the discrete “fully-reduced”  $\alpha$ - $[\text{V}^{\text{IV}}_{14}\text{As}_8\text{O}_{42}]^{4-}$  (a) and  $\beta$ - $[\text{V}^{\text{IV}}_{14}\text{As}_8\text{O}_{42}]^{4-}$  (b) polyoxoanions. Colour code: As, rose; O, red;  $\text{V}^{\text{IV}}\text{O}_x$ , sky-blue polyhedra.

Other polyoxoanions with the same or a similar elemental composition were also reported. The antiferromagnetic compound  $[\text{NH}_2(\text{CH}_2\text{CH}_2)_2\text{NH}_2]_3[\text{V}_{14}\text{As}_8\text{O}_{42}(\text{SO}_4)] \cdot 6.5\text{H}_2\text{O}$  was obtained by the hydrothermal reaction in acidic solution at  $\text{pH} = 3$  (Table 3).<sup>133</sup> Yang and colleagues showed that protonated  $[\text{NH}_2(\text{CH}_2\text{CH}_2)_2\text{NH}_2]^{2+}$  amine molecules not only compensate the negative charge of the “fully-reduced”  $\alpha$ - $[\text{SOV}^{\text{IV}}_{14}\text{As}_8\text{O}_{42}]^{6-}$  polyoxoanion but also assume space-filling and structure-directing roles. The strong hydrogen bonds between the AsPOV building blocks, organic amine molecules, and crystal water molecules result in the formation of a 3D supramolecular array. The “fully-reduced”  $\beta$ - $[\text{SO}_4@\text{V}^{\text{IV}}_{14}\text{As}_8\text{O}_{42}]^{6-}$  isomer was synthesised as the compound  $(\text{NH}_4)_2(\text{NMe}_4)_4[\text{V}_{14}\text{As}_8\text{O}_{42}(\text{SO}_4)]$  under hydrothermal conditions.<sup>134</sup> The hydrothermal

synthesis and characterisation of two other compounds  $(\text{H}_2\text{en})_{3.5}[\text{V}_{14}\text{As}_8\text{O}_{42}(\text{PO}_4)] \cdot 2\text{H}_2\text{O}$ <sup>135</sup> and  $(\text{H}_2\text{enMe})_2[\text{V}_{14}\text{As}_8\text{O}_{42}(\text{H}_2\text{O})] \cdot 3\text{H}_2\text{O}$ <sup>136</sup> based on the “fully-reduced”  $\alpha$ -polyoxoanions with encapsulated  $\text{PO}_4^{3-}$  and  $\text{H}_2\text{O}$  guests, respectively, were described as well (Table 3).

**Discrete AsPOV with rubidium counteractions.** The above series of discrete, host-guest AsPOVs also includes the “fully-reduced”  $[\text{Cl}@\text{V}^{\text{IV}}_{14}\text{As}_8\text{O}_{42}]^{5-}$  polyoxoanion, which was shown to exhibit elongated square gyrobicupola topology that is also observed for  $[\text{V}^{\text{IV}}_{16}\text{Ge}_4\text{O}_{42}(\text{OH})_4]^{8-}$  (Figure 8a). This AsPOV pentaanion is the central component of the hydrothermally prepared compound  $\text{Rb}_5[\text{V}_{14}\text{As}_8\text{O}_{42}(\text{Cl})] \cdot 2\text{H}_2\text{O}$  with a chain-like structure.<sup>116</sup> Interestingly, the  $[\text{Cl}@\text{V}^{\text{IV}}_{14}\text{As}_8\text{O}_{42}]^{5-}$  polyoxoanion could only be isolated in the presence of  $\text{Rb}^+$  cations (Table 3) and not with  $\text{Na}^+$ ,  $\text{K}^+$  or  $\text{Cs}^+$ .

**Transformation of  $\{\text{V}_{14}\text{As}_8\}$  into  $\{\text{V}_6\text{As}_8\}$ -type AsPOV.** It is worth mentioning that, in the general case, the  $[\text{V}^{\text{IV}}_{14}\text{As}_8\text{O}_{42}]^{4-}$  polyoxoanion can be formally converted into the lower-nuclearity  $[\text{V}^{\text{IV}}_6\text{As}_8\text{O}_{26}]^{4-}$  polyoxoanion by removal of the central eight-membered ring composed of edge-sharing  $\{\text{VO}_5\}$  square pyramids.<sup>137</sup> The “fully-reduced”  $[\text{V}^{\text{IV}}_6\text{As}_8\text{O}_{26}]^{4-}$  structure thus consists of four handle-like  $\{\text{As}_2\text{O}_5\}$  groups and six distorted  $\{\text{VO}_5\}$  square pyramidal units with the shortest  $\text{V}^{\text{IV}} \cdots \text{V}^{\text{IV}}$  distance of ca. 4.5 Å. Furthermore, this AsPOV contains more As than V atoms, thus giving a high As/V ratio of 4/3, a very unusual situation in the structural chemistry of *hetero*POVs discussed herein. The  $[\text{V}^{\text{IV}}_6\text{As}_8\text{O}_{26}]^{4-}$  polyoxoanion crystallised under reducing conditions at room temperature as the compound  $(\text{N}_n\text{Bu}_4)_4[\text{V}_6\text{As}_8\text{O}_{26}]$  (Table 3) and shows antiferromagnetic behaviour.

**TMC-AsPOV hybrids without specific cation-anion interactions.** The two antiferromagnetic compounds  $[\text{Zn}(2,2'\text{-bipy})_3]_2[\text{V}_{14}\text{As}_8\text{O}_{42}(\text{H}_2\text{O})] \cdot 4\text{H}_2\text{O}$  and  $[\text{Zn}(2,2'\text{-bipy})(\text{dien})]_2[\text{V}_{14}\text{As}_8\text{O}_{42}(\text{H}_2\text{O})] \cdot 2\text{H}_2\text{O}$  were prepared hydrothermally at pH = 7 using organic amines as reducing agents for the starting  $\text{V}_2\text{O}_5$  material (Table 3).<sup>138</sup> These compounds are composed of the “fully-reduced”  $\alpha$ - $[\text{H}_2\text{O}@\text{V}^{\text{IV}}_{14}\text{As}_8\text{O}_{42}]^{4-}$  polyoxoanions with approximate  $D_{2d}$  symmetries and  $[\text{Zn}(2,2'\text{-bipy})_3]^{2+}$  and  $[\text{Zn}(2,2'\text{-bipy})(\text{dien})]^{2+}$  counteractions, respectively. In contrast to  $[\text{Zn}(2,2'\text{-bipy})_3]^{2+}$ , the  $[\text{Zn}(2,2'\text{-bipy})(\text{dien})]^{2+}$  complexes are involved in extensive hydrogen bonding interactions with the oxygen atoms of the AsPOVs, thus yielding a densely packed 3D network in the crystal lattice of the  $[\text{Zn}(2,2'\text{-bipy})(\text{dien})]_2[\text{V}_{14}\text{As}_8\text{O}_{42}(\text{H}_2\text{O})] \cdot 2\text{H}_2\text{O}$  compound.

The nickel(II) and cobalt(II) analogues  $(2,2'\text{-bipy})[\text{Ni}(2,2'\text{-bipy})_3]_2[\alpha\text{-V}_{14}\text{As}_8\text{O}_{42}(\text{H}_2\text{O})] \cdot 3\text{H}_2\text{O}$  and  $[\text{Co}(2,2'\text{-bipy})_3]_2[\alpha\text{-V}_{14}\text{As}_8\text{O}_{42}(\text{H}_2\text{O})] \cdot 3\text{H}_2\text{O}$  of the  $[\text{Zn}(2,2'\text{-bipy})_3]_2[\alpha\text{-V}_{14}\text{As}_8\text{O}_{42}(\text{H}_2\text{O})] \cdot 4\text{H}_2\text{O}$  compound were also hydrothermally synthesised (Table 3).<sup>139</sup> Similarly, the inorganic-organic hybrid compounds  $[\text{Cu}(\text{en})_2]_2[\text{V}_{14}\text{As}_8\text{O}_{42}(\text{H}_2\text{O})] \cdot 2.5\text{H}_2\text{O}$ ,

$[M(1,10\text{-phen})_3]_2[V_{14}As_8O_{42}(H_2O)_{0.5}] \cdot 0.5H_2O$  ( $M = Mn, Cd$ ) and  $[Co(dien)_2]_2[V_{14}As_8O_{42}(H_2O)] \cdot 3.5H_2O$  were obtained by pH-controlled hydrothermal syntheses.<sup>140</sup> Notably, the  $\alpha$ - $[H_2O@V_{14}As_8O_{42}]^{4-}$  polyoxoanions in the crystal structure of  $[Co(dien)_2]_2[V_{14}As_8O_{42}(H_2O)] \cdot 3.5H_2O$  are linked by van der Waals forces into channels where the  $[Co(dien)_2]^{2+}$  complexes and  $H_2O$  molecules act as space-fillers.

The excitation and emission spectra of other hydrothermally prepared compounds  $[Zn(phen)_3]_2[V_{14}As_8O_{42}(H_2O)] \cdot 4H_2O$  and  $[Cd(phen)_3]_2[V_{14}As_8O_{42}(H_2O)] \cdot 2H_2O$  (Table 3) were reported that indicate fluorescence in the UV region with an emission peak at ca. 300 nm.<sup>141</sup> Although the authors claimed that these compounds feature a new type of the “fully-reduced”  $[V_{14}As_8O_{42}]^{4-}$  polyoxoanion, namely the  $\gamma$  isomer with  $d_{V...V} = 3.01 - 3.04 \text{ \AA}$ , their structures are in fact characterised by co-crystallised polyoxoanions of  $\alpha$  and  $\beta$  types with occupation factors of 0.5. For the rotational isomerism, electronic structures and acidity/basicity properties of “fully-reduced”  $[V_{14}E_8O_{50}]^{12-}$  heteroPOVs and their chalcogenide-substituted  $[V_{14}E_8O_{42}X_8]^{12-}$  derivatives ( $E = Si, Ge, Sn; X = S, Se, Te$ ), see the theoretical work of Kondinski *et al.*<sup>142</sup> For comparison, Figure 16 illustrates the  $\alpha$ -,  $\gamma$ -, and  $\beta$ -isomeric vanadium oxide skeletons of the  $\{V_{14}As_8\}$ -nuclearity AsPOVs.

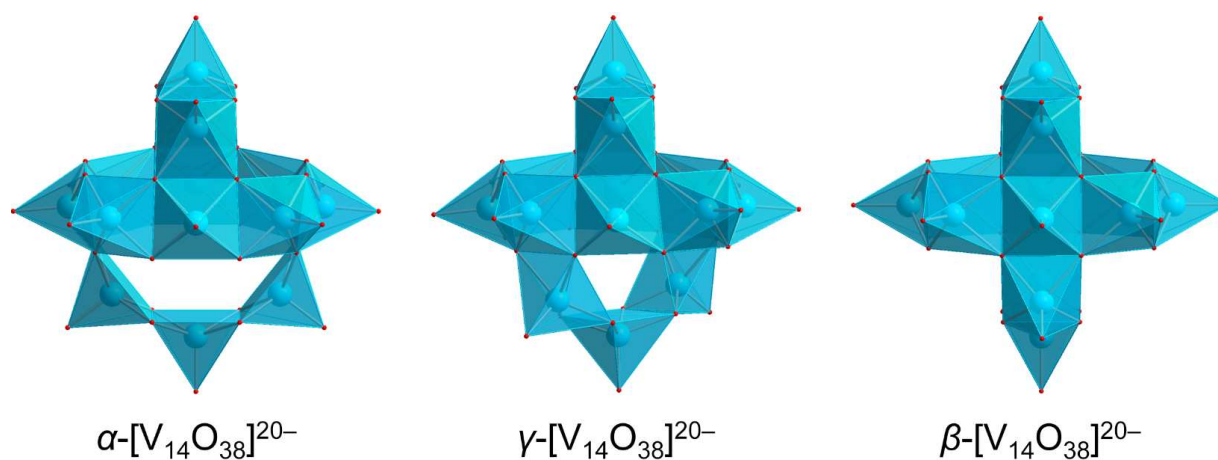


**Figure 16.** The “fully-reduced” vanadium oxide skeletons of  $\alpha$ -/ $\gamma$ -/ $\beta$ - $[V_{14}As_8O_{42}]^{4-}$  polyoxoanions. The  $\{As_2O\}$  moieties are not shown. Colour code: O, red;  $V^{IV}O_x$ , sky-blue polyhedra.

**TMC-AsPOV hybrids with specific cation-anion interactions.** A large series of  $\{V_{14}As_8O_{42}\}$ -type polyoxoanions charge-balanced and covalently coordinated with various TMC complexes were presented by Yang, Xu, Wang, Peng, Das and coworkers. The inorganic–organic hybrid compounds with the  $\alpha$ - $[V_{14}As_8O_{42}]^{4-}$  building blocks pillared by Zn(II) complexes  $[Zn(en)_2][(H_2O)Zn(en)_2V_{14}As_8O_{42}(H_2O)] \cdot H_2O$ ,  $\{(H_2O)Zn(1,10\text{-phen})_2\}_2[V_{14}As_8O_{42}(H_2O)] \cdot 4H_2O$ ,  $\{(H_2O)Zn(2,2'\text{-bipy})_2\}\{Zn(2,2'$

bipy)<sub>2</sub>V<sub>14</sub>As<sub>8</sub>O<sub>42</sub>(H<sub>2</sub>O)<sub>0.5</sub>]<sub>2</sub>[(H<sub>2</sub>O)Zn(2,2'-bipy)<sub>2</sub>V<sub>14</sub>As<sub>8</sub>O<sub>42</sub>(H<sub>2</sub>O)<sub>0.5</sub>]<sub>2</sub>[Zn(2,2'-bipy)<sub>2</sub>]<sub>2</sub>·3H<sub>2</sub>O, and [(H<sub>2</sub>O)Zn(4,4'-bipy)<sub>2</sub>]<sub>2</sub>{V<sub>14</sub>As<sub>8</sub>O<sub>42</sub>(H<sub>2</sub>O)}<sub>2</sub>·2H<sub>2</sub>O were all synthesised under hydrothermal conditions.<sup>143</sup> These compounds display differing extended structures as well as different coordination modes of the organodiamine ligands (en, 1,10-phen, 2,2'-bipy, and 4,4'-bipy) used in the synthesis reactions (Table 3). Notably, the formation of the crystalline products was shown to be strongly dependent on the acidic pH range (3 – 6), which is quite different from the pH (alkaline media) for reactions resulting in the TMC-supported GePOVs, and was seemingly not influenced by the reaction temperatures in the range 130 – 170 °C. The layered crystal structure of [Zn(en)<sub>2</sub>][(H<sub>2</sub>O)Zn(en)<sub>2</sub>V<sub>14</sub>As<sub>8</sub>O<sub>42</sub>(H<sub>2</sub>O)]·H<sub>2</sub>O features the [(H<sub>2</sub>O)Zn(en)<sub>2</sub>V<sub>14</sub>As<sub>8</sub>O<sub>42</sub>(H<sub>2</sub>O)]<sup>2-</sup> anion, in which a single [Zn(en)<sub>2</sub>(H<sub>2</sub>O)]<sup>2+</sup> moiety is attached to a terminal O atom from the eight-membered ring of the AsPOV, and the [Zn(en)<sub>2</sub>]<sup>2+</sup> complex is the counteraction. The [(H<sub>2</sub>O)Zn(1,10-phen)<sub>2</sub>]<sub>2</sub>{V<sub>14</sub>As<sub>8</sub>O<sub>42</sub>(H<sub>2</sub>O)}<sub>2</sub>·4H<sub>2</sub>O compound shows the “fully-reduced” [V<sup>IV</sup><sub>14</sub>As<sub>8</sub>O<sub>42</sub>]<sup>4-</sup> polyoxoanion whose central eight-membered ring is doubly decorated with the [(H<sub>2</sub>O)Zn(1,10-phen)<sub>2</sub>]<sup>2+</sup> complexes through covalent Zn–O bonds. The crystal structure is, furthermore, characterised by a 2D supramolecular array formed due to an extended hydrogen bond network. The crystal structure of [(H<sub>2</sub>O)Zn(2,2'-bipy)<sub>2</sub>]<sub>2</sub>{Zn(2,2'-bipy)<sub>2</sub>V<sub>14</sub>As<sub>8</sub>O<sub>42</sub>(H<sub>2</sub>O)<sub>0.5</sub>]<sub>2</sub>[(H<sub>2</sub>O)Zn(2,2'-bipy)<sub>2</sub>V<sub>14</sub>As<sub>8</sub>O<sub>42</sub>(H<sub>2</sub>O)<sub>0.5</sub>]<sub>2</sub>[Zn(2,2'-bipy)<sub>2</sub>]<sub>2</sub>·3H<sub>2</sub>O displays two crystallographically independent motifs, namely [(H<sub>2</sub>O)Zn(2,2'-bipy)<sub>2</sub>V<sub>14</sub>As<sub>8</sub>O<sub>42</sub>(H<sub>2</sub>O)<sub>0.5</sub>]<sub>2</sub>[Zn(2,2'-bipy)<sub>2</sub>]<sub>2</sub> and [(H<sub>2</sub>O)Zn(2,2'-bipy)<sub>2</sub>]<sub>2</sub>{Zn(2,2'-bipy)<sub>2</sub>V<sub>14</sub>As<sub>8</sub>O<sub>42</sub>(H<sub>2</sub>O)<sub>0.5</sub>}. The structure of the former, neutral dimer consists of two [(H<sub>2</sub>O)Zn(2,2'-bipy)<sub>2</sub>V<sub>14</sub>As<sub>8</sub>O<sub>42</sub>(H<sub>2</sub>O)<sub>0.5</sub>]<sup>2-</sup> hybrids, in which each AsPOV building block is coordinated with one [(H<sub>2</sub>O)Zn(2,2'-bipy)<sub>2</sub>]<sup>2+</sup> complex, and two [Zn(2,2'-bipy)<sub>2</sub>]<sup>2+</sup> complexes function as bridging groups between these two dianions. The structure of another neutral hybrid compound [(H<sub>2</sub>O)Zn(2,2'-bipy)<sub>2</sub>]<sub>2</sub>{Zn(2,2'-bipy)<sub>2</sub>V<sub>14</sub>As<sub>8</sub>O<sub>42</sub>(H<sub>2</sub>O)<sub>0.5</sub>} consists of the [(H<sub>2</sub>O)Zn(2,2'-bipy)<sub>2</sub>]<sup>2+</sup> and [Zn(2,2'-bipy)<sub>2</sub>]<sup>2+</sup> moieties covalently attached to the AsPOV building block via Zn–O bonds. In the structure, the [(H<sub>2</sub>O)Zn(2,2'-bipy)<sub>2</sub>]<sup>2+</sup> complex is involved in bonding to a terminal O atom from the eight-membered ring of [V<sup>IV</sup><sub>14</sub>As<sub>8</sub>O<sub>42</sub>]<sup>4-</sup> and the [Zn(2,2'-bipy)<sub>2</sub>]<sup>2+</sup> complex to that of a {VO<sub>5</sub>}-composed trimer capping the AsPOV ring. The crystal structure of [(H<sub>2</sub>O)Zn(4,4'-bipy)<sub>2</sub>]<sub>2</sub>{V<sub>14</sub>As<sub>8</sub>O<sub>42</sub>(H<sub>2</sub>O)}<sub>2</sub>·2H<sub>2</sub>O displays a 2D network where the adjacent AsPOVs are linked by two [(H<sub>2</sub>O)Zn(4,4'-bipy)<sub>2</sub>]<sup>2+</sup> fragments through covalent Zn–O bonds. Thus, each polyoxoanion is surrounded by four bridging Zn(II) complexes coordinated to the terminal O atoms of the eight-membered vanadium oxide ring. The 2D network of this compound is further expanded into a 3D supramolecular structure via hydrogen bonds between water

molecules and terminal oxygen positions of  $[V^{IV}_{14}As_8O_{42}]^{4-}$ . According to cyclic voltammograms, the above-described compounds exhibit quasi-reversible redox behaviour.

The extended solid-state structures of the hydrothermally prepared compounds  $[Zn(2,2'-bipy)_2]_2[V_{14}As_8O_{42}(H_2O)] \cdot H_2O$  (Figure 17a),  $[Cd(2,2'-bipy)_3][Cd(dien)V_{14}As_8O_{42}(H_2O)]$ , and  $[Ni(en)_2]_3[V_{14}As_8O_{42}(HPO_3)] \cdot 4H_2O$  (Table 3) display the “fully-reduced”  $\alpha$ - $[V^{IV}_{14}As_8O_{42}]^{4-}$  polyoxoanions interconnected through the corresponding TMC complexes  $[Zn(2,2'-bipy)_2]^{2+}$ ,  $[Cd(dien)]^{2+}$ , and  $[Ni(en)_2]^{2+}$ , respectively.<sup>144</sup> The Zn(II)- and Cd(II)-containing compounds organise into 1D chain structures and are characterised by overall antiferromagnetic coupling. In contrast, the Ni(II)-containing compound exhibits a 2D structure and produces no signal for  $V^{IV}$  ions in the EPR spectrum at room temperature.

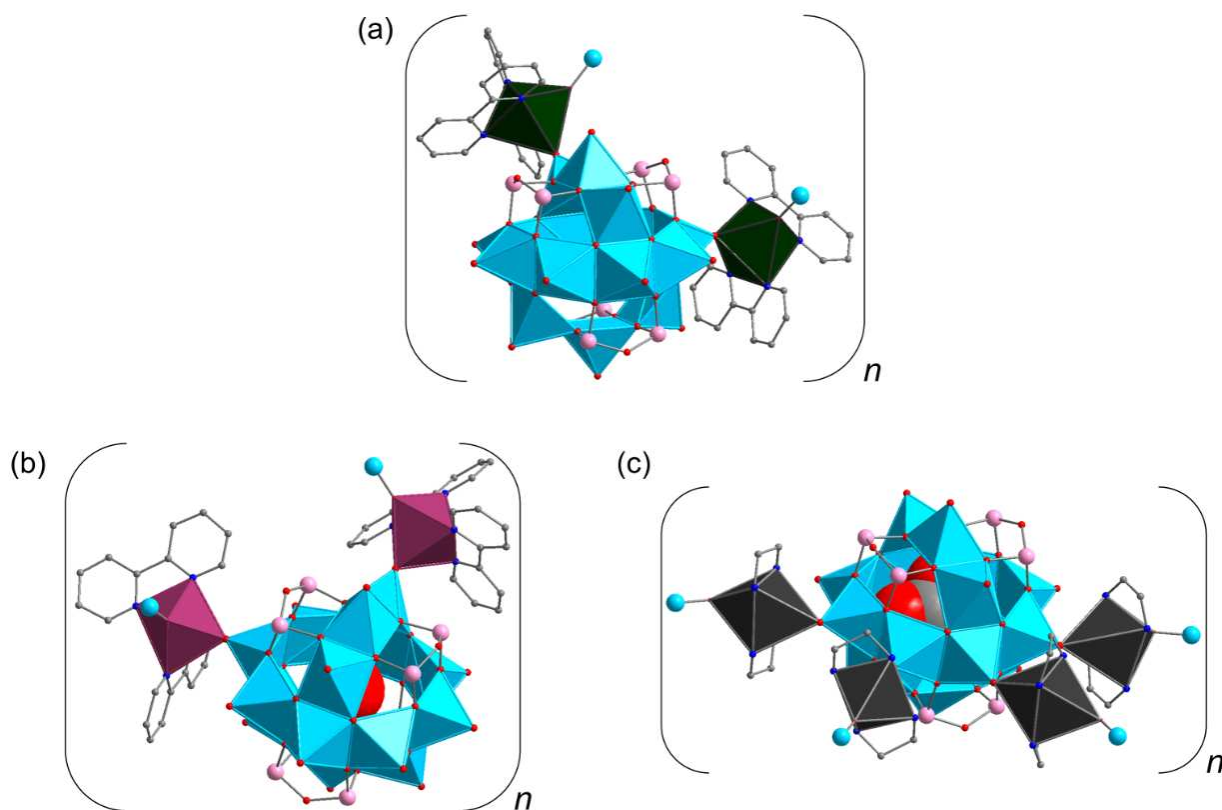


**Figure 17.** Polyhedral representations of sections of the polymeric solid-state structures of  $[Zn(2,2'-bipy)_2]_2[V_{14}As_8O_{42}(H_2O)] \cdot H_2O$  (a),  $[Co(2,2'-bipy)_2]_2[V_{14}As_8O_{42}(H_2O)] \cdot H_2O$  (b), and  $[Cu(en)_2]_3[V_{14}As_8O_{42}(CO_3)] \cdot 10H_2O$  (c; only four  $[Cu(en)_2]^{2+}$  bridging groups are shown). Hydrogen atoms are omitted for clarity. Colour code: C, grey; N, blue; As, rose; O, red;  $V^{IV}$ , sky blue;  $V^{IV}O_x$ , sky-blue polyhedra; Co, plum; Cu, black; Zn, dark green.

The antiferromagnetic compound  $[Ni(en)_2]_3[V_{14}As_8O_{42}(SO_4)] \cdot 4.5H_2O$  with a 2D layer structure was prepared under hydrothermal conditions (Table 3) and reveals strong covalent attachment between the adjacent  $\alpha$ - $[SO_4@V^{IV}_{14}As_8O_{42}]^{6-}$  polyoxoanions through



V=O–Ni–O=V connectivities.<sup>145</sup> A 2D network is formed as POV is bound to four neighbouring polyoxoanions via an octahedrally coordinated Ni(II) centre.

The compounds  $[\{\text{Ni}(\text{en})_2\}_4(4,4'\text{-bipy})_4\{\text{Ni}(\text{H}_2\text{O})_2\}]_2[\text{V}_{14}\text{As}_8\text{O}_{42}(\text{NO}_3)]_4 \cdot 16\text{H}_2\text{O}$  and  $[\text{Ni}(\text{en})_2(\text{H}_2\text{O})_2]_2[\{\text{Ni}(\text{en})_2(\text{H}_2\text{O})\}_2\text{V}_{14}\text{As}_8\text{O}_{42}(\text{NO}_3)][\{\text{Ni}(\text{en})_2\}\text{V}_{14}\text{As}_8\text{O}_{42}(\text{NO}_3)] \cdot 6\text{H}_2\text{O}$  (Table 3) were hydrothermally prepared and showed high-dimensional organic–inorganic hybrid nanostructures.<sup>146</sup> The compound bearing 4,4'-bipy ligands consists of two bridging  $[\{\text{Ni}(\text{en})_2\}_4(4,4'\text{-bipy})_4\{\text{Ni}(\text{H}_2\text{O})_2\}]^{10+}$  fragments and four  $\alpha\text{-}[\text{NO}_3@V^{\text{IV}}_{14}\text{As}_8\text{O}_{42}]^{5-}$  polyoxoanions which are joined through Ni–O bonds to form a pillared box-like structure with a cavity of ca. 600 Å<sup>3</sup> (Figure 18). In contrast to the previous compound, the compound  $[\text{Ni}(\text{en})_2(\text{H}_2\text{O})_2]_2[\{\text{Ni}(\text{en})_2(\text{H}_2\text{O})\}_2\text{V}_{14}\text{As}_8\text{O}_{42}(\text{NO}_3)][\{\text{Ni}(\text{en})_2\}\text{V}_{14}\text{As}_8\text{O}_{42}(\text{NO}_3)] \cdot 6\text{H}_2\text{O}$  is based on the “fully-reduced”  $\beta\text{-}[\text{NO}_3@V^{\text{IV}}_{14}\text{As}_8\text{O}_{42}]^{5-}$  polyoxoanions. Its crystal structure shows three crystallographically independent motifs: (i) *bis*- $\{\text{Ni}(\text{en})_2(\text{H}_2\text{O})\}$ -decorated AsPOV anion  $[\{\text{Ni}(\text{en})_2(\text{H}_2\text{O})\}_2\text{V}_{14}\text{As}_8\text{O}_{42}(\text{NO}_3)]^-$ ; (ii) 1D chain polymer consisting of  $[\{\text{Ni}(\text{en})_2\}_2\text{V}_{14}\text{As}_8\text{O}_{42}(\text{NO}_3)]^-$  monoanions; (iii)  $[\text{Ni}(\text{en})_2(\text{H}_2\text{O})_2]^{2+}$  complexes.

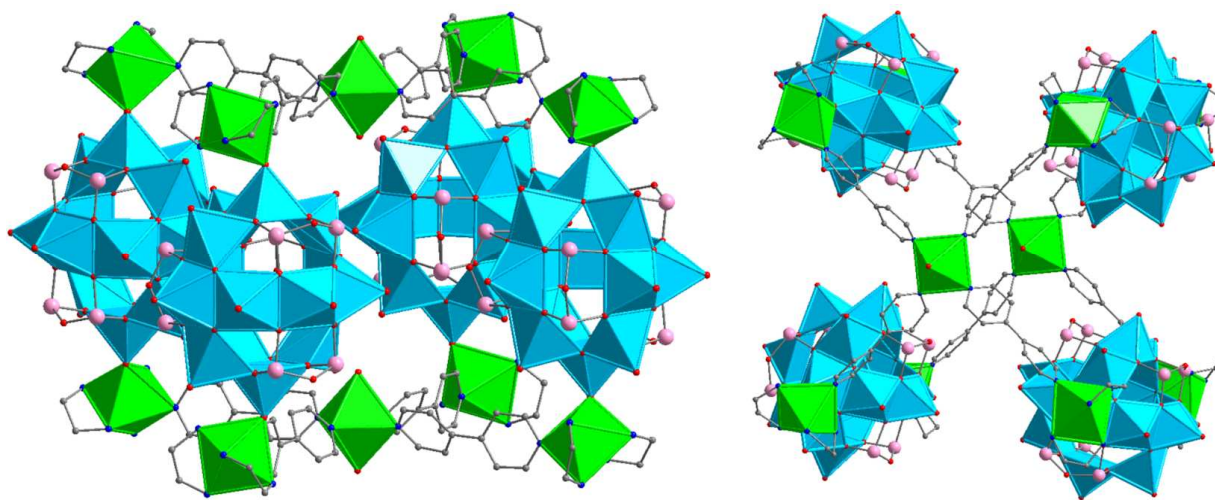


**Figure 18.** Two different views of the box-like motif found in the solid-state structure of  $[\{\text{Ni}(\text{en})_2\}_4(4,4'\text{-bipy})_4\{\text{Ni}(\text{H}_2\text{O})_2\}]_2[\text{V}_{14}\text{As}_8\text{O}_{42}(\text{NO}_3)]_4 \cdot 16\text{H}_2\text{O}$ . Hydrogen atoms and lattice water molecules are omitted for clarity. Colour code: C, grey; N, blue; As, rose; O, red;  $V^{\text{IV}}\text{O}_x$ , sky-blue polyhedra; Ni, bright green.

The hydrothermal synthesis of ‘metal-controlled’ inorganic–organic self-assemblies with compositions  $[\text{Ni}(\text{enMe})_3]_4[\text{Ni}(\text{enMe})_2][\text{V}_{14}\text{As}_8\text{O}_{42}(\text{NO}_3)]_2 \cdot 8\text{H}_2\text{O}$  and  $[\text{Co}(\text{en})_3][\text{Co}(\text{en})_2\text{V}_{14}\text{As}_8\text{O}_{42}(\text{H}_2\text{O})] \cdot 16\text{H}_2\text{O}$  (Table 3) was reported. These antiferromagnetic compounds are based on the “fully-reduced”  $\alpha\text{-}[\text{V}^{\text{IV}}_{14}\text{As}_8\text{O}_{42}]^{4-}$  polyoxoanions accommodating  $\text{NO}_3^-$  and  $\text{H}_2\text{O}$  as guests.<sup>125</sup> The crystal structure of the former AsPOV consists of  $[\text{Ni}(\text{enMe})_2\{\text{V}_{14}\text{As}_8\text{O}_{42}(\text{NO}_3)\}]_2^{8-}$  dimers, four  $[\text{Ni}(\text{enMe})_3]^{2+}$  countercations and lattice  $\text{H}_2\text{O}$  molecules. The  $[\text{Ni}(\text{enMe})_2\{\text{V}_{14}\text{As}_8\text{O}_{42}(\text{NO}_3)\}]_2^{8-}$  dimer is constructed from two

“fully-reduced”  $[\text{NO}_3@V^{IV}_{14}\text{As}_8\text{O}_{42}]^{5-}$  moieties linked through the bridging  $[\text{Ni}(\text{enMe})_2]^{2+}$  complex. The crystal structure of the latter compound is characterised by 1D chains consisting of the  $[\text{Co}(\text{en})_2V_{14}\text{As}_8\text{O}_{42}(\text{H}_2\text{O})]^{2-}$  hybrids,  $[\text{Co}(\text{en})_3]^{2+}$  countercations and lattice  $\text{H}_2\text{O}$  molecules. The  $[\text{Co}(\text{en})_2]^{2+}$  complexes act here as bridging ligands for the neighbouring AsPOVs.

Another Co(II)-containing compound with the formula  $[\text{Co}(2,2'\text{-bipy})_2]_2[V_{14}\text{As}_8\text{O}_{42}(\text{H}_2\text{O})]\cdot\text{H}_2\text{O}$  (Figure 17b) and a tubular structure was prepared hydrothermally in acidified solution (Table 3).<sup>147</sup> The crystal structure of this solid being stable up to ca. 370 °C shows closed helical chains of  $\{[\text{Co}(2,2'\text{-bipy})_2][V^{IV}_{14}\text{As}_8\text{O}_{42}(\text{H}_2\text{O})]\}_\infty$  hybrid building blocks where the  $[\text{Co}(2,2'\text{-bipy})_2]^{2+}$  complexes covalently link the  $\alpha$ -isomeric AsPOVs through Co–O bonds.

A number of high-dimensional hybrid materials based on the  $\alpha$ - $[V^{IV}_{14}\text{As}_8\text{O}_{42}]^{4-}$  building block, namely  $[\text{M}(\text{bbi})_2]_2[V_{14}\text{As}_8\text{O}_{42}(\text{H}_2\text{O})]$  (M = Co, Ni, Zn) and  $[\text{Cu}(\text{bbi})_4][V_{14}\text{As}_8\text{O}_{42}(\text{H}_2\text{O})]$  were synthesised under hydrothermal conditions (pH of ca. 5.0) where oxalic acid can act as a reducing agent for the  $V^V$  source (Table 3).<sup>148</sup> These compounds containing the soft N-donor 1,1'-(1,4-butanediyl)bis(imidazole) (= bbi,  $\text{C}_{10}\text{H}_{14}\text{N}_4$ ) extend a series of POV-templated structures including, e.g., that of the  $[\text{H}_4V_{18}\text{O}_{46}(\text{SiO})_8(\text{dab})_4(\text{H}_2\text{O})]\cdot 4\text{H}_2\text{O}$  compound bearing the bidentate dab ligand.<sup>97</sup> The isostructural  $[\text{M}(\text{bbi})_2]_2[V_{14}\text{As}_8\text{O}_{42}(\text{H}_2\text{O})]$  (M = Co, Ni, Zn) compounds with antiferromagnetic properties are characterised by a binodal (4,6)-connected 2D network structure, Schläfli symbol  $(3^4\cdot 4^2)(3^4\cdot 4^4\cdot 5^4\cdot 6^3)_2$ , where each of the neighbouring AsPOVs is covalently coordinated to four bridging  $[\text{M}(\text{bbi})_2]^{2+}$  complexes through M–O bonds. The coordination modes of the bbi ligands allow them to connect these four  $M^{2+}$  ions in such a manner that each polyoxoanion is located within a closed  $\{\text{M}(\text{bbi})\}_4$  ring. In the structure of the compound  $[\text{Cu}(\text{bbi})_4][V_{14}\text{As}_8\text{O}_{42}(\text{H}_2\text{O})]$  a 3D network is observed made up of the AsPOVs interacting covalently with the bbi-bridged  $\text{Cu}^+$  cations from the adjacent wave-like chains of the  $[\text{Cu}(\text{bbi})_n]$  moieties. The latter surrounding each polyoxoanion up and down results in the formation of 1D ladder-like  $[\text{Cu}(\text{bbi})]^+$  double chains.

The compound  $[\text{Cu}(\text{en})_2]_3[V_{14}\text{As}_8\text{O}_{42}(\text{CO}_3)]\cdot 10\text{H}_2\text{O}$  with a 2D network structure was prepared hydrothermally (Table 3) and contains  $\alpha$ - $[\text{CO}_3@V^{IV}_{14}\text{As}_8\text{O}_{42}]^{6-}$  with a carbonate ion in the inner void of the polyoxoanion.<sup>149</sup> In the solid state, each AsPOV is surrounded by six  $[\text{Cu}(\text{en})_2]^{2+}$  bridging groups with Cu–O<sub>term</sub>–V linkages (Figure 17c).

**Lanthanoid-AsPOV hybrids.** The first representatives of AsPOVs with covalently attached aqua-lanthanoid(III) complexes were reported in 2009.<sup>150</sup> Arumuganathan and Das isolated three isostructural  $[\{\text{Ln}(\text{H}_2\text{O})_6\}_2V_{14}\text{As}_8\text{O}_{42}(\text{SO}_3)]\cdot 8\text{H}_2\text{O}$  compounds (Ln = La<sup>III</sup>, Sm<sup>III</sup>, and

Ce<sup>III</sup>) from aqueous reaction solutions at room temperature using (NH<sub>4</sub>)<sub>6</sub>[V<sub>14</sub>As<sub>8</sub>O<sub>42</sub>(SO<sub>3</sub>)] and Ln(NO<sub>3</sub>)<sub>3</sub>·6H<sub>2</sub>O as starting materials (Table 3). The main structural motif of the all-inorganic {V<sub>14</sub>As<sub>8</sub>}<sup>-</sup>-type compounds represents the “fully-reduced” β-[V<sup>IV</sup><sub>14</sub>As<sub>8</sub>O<sub>42</sub>]<sup>4-</sup> polyoxoanion with approximate D<sub>2d</sub> symmetry, which encapsulate a sulfite anion. As was demonstrated by thermal analysis and mass spectrometry experiments, the aqua-Ln(III)-capped AsPOVs release gaseous SO<sub>2</sub> at temperatures 520–580 °C, whereas the (NH<sub>4</sub>)<sub>6</sub>[V<sub>14</sub>As<sub>8</sub>O<sub>42</sub>(SO<sub>3</sub>)] precursor releases SO<sub>2</sub> already at 480–520 °C. The crystal structures of these compounds display 2D layered coordination polymers where each of six [Ln(H<sub>2</sub>O)<sub>6</sub>]<sup>3+</sup> complexes surrounding the [SO<sub>3</sub>@V<sup>IV</sup><sub>14</sub>As<sub>8</sub>O<sub>42</sub>]<sup>6-</sup> polyoxoanion through one covalent Ln–O<sub>term</sub>–V bond coordinates to two other adjacent AsPOVs. Thus, the aqua-Ln(III) complexes can indeed link to AsPOVs, which resulted in the formation of extended structures where La<sup>III</sup> ions are nine-fold coordinated and reside in a monocapped square-antiprismatic coordination environment. Magnetic susceptibility studies performed for the samples with the 4<sup>f</sup>-La<sup>III</sup>, 4<sup>f</sup>-Sm<sup>III</sup> and 4<sup>f</sup>-Ce<sup>III</sup> ions indicated that [Ln(H<sub>2</sub>O)<sub>6</sub>]<sub>2</sub>[V<sub>14</sub>As<sub>8</sub>O<sub>42</sub>(SO<sub>3</sub>)]·8H<sub>2</sub>O are antiferromagnetically coupled materials, with no significant coupling between the lanthanide(III) ions and the POV.

### 3.2.5 {V<sub>15</sub>As<sub>6</sub>}<sup>-</sup>-type polyoxoanions.

**Discrete AsPOV with potassium counteractions.** The first synthesised AsPOV dates back to 1988, when Müller and Döring published the compound K<sub>6</sub>[V<sub>15</sub>As<sub>6</sub>O<sub>42</sub>(H<sub>2</sub>O)]·8H<sub>2</sub>O which was prepared by reduction of vanadate with hydrazinium sulfate in the presence of As<sub>2</sub>O<sub>3</sub> in aqueous solution at 85 °C (Table 3).<sup>151</sup> This compound is composed of the “fully-reduced” [H<sub>2</sub>O@V<sup>IV</sup><sub>15</sub>As<sub>6</sub>O<sub>42</sub>]<sup>6-</sup> polyoxoanion with crystallographic D<sub>3</sub> symmetry and six K<sup>+</sup> counteractions. The “hydrated” potassium ions provide the networking of the AsPOVs in the crystal structure (rhombohedral cell; for hexagonal cell, see K<sub>6</sub>[V<sub>15</sub>As<sub>6</sub>O<sub>42</sub>(H<sub>2</sub>O)]·6H<sub>2</sub>O).<sup>152</sup> The [H<sub>2</sub>O@V<sup>IV</sup><sub>15</sub>As<sub>6</sub>O<sub>42</sub>]<sup>6-</sup> polyoxoanion with an encapsulated H<sub>2</sub>O molecule (Figure 19a) is the first member of the series of compounds with general formula [V<sub>18-z</sub>As<sub>2z</sub>O<sub>42</sub>] (z = 3). The structural motif of [H<sub>2</sub>O@V<sup>IV</sup><sub>15</sub>As<sub>6</sub>O<sub>42</sub>]<sup>6-</sup> is derived from the [V<sub>18</sub>O<sub>42</sub>]<sup>12-</sup> structure by replacing three {VO<sub>5</sub>} units by three handle-like {As<sub>2</sub>O<sub>5</sub>} groups (for comparison, see [V<sup>IV</sup><sub>15</sub>Si<sub>6</sub>O<sub>42</sub>(OH)<sub>6</sub>]<sup>6-</sup> in Figure 6c). This polyoxoanion thus consists of fifteen distorted {VO<sub>5</sub>} square pyramids that are interlinked through the basal O vertices and edges and of six {AsO<sub>3</sub>} trigonal pyramids. Interestingly, Müller and Döring noticed that this prominent AsPOV “*may be regarded as a model for species that are formed during poisoning of the V<sub>2</sub>O<sub>5</sub> catalyst (which contains V<sup>IV</sup> centers) by arsenic*”.<sup>151</sup>



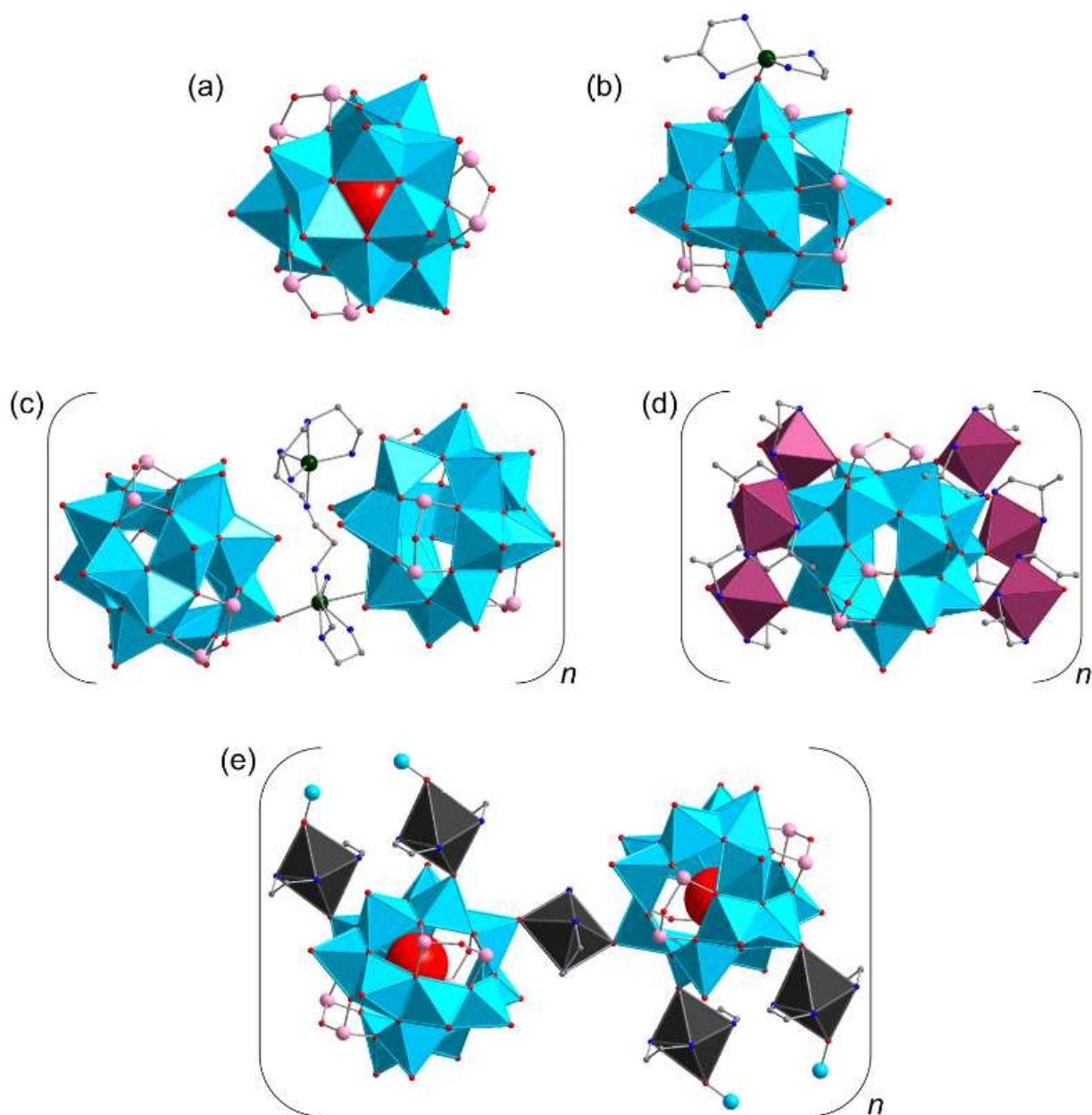


**Figure 19.** (a) The “fully-reduced”  $[\text{H}_2\text{O}@\text{V}^{\text{IV}}_{15}\text{As}_6\text{O}_{42}]^{6-}$  polyoxoanion. (b) The “fully-reduced”  $[\{\text{Zn}(\text{en})(\text{enMe})\}\text{V}^{\text{IV}}_{15}\text{As}_6\text{O}_{42}]^{4-}$  hybrid polyoxoanion. Hydrogen atoms and encapsulated water molecule are not shown. (c) A segment of the polymeric structure of  $[\text{Zn}_2(\text{dien})_3(\text{H}_2\text{O})_2]_{0.5}[\{\text{Zn}_2(\text{dien})_3\}\text{V}_{15}\text{As}_6\text{O}_{42}(\text{H}_2\text{O})]\cdot 2\text{H}_2\text{O}$ . (d) A segment of the extended solid-state structure of  $[\text{Co}(\text{enMe})_2]_3[\text{V}_{15}\text{As}_6\text{O}_{42}(\text{H}_2\text{O})]\cdot 2\text{H}_2\text{O}$ . (e) A segment of the extended solid-state structure of  $[\text{Cu}(\text{en})_2]_{1.5}[\text{H}_3\text{V}_{15}\text{As}_6\text{O}_{42}(\text{H}_2\text{O})]\cdot 3\text{H}_2\text{O}$ . Colour code: C, grey; N, blue; As, rose; O, red;  $\text{V}^{\text{IV}}$ , sky blue;  $\text{V}^{\text{IV}}\text{O}_x$ , sky-blue polyhedra; Co, plum; Cu, black; Zn, dark green.

**TMC-AsPOV hybrids without specific cation-anion interactions.** The compound  $[\text{Zn}(\text{H}_2\text{O})_4]_2[\text{H}_2\text{V}_{15}\text{As}_6\text{O}_{42}(\text{H}_2\text{O})]\cdot 2\text{H}_2\text{O}$  was obtained under hydrothermal conditions (Table 3) and is composed of the doubly protonated  $[\text{H}_2\text{O}@\text{H}_2\text{V}^{\text{IV}}_{15}\text{As}_6\text{O}_{42}]^{4-}$  polyoxoanion and two  $[\text{Zn}(\text{H}_2\text{O})_4]^{2+}$  countercations.<sup>153</sup> In the structure, these two constituents are held together by hydrogen  $\text{O}-\text{H}\cdots\text{O}_{\text{term}}$  bonds, which results in the formation of a 3D network structure. In

studies of third-order nonlinear optical (NLO) properties of  $[\text{Zn}(\text{H}_2\text{O})_4]_2[\text{H}_2\text{V}_{15}\text{As}_6\text{O}_{42}(\text{H}_2\text{O})]\cdot 2\text{H}_2\text{O}$  the compound exhibited strong nonlinear absorption.

**TMC-AsPOV hybrids with specific cation-anion interactions.** The structures of two hydrothermally synthesised compounds  $[\text{Zn}(\text{en})_2][\text{Zn}(\text{en})_2(\text{H}_2\text{O})_2][\{\text{Zn}(\text{en})(\text{enMe})\}\text{V}_{15}\text{As}_6\text{O}_{42}(\text{H}_2\text{O})]\cdot 4\text{H}_2\text{O}$  and  $[\text{Zn}_2(\text{enMe})_2(\text{en})_3][\{\text{Zn}(\text{enMe})_2\}\text{V}_{15}\text{As}_6\text{O}_{42}(\text{H}_2\text{O})]\cdot 4\text{H}_2\text{O}$  (Table 3) consist of the  $[\{\text{Zn}(\text{en})(\text{enMe})\}\text{V}_{15}\text{As}_6\text{O}_{42}(\text{H}_2\text{O})]^{4-}$  (Figure 19b) and  $[\{\text{Zn}(\text{enMe})_2\}\text{V}_{15}\text{As}_6\text{O}_{42}(\text{H}_2\text{O})]^{4-}$  hybrid polyoxoanions whose AsPOV shells are coordinatively functionalised with  $\text{Zn}^{2+}$  complexes through  $\text{Zn}-\text{O}_{\text{term}}-\text{V}$  bonds.<sup>154</sup> Charge neutrality of the compounds is achieved by cationic  $[\{\text{Zn}(\text{en})_2\}[\text{Zn}(\text{en})_2(\text{H}_2\text{O})_2]]^{4+}$  and  $[\text{Zn}_2(\text{enMe})_2(\text{en})_3]^{4+}$  complexes. By contrast, a  $[\{\{\text{Zn}(\text{en})_2\}_2\text{V}_{15}\text{As}_6\text{O}_{42}(\text{H}_2\text{O})\}_2\{\text{Zn}(\text{en})_2\}]^{2-}$  dimer in another hydrothermally prepared compound  $(\text{Hen})_2[\{\{\text{Zn}(\text{en})_2\}_2\text{V}_{15}\text{As}_6\text{O}_{42}(\text{H}_2\text{O})\}_2\{\text{Zn}(\text{en})_2\}]\cdot 3\text{H}_2\text{O}$  (Table 3) is charge-balanced by two singly protonated  $\text{Hen}^+$  cations.<sup>155</sup> The crystal structure of the latter compound shows two  $[\text{H}_2\text{O}@V_{15}\text{As}_6\text{O}_{42}\{\text{Zn}(\text{en})_2\}_2]^{2-}$  building blocks which are joined by a bridging  $[\text{Zn}(\text{en})_2]^{2+}$  unit through  $\text{Zn}-\text{O}$  bonds.

The “fully-reduced”  $[\text{H}_2\text{O}@V_{15}\text{As}_6\text{O}_{42}]^{6-}$  polyoxoanions in the crystal structures of the antiferromagnetic compounds  $[\text{Zn}_2(\text{dien})_3(\text{H}_2\text{O})_2]_{0.5}[\{\text{Zn}_2(\text{dien})_3\}\text{V}_{15}\text{As}_6\text{O}_{42}(\text{H}_2\text{O})]\cdot 2\text{H}_2\text{O}$  (Figure 19c, Table 3) and  $[\text{Ni}(2,2'\text{-bipy})_3]_2[\{\text{Ni}(\text{en})_2\}\text{V}_{15}\text{As}_6\text{O}_{42}(\text{H}_2\text{O})]\cdot 9.5\text{H}_2\text{O}$  are interlinked by  $[\text{Zn}_2(\text{dien})_3]^{2+}$  and  $[\text{Ni}(\text{en})_2]^{2+}$  moieties to form 1D helical chains and 1D infinite straight chains, respectively.<sup>156</sup> The 1D helical chains are involved in extensive hydrogen bonding interactions with discrete  $[\text{Zn}_2(\text{dien})_3(\text{H}_2\text{O})_2]^{4+}$  complexes, thus generating a 2D network structure; a further expansion of the hydrogen bond pattern involving  $[\text{Zn}_2(\text{dien})_3]^{4+}$  bridging units results in a 3D supramolecular array. The 1D chains based on the  $[\text{H}_2\text{O}@V_{15}\text{As}_6\text{O}_{42}\{\text{Ni}(\text{en})_2\}]^{4-}$  polyoxoanions have been reported as possessing molecular recognition ability for the chiral  $[\text{Ni}(2,2'\text{-bipy})_3]^{2+}$  guests.

The hydrothermally prepared compound  $[\text{Co}(\text{enMe})_2]_3[\text{V}_{15}\text{As}_6\text{O}_{42}(\text{H}_2\text{O})]\cdot 2\text{H}_2\text{O}$  (Figure 19d, Table 3) is characterised by a 2D structure where each  $[\text{H}_2\text{O}@V_{15}\text{As}_6\text{O}_{42}]^{6-}$  polyoxoanion is coordinated by six  $[\text{Co}(\text{enMe})_2]^{2+}$  moieties which in turn link the neighbouring AsPOVs to each other through  $\text{Co}-\text{O}_{\text{term}}-\text{V}$  bonds.<sup>156</sup> The crystal structure of the hydrothermally synthesised compound  $[\text{Co}(\text{en})_3][\{\text{Co}(\text{en})_2\}_2\text{V}_{15}\text{As}_6\text{O}_{42}]\cdot 4\text{H}_2\text{O}$  (Table 3) shows a 1D infinite chain structure generated by  $\text{Co}-\text{O}_{\text{apical}}-\text{V}$  linkages.<sup>157</sup> The neighbouring  $[\text{V}_{15}\text{As}_6\text{O}_{42}]^{6-}$  polyoxoanions are covalently linked through two six-coordinate cobalt(II) ions of  $\mu_2$ - $\{\text{Co}^{\text{II}}(\text{en})_2\}^{2+}$  moieties; isolated  $[\text{Co}^{\text{II}}(\text{en})_3]^{2+}$  cations reside in interchain regions. This “fully-

reduced" AsPOV exhibits weak antiferromagnetic exchange interactions between the vanadyl moieties.

A  $\{V_{15}As_6\}$ -type polyoxoanion with a higher degree of protonation was found in the hydrothermally synthesised compound  $[Cu(en)_2]_{1.5}[H_3V_{15}As_6O_{42}(H_2O)] \cdot 3H_2O$  (Table 3).<sup>158</sup> In the crystal structure, the "fully-reduced"  $[H_2O@H_3V_{15}As_6O_{42}]^{3-}$  polyoxoanions are bridged by  $[Cu(en)_2]^{2+}$  moieties leading to formation of a 1D sinusoidal chain (Figure 19e). The series of protonated  $[H_3V_{15}As_6O_{42}]^{3-}$  and  $[H_2V_{15}As_6O_{42}]^{4-}$ <sup>153</sup> polyoxoanions was further expanded by a  $[HV_{15}As_6O_{42}]^{5-}$  polyoxoanion as observed in the compound  $[Cu(enMe)_2]_{2.5}[HV_{15}As_6O_{42}(H_2O)] \cdot 2H_2O$  exhibiting antiferromagnetic properties.<sup>136</sup> This compound was prepared hydrothermally (Table 3) and shows a brick-wall-like 2D layer structure where the "fully-reduced"  $[H_2O@HV_{15}As_6O_{42}]^{5-}$  polyoxoanions are doubly-bridged by the  $[Cu(enMe)_2]^{2+}$  moieties.

### 3.2.6 $\{V_{16}As_4\}$ -type polyoxoanion.

The  $\{V_{16}As_4O_{42}\}$  building block of  $D_{2h}$  symmetry, which is derived from the general formula  $[V_{18-z}As_{2z}O_{42}]$  with  $z = 2$ , was isolated hydrothermally as the antiferromagnetic compound  $[Zn_2(dien)_3][\{Zn(dien)\}_2V_{16}As_4O_{42}(H_2O)] \cdot 3H_2O$  (Table 3).<sup>159</sup> Its crystal structure is characterised by 1D chains where the neighbouring, "fully-reduced"  $[H_2O@V_{16}As_4O_{42}]^{8-}$  polyoxoanions are bridged by dual mononuclear  $\{Zn(dien)\}^{2+}$  complexes through Zn–O bonds (Figure 20). The dinuclear  $[Zn_2(dien)_3]^{4+}$  countercations reside in the interchain regions. To point out some structural relationships, this AsPOV can formally be converted, on the one hand, into the  $\{V_{18}O_{42}\}$  archetype by replacing two diagonal handle-like  $\{As_2O_5\}$  groups in the former by two square-pyramidal  $\{VO_5\}$  units *or*, on the other hand, the formal substitution of two diagonal  $\{VO_5\}$  square pyramids – that interlock two eight-membered rings in the  $\{V_{16}As_4O_{42}\}$  building block – by two additional  $\{As_2O_5\}$  groups will result in the polyoxoanion with the composition  $\beta-[V_{14}As_8O_{42}]^{4-}$  ( $z = 4$ ).

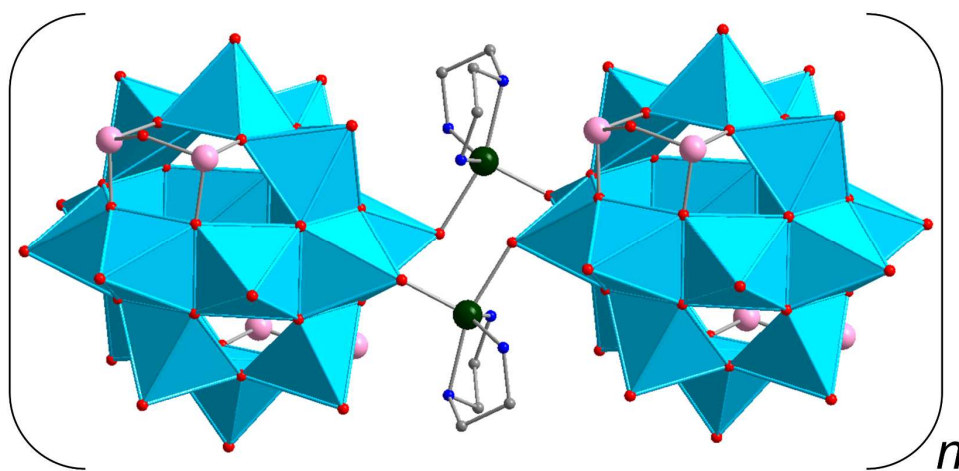


**Figure 20.** Polyhedral representation of a segment of the polymeric structure of  $[\text{Zn}_2(\text{dien})_3][\{\text{Zn}(\text{dien})\}_2\text{V}_{16}\text{As}_4\text{O}_{42}(\text{H}_2\text{O})] \cdot 3\text{H}_2\text{O}$ . Colour code: C, grey; N, blue; As, rose; O, red;  $\text{V}^{\text{IV}}\text{O}_x$ , sky-blue polyhedra; Zn, dark green.

### 3.2.7 POVs with organoarsenate ligands.

**$\{\text{O}_3\text{AsPh}\}/\{\text{O}_4\text{AsPh}\}$ -functionalised AsPOVs.** The vanadium oxide compounds containing phenylarsonate  $(\text{O}_3\text{AsPh})^{2-}$  moieties were first described in the early 1990s. The antiferromagnetic compound  $[\text{V}_2\text{O}_4(\text{PhAsO}_3\text{H})] \cdot \text{H}_2\text{O}$  with a layered mixed-valent ( $\text{V}^{\text{V}}/\text{V}^{\text{IV}}$ ) structure was hydrothermally synthesised and characterised by Huan et al.,<sup>160</sup> while the compound displaying a phenylarsonate POV structure of higher nuclearity was described by Zubieta and colleagues<sup>161,162</sup> The mixed-valent  $[\text{H}_2\{\text{V}^{\text{IV}}_2\text{V}^{\text{V}}_4\text{O}_{10}(\text{O}_3\text{AsPh})_6\}]^{2-}$  polyoxoanion was isolated as the compound  $(\text{N}_n\text{Bu}_4)_2[\text{H}_2\{\text{V}_6\text{O}_{10}(\text{O}_3\text{AsPh})_6\}] \cdot 2\text{H}_2\text{O}$  (Table 3).<sup>161</sup>

Later on, the solvothermally prepared compounds  $(\text{H}_7\text{O}_3)_2(\text{N}_n\text{Bu}_4)_2[(\text{MeOH})_2\text{V}_{12}\text{O}_{14}(\text{OH})_4(\text{O}_3\text{AsPh})_{10}] \cdot \text{H}_2\text{O}$  and  $(\text{NEt}_4)_2[\text{V}_{12}\text{O}_{12}(\text{OH})_2(\text{H}_2\text{O})_4(\text{O}_3\text{AsPh})_{10}(\text{HO}_3\text{AsPh})_4] \cdot 6\text{H}_2\text{O}$  (Table 3) exhibiting, respectively, the nanoscopic organoarsenate POV cages with compositions  $[(\text{MeOH})_2@V_{12}\text{O}_{14}(\text{OH})_4(\text{O}_3\text{AsPh})_{10}]^{4-}$  (with approx.  $D_{2h}$  symmetry) and  $[(\text{H}_2\text{O})_2@V_{12}\text{O}_{12}(\text{OH})_2(\text{H}_2\text{O})_2(\text{O}_3\text{AsPh})_{10}(\text{HO}_3\text{AsPh})_4]^{2-}$  that cannot be derived from the  $\{\text{V}_{18}\text{O}_{42}\}$  archetype.<sup>162</sup> The “fully-reduced”  $[(\text{MeOH})_2@V^{\text{IV}}_{12}\text{O}_{14}(\text{OH})_4(\text{O}_3\text{AsPh})_{10}]^{4-}$  polyoxoanion is built up of edge- and corner-sharing  $\{\text{VO}_5\}$  square pyramids, phenylarsonate tetrahedra and square pyramids and can be regarded as being composed of two  $\{\text{V}^{\text{IV}}_4\text{O}_5(\text{O}_3\text{AsPh})\}$  fragments bridged by two  $\{\text{V}^{\text{IV}}_2\text{O}_2(\text{OH})_2(\text{O}_3\text{AsPh})_4\}^{6-}$  moieties. The dianionic, “fully-reduced” AsPOV  $[(\text{H}_2\text{O})_2@V^{\text{IV}}_{12}\text{O}_{12}(\text{OH})_2(\text{H}_2\text{O})_2(\text{O}_3\text{AsPh})_{10}(\text{HO}_3\text{AsPh})_4]^{2-}$  consists of  $\{\text{VO}_5\}$  square pyramids,  $\{\text{VO}_6\}$  octahedra and phenylarsonate tetrahedra and square pyramids. The structure of this AsPOV is characterised by two  $\{\text{V}^{\text{IV}}_5\text{O}_6(\text{O}_3\text{AsPh})_3\}^{2+}$  fragments bridged by two  $\{\text{V}^{\text{IV}}(\text{OH})(\text{H}_2\text{O})(\text{O}_3\text{AsPh})_2(\text{HO}_3\text{AsPh})_2\}^{3-}$  moieties. The geometric equivalence of the  $\{\text{AsPh}\}^{4+}$  groups to  $\{\text{VO}\}^{3+}$  by virtue of the nearly identical  $\text{As}^{\text{V}}\text{-O}$  and  $\text{V}^{\text{V}}\text{-O}$  bond lengths was stressed by Khan and Zubieta.

In 2011, Zhang and Schmitt reported a unique series of symmetrical nanoscopic vanadium oxide supramolecular coordination cages functionalised with phenylarsonate ligands (Figure 21) and exploited the topologies of their hollow structures together with the template effects of the octahedral  $\{\text{X}_z(\text{H}_2\text{O})_{6-z}\}$  guest assemblies ( $\text{X} = \text{Br}, \text{Cl}$  and  $z = 2, 4, 6$ ).<sup>163</sup> Such “fully-reduced”  $\text{V}^{\text{IV}}$ , mixed-valent  $\text{V}^{\text{V}}/\text{V}^{\text{IV}}$  and fully-oxidised  $\text{V}^{\text{V}}$  AsPOVs characterised by the high-nuclearity  $\{\text{V}_{16}\text{As}_8\}$ ,  $\{\text{V}_{16}\text{As}_{10}\}$ ,  $\{\text{V}_{20}\text{As}_8\}$  and  $\{\text{V}_{24}\text{As}_8\}$  cages were found in the blue compounds  $(\text{HNEt}_3)_2\{\{\text{Br}_2(\text{H}_2\text{O})_4\}(\text{V}^{\text{IV}}\text{O})_{16}(\text{OH})_8(\text{O}_4\text{AsPh})_2(\text{O}_3\text{AsPh})_8\} \cdot 6\text{MeCN}$  and

(HNEt<sub>3</sub>)<sub>2</sub>{[Cl<sub>2</sub>(H<sub>2</sub>O)<sub>4</sub>](V<sup>IV</sup>O)<sub>16</sub>(OH)<sub>8</sub>(O<sub>4</sub>AsPh)<sub>2</sub>(O<sub>3</sub>AsPh)<sub>8</sub>}]·2H<sub>2</sub>O as well as the green compounds

$$\text{H}_5\{[\text{Cl}_4(\text{H}_2\text{O})_2](\text{V}^{\text{V}}\text{O})_{16}\text{O}_{16}(\text{O}_3\text{AsPh})_8\}\text{Cl}\cdot 4\text{H}_2\text{O}\cdot 3\text{MeCN},$$

$$[\{\text{Cl}_4(\text{H}_2\text{O})_2\}(\text{V}^{\text{V}}\text{O})_{16}(\text{V}^{\text{IV}}\text{O})_4\text{O}_{16}(\text{OH})_4(\text{O}_3\text{AsPh})_8]\cdot 7\text{H}_2\text{O}\cdot 3\text{MeCN}$$

and H<sub>10</sub>{[Cl<sub>6</sub>](V<sup>V</sup>O)<sub>16</sub>(V<sup>IV</sup>O)<sub>8</sub>O<sub>24</sub>(O<sub>3</sub>AsPh)<sub>8</sub>]Cl<sub>4</sub>·10H<sub>2</sub>O·2MeCN (Table 3). Their structures contain four- (O<sub>3</sub>AsPh) or five-fold (O<sub>4</sub>AsPh) coordinated As<sup>V</sup> centres. The isomeric, “fully-reduced” {V<sub>16</sub>As<sub>10</sub>} cages in the blue compounds consist of sixteen {VO<sub>5</sub>} square-pyramids and ten fully deprotonated phenylarsonate ligands. Their AsPOV building block represents a modified [V<sub>18</sub>O<sub>42</sub>]<sup>12-</sup> structure in which two {VO<sub>5</sub>} caps on one diagonal are replaced with two {O<sub>4</sub>AsPh} moieties and two groups by four {O<sub>3</sub>AsPh} moieties slice the structure horizontally to isolate an eight-membered {VO<sub>5</sub>}-belt (Figure 21, top). The key structural difference between the {V<sub>16</sub>As<sub>10</sub>} cages accommodating octahedral {Br<sub>2</sub>(H<sub>2</sub>O)<sub>4</sub>} and {Cl<sub>2</sub>(H<sub>2</sub>O)<sub>4</sub>} guest templates in their inner voids is that the two convex {V<sup>IV</sup><sub>4</sub>O<sub>5</sub>(O<sub>3</sub>AsPh)} moieties in the Cl-containing AsPOV are rotated by 45° (isomer 2). This structural change is the result of the considerably different ionic radii of Br<sup>-</sup> and Cl<sup>-</sup> ions and the energies of V···Br and V···Cl interactions. The encapsulated symmetrical {Br<sub>2</sub>(H<sub>2</sub>O)<sub>4</sub>} and {Cl<sub>2</sub>(H<sub>2</sub>O)<sub>4</sub>} octahedra with the Br<sup>-</sup> and Cl<sup>-</sup> ions situated in the apical positions show Br···H<sub>2</sub>O and Cl···H<sub>2</sub>O distances ranging from 3.13 to 3.36 Å and from 3.03 to 3.18 Å, respectively. In addition, Br···Br distance of 5.28 Å is slightly shorter than the Cl···Cl distance of 5.31 Å. The intramolecular V···Br and V···Cl separations are between 3.47 and 3.51 Å. It was concluded that the nature and geometry of these octahedral guest assemblies determines the nuclearity, size, and topology of the produced organoarsenate POV cages.

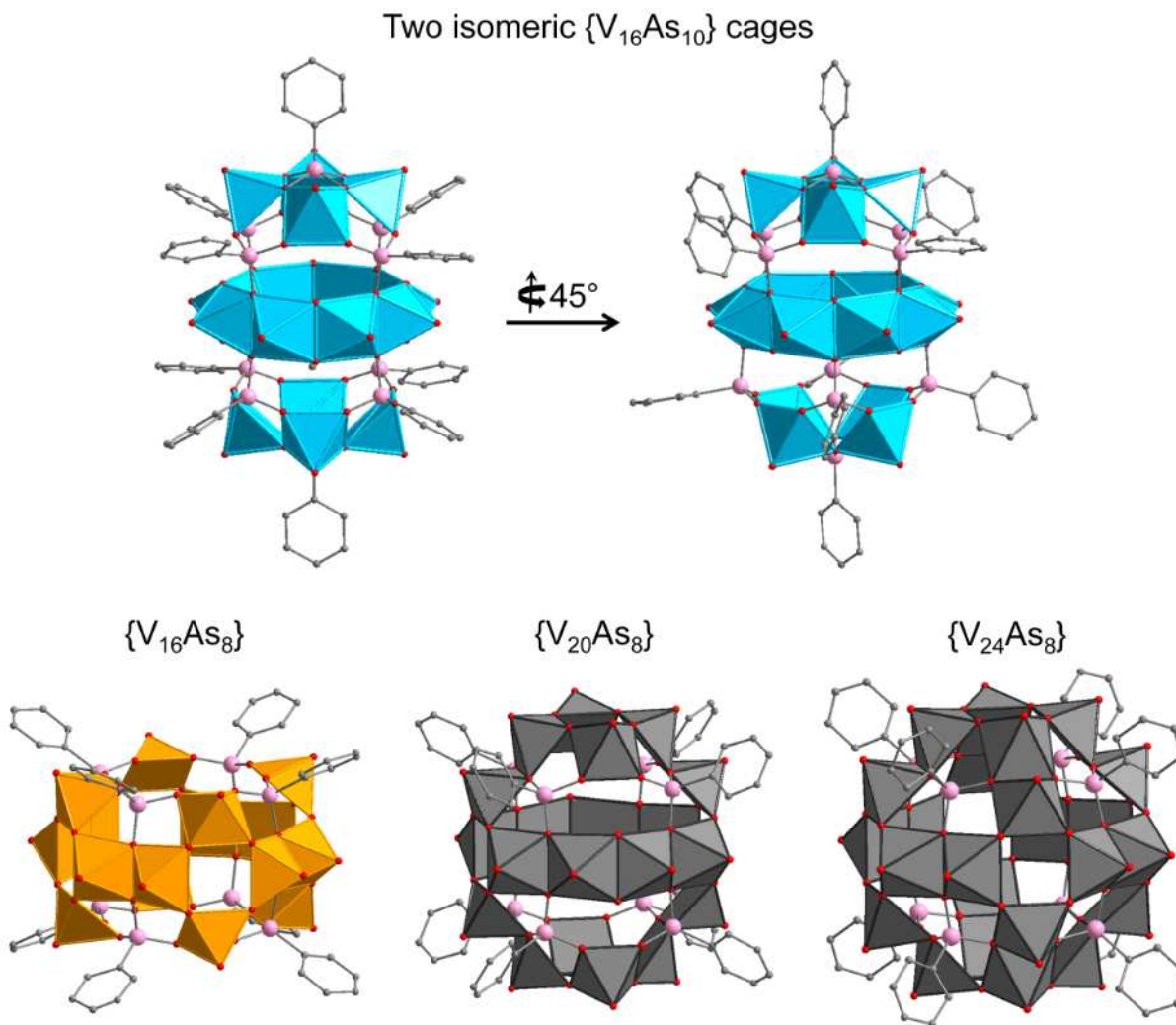


**Figure 21.** Polyhedral representations of the “fully-reduced”  $\{V_{16}As_{10}\}$ -nuclearity AsPOVs (top) as well as the fully-oxidised  $\{V_{16}As_8\}$ -nuclearity AsPOV, and the mixed-valent  $\{V_{20}As_8\}$ - and  $\{V_{24}As_8\}$ -nuclearity AsPOVs (bottom). Encapsulated octahedral guest assemblies are omitted for clarity. Colour code: C, grey; As, rose; O, red;  $V^{IV}O_x$ , sky-blue polyhedra;  $V^VO_x$ , light-orange polyhedra;  $V^V/V^{IV}O_x$ , dark-grey polyhedra.

The fully-oxidised  $\{V_{16}As_8\}$ - and mixed-valent  $\{V_{20}As_8\}$ - and  $\{V_{24}As_8\}$ -type building blocks (Figure 21, bottom) of the above-mentioned green compounds were synthesised using  $Dy(NO_3)_3 \cdot nH_2O$  ( $n \approx 6$ ), where presumably nitrate acts as an oxidant, different quantities of which was shown to influence the nuclearity of these AsPOV cages and the formal oxidation states of their V atoms. Thus, a gradual increase in the amount of the oxidant led ultimately to the fully-oxidised  $\{V_{16}As_8\}$ -nuclearity cage. The molecular structures of these three AsPOVs are constructed of sixteen, twenty and twenty-four edge- and corner-sharing  $\{VO_5\}$  square-pyramids, respectively. Each POV shell is ligated by eight phenylarsonate groups. The  $\{V_{16}As_8\}$ -toroid cage encapsulates an octahedral  $\{Cl_4(H_2O)_2\}$  guest template, in which the closest  $Cl \cdots Cl$  /  $Cl \cdots H_2O$  distances amount to 3.97 Å / 3.41 Å. The intramolecular  $V \cdots Cl$  separations range from 2.82 Å to 3.02 Å. The  $\{V_{20}As_8\}$  cage can be seen as the



toroidal structure of  $\{V_{16}As_8\}$  decorated with two  $\{(V^{IV}O)_2(\mu_2-OH)_2\}$  units and is stabilised by the  $\{Cl_4(H_2O)_2\}$  assembly as well. The  $Cl\cdots Cl$  and  $Cl\cdots H_2O$  distances in this  $\{Cl_4(H_2O)_2\}$  octahedron are 3.98 Å and 3.24 – 3.80 Å, respectively. The closest intramolecular  $V\cdots Cl$  distances lie in the range 2.81 – 3.10 Å. The two encapsulated  $H_2O$  molecules and the  $V$  ions of the  $\{(V^{IV}O)_2(\mu_2-OH)_2\}$  entities are involved in  $V\cdots O_{water}$  interactions at a distances of 2.36 Å. The  $\{V_{24}As_8\}$  cage encapsulates a  $\{Cl_6\}$  aggregate with  $d_{Cl\cdots Cl} = 3.91 - 4.01$  Å the vertices of which are capped by six square  $\{V_4O_8\}$  fragments with electrophilic inner and nucleophilic outer environments. The closest  $V\cdots Cl$  separations are in the range 2.94 – 3.033 . The Archimedean body  $\{V_{24}\}$  polyhedron (14 faces, 36 edges, 24 vertices) deduced from the mixed-valent  $\{(V^{IV}O)_{16}(V^{V}O)_8O_{24}(O_3AsPh)_8\}$  fragment that can be regarded as a Keplerate displays a truncated octahedral topology. The  $\{V_{24}\}$  polyhedron in the  $\{V_{24}As_8\}$  cage can thus be classified as one of the thirteen Archimedean solids.<sup>164</sup> The vanadium skeletons of some of the discussed organoarsenate POV cages are illustrated in Figure 22.

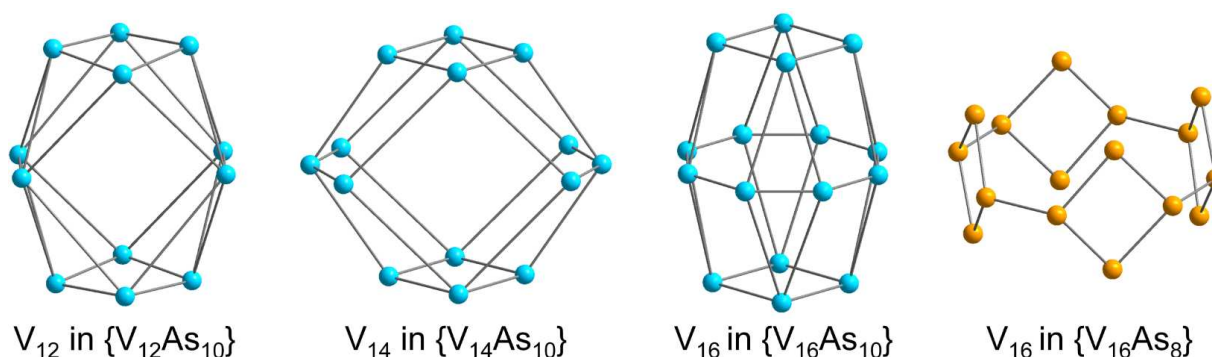


**Figure 22.** Topological representations of the vanadium skeletons deduced from some high-nuclearity organoarsenate POV cages represented in Figures 18 and 20. Colour code:  $V^{IV}$ , sky blue;  $V^V$ , light orange.

**$\{O_3AsC_6H_4-4-NH_2\}$ -functionalised AsPOVs.** The group of Schmitt also reported two nanoscopic cages with compositions  $[V_{14}O_{16}(OH)_8(O_3AsC_6H_4-4-NH_2)_{10}]^{4-}$  (Figure 23), which shows a defect AsPOV structure from the  $\{V_{16}As_{10}\}$ -nuclearity cage (isomer 1, Figure 21), and  $[V_{10}O_{18}(O_3AsC_6H_4-4-NH_2)_7(DMF)_2]^{5-}$ .<sup>165</sup> The compounds based on these AsPOVs were isolated from the condensation reactions under reducing conditions in aqueous solution (Table 3). The different nature of acids (HCl and  $HNO_3$ ) used in the synthesis of these compounds strongly influenced the nuclearity of the cages, resulting in the  $\{V_{14}As_{10}\}$ - and  $\{V_{10}As_7\}$ -type polyoxoanions, respectively. In contrast to the  $\{O_3AsPh\}/\{O_4AsPh\}$ -functionalised AsPOVs, the POV shells of these polyoxoanions are decorated with terminal (4-aminophenyl)arsonate ligands  $\{O_3AsC_6H_4-4-NH_2\}$ . Their skeleton structures are composed exclusively of  $\{VO_5\}$  square-pyramids. Whereas the electrophilic void of the

“fully-reduced”  $\{V_{14}As_{10}\}$  cage (dimensions:  $5.8 \times 5.9 \times 5.9 \text{ \AA}$ ) with an almost ideal cubic arrangement of the As atoms contains two  $Cl^-$  ions and four  $H_2O$  molecules forming a stabilising octahedral assembly, the mixed-valent asymmetric  $\{V_{10}As_7\}$  cage is characterised by a hexagonal packing due to the amine functionalities engaged in hydrogen bonds in the structure.

The  $[V_{12}O_{14}(OH)_4(O_3AsC_6H_4-4-NH_2)_{10}]^{4-}$  polyoxoanion with the  $V^{IV}/\text{arsonate}$  nuclearity  $[12(VO_5) : 10(O_3AsR)]$ , lower than that  $[14(VO_5) : 10(O_3AsR)]$  of the above-mentioned  $[V_{14}O_{16}(OH)_8(O_3AsC_6H_4-4-NH_2)_{10}]^{4-}$  polyoxoanion, was isolated as the compound  $Na_4(H_2O)_{10}[\{V_{12}O_{14}(OH)_4(H_2O)_3(O_3AsC_6H_4-4-NH_2)_{10}\}] \cdot 1.5DMF \cdot 1.25H_2O$  (Table 3) from a condensation reaction involving *p*-arsanilic acid in a  $H_2O$ /dimethylformamide (DMF) mixture.<sup>166</sup> The main structural difference between these two AsPOVs (Figure 22) is the number of the  $\{VO_5\}$  square pyramids sandwiched between two tetranuclear  $\{LV^{IV}_4O_{12}\}$  subunits where L is the (4-aminophenyl)arsonate ligand. The  $\{V_{14}As_{10}\}$  cage comprises two separated hydroxy-bridged  $\{O_4V^{IV}(OH)_2V^{IV}(OH)_2V^{IV}O_4\}$  trimers, whilst the  $\{V_{12}As_{10}\}$  cage has only two separated, partially hydrated  $\{O_4V^{IV}(OH)_2V^{IV}O_4\}$  dimers. The  $\{VO_5\}$  square pyramids in the belt of each of these molecular cages are connected to two tetranuclear  $\{LV^{IV}_4O_{12}\}$  subunits via additional eight (4-aminophenyl)arsonate ligands (Figure 23). The synthesis and structural characterisation of the compound  $Na_5[V_5O_9(O_3AsC_6H_4-4-NH_2)_4] \cdot 20.5H_2O \cdot 3DMF$  with the low-nuclearity inorganic–organic calix-type building block  $[V_5O_9(O_3AsC_6H_4-4-NH_2)_4]^{5-}$  comprising mixed-valent  $V^V/V^{IV}$  atoms were described as well (Table 3).<sup>166</sup> The preliminary magnetic studies performed for these two compounds showed the presence of antiferromagnetic exchange interactions and  $S = 0$  ground states.



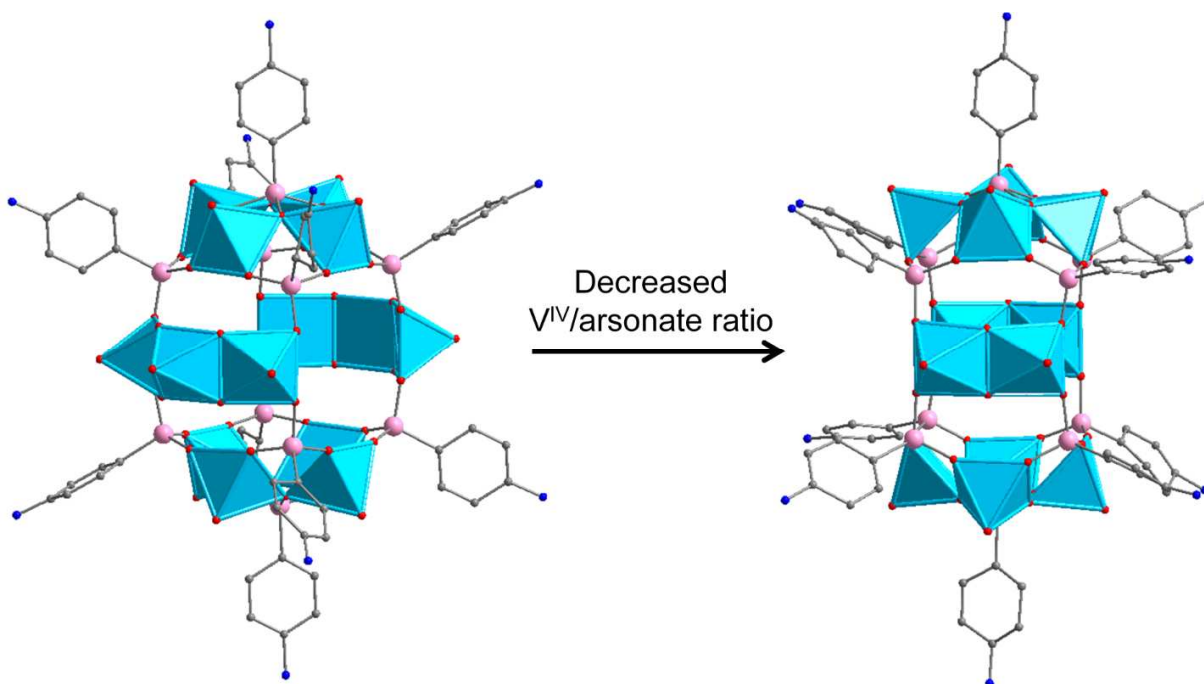


**Figure 23.** The “fully-reduced”  $[V^{IV}_{14}O_{16}(OH)_8(O_3AsC_6H_4-4-NH_2)_{10}]^{4-}$  (left) and  $[V^{IV}_{12}O_{14}(OH)_4(O_3AsC_6H_4-4-NH_2)_{10}]^{4-}$  (right) AsPOVs. H omitted for clarity. Colour code: C, grey; N, blue; As, rose; O, red;  $V^{IV}O_x$ , sky-blue polyhedra.

An example of the  $\{O_3AsC_6H_4-4-NH_2\}$ -functionalised AsPOV with a quasi-planar, polycyclic-type structure was also reported. The fully-oxidised  $[V^V_{10}O_{24}(O_3AsC_6H_4-4-NH_2)_3]^{4-}$  (Figure 24a) polyoxoanion was isolated as the compound  $(N_nBu_4)_2(NH_4)_2[V_{10}O_{24}(O_3AsC_6H_4-4-NH_2)_3]$  (Table 3).<sup>161</sup> The structure of this AsPOV can be regarded as a  $[V_9O_{21}(O_3AsC_6H_4-4-NH_2)_3]^{3-}$  toroid that encloses a  $\{VO_3\}^-$  unit in the centre of the wheel. The most unique feature of  $[V^V_{10}O_{24}(O_3AsC_6H_4-4-NH_2)_3]^{4-}$  is that it contains a wheel-type  $[V_7O_{24}]^{13-}$  substructure (Figure 24b). Remarkably, the structure of this heptanuclear  $[V_7O_{24}]^{13-}$  polyoxoanion displays striking similarities to the Anderson-type structures, e.g. of  $[TeM_6O_{24}]^{6-}$ ,<sup>167</sup>  $[M_7O_{24}]^{6-}$  ( $M = Mo, W$ ),<sup>168</sup> and  $[Bi_7I_{24}]^{3-}$ .<sup>169</sup> (Figure 24c). The overall composition of  $[V^V_{10}O_{24}(O_3AsC_6H_4-4-NH_2)_3]^{4-}$  formally consists of a double layer of polyhedra (bicapped Anderson type), with the one being composed of  $[V_7O_{24}]^{13-}$  and the second, of a  $[V_3(RAsO_3)_3]^{9+}$  ring. Another interesting feature is that it can be reversibly reduced by one electron to give the green-brown compound with composition  $[V_{10}O_{24}(O_3AsC_6H_4-4-NH_2)_3]^{5-}$ . According to electrochemical and magnetic measurements, this compound as well as the aforementioned  $(N_nBu_4)_2[H_2\{V_6O_{10}(O_3AsPh)_6\}] \cdot 2H_2O$ <sup>161</sup> are characterised by extensive electron storage and coupled electron-proton transfer processes.

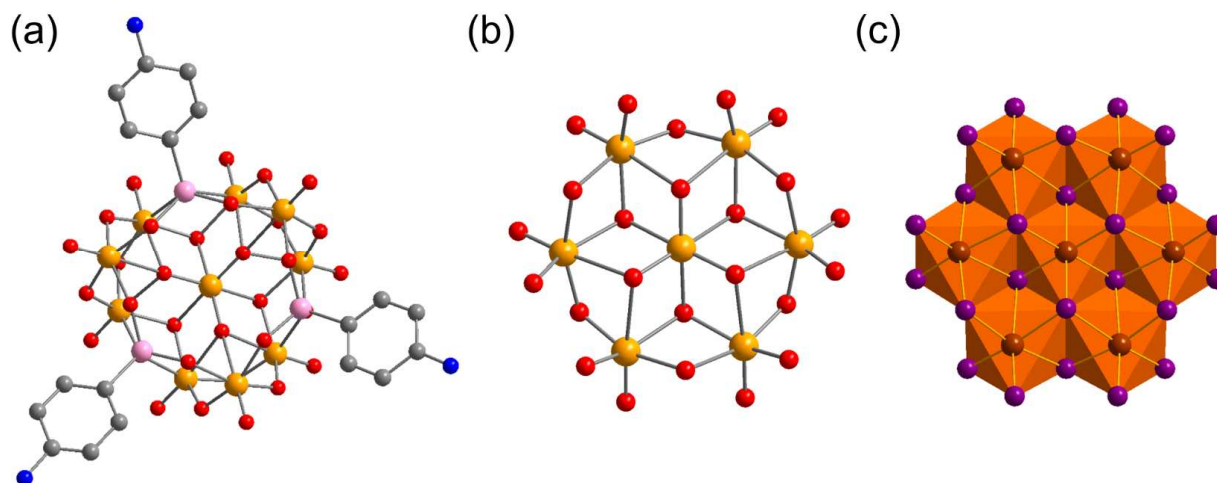


**Figure 24.** The fully-oxidised  $[V_{10}O_{24}(O_3AsC_6H_4-4-NH_2)_3]^{4-}$  polyoxoanion (a), its  $[V_7O_{24}]^{13-}$  core (b), and the structurally related  $[Bi_7I_{24}]^{3-}$  polyiodoanion (c). Colour code: C, grey; N, blue; As, rose; O, red;  $V^V$ , light orange; Bi, brown; I, violet.

### 3.2.8 Corollary for AsPOVs.

The AsPOVs discussed so far exhibit various symmetries as exemplified by  $[V^{IV}_8V^V_4As_8O_{40}]^{5-}$  and  $\beta-[V^{IV}_{14}As_8O_{42}]^{4-}$  with  $D_{4h}$ ,  $\alpha-[V^{IV}_{14}As_8O_{42}]^{4-}$  with  $D_{2d}$ ,  $[H_3KV^{IV}_4V^V_8As_3O_{39}(AsO_4)]^{6-}$  with  $C_3$ ,  $[V^{IV}_{14}As_8O_{42}]^{4-}$  with  $S_4$ ,  $[V^{IV}_{15}As_6O_{42}]^{6-}$  with  $D_3$ , and  $[V^{IV}_{16}As_4O_{42}]^{8-}$  with  $D_{2h}$ . Fully-oxidised, mixed-valent and “fully-reduced” AsPOVs with As atoms in their formal oxidation states of +3 and, more rarely, +5, were reported to date. AsPOVs a variety of structural motifs, ranging from spherical-shaped to wheel-type structures. Dimensionalities from 0D (isolated AsPOVs) to 3D were observed in the solid state. The AsPOVs easily undergo transition metal functionalisation, resulting in novel inorganic-organic frameworks where multidentate organoamines are very commonly captured by transition metal ions introduced into the backbones of the AsPOVs. The hydrogen bonds characteristically expand the dimensionality of the AsPOV structures into 3D networks.

The discovery of the seminal  $[H_2O@V^{IV}_{15}As_6O_{42}]^{6-}$  polyoxoanion<sup>151</sup> that was shown to act as a textbook example for quantum spin frustration and as a qubit with relatively long coherence lifetimes paved the way for studies focussed on the optical, electronic and magnetic properties of other *iso*- and *hetero*POVs. The nanoscale magnetism of this  $\{V_{15}\}$ -type AsPOV with a symmetrical layer structure of spin centres and spin frustration effects in the central  $V^{IV}$  triangle is now well-documented. The  $[H_2O@V^{IV}_{15}As_6O_{42}]^{6-}$  polyoxoanion is a low-spin (spin-1/2) molecular nanomagnet and its characteristics were explored extensively: non-adiabatic Landau-Zener transitions,<sup>170</sup> low-energy spin excitations by elastic neutron scattering study of  $K_6[V_{15}As_6O_{42}] \cdot 9D_2O$ ,<sup>171</sup> low-energy excitations from proton NMR and

$\mu$ SR,<sup>172</sup> adiabatic Landau-Zener-Stückelberg transitions with or without dissipation,<sup>173</sup> mechanism of ground-state selection,<sup>174</sup> local spin moment configuration determined by NMR,<sup>175</sup> static magnetisation at ultra-low temperatures,<sup>176</sup> quantum oscillations,<sup>177</sup> and direct spin-phonon transitions.<sup>178</sup> In general, such AsPOVs show extraordinary magnetic properties and can be used as models to study different fundamental phenomena as e.g. spin frustration<sup>179</sup> and frustrated spin coupling, spin-phonon bottlenecks and butterfly hysteresis,<sup>180</sup> Dzyaloshinsky-Moria interactions and other splitting effects,<sup>181</sup> molecular-scale switching,<sup>182</sup> quantum-spin tunnelling, spin coherence and low-temperature spin relaxation processes.<sup>183</sup>

**Table 3.** Selected details of synthesis and characterisation of **AsPOV**-based compounds.

Formula	Colour	Characteristics of crystal structure <sup>a</sup>	Reactants	Reaction conditions	Yield	Characterised via	Ref.
<b>V<sub>5</sub></b>							
Na <sub>5</sub> [V <sub>5</sub> O <sub>9</sub> (O <sub>3</sub> AsC <sub>6</sub> H <sub>4</sub> -4-NH <sub>2</sub> ) <sub>4</sub> ]·20.5H <sub>2</sub> O·3DMF	green		NaVO <sub>3</sub> , NaN <sub>3</sub> , <i>p</i> -arsanilic acid, H <sub>2</sub> O, DMF, N <sub>2</sub> H <sub>4</sub> ·H <sub>2</sub> O, HCl	70 °C, pH = 7.3	82%	EA, IR, UV-vis, single-crystal XRD	166
<b>V<sub>6</sub></b>							
(N <sub><i>n</i></sub> Bu <sub>4</sub> ) <sub>4</sub> [V <sub>6</sub> As <sub>8</sub> O <sub>26</sub> ]	bright green		NaVO <sub>3</sub> , H <sub>2</sub> O, NaAsO <sub>2</sub> , N <sub>2</sub> H <sub>4</sub> , <i>n</i> Bu <sub>4</sub> NBr	r.t.	50% based on As	EA, IR, TGA, single-crystal XRD, magnetometry	137
(N <sub><i>n</i></sub> Bu <sub>4</sub> ) <sub>2</sub> [H <sub>2</sub> {V <sub>6</sub> O <sub>10</sub> (O <sub>3</sub> AsPh) <sub>6</sub> }]·2H <sub>2</sub> O	dark green		PhAsO <sub>3</sub> H <sub>2</sub> , (NH <sub>4</sub> ) <sub>2</sub> Na <sub>2</sub> K <sub>2</sub> [V <sub>10</sub> O <sub>28</sub> ], (TBA)Br, MeOH, MeCN, pentane, Et <sub>2</sub> O, isopropanol	reflux, 40 min → 4 d	65%	EA, IR, UV-vis, electrochemistry, magnetometry, single-crystal XRD	161
<b>V<sub>10</sub></b>							
[V <sub>10</sub> As <sub>2</sub> O <sub>26</sub> (H <sub>2</sub> O)]·8H <sub>2</sub> O	dark green	3D network	V <sub>2</sub> O <sub>5</sub> , H <sub>3</sub> AsO <sub>4</sub> , H <sub>2</sub> C <sub>2</sub> O <sub>4</sub> , H <sub>2</sub> O, en	160 °C, 3 d, pH = 8	40% based on V	EA, IR, TGA, EPR, powder XRD, single-crystal XRD, magnetometry	118
H <sub>5</sub> [V <sub>10</sub> O <sub>18</sub> (O <sub>3</sub> AsC <sub>6</sub> H <sub>4</sub> -4-NH <sub>2</sub> ) <sub>7</sub> (DMF) <sub>2</sub> ]·7DMF·5H <sub>2</sub> O	green	hexagonal packing arrangement	NaVO <sub>3</sub> , ( <i>p</i> -aminophenyl)arsonic acid, H <sub>2</sub> O, DMF, HNO <sub>3</sub> , N <sub>2</sub> H <sub>4</sub> ·H <sub>2</sub> O	70 °C, 30 min, pH = 4	35%	EA, IR, DTA-TG, powder XRD, single-crystal XRD	165
(N <sub><i>n</i></sub> Bu <sub>4</sub> ) <sub>2</sub> (NH <sub>4</sub> ) <sub>2</sub> [V <sub>10</sub> O <sub>24</sub> (O <sub>3</sub> AsC <sub>6</sub> H <sub>4</sub> -4-NH <sub>2</sub> ) <sub>3</sub> ]	red		(TBA)Br, arsanilic acid, MeOH, (NH <sub>4</sub> ) <sub>2</sub> Na <sub>2</sub> K <sub>2</sub> [V <sub>10</sub> O <sub>28</sub> ]	reflux, 20 min → 4 °C, 20 h	45%	EA, IR, UV-vis, <sup>51</sup> V NMR, EPR, electrochemistry, single-crystal XRD	161

**V<sub>12</sub>**

(NH <sub>4</sub> ) <sub>4</sub> [V <sub>12</sub> As <sub>8</sub> O <sub>40</sub> (H <sub>2</sub> O)]·4H <sub>2</sub> O	dark green		NH <sub>4</sub> VO <sub>3</sub> , As <sub>2</sub> O <sub>3</sub> , ethyl ether (or EtOH), H <sub>2</sub> O	80 °C, 7 d	20% based on V	EA, IR, ESI-MS, TG-MS, UV-vis, powder XRD, single-crystal XRD	122
(NHEt <sub>3</sub> ) <sub>4</sub> [V <sub>12</sub> As <sub>8</sub> O <sub>40</sub> (H <sub>2</sub> O)]·H <sub>2</sub> O	dark blue		NaVO <sub>3</sub> , As <sub>2</sub> O <sub>3</sub> , NHEt <sub>3</sub> Cl, H <sub>2</sub> O, N <sub>2</sub> H <sub>4</sub> ·HCl, HCl	24 °C, 2-3 d, pH = 6.0	29% based on V	IR, magnetometry, powder XRD, single-crystal XRD, INS	121
(NHEt <sub>3</sub> ) <sub>2</sub> (NH <sub>2</sub> Me <sub>2</sub> )[V <sub>12</sub> As <sub>8</sub> O <sub>40</sub> (HCO <sub>2</sub> )] <sub>2</sub> ·2H <sub>2</sub> O, Na <sub>5</sub> [V <sub>12</sub> As <sub>8</sub> O <sub>40</sub> (HCO <sub>2</sub> )] <sub>2</sub> ·18H <sub>2</sub> O	deep green, deep blue		NaVO <sub>3</sub> ·2H <sub>2</sub> O, As <sub>2</sub> O <sub>3</sub> , N <sub>2</sub> H <sub>4</sub> ·HCl, <i>N,N</i> -dimethylformamide			EA, IR, UV-vis, TGA, magnetometry, single-crystal XRD	119
Na <sub>4</sub> [V <sub>12</sub> As <sub>8</sub> O <sub>40</sub> (H <sub>2</sub> O)]·23H <sub>2</sub> O	dark blue		NaVO <sub>3</sub> , As <sub>2</sub> O <sub>3</sub> , H <sub>2</sub> O, N <sub>2</sub> H <sub>4</sub> ·H <sub>2</sub> SO <sub>4</sub> , HCl	4 °C, 2-3 d, pH = 6.0	53% based on V	IR, magnetometry, powder XRD, single-crystal XRD, INS	121
Na <sub>4</sub> [V <sub>12</sub> As <sub>8</sub> O <sub>40</sub> (D <sub>2</sub> O)]·16.5D <sub>2</sub> O			NaVO <sub>3</sub> , As <sub>2</sub> O <sub>3</sub> , D <sub>2</sub> O, N <sub>2</sub> H <sub>4</sub> ·H <sub>2</sub> SO <sub>4</sub> , DCl	4 °C, 2-3 d, pH = 6.0		IR, magnetometry, powder XRD, single-crystal XRD, INS	121
K <sub>3</sub> [H <sub>12</sub> V <sub>12</sub> O <sub>36</sub> (AsO) <sub>2</sub> (AsO <sub>4</sub> )]·12H <sub>2</sub> O	dark green		NaVO <sub>3</sub> , As <sub>2</sub> O <sub>3</sub> , H <sub>2</sub> O, H <sub>2</sub> NC(CH <sub>2</sub> OH) <sub>3</sub> , KSCN, H <sub>2</sub> SO <sub>4</sub>	70 °C, 22 h, pH = 4.6	25% based on V	EA, IR, TGA, single-crystal XRD	116
K <sub>6</sub> [H <sub>3</sub> KV <sub>12</sub> As <sub>3</sub> O <sub>39</sub> (AsO <sub>4</sub> )]·8H <sub>2</sub> O	black grey	zig-zag chain	KVO <sub>3</sub> , H <sub>2</sub> O, As <sub>2</sub> O <sub>5</sub> ·5H <sub>2</sub> O, KSCN, H <sub>2</sub> SO <sub>4</sub>	1 h, 90 °C, pH = 3		EA, IR, EPR, magnetometry, single-crystal XRD	115
(NEt <sub>4</sub> ) <sub>2</sub> [V <sub>12</sub> O <sub>12</sub> (OH) <sub>2</sub> (H <sub>2</sub> O) <sub>4</sub> (O <sub>3</sub> AsPh) <sub>10</sub> (HO <sub>3</sub> AsPh) <sub>4</sub> ]·6H <sub>2</sub> O	light green		(N <sub>n</sub> Bu <sub>4</sub> ) <sub>3</sub> [H <sub>3</sub> V <sub>10</sub> O <sub>28</sub> ], PhAsO <sub>3</sub> H <sub>2</sub> , Et <sub>4</sub> NCl, MeOH/H <sub>2</sub> O	100 °C, 17 h → 120 °C, 3 d	30% based on V	EA, IR, TGA, single-crystal XRD	162
(H <sub>7</sub> O <sub>3</sub> ) <sub>2</sub> (N <sub>n</sub> Bu <sub>4</sub> ) <sub>2</sub> [(MeOH) <sub>2</sub> V <sub>12</sub> O <sub>14</sub> (OH) <sub>4</sub> (O <sub>3</sub> AsPh) <sub>10</sub> ]·H <sub>2</sub> O	light green		(N <sub>n</sub> Bu <sub>4</sub> ) <sub>3</sub> [H <sub>3</sub> V <sub>10</sub> O <sub>28</sub> ], PhAsO <sub>3</sub> H <sub>2</sub> , MeOH/H <sub>2</sub> O	100 °C, 17 h → 120 °C, 3 d	20% based on V	EA, IR, TGA, single-crystal XRD	162

$\text{Na}_4(\text{H}_2\text{O})_{10}[\{\text{V}_{12}\text{O}_{14}(\text{OH})_4(\text{H}_2\text{O})_3(\text{O}_3\text{AsC}_6\text{H}_4-4\text{-NH}_2)_{10}\}] \cdot 1.5\text{DMF} \cdot 1.25\text{H}_2\text{O}$	blue		$\text{NaVO}_3$ , $\text{NaN}_3$ , <i>p</i> -arsanilic acid, $\text{H}_2\text{O}$ , DMF, $\text{N}_2\text{H}_4 \cdot \text{H}_2\text{O}$ , HCl	70 °C, pH = 4.9	43%	EA, IR, UV-vis, single-crystal XRD	166
$[\text{Zn}(\text{en})_2]_2[\text{Zn}_2(\text{bpe})_2\text{V}_{12}\text{As}_8\text{O}_{40}(\text{H}_2\text{O})]$	brown	1D straight chain	$\text{NH}_4\text{VO}_3$ , $\text{As}_2\text{O}_3$ , $\text{ZnCl}_2 \cdot 7\text{H}_2\text{O}$ , bpe, en, $\text{HNO}_3$ , $\text{H}_2\text{O}$	170 °C, 7d	59% based on V	EA, FT-IR, TGA, CV, single-crystal XRD	125
$\{[\text{Zn}(\text{dien})]_2(\text{dien})_2[\text{Zn}_2\text{V}_{12}\text{As}_8\text{O}_{40}(0.5\text{H}_2\text{O})]\}_2 \cdot 6\text{H}_2\text{O}$		cluster dimers	$\text{V}_2\text{O}_5$ , $\text{As}_2\text{O}_3$ , $\text{H}_2\text{O}$ , $\text{Zn}(\text{OAc})_2 \cdot 4\text{H}_2\text{O}$ , dien	160 °C, 3 d	36% based on $\text{V}_2\text{O}_5$	EA, IR, single-crystal XRD	124
$\{[\text{Zn}(\text{enMe})_2]_2(\text{enMe})_2[\text{Zn}_2\text{V}_{12}\text{As}_8\text{O}_{40}(\text{H}_2\text{O})]\}_2 \cdot 4\text{H}_2\text{O}$	brown		$\text{V}_2\text{O}_5$ , $\text{As}_2\text{O}_3$ , enMe, $\text{Zn}(\text{OAc})_2 \cdot 4\text{H}_2\text{O}$ , $\text{H}_2\text{O}$	180 °C, 7 d	76% based on V	EA, IR, TGA, EPR, magnetometry, single-crystal XRD	123
$[\text{Zn}(\text{enMe})_2]_2[(4,4'\text{-bipy})\text{Zn}_2\text{V}_{12}\text{As}_8\text{O}_{40}(\text{H}_2\text{O})]$	brown	1D straight chain	$\text{NH}_4\text{VO}_3$ , $\text{As}_2\text{O}_3$ , $\text{ZnCl}_2 \cdot 7\text{H}_2\text{O}$ , 4,4'-bipy, enMe, $\text{HNO}_3$ , $\text{H}_2\text{O}$	170 °C, 5 d	60% based on V	EA, FT-IR, TGA, CV, magnetometry, single-crystal XRD	126
$[\text{Zn}(\text{en})_2(\text{H}_2\text{O})][\text{Zn}(\text{en})_2(4,4'\text{-bipy})\text{Zn}_2\text{V}_{12}\text{As}_8\text{O}_{40}(\text{H}_2\text{O})] \cdot 3\text{H}_2\text{O}$	brown	1D sinuate chain	$\text{NH}_4\text{VO}_3$ , $\text{As}_2\text{O}_3$ , $\text{ZnCl}_2 \cdot 7\text{H}_2\text{O}$ , 4,4'-bipy, en, $\text{HNO}_3$ , $\text{H}_2\text{O}$	170 °C, 5 d	30% based on V	EA, FT-IR, TGA, CV, single-crystal XRD	126
$\{[\text{Zn}(\text{en})_3]_2[\text{Zn}_2\text{V}_{12}\text{As}_8\text{O}_{40}(\text{H}_2\text{O})]\}_2 \cdot 4\text{H}_2\text{O} \cdot 0.25\text{bipy}$	brown	eight-shaped chiral helix	$\text{NH}_4\text{VO}_3$ , $\text{As}_2\text{O}_3$ , $\text{ZnCl}_2 \cdot 7\text{H}_2\text{O}$ , 4,4'-bipy, en, $\text{HNO}_3$ , $\text{H}_2\text{O}$	170 °C, 5 d	39% based on V	EA, FT-IR, TGA, CV, single-crystal XRD	126
$[\text{Zn}_2(\text{en})_5][\{\text{Zn}(\text{en})_2\}(\text{bpe})\text{HZn}_2\text{V}_{12}\text{As}_8\text{O}_{40}(\text{H}_2\text{O})]_2 \cdot 7\text{H}_2\text{O}$	brown	2D network	$\text{NH}_4\text{VO}_3$ , $\text{As}_2\text{O}_3$ , $\text{ZnCl}_2 \cdot 7\text{H}_2\text{O}$ , bpe, en, $\text{HNO}_3$ , $\text{H}_2\text{O}$	170 °C, 5 d	37% based on V	EA, FT-IR, TGA, CV, UV-Vis, magnetometry, single-crystal XRD	126
$[\text{Cd}(\text{en})_2]_2[\text{Cd}_2(\text{en})_2\text{V}_{12}\text{As}_8\text{O}_{40}]$	brown	1D chain	$\text{V}_2\text{O}_5$ , $\text{As}_2\text{O}_3$ , en, $\text{H}_2\text{O}$ , $\text{Cd}(\text{OAc})_2 \cdot 2\text{H}_2\text{O}$	180 °C, 6 d	52% based on V	EA, IR, TGA, EPR, magnetometry, powder XRD, single-crystal XRD	127
$[\text{Cd}(\text{enMe})_3]_2[(\text{enMe})_2\text{Cd}_2\text{V}_{12}\text{As}_8\text{O}_{40}(0.5\text{H}_2\text{O})] \cdot 5.5\text{H}_2\text{O}$	brown	layer	$\text{V}_2\text{O}_5$ , $\text{As}_2\text{O}_3$ , $\text{H}_2\text{O}$ , enMe, $\text{Cd}(\text{OAc})_2 \cdot 2\text{H}_2\text{O}$	170 °C, 3d	42% based on V	EA, IR, TGA, UV-Vis, magnetometry, powder	128

[Cd(enMe) <sub>2</sub> ] <sub>2</sub> [Cd <sub>2</sub> (enMe) <sub>2</sub> V <sub>12</sub> As <sub>8</sub> O <sub>40</sub> (0.5H <sub>2</sub> O)]	brown	1D linear chain	V <sub>2</sub> O <sub>5</sub> , As <sub>2</sub> O <sub>3</sub> , H <sub>2</sub> O, enMe (excess), Cd(OAc) <sub>2</sub> ·2H <sub>2</sub> O	170 °C, 3 d	32% based on V	XRD, single-crystal XRD EA, IR, TGA, UV–Vis, magnetometry, powder XRD, single-crystal XRD	128
<b>V<sub>13</sub></b>							
[Zn(2,2'-bipy) <sub>3</sub> ] <sub>4</sub> [(ppz){Zn(tepa)} <sub>2</sub> ZnV <sub>13</sub> As <sub>8</sub> O <sub>41</sub> (H <sub>2</sub> O)] <sub>2</sub> [V <sub>14</sub> As <sub>8</sub> O <sub>42</sub> (0.5H <sub>2</sub> O)] <sub>2</sub> ·4H <sub>2</sub> O	brown	3D network	V <sub>2</sub> O <sub>5</sub> , As <sub>2</sub> O <sub>3</sub> , H <sub>2</sub> O, dien, Zn(OAc) <sub>2</sub> ·4H <sub>2</sub> O, 2,2'-bipy	160 °C, 3 d, pH = 7.45 → 8.35	39% based on V <sub>2</sub> O <sub>5</sub>	EA, IR, TGA, magnetometry, powder XRD, single-crystal XRD	124
[[Cd(en) <sub>3</sub> ][Cd(phen)(en)(H <sub>2</sub> O) <sub>2</sub> ][Cd(en)V <sub>13</sub> As <sub>8</sub> O <sub>41</sub> (H <sub>2</sub> O)]·1.5H <sub>2</sub> O	brown		NH <sub>4</sub> VO <sub>3</sub> , As <sub>2</sub> O <sub>3</sub> , 1,10-phen, en, CdCl <sub>2</sub> ·7H <sub>2</sub> O, HNO <sub>3</sub> , H <sub>2</sub> O	170 °C, 7 d	46% based on V	EA, FT-IR, TGA, CV, powder XRD, single-crystal XRD	125
[Cd(phen) <sub>2</sub> (en)] <sub>2</sub> [Cd(phen)V <sub>13</sub> As <sub>8</sub> O <sub>41</sub> (H <sub>2</sub> O)]·21H <sub>2</sub> O·phen	brown		NH <sub>4</sub> VO <sub>3</sub> , As <sub>2</sub> O <sub>3</sub> , 1,10-phen, en, CdCl <sub>2</sub> ·7H <sub>2</sub> O, HNO <sub>3</sub> , H <sub>2</sub> O	170 °C, 7 d	55% based on V	EA, FT-IR, TGA, CV, magnetometry, powder XRD, single-crystal XRD	125
[Cd(dien) <sub>2</sub> ] <sub>2</sub> [Cd(dien)V <sub>13</sub> As <sub>8</sub> O <sub>41</sub> (H <sub>2</sub> O)]·4H <sub>2</sub> O	brown		V <sub>2</sub> O <sub>5</sub> , As <sub>2</sub> O <sub>3</sub> , dien, H <sub>2</sub> O, Cd(OAc) <sub>2</sub> ·2H <sub>2</sub> O	180 °C, 6 d	61% based on V	EA, IR, EPR, TGA, magnetometry, single-crystal XRD	127
{[V <sub>13</sub> As <sub>8</sub> NiClO <sub>41</sub> ][Ni(en) <sub>2</sub> (H <sub>2</sub> O)][Ni(en) <sub>2</sub> ]}{[Ni(en) <sub>2</sub> (H <sub>2</sub> O) <sub>2</sub> ] <sub>0.5</sub> }·4H <sub>2</sub> O	black	1D chain	V <sub>2</sub> O <sub>5</sub> , As <sub>2</sub> O <sub>3</sub> , H <sub>2</sub> C <sub>2</sub> O <sub>4</sub> ·2H <sub>2</sub> O, en, NiCl <sub>2</sub> ·6H <sub>2</sub> O, H <sub>2</sub> O	160 °C, 3 d	68% based on V	EA, IR, TGA, magnetometry, single-crystal XRD	129
<b>V<sub>14</sub></b>							
(NH <sub>4</sub> ) <sub>6</sub> [V <sub>14</sub> As <sub>8</sub> O <sub>42</sub> (SO <sub>3</sub> )]	brown		NH <sub>4</sub> VO <sub>3</sub> , As <sub>2</sub> O <sub>3</sub> , H <sub>2</sub> O, Na <sub>2</sub> S <sub>2</sub> O <sub>4</sub> , NH <sub>3</sub> , NH <sub>4</sub> SCN	80 °C, 1–2 d (not stirred)		EA, IR, UV-vis, single-crystal XRD	130
(NH <sub>4</sub> ) <sub>6</sub> [V <sub>14</sub> As <sub>8</sub> O <sub>42</sub> (SO <sub>4</sub> )]	brown		NH <sub>4</sub> VO <sub>3</sub> , As <sub>2</sub> O <sub>3</sub> , H <sub>2</sub> O, N <sub>2</sub> H <sub>6</sub> SO <sub>4</sub> , NH <sub>3</sub> , NH <sub>4</sub> SCN	90 °C, 3 d (not stirred)		EA, IR, UV-vis, single-crystal XRD	130
(NMe <sub>4</sub> ) <sub>4</sub> [V <sub>14</sub> As <sub>8</sub> O <sub>42</sub> (H <sub>2</sub> O)]	dark green		NaVO <sub>3</sub> , As <sub>2</sub> O <sub>3</sub> , NMe <sub>4</sub> Cl, H <sub>2</sub> O, N <sub>2</sub> H <sub>5</sub> Cl	70 °C, 7 d (not stirred)		EA, IR, UV-vis, single-crystal XRD	130
(NMe <sub>4</sub> ) <sub>4</sub> [V <sub>14</sub> As <sub>8</sub> O <sub>42</sub> (H <sub>2</sub> O) <sub>0.5</sub> ]	dark		V <sub>2</sub> O <sub>5</sub> , As <sub>2</sub> O <sub>3</sub> , Me <sub>4</sub> NOH, H <sub>2</sub> O	200 °C, 2 d	89% based	EA, IR, single-crystal	131

	brown				on V	XRD	
$(\text{NH}_4)_2(\text{NMe}_4)_4[\text{V}_{14}\text{As}_8\text{O}_{42}(\text{SO}_4)]$	black		$\text{NH}_4\text{VO}_3$ , $\text{As}_2\text{O}_3$ , $\text{NiSO}_4 \cdot 6\text{H}_2\text{O}$ , $\text{NMe}_4\text{OH}$ , $\text{H}_2\text{O}$	160 °C, 5 d	54% based on V	EA, IR, TGA, single- crystal XRD	134
$(\text{NEt}_4)_3[\text{H}_6\text{V}_{12}\text{AsO}_{40}(\text{VO})_2] \cdot 20\text{H}_2\text{O}$	dark red		$\text{NH}_4\text{VO}_3$ , $\text{Na}_2\text{HAsO}_4$ , $\text{NH}_2\text{OH}$ , $\text{HCl}$ , $\text{H}_2\text{O}$ , $\text{Et}_4\text{NBr}$	reflux temperature (1.5 h) → r.t.		EA, single-crystal XRD	117
$(\text{H}_2\text{en})_{3.5}[\text{V}_{14}\text{As}_8\text{O}_{42}(\text{PO}_4)] \cdot 2\text{H}_2\text{O}$	black		$\text{V}_2\text{O}_5$ , $\text{As}_2\text{O}_3$ , $\text{H}_3\text{PO}_4$ , en, $\text{H}_2\text{C}_2\text{O}_4 \cdot 2\text{H}_2\text{O}$ , $\text{H}_2\text{O}$	160 °C, 3 d	80% based on V	EA, IR, TGA, XPS, ESR, single-crystal XRD	135
$(\text{H}_2\text{enMe})_2[\text{V}_{14}\text{As}_8\text{O}_{42}(\text{H}_2\text{O})] \cdot 3\text{H}_2\text{O}$	black	triple clusters	$\text{NH}_4\text{VO}_3$ , $\text{As}_2\text{O}_3$ , $\text{FeSO}_4 \cdot 4\text{H}_2\text{O}$ , $\text{H}_3\text{PO}_4$ , enMe, $\text{H}_2\text{C}_2\text{O}_4 \cdot 2\text{H}_2\text{O}$ , $\text{H}_2\text{O}$ , $\text{NH}_3 \cdot \text{H}_2\text{O}$	160 °C, 3 d	80% based on V	EA, IR, UV-vis, XPS, EPR, powder XRD, single-crystal XRD, magnetometry	136
$(\text{Hen})_2(\text{H}_2\text{en})[\text{V}_{14}\text{As}_8\text{O}_{42}(\text{H}_2\text{O})] \cdot 2.33\text{H}_2\text{O}$	black		$\text{V}_2\text{O}_5$ , $\text{As}_2\text{O}_3$ , $\text{CuCl}_2 \cdot 2\text{H}_2\text{O}$ , en, $\text{H}_2\text{O}$ , $\text{HCl}$	170 °C, 7 d, pH = 6.0	64% based on V	EA, IR, TGA, single- crystal XRD	140
$[\text{NH}_2(\text{CH}_2)_4\text{NH}_2]_4[\text{V}_{14}\text{As}_8\text{O}_{42}(\text{SO}_4)] \cdot (\text{HSO}_4)_2$	black	layer	$\text{VO}_2 \cdot \text{H}_2\text{O}$ , $\text{As}_2\text{O}_5$ , ppz, $\text{H}_2\text{O}$	180 °C, 6 d		EA, IR, TGA, single- crystal XRD	132
$[\text{NH}_2(\text{CH}_2\text{CH}_2)_2\text{NH}_2]_3[\text{V}_{14}\text{As}_8\text{O}_{42}(\text{SO}_4)] \cdot 6.5\text{H}_2\text{O}$	brown		$\text{VO}_2 \cdot \text{H}_2\text{O}$ , $\text{As}_2\text{O}_5$ , $\text{HN}(\text{CH}_2\text{CH}_2)_2\text{NH}$ , $\text{H}_2\text{O}$	180 °C, 6 d	76% based on V	EA, IR, TGA, single- crystal XRD, magnetometry	133
$\text{H}_6[\text{Cl}_2\text{V}_{14}\text{O}_{16}(\text{OH})_8(\text{O}_3\text{AsC}_6\text{H}_4\text{-4-}\text{NH}_2)_{10}] \cdot 8\text{DMF} \cdot 16\text{H}_2\text{O}$	turquoise		$\text{NaVO}_3$ , ( <i>p</i> - aminophenyl)arsonic acid, $\text{H}_2\text{O}$ , $\text{DMF}$ , $\text{HCl}$ , $\text{N}_2\text{H}_4 \cdot \text{H}_2\text{O}$	70 °C, 30 min, pH = 4.5	19%	EA, IR, ESI-MS, UV-vis, single-crystal XRD	165
$\text{K}_7[\text{V}_{14}\text{AsO}_{40}] \cdot 12\text{H}_2\text{O}$	dark blue		$\text{KVO}_3$ , $\text{As}_2\text{O}_5 \cdot$ $5/3\text{H}_2\text{O}$ , $\text{KSCN}$ , $\text{H}_2\text{O}$ , $\text{H}_2\text{SO}_4$ , $\text{KOH}$	70-75 °C, 16 h, pH = 4.6		EA, IR, Raman, TGA, UV-vis, EPR, single- crystal XRD, magnetometry	106
$\text{Rb}_5[\text{V}_{14}\text{As}_8\text{O}_{42}(\text{Cl})] \cdot 2\text{H}_2\text{O}$	brown		$\text{V}_2\text{O}_5$ , $\text{V}_2\text{O}_3$ , V (mesh), $\text{H}_5\text{As}_3\text{O}_{10}$ , $\text{RbOH}$ , $\text{H}_2\text{O}$	200 °C, 2.5 d	40% based on V	EA, IR, UV-vis, single- crystal XRD	116



[Zn(bbi) <sub>2</sub> ] <sub>2</sub> [V <sub>14</sub> As <sub>8</sub> O <sub>42</sub> (H <sub>2</sub> O)]	dark green	2D network	NH <sub>4</sub> VO <sub>3</sub> , bbi, ZnCl <sub>2</sub> ·2H <sub>2</sub> O, NaOAc, H <sub>2</sub> C <sub>2</sub> O <sub>4</sub> ·2H <sub>2</sub> O, tris(hydroxymethyl)amino-methane), Na <sub>3</sub> AsO <sub>4</sub> ·H <sub>2</sub> O, H <sub>2</sub> O, HCl		88% based on V	EA, IR, powder XRD, magnetometry	148
[Zn(2,2'-bipy) <sub>2</sub> ] <sub>2</sub> [V <sub>14</sub> As <sub>8</sub> O <sub>42</sub> (H <sub>2</sub> O)]·H <sub>2</sub> O	brown	1D tubular chain	V <sub>2</sub> O <sub>5</sub> , As <sub>2</sub> O <sub>5</sub> , Zn(OAc) <sub>2</sub> ·2H <sub>2</sub> O, 2,2'-bipy, NMe <sub>4</sub> OH, H <sub>2</sub> O	160 °C, 6 d	33% based on V	EA, IR, EPR, single-crystal XRD, magnetometry	144
[Zn(2,2'-bipy) <sub>3</sub> ] <sub>2</sub> [V <sub>14</sub> As <sub>8</sub> O <sub>42</sub> (H <sub>2</sub> O)]·4H <sub>2</sub> O	brown		V <sub>2</sub> O <sub>5</sub> , As <sub>2</sub> O <sub>3</sub> , Zn(OAc) <sub>2</sub> ·2H <sub>2</sub> O, 2,2'-bipy, ppz, H <sub>2</sub> O	180 °C, 6 d	73% based on V	EA, IR, EPR, TGA, powder XRD, single-crystal XRD, magnetometry	138
[{(H <sub>2</sub> O)Zn(4,4'-bipy)} <sub>2</sub> ] <sub>2</sub> [V <sub>14</sub> As <sub>8</sub> O <sub>42</sub> (H <sub>2</sub> O)]·2H <sub>2</sub> O	black	2D network	V <sub>2</sub> O <sub>5</sub> , As <sub>2</sub> O <sub>3</sub> , Zn(OAc) <sub>2</sub> ·2H <sub>2</sub> O, 4,4'-bipy, H <sub>2</sub> O	160 °C, 7 d	23% based on V	EA, IR, XPS, TGA, CV, single-crystal XRD	143
[Zn(2,2'-bipy)(dien)] <sub>2</sub> [V <sub>14</sub> As <sub>8</sub> O <sub>42</sub> (H <sub>2</sub> O)]·2H <sub>2</sub> O	brown		V <sub>2</sub> O <sub>5</sub> , As <sub>2</sub> O <sub>3</sub> , Zn(OAc) <sub>2</sub> ·2H <sub>2</sub> O, 2,2'-bipy, dien, H <sub>2</sub> O	180 °C, 6 d	68% based on V	EA, IR, EPR, TGA, powder XRD, single-crystal XRD, magnetometry	138
[{(H <sub>2</sub> O)Zn(1,10-phen)} <sub>2</sub> ] <sub>2</sub> [V <sub>14</sub> As <sub>8</sub> O <sub>42</sub> (H <sub>2</sub> O)]·4H <sub>2</sub> O	black	2D supermolecular array	V <sub>2</sub> O <sub>5</sub> , As <sub>2</sub> O <sub>3</sub> , Zn(OAc) <sub>2</sub> ·2H <sub>2</sub> O, 1,10-phen, H <sub>2</sub> O	160 °C, 7 d	39% based on V	EA, IR, XPS, TGA, CV, single-crystal XRD	143
[Zn(phen) <sub>3</sub> ] <sub>2</sub> [V <sub>14</sub> As <sub>8</sub> O <sub>42</sub> (H <sub>2</sub> O)]·4H <sub>2</sub> O	brown	layer-like arrangement	V <sub>2</sub> O <sub>5</sub> , As <sub>2</sub> O <sub>3</sub> , Zn(OAc) <sub>2</sub> ·6H <sub>2</sub> O, phen, dien, H <sub>2</sub> O	180 °C, 3 d	62% based on V	EA, IR, TGA, single-crystal XRD, fluorescence	141
[Zn(en) <sub>2</sub> ][(H <sub>2</sub> O)Zn(en) <sub>2</sub> V <sub>14</sub> As <sub>8</sub> O <sub>42</sub> (H <sub>2</sub> O)]·H <sub>2</sub> O	black	infinite 1D channels	NH <sub>4</sub> VO <sub>3</sub> , As <sub>2</sub> O <sub>3</sub> , Zn(NO <sub>3</sub> ) <sub>2</sub> ·6H <sub>2</sub> O, HNO <sub>3</sub> , en,	160 °C, 7 d	45% based on V	EA, IR, TGA, CV, single-crystal XRD	143

$[(\text{H}_2\text{O})\text{Zn}(2,2'\text{-bipy})_2]\{\text{Zn}(2,2'\text{-bipy})_2\}\text{V}_{14}\text{As}_8\text{O}_{42}(\text{H}_2\text{O})_{0.5}\}_2\{[(\text{H}_2\text{O})\text{Zn}(2,2'\text{-bipy})_2\text{V}_{14}\text{As}_8\text{O}_{42}(\text{H}_2\text{O})_{0.5}\}_2\{\text{Zn}(2,2'\text{-bipy})_2\}_2\}\cdot 3\text{H}_2\text{O}$	black	cluster dimers	$\text{H}_2\text{O}$ $\text{V}_2\text{O}_5$ , $\text{As}_2\text{O}_3$ , $\text{Zn}(\text{OAc})_2\cdot 2\text{H}_2\text{O}$ , 2,2'-bipy, $\text{H}_2\text{O}$	160 °C, 7 d	29% based on V	EA, IR, XPS, TGA, CV, single-crystal XRD	143
$[\text{Cd}(\text{phen})_3]_2[\text{V}_{14}\text{As}_8\text{O}_{42}(\text{H}_2\text{O})]\cdot 2\text{H}_2\text{O}$	brown	layer-like arrangement	$\text{V}_2\text{O}_5$ , $\text{As}_2\text{O}_3$ , $\text{Cd}(\text{OAc})_2\cdot 6\text{H}_2\text{O}$ , phen, dien, $\text{H}_2\text{O}$	150 °C, 5 d	63% based on V	EA, IR, TGA, single-crystal XRD, fluorescence	141
$[\text{Cd}(1,10\text{-phen})_3]_2[\text{V}_{14}\text{As}_8\text{O}_{42}(\text{H}_2\text{O})_{0.5}]\cdot 0.5\text{H}_2\text{O}$	black		$\text{NaVO}_3\cdot 2\text{H}_2\text{O}$ , $\text{As}_2\text{O}_3$ , $\text{Cd}(\text{OAc})_2$ , 1,10-phen, NaOAc/HOAc	175 °C, 5 d	50% based on V	EA, IR, EPR, TGA, CV single-crystal XRD	140
$[\text{Cd}(2,2'\text{-bipy})_3][\text{Cd}(\text{dien})\text{V}_{14}\text{As}_8\text{O}_{42}(\text{H}_2\text{O})]$	brown	1D wave-like chain	$\text{V}_2\text{O}_5$ , $\text{As}_2\text{O}_3$ , $\text{CdSO}_4\cdot 8\text{H}_2\text{O}$ , 2,2'-bipy, $\text{H}_2\text{C}_2\text{O}_4\cdot 2\text{H}_2\text{O}$ , dien, $\text{H}_2\text{O}$	160 °C, 3 d	51% based on V	EA, IR, EPR, single-crystal XRD, magnetometry	144
$[\text{Cu}(\text{en})_2]_2[\text{V}_{14}\text{As}_8\text{O}_{42}(\text{H}_2\text{O})]\cdot 2.5\text{H}_2\text{O}$	brown	1D chain	$\text{NH}_4\text{VO}_3$ , $\text{As}_2\text{O}_3$ , $\text{CuCl}_2\cdot 2\text{H}_2\text{O}$ , en, $\text{HNO}_3$ , $\text{H}_2\text{O}$	160 °C, 7 d	33% based on V	EA, IR, TGA, single-crystal XRD	140
$[\text{Cu}(\text{en})_2]_3[\text{V}_{14}\text{As}_8\text{O}_{42}(\text{CO}_3)]\cdot 10\text{H}_2\text{O}$	black	2D layered network	$\text{V}_2\text{O}_5$ , $\text{As}_2\text{O}_3$ , $\text{CuCl}_2\cdot 2\text{H}_2\text{O}$ , en, $\text{H}_2\text{C}_2\text{O}_4\cdot 2\text{H}_2\text{O}$ , $\text{H}_2\text{O}$	160 °C, 3 d	80% based on V	EA, IR, TGA, single-crystal XRD	149
$[\text{Cu}(\text{bbi})_4][\text{V}_{14}\text{As}_8\text{O}_{42}(\text{H}_2\text{O})]$	green	3D network	$\text{NH}_4\text{VO}_3$ , bbi, $\text{Cu}(\text{OAc})_2\cdot 3\text{H}_2\text{O}$ , NaOAc, $\text{H}_2\text{C}_2\text{O}_4\cdot 2\text{H}_2\text{O}$ , tris(hydroxymethyl)amino-methane), $\text{Na}_3\text{AsO}_4\cdot \text{H}_2\text{O}$ , $\text{H}_2\text{O}$ , HCl	170 °C, 5 d	62% based on V	EA, IR, single-crystal XRD	148
$[\text{Ni}(\text{bbi})_2]_2[\text{V}_{14}\text{As}_8\text{O}_{42}(\text{H}_2\text{O})]$	dark green	2D network	$\text{NH}_4\text{VO}_3$ , bbi, $\text{Ni}(\text{NO}_3)_2\cdot 6\text{H}_2\text{O}$ , NaOAc, $\text{H}_2\text{C}_2\text{O}_4\cdot 2\text{H}_2\text{O}$ ,	170 °C, 5 d	82% based on V	EA, IR, powder XRD, single-crystal XRD, magnetometry	148

[Ni(en) <sub>2</sub> ] <sub>3</sub> [V <sub>14</sub> As <sub>8</sub> O <sub>42</sub> (SO <sub>4</sub> )]·4.5H <sub>2</sub> O	black	2D sinusoidal layer	tris(hydroxymethyl)aminomethane), Na <sub>3</sub> AsO <sub>4</sub> ·H <sub>2</sub> O, H <sub>2</sub> O, HCl V <sub>2</sub> O <sub>5</sub> , As <sub>2</sub> O <sub>3</sub> , en, H <sub>2</sub> C <sub>2</sub> O <sub>4</sub> ·2H <sub>2</sub> O, H <sub>2</sub> O, NiSO <sub>4</sub> ·6H <sub>2</sub> O	160 °C, 3 d	73% based on V	EA, IR, EPR, XPS, single-crystal XRD, magnetometry	145
[Ni(en) <sub>2</sub> ] <sub>3</sub> [V <sub>14</sub> As <sub>8</sub> O <sub>42</sub> (HPO <sub>3</sub> )]·4H <sub>2</sub> O	brown	2D puckery layer	V <sub>2</sub> O <sub>5</sub> , As <sub>2</sub> O <sub>3</sub> , H <sub>3</sub> PO <sub>3</sub> , en, Ni, Ni(OAc) <sub>2</sub> ·4H <sub>2</sub> O, H <sub>2</sub> O	160 °C, 4 d	16% based on V	EA, IR, EPR, single-crystal XRD	144
(2,2'-bipy) <sub>3</sub> [Ni(2,2'-bipy) <sub>2</sub> ] <sub>2</sub> [V <sub>14</sub> As <sub>8</sub> O <sub>42</sub> (H <sub>2</sub> O)]·3H <sub>2</sub> O	brown		V <sub>2</sub> O <sub>5</sub> , As <sub>2</sub> O <sub>3</sub> , H <sub>2</sub> O, Ni(OAc) <sub>2</sub> ·4H <sub>2</sub> O, en, 2,2'-bipy	160 °C, 3 d	46% based on V	EA, IR, EPR, TGA, UV-vis, XPS, single-crystal XRD	139
[Ni(enMe) <sub>3</sub> ] <sub>4</sub> [Ni(enMe) <sub>2</sub> ] <sub>2</sub> [V <sub>14</sub> As <sub>8</sub> O <sub>42</sub> (NO <sub>3</sub> )] <sub>2</sub> ·8H <sub>2</sub> O	black	cluster dimers	NH <sub>4</sub> VO <sub>3</sub> , As <sub>2</sub> O <sub>3</sub> , Ni(NO <sub>3</sub> ) <sub>2</sub> ·6H <sub>2</sub> O, bpp, enMe, HNO <sub>3</sub> , H <sub>2</sub> O	170 °C, 7 d	45% based on V	EA, IR, TGA, CV, powder XRD, single-crystal XRD, magnetometry	125
[{Ni(en) <sub>2</sub> ] <sub>4</sub> (4,4'-bipy) <sub>4</sub> {Ni(H <sub>2</sub> O) <sub>2</sub> }] <sub>2</sub> [V <sub>14</sub> As <sub>8</sub> O <sub>42</sub> (NO <sub>3</sub> )] <sub>4</sub> ·16H <sub>2</sub> O	black	box-like framework	NH <sub>4</sub> VO <sub>3</sub> , As <sub>2</sub> O <sub>3</sub> , Ni(NO <sub>3</sub> ) <sub>2</sub> ·6H <sub>2</sub> O, 4,4'-bipy, HNO <sub>3</sub> , en, H <sub>2</sub> O	170 °C, 5 d	70% based on V	EA, IR, TGA, CV, single-crystal XRD, magnetometry	146
[Ni(en) <sub>2</sub> (H <sub>2</sub> O) <sub>2</sub> ] <sub>2</sub> [{Ni(en) <sub>2</sub> (H <sub>2</sub> O) <sub>2</sub> ] <sub>2</sub> V <sub>14</sub> As <sub>8</sub> O <sub>42</sub> (NO <sub>3</sub> )] <sub>2</sub> [Ni(en) <sub>2</sub> ] <sub>2</sub> V <sub>14</sub> As <sub>8</sub> O <sub>42</sub> (NO <sub>3</sub> )]·6H <sub>2</sub> O	black	1D chain	NH <sub>4</sub> VO <sub>3</sub> , As <sub>2</sub> O <sub>3</sub> , Ni(NO <sub>3</sub> ) <sub>2</sub> ·6H <sub>2</sub> O, 1,3-bis(4-pyridyl)propane, HNO <sub>3</sub> , en, H <sub>2</sub> O	170 °C, 5 d	10% based on V	EA, IR, single-crystal XRD	146
[Co(2,2'-bipy) <sub>2</sub> ] <sub>2</sub> [V <sub>14</sub> As <sub>8</sub> O <sub>42</sub> (H <sub>2</sub> O)]·H <sub>2</sub> O	black	1D tubular chain	VOSO <sub>4</sub> , As <sub>2</sub> O <sub>3</sub> , CoC <sub>2</sub> O <sub>4</sub> ·2H <sub>2</sub> O, 2,2'-bipy, H <sub>2</sub> O, dien	160 °C, 9 d, pH = 5.5	30% based on V	EA, IR, TGA, single-crystal XRD, magnetometry	147
[Co(2,2'-bipy) <sub>3</sub> ] <sub>2</sub> [V <sub>14</sub> As <sub>8</sub> O <sub>42</sub> (H <sub>2</sub> O)]·3H <sub>2</sub> O	brown		V <sub>2</sub> O <sub>5</sub> , As <sub>2</sub> O <sub>3</sub> , H <sub>3</sub> PO <sub>3</sub> , H <sub>2</sub> O, H <sub>2</sub> C <sub>2</sub> O <sub>4</sub> ·2H <sub>2</sub> O,	160 °C, 3 d	52% based on V	EA, IR, TGA, UV-vis, XPS, EPR, single-	139

			Co(OAc) <sub>2</sub> ·4H <sub>2</sub> O, en, 2,2'-bipy			crystal XRD	
[Co(dien) <sub>2</sub> ] <sub>2</sub> [V <sub>14</sub> As <sub>8</sub> O <sub>42</sub> (H <sub>2</sub> O)]·3.5H <sub>2</sub> O	brown	soft channels	V <sub>2</sub> O <sub>5</sub> , Na <sub>3</sub> AsO <sub>4</sub> , CoCl <sub>2</sub> ·6H <sub>2</sub> O, dien, H <sub>2</sub> O, H <sub>2</sub> SO <sub>4</sub>	170 °C, 7 d, pH = 8.0	33% based on V	EA, IR, TGA, single-crystal XRD	140
[Co(bbi) <sub>2</sub> ] <sub>2</sub> [V <sub>14</sub> As <sub>8</sub> O <sub>42</sub> (H <sub>2</sub> O)]	dark green	2D network	V <sub>2</sub> O <sub>5</sub> , bbi, Co(OAc) <sub>2</sub> ·4H <sub>2</sub> O, H <sub>2</sub> C <sub>2</sub> O <sub>4</sub> ·2H <sub>2</sub> O, NaOAc, tris(hydroxymethyl)aminomethane), Na <sub>3</sub> AsO <sub>4</sub> ·H <sub>2</sub> O, H <sub>2</sub> O, HCl	170 °C, 5 d	55% based on V	EA, IR, powder XRD, single-crystal XRD, magnetometry	148
[Co(en) <sub>3</sub> ][Co(en) <sub>2</sub> V <sub>14</sub> As <sub>8</sub> O <sub>42</sub> (H <sub>2</sub> O)]·16H <sub>2</sub> O	black	1D chain	NH <sub>4</sub> VO <sub>3</sub> , As <sub>2</sub> O <sub>3</sub> , Co(NO <sub>3</sub> ) <sub>2</sub> ·6H <sub>2</sub> O, 4,4'-bipy, en, HNO <sub>3</sub> , H <sub>2</sub> O	170 °C, 7 d	40% based on V	EA, IR, TGA, CV, powder XRD, single-crystal XRD	125
[Mn(1,10-phen) <sub>3</sub> ] <sub>2</sub> [V <sub>14</sub> As <sub>8</sub> O <sub>42</sub> (H <sub>2</sub> O) <sub>0.5</sub> ]·0.5H <sub>2</sub> O	green		NH <sub>4</sub> VO <sub>3</sub> , As <sub>2</sub> O <sub>3</sub> , KMnO <sub>4</sub> , 1,10-phen, H <sub>2</sub> O	160 °C, 7 d	10% based on V	EA, IR, EPR, TGA, single-crystal XRD	140
[{La(H <sub>2</sub> O) <sub>6</sub> ] <sub>2</sub> V <sub>14</sub> As <sub>8</sub> O <sub>42</sub> (SO <sub>3</sub> )]·8H <sub>2</sub> O	brown	2D layered network	(NH <sub>4</sub> ) <sub>6</sub> [V <sub>14</sub> As <sub>8</sub> O <sub>42</sub> (SO <sub>3</sub> )], La(NO <sub>3</sub> ) <sub>3</sub> ·6H <sub>2</sub> O, H <sub>2</sub> O	7d	32% based on (NH <sub>4</sub> ) <sub>6</sub> [V <sub>14</sub> As <sub>8</sub> O <sub>42</sub> (SO <sub>3</sub> )]	EA, IR, EPR, TGA, powder XRD, single-crystal XRD	150
[{Ce(H <sub>2</sub> O) <sub>6</sub> ] <sub>2</sub> V <sub>14</sub> As <sub>8</sub> O <sub>42</sub> (SO <sub>3</sub> )]·8H <sub>2</sub> O	brown	2D layered network	(NH <sub>4</sub> ) <sub>6</sub> [V <sub>14</sub> As <sub>8</sub> O <sub>42</sub> (SO <sub>3</sub> )], Ce(NO <sub>3</sub> ) <sub>3</sub> ·6H <sub>2</sub> O, H <sub>2</sub> O	7d	32% based on (NH <sub>4</sub> ) <sub>6</sub> [V <sub>14</sub> As <sub>8</sub> O <sub>42</sub> (SO <sub>3</sub> )]	EA, IR, EPR, TGA, powder XRD, single-crystal XRD	150
[{Sm(H <sub>2</sub> O) <sub>6</sub> ] <sub>2</sub> V <sub>14</sub> As <sub>8</sub> O <sub>42</sub> (SO <sub>3</sub> )]·8H <sub>2</sub> O	brown	2D layered network	(NH <sub>4</sub> ) <sub>6</sub> [V <sub>14</sub> As <sub>8</sub> O <sub>42</sub> (SO <sub>3</sub> )], Sm(NO <sub>3</sub> ) <sub>3</sub> ·6H <sub>2</sub> O, H <sub>2</sub> O	7d	27% based on (NH <sub>4</sub> ) <sub>6</sub> [V <sub>14</sub> As <sub>8</sub> O <sub>42</sub> (SO <sub>3</sub> )]	EA, IR, EPR, TGA, powder XRD, single-crystal XRD	150

$K_6[V_{15}As_6O_{42}(H_2O)] \cdot 8H_2O$	brown	3D network	$KVO_3$ , $As_2O_3$ , $KSCN$ , $KOH$ , $H_2O$ , $N_2H_4 \cdot H_2SO_4$	$85 \rightarrow 20^\circ C$ , $pH = 8.4$	55%	EA, IR, TGA, single-crystal XRD, magnetometry	151
$[Zn(H_2O)_4]_2[H_2V_{15}As_6O_{42}(H_2O)] \cdot 2H_2O$	black		$V_2O_5$ , $As_2O_3$ , $H_2C_2O_4 \cdot 2H_2O$ , en, $Zn(OAc)_2 \cdot 2H_2O$ , $H_2O$	$160^\circ C$ , 3 d	53% based on As	EA, IR, ESR, single-crystal XRD, magnetometry, third-order NLO	153
$[Zn(en)_2][Zn(en)_2(H_2O)_2][\{Zn(en)(enMe)\}V_{15}As_6O_{42}(H_2O)] \cdot 4H_2O$	black		$V_2O_5$ , $As_2O_3$ , en, enMe, $Zn(OAc)_2 \cdot 2H_2O$ , $H_2O$	$160^\circ C$ , 6 d, $pH = 8.5$	52% based on V	EA, IR, TGA, single-crystal XRD	154
$[Zn_2(enMe)_2(en)_3][\{Zn(enMe)_2\}V_{15}As_6O_{42}(H_2O)] \cdot 4H_2O$	black		$V_2O_5$ , $As_2O_3$ , en, enMe, $Zn(OAc)_2 \cdot 2H_2O$ , $H_2O$	$160^\circ C$ , 6 d	37% based on V	EA, IR, TGA, single-crystal XRD	154
$(Hen)_2[\{Zn(en)_2\}_2V_{15}As_6O_{42}(H_2O)]_2[Zn(en)_2] \cdot 3H_2O$	black	cluster dimers	$VOSO_4$ , $As_2O_3$ , $ZnO$ , en, $HCl$ , $H_2O$	$160^\circ C$ , 4 d, $pH = 7$	58% based on V	EA, IR, TGA, single-crystal XRD	155
$[Zn_2(dien)_3(H_2O)_2]_{0.5}[\{Zn_2(dien)_3\}V_{15}As_6O_{42}(H_2O)] \cdot 2H_2O$	brown	1D helical chain	$V_2O_5$ , $As_2O_3$ , dien, $Zn(OAc)_2 \cdot 2H_2O$ , $H_2O$	$160^\circ C$ , 3 d	57% based on V	EA, IR, TGA, EPR, single-crystal XRD	156
$[Cu(en)_2]_{1.5}[H_3V_{15}As_6O_{42}(H_2O)] \cdot 3H_2O$	black	1D sinusoidal chain	$V_2O_5$ , $As_2O_3$ , $H_2C_2O_4 \cdot 2H_2O$ , $CuSO_4 \cdot 5H_2O$ , en, $H_2O$	$160^\circ C$ , 3 d	67% based on V	EA, IR, single-crystal XRD	158
$[Cu(enMe)_2]_{2.5}[HV_{15}As_6O_{42}(H_2O)] \cdot 2H_2O$	black	brick-wall-like 2D layer	$V_2O_5$ , $As_2O_3$ , $H_2SO_4$ , enMe, $H_2C_2O_4 \cdot 2H_2O$ , $CuSO_4 \cdot 5H_2O$ , $H_2O$ , $NH_3 \cdot H_2O$	$160^\circ C$ , 3 d, $pH = 10$	51% based on V	EA, IR, TGA, UV-vis, EPR, XPS, magnetometry, single-crystal XRD	136
$[Ni(2,2'-bipy)_3]_2[\{Ni(en)_2\}V_{15}As_6O_{42}(H_2O)] \cdot 9.5H_2O$	brown	1D straight chain	$V_2O_5$ , $As_2O_3$ , 2,2'-bipy, $Ni(OAc)_2 \cdot 4H_2O$ , en, $H_2O$	$160^\circ C$ , 3 d	65% based on V	EA, IR, TGA, EPR, single-crystal XRD	156
$[Co(en)_3][\{Co(en)_2\}_2V_{15}As_6O_{42}] \cdot 4H_2O$	black	1D chain	$V_2O_5$ , $As_2O_3$ , $H_3PO_3$ , $Co(OAc)_2$ , en, $H_2O$	$160^\circ C$ , 3 d	78%	IR, single-crystal XRD, magnetometry	157
$[Co(enMe)_2]_3[V_{15}As_6O_{42}(H_2O)] \cdot 2H_2O$	brown	2D framework	$V_2O_5$ , $As_2O_3$ , enMe, $H_2C_2O_4 \cdot 2H_2O$ , $CoSO_4 \cdot 4H_2O$ , $H_2O$	$160^\circ C$ , 6 d	27% based on V	EA, IR, TGA, EPR, single-crystal XRD	156

**V<sub>16</sub>**

(HNEt <sub>3</sub> ) <sub>2</sub> [Br <sub>2</sub> (H <sub>2</sub> O) <sub>4</sub> ](VO) <sub>16</sub> (OH) <sub>8</sub> (O <sub>4</sub> AsPh) <sub>2</sub> (O <sub>3</sub> AsPh) <sub>8 <td>blue</td> <td></td> <td>VBr<sub>3</sub>, PhAsO<sub>3</sub>H<sub>2</sub>, NEt<sub>3</sub>, MeCN</td> <td>80 °C, 30 min</td> <td>62% based on V</td> <td>EA, IR, ESI-MS, powder XRD, single-crystal XRD</td> <td>163</td> </sub>	blue		VBr <sub>3</sub> , PhAsO <sub>3</sub> H <sub>2</sub> , NEt <sub>3</sub> , MeCN	80 °C, 30 min	62% based on V	EA, IR, ESI-MS, powder XRD, single-crystal XRD	163
(HNEt <sub>3</sub> ) <sub>2</sub> [Cl <sub>2</sub> (H <sub>2</sub> O) <sub>4</sub> ](VO) <sub>16</sub> (OH) <sub>8</sub> (O <sub>4</sub> AsPh) <sub>2</sub> (O <sub>3</sub> AsPh) <sub>82</sub> O	blue		VCl <sub>3</sub> , PhAsO <sub>3</sub> H <sub>2</sub> , NEt <sub>3</sub> , MeCN	80 °C, 30 min	65% based on V	EA, IR, ESI-MS, powder XRD, single-crystal XRD	163
H <sub>5</sub> [{Cl <sub>4</sub> (H <sub>2</sub> O) <sub>2</sub> }(VO) <sub>16</sub> O <sub>16</sub> (O <sub>3</sub> AsPh) <sub>8</sub> ]Cl·4H <sub>2</sub> O·3MeCN	green		VCl <sub>3</sub> , Dy(NO <sub>3</sub> ) <sub>3</sub> ·xH <sub>2</sub> O, PhAsO <sub>3</sub> H <sub>2</sub> , NEt <sub>3</sub> , MeCN	80 °C, 30 min	12% based on V	EA, IR, ESI-MS, powder XRD, single-crystal XRD	163
[Zn <sub>2</sub> (dien) <sub>3</sub> ][{Zn(dien)} <sub>2</sub> V <sub>16</sub> As <sub>4</sub> O <sub>42</sub> (H <sub>2</sub> O)]·3H <sub>2</sub> O	brown	1D linear chain	V <sub>2</sub> O <sub>5</sub> , As <sub>2</sub> O <sub>3</sub> , H <sub>2</sub> O, dien, Zn(OAc) <sub>2</sub> ·4H <sub>2</sub> O	170 °C, 4 d pH = 7.15 → 8.05	31% based on V <sub>2</sub> O <sub>5</sub>	EA, IR, TGA, magnetometry, single-crystal XRD	159

**V<sub>20</sub>**

[{Cl <sub>4</sub> (H <sub>2</sub> O) <sub>2</sub> }(VO) <sub>20</sub> O <sub>16</sub> (OH) <sub>4</sub> (O <sub>3</sub> AsPh) <sub>8</sub> ]·7H <sub>2</sub> O·3MeCN	green		VCl <sub>3</sub> , Dy(NO <sub>3</sub> ) <sub>3</sub> ·xH <sub>2</sub> O, PhAsO <sub>3</sub> H <sub>2</sub> , NEt <sub>3</sub> , MeCN	80 °C, 30 min	58% based on V	EA, IR, ESI-MS, powder XRD, single-crystal XRD	163
--	-------	--	--	---------------	----------------	--	-----

**V<sub>24</sub>**

H <sub>10</sub> [{Cl <sub>6</sub> }(VO) <sub>24</sub> O <sub>24</sub> (O <sub>3</sub> AsPh) <sub>8</sub> ]Cl <sub>4</sub> ·10H <sub>2</sub> O·2MeCN	green		VCl <sub>3</sub> , Dy(NO <sub>3</sub> ) <sub>3</sub> ·xH <sub>2</sub> O, PhAsO <sub>3</sub> H <sub>2</sub> , NEt <sub>3</sub> , MeCN	80 °C, 30 min	52% based on V	EA, IR, ESI-MS, powder XRD, single-crystal XRD	163
---	-------	--	--	---------------	----------------	--	-----

<sup>a</sup> Dimensionality resulting from hydrogen bonding networks is not considered.

### 3.3 Polyoxovanadatoantimonates (SbPOVs).

#### 3.3.1 Discrete SbPOVs.

***{V<sub>14</sub>Sb<sub>8</sub>}*-type polyoxoanions.** The “fully-reduced”  $\alpha$ -[H<sub>2</sub>O@V<sup>IV</sup><sub>14</sub>Sb<sub>8</sub>O<sub>42</sub>]<sup>4-</sup> polyoxoanion, with rhombicuboctahedral topology and isostructural to  $\alpha$ -[V<sup>IV</sup><sub>14</sub>As<sub>8</sub>O<sub>42</sub>]<sup>4-</sup> (Figure 15a), was isolated as the compound [(H<sub>2</sub>en)<sub>2</sub>{V<sub>14</sub>Sb<sub>8</sub>O<sub>42</sub>(H<sub>2</sub>O)}]·(en)·4H<sub>2</sub>O under hydrothermal conditions<sup>184</sup> (Table 4). Its crystal structure shows a 1D double-chain in which the sphere-like  $\alpha$ -isomeric SbPOVs are interlinked through non-bonding Sb···O contacts of 2.74 and 2.79 Å. The intermolecular N–H···O hydrogen bonds between the terminal oxygen atoms of the SbPOVs and the hydrogen atoms of ethylenediamine molecules were observed.

The  $\beta$ -isomeric [V<sup>IV</sup><sub>14</sub>Sb<sub>8</sub>O<sub>42</sub>]<sup>4-</sup> polyoxoanion is a component of the solvothermally prepared ammonium salt (NH<sub>4</sub>)<sub>4</sub>[V<sub>14</sub>Sb<sub>8</sub>O<sub>42</sub>]·2H<sub>2</sub>O (Table 4).<sup>185</sup> The structure is further characterised by comparably short intercluster Sb···O contacts of 2.83–2.98 Å.

***{V<sub>15</sub>Sb<sub>6</sub>}*-type polyoxoanion.** The compound (H<sub>3</sub>tren)<sub>2</sub>[V<sub>15</sub>Sb<sub>6</sub>O<sub>42</sub>]·0.33(tren)·*n*H<sub>2</sub>O (*n* = 3–5) was obtained under solvothermal conditions (Table 4),<sup>186</sup> comprising an isostructural antimony analogue [V<sup>IV</sup><sub>15</sub>Sb<sub>6</sub>O<sub>42</sub>]<sup>6-</sup> of the molecular magnet [H<sub>2</sub>O@V<sup>IV</sup><sub>15</sub>As<sub>6</sub>O<sub>42</sub>]<sup>6-</sup>. The nanosized structure of this “fully-reduced” polyoxoanion (Figure 25a, left) is viewed as a derivative of the {V<sub>18</sub>O<sub>42</sub>} archetype where three {VO<sub>5</sub>} square-pyramids are substituted by three handle-like {Sb<sub>2</sub>O<sub>5</sub>} groups. The structure features {V<sub>15</sub>}-nuclearity building blocks being arranged in hexagonal layers via weak, intercluster  $\Delta$ (Sb– $\mu$ -O···Sb– $\mu$ -O···Sb– $\mu$ -O) interactions within the distances of *ca.* 2.9 Å, thus resulting in the formation of trimeric super-structures ([V<sup>IV</sup><sub>15</sub>Sb<sub>6</sub>O<sub>42</sub>]<sup>6-</sup>)<sub>3</sub>. The spin-1/2 ground structure of the [V<sup>IV</sup><sub>15</sub>Sb<sub>6</sub>O<sub>42</sub>]<sup>6-</sup> polyoxoanion “represents an interesting reference system for the concise characterisation of the microscopic magnetism of these spin 1/2 triangle systems”<sup>186</sup> (Figure 25a, right).

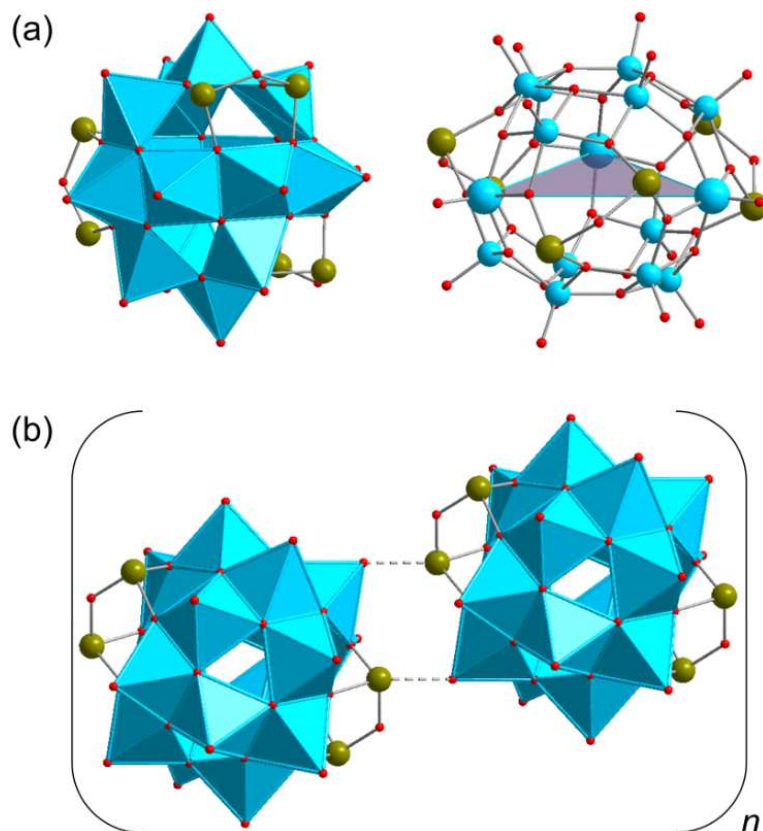


**Figure 25.** (a) Left: Polyhedral representation of the “fully-reduced”  $[V_{15}Sb_6O_{42}]^{6-}$  polyoxoanion isolated as the compound  $(H_3tren)_2[V_{15}Sb_6O_{42}] \cdot 0.33(tren) \cdot nH_2O$  with  $n = 3-5$ . Right: Ball-and-stick representation of  $[V_{15}Sb_6O_{42}]^{6-}$  emphasising the equilateral  $S = 1/2 V_{15}^{IV}$  triangle that defines the low-temperature magnetic properties. (b) A segment of the extended solid-state structure of  $(H_2aep)_4[V_{16}Sb_4O_{42}] \cdot 2H_2O$ , highlighting the weak  $Sb \cdots O$  interactions that interlink the neighbouring  $SbPOVs$ . Colour code: Sb, dark yellow; O, red;  $V^{IV}$ , sky blue;  $V^{IV}O_x$ , sky-blue polyhedra.

**$\{V_{16}Sb_4\}$ -type polyoxoanion.** The above class of  $SbPOV$ -based compounds with the general formula  $[(Hamine)_m V_{18-z} Sb_{2z} O_{42}] \cdot nH_2O$  ( $z = 2-4$ ) was extended by a new member of this series, namely  $(H_2aep)_4[V_{16}Sb_4O_{42}] \cdot 2H_2O$ , prepared under solvothermal conditions (Table 4).<sup>185</sup> This compound is composed of the “fully-reduced”  $[V_{16}Sb_4O_{42}]^{8-}$  polyoxoanion ( $D_{2h}$  symmetry) charge-balanced by four doubly protonated  $(C_6H_{17}N_3)^{2+}$  groups (=  $H_2aep$ ). The structure of the  $SbPOV$  showing the common rhombicuboctahedral topology consists of sixteen  $\{VO_5\}$  square pyramids and four  $\{SbO_3\}$  trigonal pyramids and can be interpreted as being derived from the  $\{V_{18}O_{42}\}$  archetype when replacing two  $\{VO_5\}$  units in the latter with two  $\{Sb_2O_5\}$  groups. In the structure of  $(H_2aep)_4[V_{16}Sb_4O_{42}] \cdot 2H_2O$ , the  $SbPOVs$  are connected into infinite chains via intercluster  $Sb \cdots O$  interactions of ca. 2.85 Å (Figure 25b).



### 3.3.2 Vanadyl(IV)-extended SbPOV.

The solvothermal synthesis of the compound  $[V_{16}Sb_4O_{42}(H_2O)\{VO(dach)_2\}_4]\cdot(dach)\cdot 10H_2O$  containing a neutral SbPOV building block<sup>187</sup> (Table 4) can be derived from a general composition  $\{V_{18-2}Sb_{22}O_{42}\}$  showing a modified  $[V_{18}O_{42}]^{12-}$  structure where two  $[VO_5]^{6-}$  square pyramids are replaced by two diagonal-lying, handle-like  $[Sb_2O_5]^{4-}$  groups (Figure 26). The terminal O atoms of two diagonally oriented, non-substituted  $\{VO_5\}$  square pyramids and those from the two  $\{VO_5\}$  square-pyramids interlocking two orthogonal eight-membered rings are involved in the bonding to the four square-pyramidal  $[V^{IV}O(dach)_2]^{2+}$  complexes. These  $\{N_4VO\}$ -type constituents cause charge neutrality. Their coordination results in the discrete  $[V_{16}Sb_4O_{42}\{VO(dach)_2\}_4]$  nanostructure with a diameter of ca. 17.5 Å. The compound is soluble in polar organic solvents (methanol, ethanol, and dimethylformamide) and may find application in homogeneous redox catalysis. According to the magnetic susceptibility data, the coupling between the O-bridged  $V^{IV}$  ions of the four  $\{N_4VO\}$  groups and those of the  $\{V_{16}Sb_4O_{42}\}$  building block is very weak. The “fully-reduced”  $[H_2O@V^{IV}_{16}Sb_4O_{42}]^{8-}$  polyoxoanion ( $D_{2h}$  symmetry) itself is characterised by strong antiferromagnetic coupling between the spin-1/2 vanadyl  $\{VO\}^{2+}$  moieties.

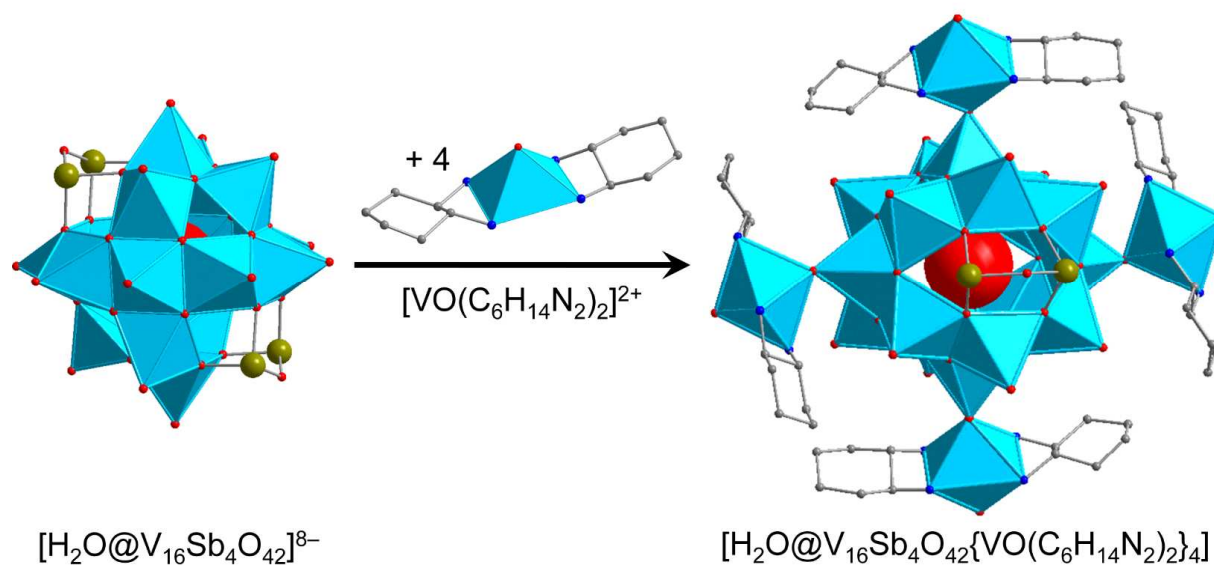


**Figure 26.** The “fully-reduced”  $[H_2O@V^{IV}_{16}Sb_4O_{42}\{VO(dach)_2\}_4]$  self-assembly (right) and its constituents,  $[H_2O@V^{IV}_{16}Sb_4O_{42}]^{8-}$  (left) and  $[V^{IV}O(dach)_2]^{2+}$  (middle). Hydrogen atoms are not shown. Colour code: C, grey; N, blue; Sb, dark yellow; O, red;  $V^{IV}O_x$ , sky-blue polyhedra.

### 3.3.3 SbPOVs with covalent Sb–N bonds.

First organo-SbPOV structures formed due to the covalent attachment of the primary and secondary amines to the SbPOVs were reported in 2011.<sup>188</sup> The compounds  $[V_{14}Sb_8(Haep)_4O_{42}(H_2O)] \cdot 4H_2O$  and  $(H_2aep)_2[V_{15}Sb_6(Haep)_2O_{42}(H_2O)] \cdot 2.5H_2O$  were hydrothermally synthesised upon adjustment of pH to the alkaline media (Table 4). The crystal structures of these compounds show hexagonal layers and rows of SbPOVs with intercluster  $Sb \cdots O$  distances of ca. 2.73 Å in the (001) and of > 3 Å in the (100) planes. The Sb atoms of the  $\beta$ - $[H_2O@V^{IV}_{14}Sb_8O_{42}]^{4-}$  and  $[H_2O@V^{IV}_{15}Sb_6O_{42}]^{6-}$  polyoxoanions are covalently bound to ammonium groups  $(C_6H_{16}N_3)^+$  (= Haep), thus resulting in Sb–N bonds lengths ranging from 2.50 to 2.54 Å. Interestingly, the molecular charge of the  $\{V_{14}\}$ -nuclearity polyoxoanion is completely neutralised by the four monoprotonated 1-(2-aminoethyl)piperazine groups, while the charge of the  $\{V_{15}\}$ -nuclearity polyoxoanion in the respective compound is only partly compensated by two Haep groups covalently attached to the Sb atoms of the  $\{Sb_2O_5\}$  handle-like groups (Figure 27). Hence,  $[V_{14}Sb_8(Haep)_4O_{42}(H_2O)] \cdot 4H_2O$  is a neutral compound and  $(H_2aep)_2[V_{15}Sb_6(Haep)_2O_{42}(H_2O)] \cdot 2.5H_2O$  is a zwitterionic complex composed of two doubly protonated  $(C_6H_{17}N_3)^{2+}$  amine counteranions (= H<sub>2</sub>aep) and the “fully-reduced”  $[H_2O@V^{IV}_{15}Sb_6(Haep)_2O_{42}]^{4-}$  polyoxoanion. The  $(C_6H_{16}N_3)^+$  groups in the compound  $[V_{14}Sb_8(Haep)_4O_{42}(H_2O)] \cdot 4H_2O$  coordinate to the Sb sites of the handle-like  $\{Sb_2O_5\}$  groups through terminal  $NH_2$  groups of 1-(2-aminoethyl)piperazinium as well as the N atoms of the piperazinium rings. The amine ligands in  $[H_2O@V^{IV}_{15}Sb_6(Haep)_2O_{42}]^{4-}$  favour only the second coordination type to the  $Sb^{III}$  atoms. The magnetic properties of two compounds are characterised by strong antiferromagnetic interactions between the spin-1/2 vanadyl  $\{VO\}^{2+}$  moieties. In line with the low or neutral charge of the clusters, both compounds are soluble in methanol and ethanol. The UV/Vis spectra of their solutions are characterised by a strong absorption band at ca. 230 nm and a weaker shoulder at ca. 280 nm.

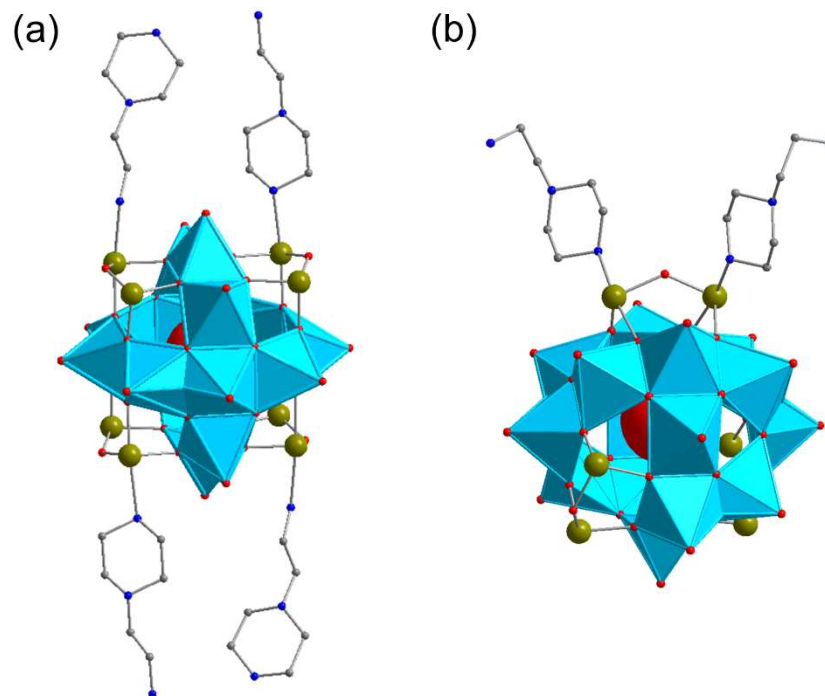


**Figure 27.** The “fully-reduced” organo-SbPOVs  $[\text{H}_2\text{O}@V^{IV}_{14}\text{Sb}_8(\text{Haep})_4\text{O}_{42}]$  (a) and  $[\text{H}_2\text{O}@V^{IV}_{15}\text{Sb}_6(\text{Haep})_2\text{O}_{42}]^{4-}$  (b). Colour code: C, grey; N, blue; Sb, dark yellow; O, red;  $V^{IV}\text{O}_x$ , sky-blue polyhedra.

### 3.3.4 TMC-supported SbPOVs.

**Zinc-SbPOV hybrids.** Two organic–inorganic hybrid solids  $[\text{Zn}_2(\text{dien})_3][\{\text{Zn}(\text{dien})\}_2\text{V}_{16}\text{Sb}_4\text{O}_{42}(\text{H}_2\text{O})]\cdot 4\text{H}_2\text{O}$  and  $[\text{Zn}(\text{dien})_2]_2[\{\text{Zn}(\text{dien})\}_2(\text{V}_{14}\text{Sb}_8\text{O}_{42})_2(\text{H}_2\text{O})]\cdot 4\text{H}_2\text{O}$  were obtained by pH-controlled hydrothermal syntheses (Table 4).<sup>189</sup> These compounds contain the  $[\text{V}^{IV}_{16}\text{Sb}_4\text{O}_{42}]^{8-}$  and  $\beta$ - $[\text{V}^{IV}_{14}\text{Sb}_8\text{O}_{42}]^{4-}$  building blocks and in the solid state are arranged as 1D infinite linear and zig-zag chains, respectively. In the structure of the former compound, neighbouring  $[\text{H}_2\text{O}@V_{16}\text{Sb}_4\text{O}_{42}]^{8-}$  polyoxoanions with  $D_{2h}$  symmetry are linked by the  $[\text{Zn}(\text{dien})]^{2+}$  bridging groups via covalent Zn–O bonds (Figure 28a), while the  $[\text{Zn}_2(\text{dien})_3]^{4+}$  complexes resemble structurally discrete counteranions. Similarly to the previous compound, the crystal structure of  $[\text{Zn}(\text{dien})_2]_2[\{\text{Zn}(\text{dien})\}_2(\text{V}_{14}\text{Sb}_8\text{O}_{42})_2(\text{H}_2\text{O})]\cdot 4\text{H}_2\text{O}$  contains neighbouring  $\beta$ - $[\text{V}^{IV}_{14}\text{Sb}_8\text{O}_{42}]^{4-}$  polyoxoanions that are bridged by single  $[\text{Zn}(\text{dien})]^{2+}$  moieties through covalent Zn–O bonds (Figure 28b). The two  $[\text{Zn}(\text{dien})_2]^{2+}$  cations compensate the negative charge of the  $[\{\text{Zn}(\text{dien})\}_2(\text{V}_{14}\text{Sb}_8\text{O}_{42})_2(\text{H}_2\text{O})]^{4-}$  assembly.

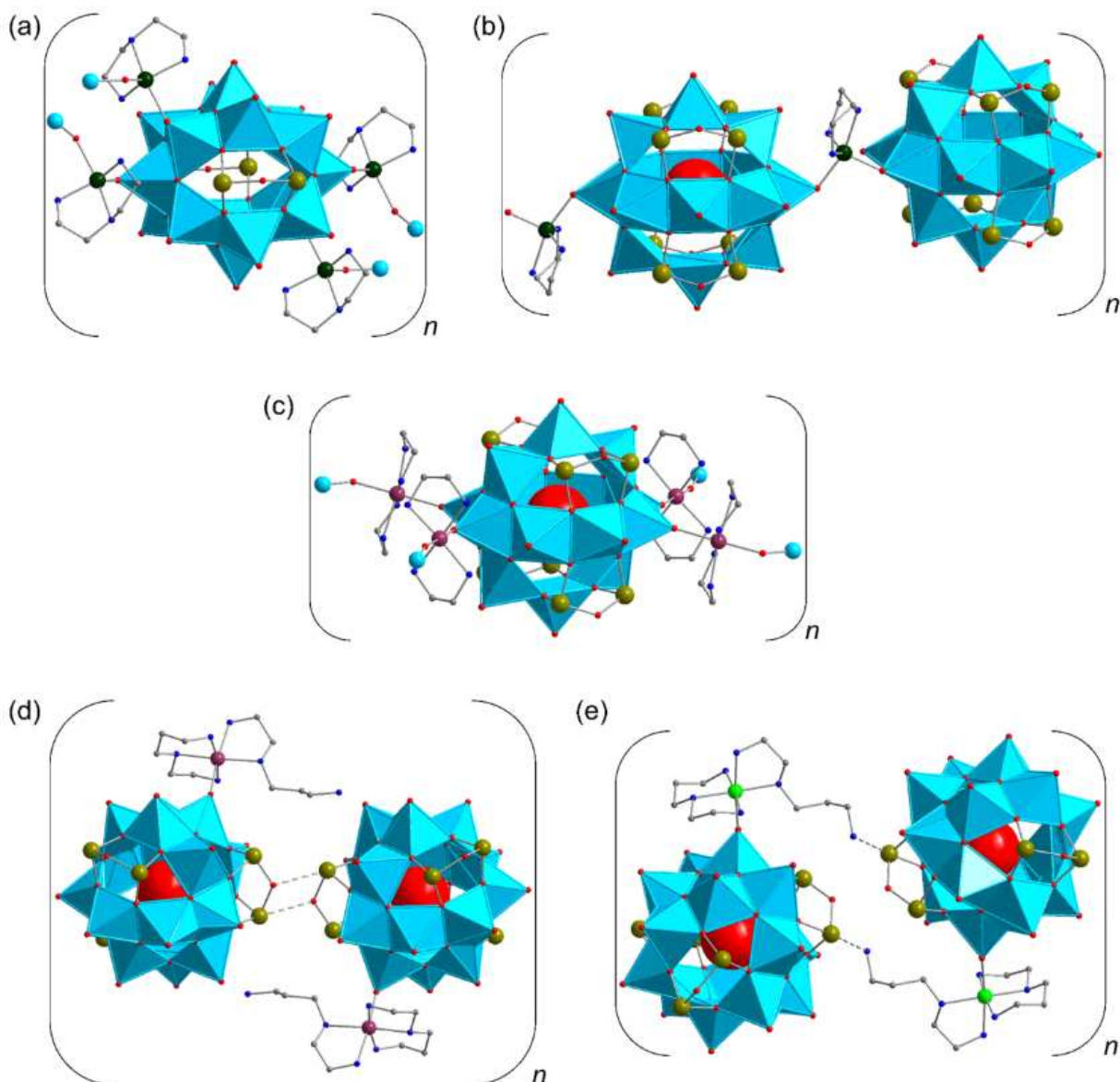


**Figure 28.** (a,b) Fragments from the 1D infinite linear (a) and zig-zag (b) chains in the crystal structures of  $[\text{Zn}_2(\text{dien})_3][\{\text{Zn}(\text{dien})\}_2\text{V}_{16}\text{Sb}_4\text{O}_{42}(\text{H}_2\text{O})]\cdot 4\text{H}_2\text{O}$  and  $[\text{Zn}(\text{dien})_2]_2[\{\text{Zn}(\text{dien})\}_2(\text{V}_{14}\text{Sb}_8\text{O}_{42})_2(\text{H}_2\text{O})]\cdot 4\text{H}_2\text{O}$ . (c) A fragment from the extended solid-state structure of  $[\{\text{Co}(\text{en})_2\}_2\text{V}_{14}\text{Sb}_8\text{O}_{42}(\text{H}_2\text{O})]\cdot 6\text{H}_2\text{O}$ , illustrating the “fully-reduced”  $\beta\text{-}[\text{H}_2\text{O}@V_{14}\text{Sb}_8\text{O}_{42}]^{4-}$  polyoxoanion decorated with four bridging  $[\text{Co}(\text{en})_2]^{2+}$  groups. (d,e) Pairs of  $[\text{H}_2\text{O}@V_{15}\text{Sb}_6\text{O}_{42}\text{M}(\text{aepda})_2]^{4-}$  hybrid polyoxoanions (M = Co, left; M = Ni, right) formed by weak  $\text{Sb}\cdots\text{O}$  (d) and  $\text{Sb}\cdots\text{N}$  (e) interactions in the solid-state structures of  $[\text{Co}(\text{aepda})_2]_2[\{\text{Co}(\text{aepda})_2\}\text{V}_{15}\text{Sb}_6\text{O}_{42}(\text{H}_2\text{O})]\cdot 5\text{H}_2\text{O}$  and  $[\text{Ni}(\text{aepda})_2]_2[\{\text{Ni}(\text{aepda})_2\}\text{V}_{15}\text{Sb}_6\text{O}_{42}(\text{H}_2\text{O})]\cdot 8\text{H}_2\text{O}$ , respectively. Colour code: C, grey; N, blue; Sb, dark yellow; O, red;  $V^{\text{IV}}$ , sky blue;  $V^{\text{IV}}\text{O}_x$ , sky-blue polyhedra; Co, plum; Ni, bright green; Zn, dark green.

A  $[\text{H}_2\text{O}@V_{16}\text{Sb}_4\text{O}_{42}]^{8-}$  polyoxoanion in which the geometric position of the handle-like  $\{\text{Sb}_2\text{O}_5\}$  groups reduce the symmetry of the  $\{\text{V}_{16}\}$  skeleton to  $C_2$  (vs.  $D_{2h}$  symmetry reported for all hitherto characterised  $\{\text{V}_{16}\}$ -nuclearity AsPOVs and SbPOVs) was also identified (Figure 29).<sup>190</sup> For comparison, the  $[\text{V}_{16}\text{Si}_4\text{O}_{46}]^{12-}$  polyoxoanion illustrated in Figure 6a has  $D_{2h}$  symmetry, whereas the  $[\text{V}_{16}\text{Ge}_4\text{O}_{42}(\text{OH})_4]^{8-}$  in Figure 8a also displays  $C_2$  symmetry.

Such changes in the SbPOV structure influenced the geometrical parameters, specifically the V...V distances of this polyoxoanion. While the shortest non-bonding V...V distances in the  $C_2$ -symmetrical  $[H_2O@V_{16}Sb_4O_{42}]^{8-}$  structure are between 2.73 and 3.10 Å, those in the isonuclear, but  $D_{2h}$ -symmetrical analogues fall in the range 2.85 – 3.06 Å in  $(H_2aep)_4[V_{16}Sb_4O_{42}] \cdot 2H_2O$ ,<sup>185</sup> 2.92 – 3.03 Å in  $[V_{16}Sb_4O_{42}(H_2O)\{VO(dach)_2\}_4] \cdot (dach) \cdot 10H_2O$ ,<sup>187</sup> and 2.92 – 3.05 Å in  $[Zn_2(dien)_3][\{Zn(dien)\}_2V_{16}Sb_4O_{42}(H_2O)] \cdot 4H_2O$ .<sup>189</sup> The “fully-reduced”  $[H_2O@V^IV_{16}Sb_4O_{42}]^{8-}$  polyoxoanion with its new *pseudorhombicuboctahedral* topology is a component of the  $[Zn(tren)(H_2tren)]_2[V_{16}Sb_4O_{42}(H_2O)] \cdot nH_2O$  compound ( $n = 6-10$ ) obtained under solvothermal conditions (Table 4). Two trigonal bipyramidal  $\{Zn(tren)(H_2tren)\}^{4+}$  complexes assume the role of countercations. The crystal structure of this compound that is soluble in methanol and ethanol contains channels between the SbPOVs arranged in the pairs by weak intercluster Sb...O interactions because of the specific orientation of the handle-like  $[Sb_2O_5]^{4-}$  groups. The intermolecular N–H...O hydrogen bonds between the cations, polyoxoanions and  $H_2O$  molecules expand the structure of  $[Zn(tren)(H_2tren)]_2[V_{16}Sb_4O_{42}(H_2O)] \cdot nH_2O$  into a 3D network. The low-field magnetic susceptibility studies revealed that the  $C_2$ -symmetrical  $[H_2O@V^IV_{16}Sb_4O_{42}]^{8-}$  polyoxoanion exhibits strong antiferromagnetic coupling between the spin-1/2 vanadyl  $\{VO\}^{2+}$  moieties. Remarkably, a significant difference in the susceptibility data was found between the compounds  $[Zn(tren)(H_2tren)]_2[V_{16}Sb_4O_{42}(H_2O)] \cdot nH_2O$  (with  $C_2$ -symmetrical  $\{V_{16}\}$  spin polytope) and  $[Zn_2(dien)_3][\{Zn(dien)\}_2V_{16}As_4O_{42}(H_2O)] \cdot 3H_2O$ <sup>159</sup> (with  $D_{2h}$ -symmetrical  $\{V_{16}\}$  spin polytope), thus showing the effect of the pnictogen oxide positions on the magnetism of the isonuclear, but not isostructural AsPOV and SbPOV structures.

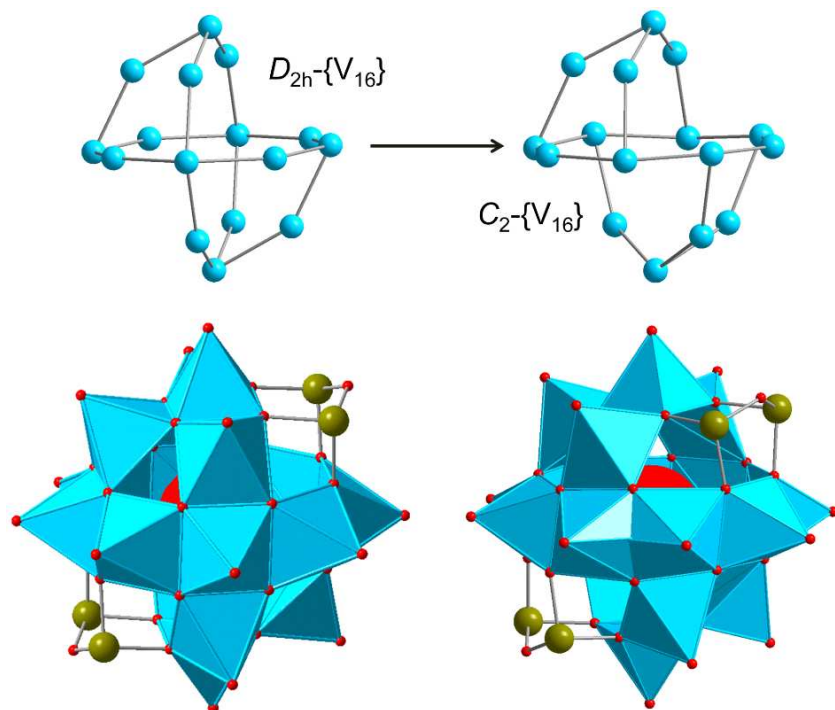


**Figure 29.** The “fully-reduced”  $[\text{H}_2\text{O}@V_{16}^{\text{IV}}\text{Sb}_4\text{O}_{42}]^{8-}$  polyoxoanion featuring  $\{\text{V}_{16}\}$  skeletons with different symmetries ( $D_{2h}$  and  $C_2$ ). Colour code: Sb, dark yellow; O, red;  $V^{\text{IV}}$ , sky blue;  $V^{\text{IV}}\text{O}_x$ , sky-blue polyhedra.

**Cobalt- and Nickel-SbPOV hybrids.** The compound  $[\{\text{Co}(\text{en})_2\}_2\text{V}_{14}\text{Sb}_8\text{O}_{42}(\text{H}_2\text{O})] \cdot 6\text{H}_2\text{O}$  prepared under hydrothermal conditions (Table 4) was the first example of functionalisation of a POV building block with antimony.<sup>191</sup> The crystal structure features 2D arrays of the spherical  $\beta\text{-}[\text{H}_2\text{O}@V_{14}^{\text{IV}}\text{Sb}_8\text{O}_{42}]^{4-}$  polyoxoanions that are joined through the covalent bonds between the apical oxygen atoms of the  $\beta\text{-SbPOVs}$  and the bridging  $\text{Co}^{2+}$  ions of the  $[\text{Co}(\text{en})_2]^{2+}$  complexes (Figure 28c). Similar to the  $\beta\text{-}[V_{14}^{\text{IV}}\text{As}_8\text{O}_{42}]^{4-}$  polyoxoanion (Figure 15b), this “fully-reduced” SbPOV represents a modified  $[\text{V}_{18}\text{O}_{42}]^{12-}$  structure whose four  $\{\text{VO}_5\}$  square pyramids are replaced by four handle-like  $\{\text{Sb}_2\text{O}_5\}$  groups.

The compounds  $[\text{Co}(\text{tren})(\text{H}_2\text{O})]_3[\text{V}_{15}\text{Sb}_6\text{O}_{42}(\text{H}_2\text{O})] \cdot \text{H}_2\text{O}$ ,  $[\text{Co}_2(\text{tren})_3]_2[\text{Co}(\text{tren})(\text{en})][\{\text{V}_{15}\text{Sb}_6\text{O}_{42}(\text{H}_2\text{O})(\text{Co}(\text{tren})_2)\}\text{V}_{15}\text{Sb}_6\text{O}_{42}(\text{H}_2\text{O})] \cdot n\text{H}_2\text{O}$  ( $n \approx 11$ ), and  $[\text{Co}(\text{tren})(\text{H}_2\text{tren})]_2[\text{V}_{16}\text{Sb}_4\text{O}_{42}(\text{H}_2\text{O})] \cdot 6\text{H}_2\text{O}$  containing distinct  $\text{Co}^{2+}$  complexes, namely  $[\text{Co}(\text{tren})(\text{H}_2\text{O})]^{2+}$ ,  $[\text{Co}_2(\text{tren})_3]^{4+}$ ,  $[\text{Co}(\text{tren})(\text{en})]^{2+}$ ,  $[\text{Co}(\text{tren})_2]^{2+}$ , and  $[\text{Co}(\text{tren})(\text{H}_2\text{tren})]^{4+}$  were synthesised under solvothermal conditions using different concentrations of amine molecules (Table 4).<sup>192</sup> Notably, the solvothermal reaction yielding  $[\text{Co}_2(\text{tren})_3]_2[\text{Co}(\text{tren})(\text{en})][\{\text{V}_{15}\text{Sb}_6\text{O}_{42}(\text{H}_2\text{O})(\text{Co}(\text{tren})_2)\}\text{V}_{15}\text{Sb}_6\text{O}_{42}(\text{H}_2\text{O})] \cdot n\text{H}_2\text{O}$  included a partial decomposition of tren molecules yielding bidentate en ligands. The inorganic-organic hybrid solids presented above are based on the  $[\text{H}_2\text{O}@V_{15}^{\text{IV}}\text{Sb}_6\text{O}_{42}]^{6-}$  or  $[\text{H}_2\text{O}@V_{16}^{\text{IV}}\text{Sb}_4\text{O}_{42}]^{8-}$  polyoxoanions with diameters of ca. 11 Å. The “fully-reduced” SbPOV

shells with the shortest V...V distances of 2.81 – 3.07 Å are derived from the  $\{V_{18}O_{42}\}$  shell showing  $D_{4d}$  symmetry, i.e.  $3 \{VO_5\} \leftrightarrow 3 \{Sb_2O_5\}$ . The  $[H_2O@V^{IV}_{15}Sb_6O_{42}]^{6-}$  polyoxoanion in the crystal structure of  $[Co(tren)(H_2O)]_3[V_{15}Sb_6O_{42}(H_2O)] \cdot H_2O$  are involved in weak Sb...O intercluster interactions, with the shortest one being ca. 2.90 Å. These Sb...O interactions are comparable with those identified e.g., in the 2D layered structures of the compounds  $(H_2en)_2[V^{IV}_{14}Sb_8O_{42}(H_2O)] \cdot 3H_2O$  ( $d_{Sb...O} = 2.72 - 2.92$  Å) and  $(H_2ppz)_2[V^{IV}_{14}Sb_8O_{42}(H_2O)]$  ( $d_{Sb...O} = 2.83 - 3.01$  Å) with the discrete  $\beta$ -isomeric SbPOV motifs ( $d_{V...V} = 2.90 - 3.10$  Å).<sup>193</sup> The solvothermal formation of these compounds is accompanied by a decomposition of *N,N,N',N'*-tetramethylethylenediamine to ethylenediamine and *in situ* fragmentation of 1-methylpiperazine to piperazine, respectively. Like for the compounds  $(H_2en)_2[V_{14}Sb_8O_{42}(H_2O)] \cdot 3H_2O$  and  $(H_2ppz)_2[V_{14}Sb_8O_{42}(H_2O)]$ ,  $O_{SbPOV} \cdots H_{amine}$  hydrogen bonds are observed in the crystal structure of  $[Co(tren)(H_2O)]_3[V_{15}Sb_6O_{42}(H_2O)] \cdot H_2O$ . The crystal structure of  $[Co_2(tren)_3]_2[Co(tren)(en)]\{[V_{15}Sb_6O_{42}(H_2O)(Co(tren)_2)]V_{15}Sb_6O_{42}(H_2O)\} \cdot nH_2O$  ( $n \approx 11$ ) is characterised by short Sb...N interactions (2.60 Å, 2.65 Å, and 2.74 Å), which engage the N atoms of primary amine molecules (tren) and the Sb atoms of the SbPOVs. Relatively short Sb...O intercluster contacts (2.88 – 2.93 Å) were also observed. The observed N–H...O hydrogen bonds generate a 3D network. Interestingly, the central  $[H_2O@V^{IV}_{16}Sb_4O_{42}]^{8-}$  polyanion of the compound  $[Co(tren)(H_2tren)]_2[V_{16}Sb_4O_{42}(H_2O)] \cdot 6H_2O$  is isostructural to that of  $[Zn(tren)(H_2tren)]_2[V_{16}Sb_4O_{42}(H_2O)] \cdot nH_2O$  ( $n = 6 - 10$ )<sup>190</sup> (see Figure 29) and can be viewed as being derived from the  $T_d$ -symmetric  $\{V_{18}O_{42}\}$  shell, i.e. by formal metathesis  $2 \{VO_5\} \leftrightarrow 2 \{Sb_2O_5\}$ . The shortest V...V distances in this  $C_2$ -symmetrical SbPOV polyoxoanion are in the range 2.73 – 3.09 Å.

The compounds  $[Co(aepda)_2]_2\{[Co(aepda)_2]V_{15}Sb_6O_{42}(H_2O)\} \cdot 5H_2O$  and  $[Ni(aepda)_2]_2\{[Ni(aepda)_2]V_{15}Sb_6O_{42}(H_2O)\} \cdot 8H_2O$  (aepda = *N*-(2-aminoethyl)-1,3-propanediamine =  $C_5H_{15}N_3$ ) were also obtained under solvothermal conditions<sup>194</sup> (Table 4) and their crystal structures feature the  $[H_2O@V^{IV}_{15}Sb_6O_{42}]^{6-}$  polyoxoanion being structurally related to the well-known  $\{V_{18}O_{42}\}$  archetype, as is the case for the AsPOV analogue  $[H_2O@V^{IV}_{15}As_6O_{42}]^{6-}$ . Each of these  $[H_2O@V^{IV}_{15}Sb_6O_{42}]^{6-}$  polyoxoanions comprises a terminal oxygen position covalently bonded to the transition metal complexes  $[M(aepda)_2]^{2+}$  ( $M = Co, Ni$ ). As a result, the  $M^{2+}$  centre has an octahedral  $M(N_{aepda})_5O_{SbPOV}$  coordination environment. The two remaining  $[M(aepda)_2]^{2+}$  moieties in each compound serve as charge-balancing cations. As in the case of several other TMC-functionalised *hetero*POVs, the paramagnetic  $M^{2+}$  ions ( $M = Co, Ni$ ) from the terminally coordinated  $[M(aepda)_2]^{2+}$  complexes couple only very weakly with the spin-1/2 vanadyl  $\{VO\}^{2+}$  moieties of the



$[\text{H}_2\text{O}@\text{V}^{\text{IV}}_{15}\text{Sb}_6\text{O}_{42}]^{6-}$  polyoxoanions. In the crystal structure of the compound comprising  $\text{Co}^{2+}$  ions, the polyoxoanions are connected through weak intercluster  $\text{Sb}\cdots\text{O}$  (3.13 Å) interaction, thus forming pairs of SbPOVs (Figure 28d). In contrast, in the crystal structure of the compound containing  $\text{Ni}^{2+}$  ions pairs of SbPOVs linked by weak  $\text{Sb}\cdots\text{N}$  contacts (2.65 Å) are observed. These  $\text{Sb}\cdots\text{N}$  interactions involve the Sb atoms of the “fully-reduced”  $[\text{H}_2\text{O}@\text{V}^{\text{IV}}_{15}\text{Sb}_6\text{O}_{42}]^{6-}$  polyoxoanion and the N atoms of the propylamine chains from the adjoined  $[\text{Ni}(\text{aepda})_2]^{2+}$  fragments (Figure 28e). In addition, intermolecular  $\text{N}-\text{H}\cdots\text{O}$  hydrogen bonds generating higher dimensional networks were observed in the structures of both these compounds.

A dimeric  $\{[\text{Ni}_2(\text{tren})_3(\text{V}_{15}\text{Sb}_6\text{O}_{42}(\text{H}_2\text{O})_{0.5})]_2\}^{4-}$  fragment where two “fully-reduced”  $[\text{V}^{\text{IV}}_{15}\text{Sb}_6\text{O}_{42}(\text{H}_2\text{O})_{0.5}]^{6-}$  polyoxoanions (shortest  $d_{\text{V}\cdots\text{V}} = 2.84 - 3.08$  Å) are bridged by an *in situ*-produced  $[\text{Ni}_2(\text{tren})_3]^{4+}$  complex via a multidentate  $\mu$ -1,7 tren ligand was identified in the solvothermally synthesised, highly insoluble compound  $[\text{Ni}(\text{Htren})_2][\text{Ni}_2(\text{tren})_3(\text{V}_{15}\text{Sb}_6\text{O}_{42}(\text{H}_2\text{O})_{0.5})]_2 \cdot \text{H}_2\text{O}$  (Table 4).<sup>195</sup> Its crystal structure is characterised by double chains along the crystallographic *b* axis, formed by short  $\text{Sb}\cdots\text{N}$  contacts ( $d_{\text{Sb}\cdots\text{N}} = \text{ca. } 2.69$  Å) between the neighbouring heterometallic dimers. Again, an additional  $[\text{Ni}(\text{Htren})_2]^{4+}$  complex with protonated tren ligands acts as counteranion. For comparison, the covalent Sb–N distances in the structures of the aforementioned compounds  $[\text{V}_{14}\text{Sb}_8(\text{Haep})_4\text{O}_{42}(\text{H}_2\text{O})] \cdot 4\text{H}_2\text{O}$  and  $(\text{H}_2\text{aep})_2[\text{V}_{15}\text{Sb}_6(\text{Haep})_2\text{O}_{42}(\text{H}_2\text{O})] \cdot 2.5\text{H}_2\text{O}$  (Figure 27) are  $d_{\text{Sb}-\text{N}} = 2.53$  and  $2.54$  Å and  $d_{\text{Sb}-\text{N}} = 2.50$  and  $2.54$  Å, respectively.<sup>188</sup> A 3D network in the crystal structure of  $[\text{Ni}_2(\text{tren})_3(\text{V}_{15}\text{Sb}_6\text{O}_{42}(\text{H}_2\text{O})_{0.5})]_2[\text{Ni}(\text{Htren})_2] \cdot \text{H}_2\text{O}$  is generated by a complex hydrogen bonding pattern between H atoms of water molecules and the amine moieties and oxygen atoms of the SbPOVs.

Two pseudopolymorphic compounds with compositions  $[\text{Ni}(\text{dien})_2]_3[\text{V}_{15}\text{Sb}_6\text{O}_{42}(\text{H}_2\text{O})] \cdot n\text{H}_2\text{O}$  ( $n = 12$  and  $8$ ) and the compound  $[\text{Ni}(\text{dien})_2]_4[\text{V}_{16}\text{Sb}_4\text{O}_{42}(\text{H}_2\text{O})]$  were prepared solvothermally by adjusting the reaction temperature (Table 4).<sup>196</sup> The pseudopolymorphs display the spherical  $[\text{H}_2\text{O}@\text{V}^{\text{IV}}_{15}\text{Sb}_6\text{O}_{42}]^{6-}$  polyoxoanions which are virtually isostructural to the molecular magnet  $[\text{H}_2\text{O}@\text{V}^{\text{IV}}_{15}\text{As}_6\text{O}_{42}]^{6-}$ . The structural motif of the “fully-reduced”  $[\text{V}^{\text{IV}}_{15}\text{Sb}_6\text{O}_{42}]^{6-}$  polyoxoanion is shown in Figure 25a and that of  $[\text{V}^{\text{IV}}_{16}\text{Sb}_4\text{O}_{42}]^{8-}$ , a component of the compound  $[\text{Ni}(\text{dien})_2]_4[\text{V}_{16}\text{Sb}_4\text{O}_{42}(\text{H}_2\text{O})]$ , is illustrated in Figure 26. Interestingly, the crystal structures of the pseudopolymorphs possess different composition of the asymmetric units that involve four crystallographically independent  $[\text{H}_2\text{O}@\text{V}^{\text{IV}}_{15}\text{Sb}_6\text{O}_{42}]^{6-}$  polyoxoanions and twelve  $[\text{Ni}(\text{dien})_2]^{2+}$  complexes adopting the *s-fac*, *mer*-, and *u-fac*-configurations (tetragonal space group) or a third of the polyoxoanion and a *mer*- $[\text{Ni}(\text{dien})_2]^{2+}$  complex (rhombohedral space group). In the crystal structure of the



compound crystallising in the tetragonal space group, the SbPOVs are arranged as tetrameric superstructures with composition  $([\text{H}_2\text{O}@V^{IV}_{15}\text{Sb}_6\text{O}_{42}]^{6-})_4$  (layer-like arrangement). The individual polyoxoanions are held together by weak  $\text{Sb}\cdots\text{O}$  interactions (2.68 to 2.97 Å), which are significantly shorter than the sum of van der Waals radii (3.52 Å) for Sb and O atoms. For the structure crystallising in the rhombohedral space group, the shortest intercluster  $\text{Sb}\cdots\text{O}$  distances exceed 5 Å, because of a triangular-like arrangement of dicationic *mer*- $[\text{Ni}(\text{dien})_2]^{2+}$  complexes around the  $[\text{V}^{IV}_{15}\text{Sb}_6\text{O}_{42}]^{6-}$  polyoxoanions. The 3D network structure of this compound is realised by intermolecular  $\text{N}-\text{H}\cdots\text{O}$  hydrogen bonding interactions. The compound  $[\text{Ni}(\text{dien})_2]_4[\text{V}_{16}\text{Sb}_4\text{O}_{42}(\text{H}_2\text{O})]$  comprises octahedrally coordinated  $\text{Ni}^{2+}$  ions in the  $[\text{Ni}(\text{dien})_2]^{2+}$  cations adopting the *s-fac*- and *u-fac*-configurations. In the crystal structure of  $[\text{Ni}(\text{dien})_2]_4[\text{V}_{16}\text{Sb}_4\text{O}_{42}(\text{H}_2\text{O})]$ , the  $[\text{H}_2\text{O}@V^{IV}_{16}\text{Sb}_4\text{O}_{42}]^{8-}$  polyoxoanions are arranged in layers in the (100) plane.

**Iron-SbPOV hybrids.** The solvothermally synthesised compound  $[\{\text{Fe}(\text{dach})_2\}_3\{\text{V}_{15}\text{Sb}_6\text{O}_{42}(\text{H}_2\text{O})\}]\cdot 8\text{H}_2\text{O}$  with the unique porous 3D network topology in its extended solid-state structure (Figure 30) is the first example of an iron-augmented SbPOV architecture also exhibiting a unique magnetic structure.<sup>197</sup> The amine molecules used in the synthesis of this compound (Table 4) were shown to carry out versatile functions, acting as ligands, solvents, and reducing agents. In the structure, the  $[\text{H}_2\text{O}@V^{IV}_{15}\text{Sb}_6\text{O}_{42}]^{6-}$  polyoxoanion is expanded by six *in situ*-generated  $[\text{Fe}(\text{dach})_2]^{2+}$  complexes, which coordinate terminally to the polyoxoanion via Fe–O bonds to form octahedral  $\{\text{FeN}_4\text{O}_2\}$  units that further interlink the adjoined SbPOVs. Relatively strong  $\text{N}-\text{H}\cdots\text{O}$  hydrogen bonds were observed. The compound is further characterised by an optical energy gap of 2.47 eV. The low-field magnetic susceptibility revealed ferromagnetic exchange interactions between the spin-1/2 vanadyl  $\{\text{VO}\}^{2+}$  moieties of the polyoxoanion and the high-spin ( $S = 2$ )  $\text{Fe}^{2+}$  ions of the adjoined  $[\text{Fe}(\text{dach})_2]^{2+}$  complexes. We note that this heterometal-vanadyl coupling differs significantly from that established for the aforementioned TMC-supported AsPOVs and SbPOVs, which showed only weak or negligible, and mostly antiferromagnetic interactions between the spin centres of the central building blocks and the attached TMC fragments.

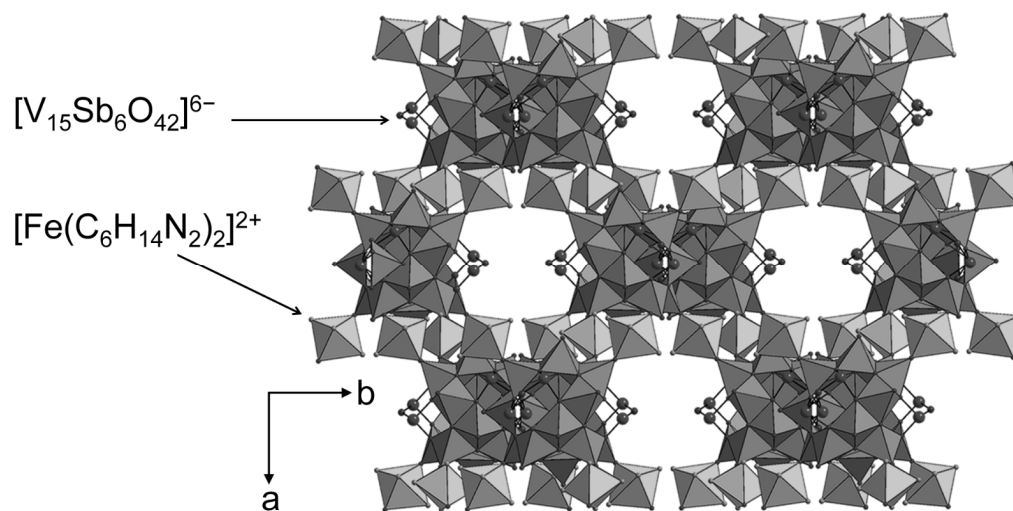


**Figure 30.** 3D network in the crystal structure of  $[[Fe(dach)_2]_3\{V_{15}Sb_6O_{42}(H_2O)\}] \cdot 8H_2O$ . The channels along  $[-110]$  are shown. Crystal solvent (water) molecules are omitted for clarity.

**Table 4.** Selected details of synthesis and characterisation of **SbPOV**-based compounds.

Formula	Colour	Characteristics of crystal structure <sup>a</sup>	Reactants	Reaction conditions	Yield	Characterised via	Ref.
<b>V<sub>14</sub></b>							
(NH <sub>4</sub> ) <sub>4</sub> [V <sub>14</sub> Sb <sub>8</sub> O <sub>42</sub> ]·2H <sub>2</sub> O	green brown	layer-like arrangement	NH <sub>4</sub> VO <sub>3</sub> , Sb <sub>2</sub> O <sub>3</sub> , theed, H <sub>2</sub> O	150 °C, 14 d	40% based on Sb	powder XRD, single-crystal XRD	185
(H <sub>2</sub> en) <sub>2</sub> [V <sub>14</sub> Sb <sub>8</sub> O <sub>42</sub> (H <sub>2</sub> O)]·3H <sub>2</sub> O	black	layer-like arrangement	NH <sub>4</sub> VO <sub>3</sub> , Sb <sub>2</sub> O <sub>3</sub> , N,N,N',N'-tetramethylethylenediamine, H <sub>2</sub> O	180 °C, 7 d	37% based on Sb	EA, IR, single-crystal XRD	193
(H <sub>2</sub> ppz) <sub>2</sub> [V <sub>14</sub> Sb <sub>8</sub> O <sub>42</sub> (H <sub>2</sub> O)]	black	layer-like arrangement	NH <sub>4</sub> VO <sub>3</sub> , Sb <sub>2</sub> O <sub>3</sub> , 1-methylpiperazine, H <sub>2</sub> O	180 °C, 7 d		powder XRD, SEM, single-crystal XRD	193
[(H <sub>2</sub> en) <sub>2</sub> {V <sub>14</sub> Sb <sub>8</sub> O <sub>42</sub> (H <sub>2</sub> O)}]·(en)·4H <sub>2</sub> O	black	1D double chain	VOSO <sub>4</sub> , Sb <sub>2</sub> O <sub>3</sub> , H <sub>2</sub> O, C <sub>2</sub> N <sub>2</sub> H <sub>8</sub> (en)	pH = 7.5, 175 °C, 4 d	61% based on Sb	EA, ICP, IR, single-crystal XRD	184
[V <sub>14</sub> Sb <sub>8</sub> (Haep) <sub>4</sub> O <sub>42</sub> (H <sub>2</sub> O)]·4H <sub>2</sub> O	brown green	chain	NH <sub>4</sub> VO <sub>3</sub> , Sb <sub>2</sub> O <sub>3</sub> , aep, H <sub>2</sub> O	180 °C, 7 d	24% based on Sb	EA, UV-vis, DTA-TGA, single-crystal XRD, magnetometry	188
[Zn(dien) <sub>2</sub> ] <sub>2</sub> [[Zn(dien)] <sub>2</sub> (V <sub>14</sub> Sb <sub>8</sub> O <sub>42</sub> ) <sub>2</sub> (H <sub>2</sub> O)]·4H <sub>2</sub> O	brown	1D zig-zag chain	Sb <sub>2</sub> O <sub>3</sub> , V <sub>2</sub> O <sub>5</sub> , Zn(OAc) <sub>2</sub> ·2H <sub>2</sub> O, dien, H <sub>2</sub> O, NaOH	pH = 9.5, 180 °C, 7 d	25% based on V	EA, IR, XPS, TGA, single-crystal XRD	189
[[Co(en) <sub>2</sub> ] <sub>2</sub> V <sub>14</sub> Sb <sub>8</sub> O <sub>42</sub> (H <sub>2</sub> O)]·6H <sub>2</sub> O	black	2D network	V <sub>2</sub> O <sub>5</sub> , Sb <sub>2</sub> O <sub>3</sub> , H <sub>2</sub> C <sub>2</sub> O <sub>4</sub> ·2H <sub>2</sub> O, CoC <sub>2</sub> O <sub>4</sub> ·2H <sub>2</sub> O, H <sub>2</sub> O, en	pH = 9.0, 160 °C, 9 d	46% based on Sb	EA, ICP, IR, single-crystal XRD	191
<b>V<sub>15</sub></b>							
(H <sub>3</sub> tren) <sub>2</sub> [V <sub>15</sub> Sb <sub>6</sub> O <sub>42</sub> ]·0.33(tren)·nH <sub>2</sub> O ( <i>n</i> = 3–5)	brown greenish	hexagonal layer	NH <sub>4</sub> VO <sub>3</sub> , Sb <sub>2</sub> O <sub>3</sub> , tren, H <sub>2</sub> O	150 °C, 7 d	70% based on Sb	EA, IR, UV-vis, Raman, DTA-TGA-MS, single-crystal XRD, magnetometry	186

$(\text{H}_2\text{aep})_2[\text{V}_{15}\text{Sb}_6(\text{Haep})_2\text{O}_{42}(\text{H}_2\text{O})]\cdot 2.5\text{H}_2\text{O}$	black	rows	$\text{NH}_4\text{VO}_3$ , $\text{Sb}_2\text{O}_3$ , aep, $\text{H}_2\text{O}$	160 °C, 7 d	64% based on Sb	EA, UV-vis, DTA-TGA, single-crystal XRD, magnetometry	188
$[\text{Ni}(\text{dien})_2]_3[\text{V}_{15}\text{Sb}_6\text{O}_{42}(\text{H}_2\text{O})]\cdot n\text{H}_2\text{O}$ ( $n = 8, 12$ )	brown	layer-like arrangement	$\text{NH}_4\text{VO}_3$ , $\text{Sb}_2\text{O}_3$ , $\text{NiCl}_2\cdot 6\text{H}_2\text{O}$ , dien, $\text{H}_2\text{O}$	130 °C / 150 °C, 7 d	36% based on Sb	EA, IR, DTA-TGA, single-crystal XRD, SEM	196
$[\text{Ni}(\text{aepda})_2]_2[\text{Ni}(\text{aepda})_2]\text{V}_{15}\text{Sb}_6\text{O}_{42}(\text{H}_2\text{O})\cdot 8\text{H}_2\text{O}$	brown	double clusters	$\text{NH}_4\text{VO}_3$ , $\text{Sb}_2\text{O}_3$ , $\text{NiCl}_2\cdot 6\text{H}_2\text{O}$ , aepda, $\text{H}_2\text{O}$	150 °C, 7 d	60% based on Sb	EA, IR, DTA-TGA, powder XRD, single-crystal XRD, SEM, magnetometry	194
$[\text{Ni}(\text{Htren})_2][\text{Ni}_2(\text{tren})_3(\text{V}_{15}\text{Sb}_6\text{O}_{42}(\text{H}_2\text{O})_{0.5})]_2\cdot \text{H}_2\text{O}$	brown	1D double chain	$\text{NH}_4\text{VO}_3$ , $\text{Sb}_2\text{O}_3$ , $\text{NiCl}_2\cdot 6\text{H}_2\text{O}$ , tren, $\text{H}_2\text{O}$	150 °C, 5 d		EA, IR, UV-vis, powder XRD, single-crystal XRD	195
$[\text{Co}(\text{aepda})_2]_2[\{\text{Co}(\text{aepda})_2\}\text{V}_{15}\text{Sb}_6\text{O}_{42}(\text{H}_2\text{O})]\cdot 5\text{H}_2\text{O}$	brown	double clusters	$\text{NH}_4\text{VO}_3$ , $\text{Sb}_2\text{O}_3$ , $\text{CoCl}_2\cdot 6\text{H}_2\text{O}$ , aepda, $\text{H}_2\text{O}$	130 °C, 7 d	45% based on Sb	EA, IR, DTA-TGA, single-crystal XRD, SEM, magnetometry	194
$[\text{Co}(\text{tren})(\text{H}_2\text{O})]_3[\text{V}_{15}\text{Sb}_6\text{O}_{42}(\text{H}_2\text{O})]\cdot \text{H}_2\text{O}$	dark brown	2D network	$\text{NH}_4\text{VO}_3$ , $\text{Sb}_2\text{O}_3$ , $\text{CoCl}_2\cdot 6\text{H}_2\text{O}$ , tren (conc. 50%)	170 °C, 7 d	60% based on Sb	EA, IR, EDXS, DTA-TG, powder XRD, single-crystal XRD	192
$[\text{Co}_2(\text{tren})_3]_2[\text{Co}(\text{tren})(\text{en})][\{\text{V}_{15}\text{Sb}_6\text{O}_{42}(\text{H}_2\text{O})(\text{Co}(\text{tren})_2)\}\text{V}_{15}\text{Sb}_6\text{O}_{42}(\text{H}_2\text{O})]\cdot n\text{H}_2\text{O}$ ( $n \approx 11$ )	brown	1D double chain	$\text{NH}_4\text{VO}_3$ , $\text{Sb}_2\text{O}_3$ , $\text{CoCl}_2\cdot 6\text{H}_2\text{O}$ , tren (conc. 75%)	170 °C, 7 d	35% based on Sb	EA, IR, EDXS, DTA-TG, powder XRD, single-crystal XRD	192
$[\{\text{Fe}(\text{dach})_2\}_3\{\text{V}_{15}\text{Sb}_6\text{O}_{42}(\text{H}_2\text{O})\}]\cdot 8\text{H}_2\text{O}$	dark red	porous 3D network	$\text{NH}_4\text{VO}_3$ , $\text{Sb}_2\text{O}_3$ , $\text{FeSO}_4\cdot 7\text{H}_2\text{O}$ , dach, $\text{H}_2\text{O}$	160 °C, 7 d	23% based on V	EA, IR, UV-vis, single-crystal XRD, magnetometry	197
<b>V<sub>16</sub></b> $(\text{H}_2\text{aep})_4[\text{V}_{16}\text{Sb}_4\text{O}_{42}]\cdot 2\text{H}_2\text{O}$	brown	chain	$\text{NH}_4\text{VO}_3$ , $\text{Sb}_2\text{O}_3$ , aep, $\text{H}_2\text{O}$	150 °C, 7 d		single-crystal XRD	185

$[\text{Zn}_2(\text{dien})_3][\{\text{Zn}(\text{dien})\}_2\text{V}_{16}\text{Sb}_4\text{O}_{42}(\text{H}_2\text{O})] \cdot 4\text{H}_2\text{O}$	brown red	1D linear chain	$\text{Sb}_2\text{O}_3$ , $\text{V}_2\text{O}_5$ , $\text{Zn}(\text{OAc})_2 \cdot 2\text{H}_2\text{O}$ , dien, $\text{H}_2\text{O}$ , NaOH	pH = 7.8–8.3, 180 °C, 7 d	75% based on V	EA, IR, XPS, TGA, single-crystal XRD	189
$[\text{Zn}(\text{tren})(\text{H}_2\text{tren})]_2[\text{V}_{16}\text{Sb}_4\text{O}_{42}(\text{H}_2\text{O})] \cdot n\text{H}_2\text{O}$ ( $n = 6-10$ )	brown	layer-like arrangement	$\text{NH}_4\text{VO}_3$ , $\text{Sb}_2\text{O}_3$ , $\text{Zn}(\text{NO}_3)_2 \cdot 6\text{H}_2\text{O}$ , tren, $\text{H}_2\text{O}$	pH = 12.5, 130 °C, 7 d	47% based on Sb	EA, IR, DTA-TGA, powder XRD, single- crystal XRD, SEM, magnetometry	190
$[\text{Ni}(\text{dien})_2]_4[\text{V}_{16}\text{Sb}_4\text{O}_{42}(\text{H}_2\text{O})]$	black	layer-like arrangement	$\text{NH}_4\text{VO}_3$ , $\text{Sb}_2\text{VO}_5$ , $\text{NiCl}_2 \cdot 6\text{H}_2\text{O}$ , dien, $\text{H}_2\text{O}$	150 °C, 7 d		powder XRD, single- crystal XRD, SEM	196
$[\text{Co}(\text{tren})(\text{H}_2\text{tren})]_2[\text{V}_{16}\text{Sb}_4\text{O}_{42}(\text{H}_2\text{O})] \cdot 6\text{H}_2\text{O}$	brown	layer-like arrangement	$\text{NH}_4\text{VO}_3$ , $\text{Sb}_2\text{O}_3$ , $\text{CoCl}_2 \cdot 6\text{H}_2\text{O}$ , tren (conc. 25%)	130 °C, 7 d	30% based on Sb	EA, IR, EDXS, DTA- TG, powder XRD, single-crystal XRD	192
<b>V<sub>20</sub></b> $[\text{V}_{16}\text{Sb}_4\text{O}_{42}(\text{H}_2\text{O})\{\text{VO}(\text{dach})_2\}_4] \cdot (\text{dach}) \cdot 10\text{H}_2\text{O}$	dark brown	porous 3D network	$\text{Sb}_2\text{O}_3$ , $\text{NH}_4\text{VO}_3$ , dach, $\text{H}_2\text{O}$	150 °C, 7 d	60% based on V	EA, IR, EDXS, UV-vis, single-crystal XRD, magnetometry	187

<sup>a</sup> Dimensionality resulting from hydrogen bonding networks is not considered.

### 3.3.5 Corollary for SbPOVs.

All hitherto reported SbPOVs are based on the  $\{V_{14}\}$ -,  $\{V_{15}\}$ -, and  $\{V_{16}\}$ -type skeletons composed exclusively of  $V^{IV}$  ions. The different symmetries of these “fully-reduced” SbPOVs were determined as  $D_{2d}$  for  $\alpha$ - $[V^{IV}_{14}Sb_8O_{42}]^{4-}$ ,  $D_{2h}$  for  $\beta$ - $[V^{IV}_{14}Sb_8O_{42}]^{4-}$ ,  $D_3$  for  $[V^{IV}_{15}Sb_6O_{42}]^{6-}$ , and  $D_{2h}$  and  $C_2$  for  $[V^{IV}_{16}Sb_4O_{42}]^{8-}$ . No mixed-valent SbPOVs have yet been reported. The SbPOV-based compounds display 1D, 2D and 3D solid-state structures where the polyoxoanions were found to form weak intercluster  $Sb \cdots O$  and/or  $Sb \cdots N$  interactions. On one hand, the SbPOVs exhibit interesting reactivity towards the covalent attachment of organic amines, which can reduce or fully balance the high negative molecular charge of the polyoxoanion shell. On the other hand, the SbPOVs also allow for functionalization with transition metal complexes to generate TMC-supported SbPOV structures, which are of considerable interest due to the addition of multiple spin centres with different magnetic moments. The possible influence of these adjoined TMC fragments on the spin (de)coherence in SbPOVs with an odd number of  $V^{IV}$  atoms (and spin-1/2 ground states) remains as an interesting problem.  $S = 0$  ground states were established for the  $\{V_{14}\}$ - and  $\{V_{16}\}$ -nuclearity building blocks with the even number of  $V^{IV}$  atoms.

The study of the chemical and physical properties and reactivity of the SbPOVs has been motivated, in particular, by the following points closely related to catalysis:

- (i) The  $Sb^{III}$  ions exhibited stabilising effects on the Keggin-type POM structures at high temperatures ( $> 450$  °C) and this played an important role in employing the Sb-modified POMs as catalysts, e.g. for the oxidative dehydrogenation of ethane to ethylene.<sup>198</sup>
- (ii) Since Sb-modified vanadium catalysts were shown to selectively oxidise *o*-xylene to phthalic anhydride,<sup>199</sup> SbPOVs might find potential applications as pre- or catalysts in heterogeneous selective oxidation reactions.

## 4. Summary and outlook

We reviewed the structural aspects and key properties of heavier group 14 and 15 element-functionalised POVs and their inorganic-organic hybrid compounds involving transition metal and lanthanoid complexes as charge compensating units and structure modifiers. We provided an overview of the synthetic routes to SiPOVs, GePOVs, AsPOVs and SbPOVs whose central structural motifs typically are derived from the  $\{V_{18}O_{42}\}$  archetype and display rhombicuboctahedral topologies. The  $V^{4+}$  cations in these robust polyoxoanions incorporating handle-like  $\{E_2O_7\}$  /  $\{E_2O_5S_2\}$  ( $E = Si$  or  $Ge$ ) and  $\{E_2O_5\}$  ( $E = As$  or  $Sb$ ) groups adopt the very common square-pyramidal  $\{VO_5\}$  coordination geometry, although a number of compounds involving  $\{VO_6\}$  octahedra and  $\{VO_4\}$  tetrahedra were also reported. Note

that the crystal chemical aspects of vanadium oxide polyhedra were comprehensively analysed by Schindler *et al.*, in 2000<sup>200</sup> and were, therefore, not discussed herein. The topological aspects of POV macropolyhedra can be found in the work of King dating back to 1995.<sup>201</sup>

It was shown that the  $\{\text{Ge}_2\text{O}_5\text{S}_2\}$  and  $\{\text{As}_2\text{O}_5\}/\{\text{Sb}_2\text{O}_5\}$  substituents in the  $\{\text{V}_{15}\text{E}_6\}$ -type building blocks play crucial roles in superexchange interactions within the central spin-1/2  $\{\text{V}_3\}$  triangle that define the low-temperature magnetism of these *hetero*POVs. Even though the  $[\text{H}_2\text{O}@\text{V}_{15}\text{Ge}_6\text{O}_{42}\text{S}_6]^{12-}$ <sup>102</sup> and  $[\text{V}_{15}\text{Sb}_6\text{O}_{42}]^{6-}$ <sup>186</sup> polyoxoanions feature spin topologies very similar to that of the prominent molecular magnet  $[\text{H}_2\text{O}@\text{V}_{15}\text{As}_6\text{O}_{42}]^{6-}$ ,<sup>151</sup> the magnetic exchange properties of the  $\{\text{Ge}_2\text{O}_5\text{S}_2\}$ -modified POVs differed significantly from those of the corresponding As- and Sb-functionalised POVs.

As was demonstrated by a large number of studies, the discrete *hetero*POVs can be extended further towards the hybrid inorganic-organic frameworks by introducing TMCs or lanthanoid salts to the reactions mixtures. These TMCs and lanthanoid complex cations commonly act as bridging ligands between the neighbouring *hetero*POVs and often exhibit unusual coordination geometries and connectivities. The transition metal ions ( $\text{Mn}^{2+}$ ,  $\text{Fe}^{2+}$ ,  $\text{Co}^{2+}$ ,  $\text{Ni}^{2+}$ ,  $\text{Cu}^{2+}$ ,  $\text{Zn}^{2+}$ ,  $\text{Cd}^{2+}$ ) can be introduced into the backbone structures of the vanadium oxide shells to facilitate the linking of these *hetero*POVs into 1D, 2D and 3D networks and to enrich / modify their magnetic properties. We did not highlight the structural chemistry of TMC fragments in these structures; discussion on their coordination geometries and bonding patterns can be found in the original literature. The use of adjoined inorganic moieties (e.g. lanthanoid complex cations<sup>150</sup>) was shown to result in high coordination numbers (up to 6) for the POV shells and, thus, to remarkably increase the overall thermal stabilities of these *hetero*POV-based materials (even exceeding 500 °C). The transition metal functionalisation of the polynuclear molecular vanadium oxides open up new possibilities for making new *hetero*POV spin architectures with e.g. spin-glass behaviour by virtue of the fact that the vanadyl  $\{\text{VO}\}^{2+}$  moieties in these polyoxoanions can be replaced by divalent transition metal ions.

Another way to improve the thermal stability of *hetero*POVs may be through the preparation of *hetero*POV-based ionic liquids, which can be achieved by pairing negatively charged *hetero*POV building blocks with appropriate cations such as imidazolium, pyridinium, phosphonium species. For instance, a number of Keggin and Lindqvist polyoxomolybdate and polyoxotungstate-based ionic liquids<sup>202</sup> and tetraalkylphosphonium decavanadates<sup>203</sup> have been reported.

The reactivity of *hetero*POVs towards organic groups was also illustrated. The organic amines usually introduced in the reaction mixtures are commonly not only acting as reducing agents, but also as structure-directing and charge-compensating groups and, furthermore, display interesting transformations under hydro-/solvothermal conditions in the presence of  $V^V$  sources. The organic functionalisation of magnetic polyoxoanions, as exemplified by  $[H_2O@V^{IV}_{14}Sb_8(Haep)_4O_{42}]$  and  $[H_2O@V^{IV}_{15}Sb_6(Haep)_2O_{42}]^{4-}$ ,<sup>188</sup> enabled their dissolution in polar protic solvents (methanol, ethanol, etc.). It also can partly or fully compensate the high negative charges of the *hetero*POVs, an important issue for molecular deposition and subsequent (micro)spectroscopic studies with this class of compounds. Such a direct covalent attachment of organic ligands allows for the expansion of *hetero*POVs into classical coordination clusters and may significantly influence their redox and acid-base properties.<sup>204</sup>

The relevance of the presented polyoxoanions to different fields of chemical and physical sciences was briefly discussed. The *hetero*POVs are envisaged to find potential applications in molecular electronics and spintronics, optics, sorption, catalysis and artificial photosynthesis.<sup>205</sup> However, the search for *hetero*POV compounds with sufficient solubility in organic solvents and a high structural and thermal stability is crucial in this context. The synthesis of new discrete and multidimensional SiPOVs, GePOVs, AsPOVs and SbPOVs is highly desirable in order to discover strategies for altering their chemical and physical properties.

Since the ratio of  $V^V/V^{IV}$  and  $V^{IV}/V^{III}$  redox couples and molecular connectivities are strongly influenced by the nature of the heteroelements, and since the overall  $E/V^V/V^{IV}/V^{III}$  ratio impacts the overall properties of the *hetero*POV to a large extent, the chemical modification of the conventional POV shells by heavier metal ions from groups 14 such as Sn and Pb is appealing and worthwhile. For example, functionalisation of POVs with bismuth, the heaviest group-15 element, resulted in interesting photocatalytic activity of the designed molecular bismuth vanadium oxide clusters.<sup>206</sup> The reactivities of SiPOVs, GePOVs, AsPOVs and SbPOVs towards transition metals e.g. from the platinum group and actinoids are yet to be discovered. Integration of lanthanoid ions into *hetero*POV shells may lead to interesting magnetic phenomena as well as visible-light photocatalytic properties.<sup>207</sup> The controlled interlinking of *hetero*POV spin structures is of high importance for the development of smart materials with electron storage functions and inter-site communications. The coexistence of (partly) delocalised 3d-vanadium electron density with localised spins of transition metals and lanthanoids in the mixed-valent *hetero*POV-based



inorganic-organic hybrid materials may result in unusual spintronic effects, “*in particular, if the corresponding charge transport can be confined to one or two dimensions*”.<sup>114</sup>

The molecular magnetism of *heteroPOVs* described so far is characterised by the presence of strong antiferromagnetic exchange interactions between the vanadium spin centres, with the exception of several compounds showing ferrimagnetic ordering characteristics. Because there are some indications of ferromagnetic coupling interactions in *heteroPOVs* (see the mixed-valent  $[\text{HCO}_2@V^{\text{IV}}_6V^{\text{V}}_6\text{As}_8\text{O}_{40}]^{3-}$  polyoxoanion<sup>119,120</sup>) as well as *alkoxoPOVs* (see the mixed-valent  $[V^{\text{IV}}_4V^{\text{V}}_2\text{O}_7(\text{OR})_{12}]$  compound<sup>78</sup> and the mixed-valent  $[V^{\text{III}}V^{\text{IV}}_5\text{O}_6(\text{OMe})_8(\text{calix})(\text{MeOH})]^-$  polyoxoanion<sup>207</sup> where calix = *p-tert-butylcalix[4]arene*), the magnetic properties of these compounds should be explored in more detail. Building a deeper understanding of the magnetism of the mixed-valent, “fully-reduced” and “highly-reduced” SiPOVs, GePOVs, AsPOVs and SbPOVs, which can potentially act as “nanoscale quantum magnets” and spin qubits remains challenging, because of the absence of magnetochemical models suitable for the fitting of their magnetic susceptibility data.

Only a few studies have employed quantum chemical models to study the electronic structures of fully-oxidised POVs<sup>208</sup> and of some of the herein-described “fully-reduced”, semimetal-functionalised POVs with the  $V_{14}$  and  $V_{15}$  nuclearities.<sup>209</sup> Reliable computational methods for assessing the electronic and magnetic properties of the mixed-valent *heteroPOVs* are still being developed.

The biological and medicinal relevance of POVs<sup>210</sup> deserves mention, as the archetypal decavanadate  $[V_{10}O_{28}]^{6-}$  has demonstrated non-trivial chemical behaviour and reactivity towards biomolecules,<sup>211</sup> e.g.: (i) inhibition of various enzymes,<sup>212</sup> (ii) hydrolytic DNA cleavage,<sup>213</sup> (iii) inhibition of oxygen consumption<sup>214</sup> in membranes. The interactions of other, lower nuclearity, but more labile oxovanadates ( $[\text{VO}_4]^{3-}$  as a structural and electronic analogue of phosphate,  $[\text{V}_2\text{O}_7]^{4-}$ , and  $[\text{V}_4\text{O}_{12}]^{4-}$ ) with enzymes<sup>215</sup> have also been recognised and well-documented.<sup>1,216</sup> Over the past two decades, much attention has been paid to biochemical, cell biological, antidiabetic and antitumor studies involving vanadium<sup>217,218,219</sup> and organic biomolecules for the reason that “*understanding the nature of protein interactions with oxovanadates and other oxometalates is important for further development of drugs based on vanadium complexes and polyoxoanions*”.<sup>1</sup> In view of the biological innocuity of bismuth and its extensive uses in medicine, pharmaceuticals, and cosmetics, the class of bismuthate polyoxovanadates is relevant to biochemical studies.

Although the number of reports on magnetic *heteroPOVs* has grown substantially in the last few decades, the field is hampered by the lack of systematic research on this class of

molecular compounds. Many questions concerning their inorganic synthesis, reactivity in aqueous and non-aqueous solutions, molecular magnetism, spectroscopy (in particular, NMR studies in solution and in the solid state), excited states and computational application remain entirely open. The benefits of effective adjustment of the *heteroPOV* building block's properties from the standpoint of chemical reactivity, electrochemistry, molecular magnetism, photophysics and surface physics will be remarkable.

Finally, we note that the self-assembly formation mechanisms of *heteroPOVs* remain poorly understood and for the development of rational syntheses these mechanisms should be unveiled. There are first promising attempts in this direction: *in situ* energy-dispersive X-ray diffraction experiments were performed under hydrothermal conditions in order to gain insight into the synthetic parameters influencing the formation of SbPOVs.<sup>220</sup> These studies were able to demonstrate directly that e.g. the amine concentration plays a crucial role for the crystallisation of a distinct SbPOV, where the formation of  $[V_{14}Sb_8(Haep)_4O_{42}(H_2O)] \cdot 4H_2O$ <sup>188</sup> is observed at the lowest amine concentration, whereas  $(H_2aep)_2[V_{15}Sb_6(Haep)_2O_{42}(H_2O)] \cdot 2.5H_2O$ <sup>188</sup> crystallised at slightly larger amine concentration and finally the SbPOV with the highest number of  $V^{IV}$  centres,  $(H_2aep)_4[V_{16}Sb_4O_{42}] \cdot 2H_2O$ ,<sup>185</sup> was obtained at the highest amine concentration. In addition, solvothermal syntheses performed under static conditions yields mixtures of these three SbPOVs while stirring afforded formation of phase pure materials at a distinct amount of amine in the reaction slurries. These empirical *in situ* studies pave the way for a more comprehensive understanding of the complex self-assembly processes in vanadate reaction solutions, in line with similarly revealing *in situ* spectroscopy studies in the chemistry of other polyoxometalate families.<sup>221</sup>

**ACKNOWLEDGMENTS** K.Y.M. is grateful to the Deutsche Forschungsgemeinschaft (DFG) for a postdoctoral reintegration fellowship and the Jülich-Aachen Research Alliance – Future Information Technology (JARA-FIT) for a Seed Fund grant. We thank Dr. Claire Besson, Dr. Jeff Rawson (RWTH Aachen University) and Dr. Natalya Izarova (Forschungszentrum Jülich) for helpful suggestions.

## ABBREVIATIONS

### *Methods*

CV	cyclic voltammetry
DFT	density functional theory

---

EA	elemental analysis
EDXS	energy-dispersive X-ray spectroscopy
EMP	electron microprobe
EPR	electron paramagnetic resonance
ESI-MS	electrospray ionisation mass spectrometry
INS	inelastic neutron scattering
IR	infrared spectroscopy
NMR	nuclear magnetic resonance
powder XRD	powder X-ray diffraction
SEM	scanning electron micrograph
single-crystal XRD	single-crystal X-ray diffraction
TGA	thermogravimetric analysis
UV-vis	ultraviolet-visible spectroscopy
XPS	X-ray photoelectron spectroscopy
<i>Inorganic compounds</i>	
POV	polyoxovanadate
<i>heteroPOV</i>	heteropolyoxovanadate
<i>alkoxoGePOV</i>	polyoxoalkoxovanadium germanate
AsPOV	polyoxovanadoarsenate
GePOV	polyoxovanadogermanate
SiPOV	polyoxovanadosilicate
SbPOV	polyoxovanadoantimonate
TMC	transition metal complex
<i>Organic compounds</i>	
2,2'-bipy	2,2'-bipyridine
aep	1-(2-aminoethyl)piperazine
aepda	<i>N</i> -(2-aminoethyl)-1,3-propanediamine
bbi	1,1'-(1,4-butanediyl)bis(imidazole)
bpe	1,2-bis(4-pyridyl)ethylene
dab	1,4-diaminobutane
dach	(±)- <i>trans</i> -1,2-cyclohexanediamine
dien	diethylenetriamine
en	ethylenediamine
enMe	1,2-diaminopropane
pdn	1,3-propanediamine

phen	1,10-phenanthroline
ppz	piperazine
salen	<i>N,N'</i> -(ethylene)bis(salicylideneimine)
teos	tetraethyl orthosilicate
tepa	tetraethylenepentamine
theed	<i>N,N,N',N'</i> -tetrakis(2-hydroxyethyl)ethylenediamine
tren	tris(2-aminoethyl)amine

---

## References

<sup>1</sup> D. C. Crans, *Comments Inorg. Chem.*, 1994, **16**, 35 and references cited therein.

<sup>2</sup> (a) N. D. Chasteen, *Vanadium in Biological Systems: Physiology and Biochemistry*, ed. N. D. Chasteen, Kluwer Academic Publishers, Boston, 1990. (b) D. Rehder, *Angew. Chem., Int. Ed. Engl.*, 1991, **30**, 148. (c) D. C. Crans, C. M. Simone and J. S. Blanchard, *J. Am. Chem. Soc.*, 1992, **114**, 4926. (d) A. Butler and C. J. Carrano, *Coord. Chem. Rev.*, 1991, **109**, 61.

<sup>3</sup> F. A. Cotton, G. Wilkinson, C. A. Murillo and M. Bochmann, *Advanced Inorganic Chemistry*, 6th Edition, Wiley Interscience, New York, 1999, p. 714.

<sup>4</sup> A. S. Tracey, G. R. Willsky and E. S. Takeuchi, *Vanadium: Chemistry, Biochemistry, Pharmacology and Practical Applications*, CRC Press, Boca Raton, 2007.

<sup>5</sup> (a) R. D. Srivastava, *Heterogeneous Catalytic Science*; CRC Press, Boca Raton, 1988. (b) G. Busca and G. Centi, *J. Am. Chem. Soc.*, 1989, **111**, 46. (c) G. Deo, F. D. Hardcastle, M. Richards, A. M. Hirt and I. E. Wachs, In *Novel Materials in Heterogeneous Catalysis*, ed. R. T. K. Baker, L. L. Murrell, American Chemical Society, Washington, D.C., 1990. (d) D. Patel, P. J. Anderson and H. H. Kung, *J. Catal.*, 1990, **125**, 132. (e) F.-L. Wang and W.-S. Lee, *J. Chem. Soc., Chem. Commun.*, 1991, 1760. (f) B. I. Whittington and J. R. Anderson, *J. Phys. Chem.*, 1993, **97**, 1032. (g) P. Dinka, K. Prandová and M. Hronec, *Appl. Clay Sci.*, 1998, **13**, 467. (h) A. G. J. Ligtenberg, R. Hage and B. L. Feringa, *Coord. Chem. Rev.*, 2003, **237**, 89. (i) J. Pless, B. Bardin, H.-S. Kim, D. Ko, M. Smith, R. Hammond, P. Stair and K. Poeppelmeier, *J. Catal.*, 2004, **223**, 419. (j) A. R. Gaspar, D. V. Evtuguin and C. P. Neto, *Ind. Eng. Chem. Res.*, 2004, **43**, 7754. (k) J. D. Pless, D. Ko, R. R. Hammond, B. B. Bardin, P. C. Stair and K. R. Poeppelmeier, *J. Catal.*, 2004, **223**, 419. (l) Z. Strassberger, E. V. Ramos-Fernandez, A. Boonstra, R. Jorna, S. Tanase and G. Rothenberg, *Dalton Trans.*, 2013, **42**, 5546.

<sup>6</sup> (a) P. Csermely, A. Martonosi, G. C. Levy and A. J. Ejchart, *Biochem. J.*, 1985, **230**, 807. (b) D. C. Crans and S. M. Schelble, *Biochemistry*, 1990, **29**, 6697. (c) D. C. Crans and C. M. Simone, *Biochemistry*, 1991, **30**, 6734. (d) See also a special issue of *Coord. Chem. Rev.*, 2003, **237**, 3.

<sup>7</sup> (a) J. Livage, *Chem. Mater.*, 1991, **3**, 578. (b) C. J. Brinker and G. W. Scherer, *Sol-Gel Science*; Academic Press, New York, 1991. (c) J. Livage, *Solid State Ionics*, 1996, **86–88**, 935. See, also: (d)

- F. J. Anaissi, G. J. F. Demets, H. E. Toma and A. C. V. Coelho, *J. Electroanal. Chem.*, 1999, **464**, 48.
- <sup>8</sup> A. R. Raju, C. N. R. Rao, *J. Chem. Soc., Chem. Commun.*, 1991, 1260.
- <sup>9</sup> (a) H. T. Evans Jr. and S. Landergren, in *Handbook of Geochemistry*, ed. K. H. Wedepohl, Springer, Berlin, 1978; Vol. II/2, Chapter 23. (b) H. T. Evans, Jr. and J. S. White, Jr. *Mineral. Rec.*, 1987, **18**, 333.
- <sup>10</sup> J. Do and A. J. Jacobson, *Inorg. Chem.*, 2001, **40**, 2468.
- <sup>11</sup> (a) M. G. Kanatzidis, C.-G. Wu, H. O. Marcy and C. R. Kannewurf, *J. Am. Chem. Soc.*, 1989, **111**, 4139. (b) M. Z. A. Munshi, W. H. Smyrl and C. Schmidtke, *Chem. Mater.*, 1990, **2**, 530. (c) J.-M. Amarilla, B. Casal, J.-C. Galvan and E. Ruiz-Hitzky, *Chem. Mater.*, 1992, **4**, 62.
- <sup>12</sup> (a) G. C. Bond and S. F. Tahir, *Appl. Catal.*, 1991, **71**, 1. (b) M. S. El-Shall, W. Slack, W. Vann, D. Kane and D. Hanley, *J. Phys. Chem.*, 1994, **98**, 3067. (c) S. Surnev, M. G. Ramsey and F. P. Netzer, *Prog. Surf. Sci.*, 2003, **73**, 117. (d) R. Schlögl and S. B. Abd Hamid, *Angew. Chem., Int. Ed.*, 2004, **43**, 1628.
- <sup>13</sup> (a) C. R. Walk and J. S. Gore, *J. Electrochem. Soc.*, 1975, **122**, 68C. (b) M. S. Whittingham, *J. Electrochem. Soc.*, 1976, **123**, 315. (c) M. S. Whittingham, R. Chen, T. Chirayil and P. Y. Zavalij, *Proc. Electrochem. Soc.*, 1996, **95–96**, 76. (d) P. Gomez-Romero, *Adv. Mater.*, 2001, **13**, 163. (e) A. Bose, P. He, C. Liu, B. D. Ellman, R. J. Twieg and S. D. Huang, *J. Am. Chem. Soc.*, 2002, **124**, 4. (f) L. Chen, F. Jiang, Z. Lin, Y. Zhou, C. Yue and M. Hong, *J. Am. Chem. Soc.*, 2005, **127**, 8588. (g) L. Li, S. Kim, W. Wang, M. Vijayakumar, Z. Nie, B. Chen, J. Zhang, G. Xia, J. Hu, G. Graff, J. Liu and Z. Yang, *Adv. Energy Mater.*, 2011, **1**, 394. (h) S. Uematsu, Z. Quan, Y. Suganuma and N. Sonoyama, *J. Power Sourc.*, 2012, **217**, 13.
- <sup>14</sup> See, e.g.: H.-U. Meisch and L. J. M. Becker, *Biochim. Biophys. Acta (BBA) - Bioenergetics*, 1981, **636**, 119.
- <sup>15</sup> (a) J. Livage, *Coord. Chem. Rev.*, 1998, **178–180**, 999. (b) Y. Hayashi, *Coord. Chem. Rev.*, 2011, **255**, 2270.
- <sup>16</sup> (a) M. T. Pope and A. Müller, *Angew. Chem., Int. Ed. Engl.*, 1991, **30**, 34. (b) L. Cronin, P. Kögerler and A. Müller, *J. Solid State Chem.*, 2000, **152**, 57. (c) A. Müller, P. Kögerler and H. Bögge, *Struct. Bond.*, 2000, **96**, 203. (d) D.-L. Long, R. Tsunashima and L. Cronin, *Angew. Chem., Int. Ed.*, 2010, **49**, 1736.
- <sup>17</sup> See for example (a) B. Dong, J. Peng, A. Tian, J. Sha, L. Li and H. Liu, *Electrochim. Acta*, 2007, **52**, 3804. (b) T. D. Keene, D. M. D'Alessandro, K. W. Krämer, J. R. Price, D. J. Price, S. Decurtins and C. J. Kepert, *Inorg. Chem.*, 2012, **51**, 9192 and references cited therein.
- <sup>18</sup> (a) L. Chen, F. Jiang, Z. Lin, Y. Zhou, C. Yue and M. Hong, *J. Am. Chem. Soc.*, 2005, **127**, 8588. See also: (b) Q. Chen and J. Zubieta, *Coord. Chem. Rev.*, 1992, **114**, 107.
- <sup>19</sup> W. G. Klemperer, T. A. Marquart and O. M. Yaghi, *Angew. Chem., Int. Ed. Engl.*, 1992, **31**, 49.
- <sup>20</sup> G. Huan, A. J. Jacobson, and V. W. Day, *Angew. Chem., Int. Ed. Engl.*, 1991, **30**, 422.

- <sup>21</sup> (a) F. J. Rossotti and H. Rossotti, *Acta Chem. Scandinav.*, 1956, **10**, 957. (b) P. A. Durif and M. T. Averbuch-Pouchot, *Acta Cryst.*, 1980, **B36**, 680. (c) A. S. J. Wery, J. M. Gutierrez-Zorrilla, A. Luque, P. Roman and M. Martinez-Ripoll, *Polyhedron*, 1996, **15**, 4555. (d) G. Johnson, R. K. Murmann, R. Deavin and W. P. Griffith, *Inorg. Synth.*, 2007, **19**, 140.
- <sup>22</sup> J. L. Ferreira da Silva, M. F. Minas da Piedade and M. T. Duarte, *Inorg. Chim. Acta*, 2003, **356**, 222.
- <sup>23</sup> (a) M. Aureliano and D. C. Crans, *J. Inorg. Biochem.*, 2009, **103**, 536. (b) M. Aureliano, *Dalton Trans.*, 2009, 9093. (c) M. Aureliano, G. Fraqueza and C. A. Ohlin, *Dalton Trans.*, 2013, **42**, 11770.
- <sup>24</sup> J. M. Hughes, W. S. Wise, M. E. Gunter, J. P. Morton and J. Rakovan, *Canad. Mineral.*, 2008, **46**, 1365 and reference cited therein.
- <sup>25</sup> (a) W. Bensch, P. Hug, A. Reller and H. R. Oswald, *Mater. Res. Bull.*, 1989, **24**, 403. (b) S. Aschwanden, H. W. Schmale, A. Reller and H. R. Oswald, *Mater. Res. Bull.*, 1993, **28**, 575.
- <sup>26</sup> E. E. Hamilton, P. E. Fanwick and J. J. Wilker, *J. Am. Chem. Soc.*, 2002, **124**, 78.
- <sup>27</sup> (a) J. Fuchs, S. Mahjour and J. Pickardt, *Angew. Chem., Int. Ed. Engl.*, 1976, **15**, 374. (b) G.-Y. Yang, D.-W. Gao, Y. Chen, J.-Q. Xu, Q.-X. Zeng, H.-R. Sun, Z.-W. Pei, Q. Su, Y. Xing, Y.-H. Ling and H.-Q. Jia, *Acta Cryst.*, 1998, **C54**, 616.
- <sup>28</sup> V. W. Day, W. G. Klemperer and O. M. Yaghi, *J. Am. Chem. Soc.*, 1989, **111**, 4518.
- <sup>29</sup> V. W. Day, W. G. Klemperer and D. J. Maltbie, *J. Am. Chem. Soc.*, 1987, **109**, 2991.
- <sup>30</sup> (a) V. W. Day, W. G. Klemperer and O. M. Yaghi, *J. Am. Chem. Soc.*, 1989, **111**, 5959. (b) W. G. Klemperer, T. A. Marquart and O. M. Yaghi, *Mater. Chem. Phys.*, 1991, **29**, 97. (c) N. Kawanami, T. Ozeki and A. Yagasaki, *J. Am. Chem. Soc.*, 2000, **122**, 1239. (d) T. Kurata, Y. Hayashi and K. Isobe, *Chem. Lett.*, 2010, **39**, 708.
- <sup>31</sup> D. Hou, K. D. Hagen and C. L. Hill, *J. Am. Chem. Soc.*, 1992, **114**, 5864.
- <sup>32</sup> D. Hou, K. S. Hagen and C. L. Hill, *J. Chem. Soc., Chem. Commun.*, 1993, 426.
- <sup>33</sup> J. Marrot, K. Barthelet, C. Simonnet and D. Riou, *C. R. Chim.*, 2005, **8**, 971.
- <sup>34</sup> (a) Y. Hayashi, N. Miyakoshi, T. Shinguchi and A. Uehara, *Chem. Lett.*, 2001, 170. (b) K. Okaya, T. Kobayashi, Y. Koyama, Y. Hayashi and K. Isobe, *Eur. J. Inorg. Chem.*, 2009, 5156 and references cited therein. (c) J. Forster, B. Rösner, M. M. Khusniyarov, C. Streb, *Chem. Commun.*, 2011, **47**, 3114.
- <sup>35</sup> (a) A. Müller, E. Krickemeyer, M. Penk, H.-J. Walberg and H. Bögge, *Angew. Chem., Int. Ed.*, 1987, **26**, 1045. (b) A. Müller, M. Penk, R. Rohlfing, E. Krickemeyer and J. Döring, *Angew. Chem., Int. Ed. Engl.*, 1990, **29**, 926. (c) G. B. Karet, Z. Sun, W. E. Streib, J. C. Bollinger, D. N. Hendrickson and G. Christou, *Chem. Commun.*, 1999, 2249.
- <sup>36</sup> Y. Chen, X. Gu, J. Peng, Z. Shi, H. Yu, E. Wang and N. Hu, *Inorg. Chem. Commun.*, 2004, **7**, 705.
- <sup>37</sup> M. I. Khan, S. Ayes, R. J. Doedens, M. Yu and C. J. O'Connor, *Chem. Commun.*, 2005, 4658.
- <sup>38</sup> Y. Hayashi, K. Fukuyama, T. Takatera and A. Uehara, *Chem. Lett.*, 2000, 770.

- <sup>39</sup> A. Müller, R. Sessoli, E. Krickemeyer, H. Bögge, J. Meyer, D. Gatteschi, L. Pardi, J. Westphal, K. Hovemeier, R. Rohlfing, J. Döring, F. Hellweg, C. Beugholt and M. Schmidtman, *Inorg. Chem.*, 1997, **36**, 5239.
- <sup>40</sup> A. Müller, E. Krickemeyer, M. Penk, R. Rohlfing, A. Armatage and H. Bögge, *Angew. Chem., Int. Ed. Engl.*, 1991, **30**, 1674.
- <sup>41</sup> L. Suber, M. Bonamico and V. Fares, *Inorg. Chem.*, 1997, **36**, 2030.
- <sup>42</sup> A. Müller, R. Rohlfing, J. Döring and M. Penk, *Angew. Chem., Int. Ed. Engl.*, 1991, **30**, 588.
- <sup>43</sup> See for example (a) K. Hegetschweiler, B. Morgenstern, J. Zubieta, P. J. Hagrman, N. Lima, R. Sessoli and F. Totti, *Angew. Chem., Int. Ed.*, 2004, **43**, 3436. (b) I. S. Tidmarsh, R. H. Laye, P. R. Brearley, M. Shanmugam, E. C. Sañudo, L. Sorace, A. Caneschi and E. J. L. McInnes, *Chem. Commun.*, 2006, 2560. (c) R. H. Laye, Q. Wei, P. V. Mason, M. Shanmugam, S. J. Teat, E. K. Brechin, D. Collison and E. J. L. McInnes, *J. Am. Chem. Soc.*, 2006, **128**, 9020. (d) I. S. Tidmarsh, E. Scales, P. R. Brearley, J. Wolowska, L. Sorace, A. Caneschi, R. H. Laye and E. J. L. McInnes, *Inorg. Chem.*, 2007, **46**, 9743. (e) I. S. Tidmarsh, R. H. Laye, P. R. Brearley, M. Shanmugam, E. C. Sañudo, L. Sorace, A. Caneschi and E. J. L. McInnes, *Chem. Eur. J.*, 2007, **13**, 6329. (f) C. Aronica, G. Chastanet, E. Zueva, S. A. Borshch, J. M. Clemente-Juan and D. Luneau, *J. Am. Chem. Soc.*, 2008, **130**, 2365.
- <sup>44</sup> C.-L. Wang, Z.-B. Zhang, J. Fu, Y. Xu and D.-R. Zhu, *Chem. Eur. J.*, 2012, **18**, 11909.
- <sup>45</sup> G. K. Johnson and E. O. Schlemper, *J. Am. Chem. Soc.*, 1978, **100**, 3645.
- <sup>46</sup> I. D. Brown and D. Altermatt, *Acta Cryst.*, 1985, **B41**, 244.
- <sup>47</sup> See, e.g.: B. Dong, C. J. Gómez-García, J. Penga, S. Benmansour and J. Ma, *Polyhedron*, 2007, **26**, 1310.
- <sup>48</sup> (a) B. J. Suh, D. Procissi, P. Kögerler, E. Micotti, A. Lascialfari and F. Borsa, *J. Magn. Magn. Mater.*, 2004, **272–276**, e759. (b) D. Rehder, *Coord. Chem. Rev.*, 2008, **252**, 2209.
- <sup>49</sup> (a) D. K. Walanda, R. C. Burns, G. A. Lawrance, E. I. von Nagy-Felsobuki, *Inorg. Chim. Acta*, 2000, **305**, 118. (b) Z. L. Chen, G. Owens and R. Naidu, *Analyt. Chim. Acta*, 2007, **585**, 32.
- <sup>50</sup> L. A. Truffandier, F. Boucher, C. Payen, R. Hajjar, Y. Millot, C. Bonhomme and N. Steunou, *J. Am. Chem. Soc.*, 2010, **132**, 4653.
- <sup>51</sup> S. Ard, C. J. Dibble, S. T. Akin and M. A. Duncan, *J. Phys. Chem. C*, 2011, **115**, 6438 and references cited therein.
- <sup>52</sup> (a) X. Zhang and H. Schwarz, *Chem. Eur. J.*, 2010, **16**, 1163. See, also: (b) D. Schröder, M. Engeser, M. Brönstrup, C. Daniel, J. Spandl and H. Hartl, *Int. J. Mass Spectrom.*, 2003, **228**, 743. (c) S. Feyel, D. Schröder and H. Schwarz, *J. Phys. Chem. A*, 2006, **110**, 2647. (d) S. Feyel, D. Schröder, X. Rozanska, J. Sauer and H. Schwarz, *Angew. Chem., Int. Ed.*, 2006, **45**, 4677. (e) S. Feyel, D. Schröder and H. Schwarz, *Eur. J. Inorg. Chem.*, 2008, 4961.
- <sup>53</sup> I. Lindqvist, *Ark. Kemi*, 1953, **5**, 247.
- <sup>54</sup> (a) Y. Hayashi, Y. Ozawa and K. Isobe, *Chem. Lett.*, 1989, 425. (b) H. K. Chae, W. G. Klemperer and V. W. Day, *Inorg. Chem.*, 1989, **28**, 1423. (c) Q. Chen, and J. Zubieta, *Inorg. Chem.*, 1990, **29**,

1458. (d) Y. Hayashi, Y. Ozawa and K. Isobe, *Inorg. Chem.*, 1991, **30**, 1025. (e) M. I. Khan, Q. Chen, J. Zubieta and D. P. Goshorn, *Inorg. Chem.*, 1992, **31**, 1556. (f) Q. Chen, D. P. Goshorn, C. P. Scholes, X. Tan and J. Zubieta, *J. Am. Chem. Soc.*, 1992, **114**, 4667. (g) M. I. Khan, Q. Chen, H. Höpe, S. Parkin, C. J. O'Connor and J. Zubieta, *Inorg. Chem.*, 1993, **32**, 2929. (h) D. Hou, G.-S. Kim, K. S. Hagen and K. L. Hill, *Inorg. Chim. Acta*, 1993, **211**, 127. (i) M. I. Khan, J. Zubieta, *Prog. Inorg. Chem.*, 1995, **43**, 1. (j) A. Müller, J. Meyer, H. Bögge, A. Stämmeler and A. Botar, *Z. Anorg. Allg. Chem.*, 1995, **621**, 1818. (k) M. Piepenbrink, M. U. Triller, N. H. J. Gorman and B. Krebs, *Angew. Chem., Int. Ed.*, 2002, **41**, 2523. (l) J. Spandl, C. Daniel, I. Brüdgam and H. Hartl, *Angew. Chem., Int. Ed.*, 2003, **42**, 1163. (m) C. Daniel and H. Hartl, *J. Am. Chem. Soc.*, 2005, **127**, 13978. (n) M. A. Augustyniak-Jabokow, C. Daniel, H. Hartl, J. Spandl and Y. V. Yablokov, *Inorg. Chem.*, 2008, **47**, 322. (o) C. Daniel and H. Hartl, *J. Am. Chem. Soc.*, 2009, **131**, 5101.

<sup>55</sup> J. F. Keggin, *Proc. R. Soc. Lond. A*, 1934, **144**, 75.

<sup>56</sup> (a) R. Kato, A. Kobayashi and Y. Sasaki, *J. Am. Chem. Soc.*, 1980, **102**, 6572. (b) R. Kato, A. Kobayashi and Y. Sasaki, *Inorg. Chem.*, 1982, **21**, 240. (c) S. Nakamura, T. Yamawaki, K. Kusaka, T. Otsuka and T. Ozeki, *J. Clust. Sci.*, 2006, **17**, 245.

<sup>57</sup> J. M. Maestre, J. M. Poblet, C. Bo, N. Casañ-Pastor and P. Gomez-Romero, *Inorg. Chem.*, 1998, **37**, 3444.

<sup>58</sup> A. Müller, J. Döring, H. Bögge and E. Krickemeyer, *Chimia*, 1988, **42**, 300.

<sup>59</sup> T. Yamase, M. Suzuki and K. Ohtaka, *J. Chem. Soc., Dalton Trans.*, 1997, 2463.

<sup>60</sup> M. T. Pope, *Nature*, 1992, **355**, 27.

<sup>61</sup> T. H. Noh, E. Heo, K. H. Park and O.-S. Jung, *J. Am. Chem. Soc.*, 2011, **133**, 1236.

<sup>62</sup> (a) K. Hiratani, M. Goto, Y. Nagawa, K. Kasuga and K. Fujiwara, *Chem. Lett.*, 2000, **29**, 1364. (b) J. Garric, J.-M. Léger and I. Huc, *Chem. Eur. J.*, 2007, **13**, 8454. (c) H. J. Shin, J. H. Jung, K. Motobayashi, S. Yanagisawa, Y. Morikawa, Y. Kim and M. Kawai, *Nat. Mater.*, 2010, **9**, 442.

<sup>63</sup> (a) J. Cioslowski and E. D. Fleischmann, *J. Chem Phys.*, 1991, **94**, 3730. (b) J. Cioslowski, *J. Am. Chem. Soc.*, 1991, **113**, 4139. (c) Y. Chai, T. Guo, C. Jin, R. E. Haufler, L. P. F. Chibante, J. Fure, L. Wang, J. M. Alford and R. E. Smalley, *J. Phys. Chem.*, 1991, **95**, 7564. (d) M. Saunders, H. A. Jimenez-Vazquez, R. J. Cross, S. Mroczkowski, M. L. Gross, D. E. Giblin and R. J. Poreda, *J. Am. Chem. Soc.*, 1994, **116**, 2193. (e) J. Cioslowski and Q. Lin, *J. Am. Chem. Soc.*, 1995, **117**, 2553. (f) Y. H. Hu and E. Ruckenstein, *J. Am. Chem. Soc.*, 2005, **127**, 11277. (g) M. Yamada, T. Nakahodo, T. Wakahara, T. Tsuchiya, Y. Maeda, T. Akasaka, M. Kako, K. Yoza, E. Horn, N. Mizorogi, K. Kobayashi and S. Nagase, *J. Am. Chem. Soc.*, 2005, **127**, 14570. (h) Z. Ge, J. C. Duchamp, T. Cai, H. W. Gibson and H. C. Dorn, *J. Am. Chem. Soc.*, 2005, **127**, 16292. (i) Y. Takano, S. Obuchi, N. Mizorogi, R. García, M. Á. Herranz, M. Rudolf, S. Wolfrum, D. M. Guldi, N. Martín, S. Nagase and T. Akasaka, *J. Am. Chem. Soc.*, 2012, **134**, 16103. (j) S. Maki, E. Nishibori, I. Terauchi, M. Ishihara, S. Aoyagi, M. Sakata, M. Takata, H. Umemoto, T. Inoue and H. Shinohara, *J. Am. Chem. Soc.*, 2013, **135**, 918.

<sup>64</sup> X. Fang, P. Kögerler, L. Isaacs, S. Uchida and N. Mizuno, *J. Am. Chem. Soc.*, 2009, **131**, 432.



- <sup>65</sup> K. Kurotobi and Y. Murata, *Science*, 2011, **333**, 613.
- <sup>66</sup> (a) P. N. W. Baxter, in *Comprehensive Supramolecular Chemistry*, Vol. 9, ed. J. L. Atwood, J. E. D. Davies, D. D. MacNicol, F. Vögtle, Pergamon/Elsevier, New York, 1996, p. 200. (b) L. Cronin, in *Comprehensive Coordination Chemistry II*, vol. 7, ed. J. A. McCleverty, T. B. Meyer, Elsevier, Amsterdam, 2004, pp. 1–56 and references cited therein.
- <sup>67</sup> H. Wan, C. Wang, Y. Zhang, H. Miao, S. Zhou and Y. Xu, *Inorg. Chem.*, 2014, **53**, 10498.
- <sup>68</sup> (a) A. Müller, E. Diemann, E. Krickemeyer and S. Che, *Naturwissenschaften*, 1993, **80**, 77. (b) M.-M. Rohmer, M. Bénard, J. Maestre and J.-M. Poblet, *Coord. Chem. Rev.*, 1998, **178–180**, 1019.
- <sup>69</sup> A. Müller, P. Kögerler and C. Kuhlmann, *Chem. Commun.*, 1999, 1347.
- <sup>70</sup> (a) K. Kastner, J. T. Margraf, T. Clark and C. Streb, *Chem. Eur. J.*, 2014, **20**, 12269. (b) K. Kastner, J. Forster, H. Ida, G. N. Newton, H. Oshio and C. Streb, *Chem. Eur. J.*, 2015, **21**, 7686.
- <sup>71</sup> T. Kurata, A. Uehara, Y. Hayashi and K. Isobe, *Inorg. Chem.*, 2005, **44**, 2524.
- <sup>72</sup> K. Yu. Monakhov, O. Linnenberg, P. Kozłowski, J. van Leusen, C. Besson, T. Secker, A. Ellern, X. López, J. M. Poblet and P. Kögerler, *Chem. Eur. J.*, 2015, **21**, 2387.
- <sup>73</sup> J. Tucher, K. Peuntinger, J. T. Margraf, T. Clark, D. M. Guldi and C. Streb, *Chem. Eur. J.*, 2015, **21**, 8716.
- <sup>74</sup> A. Müller, H. Reuter and S. Dillinger, *Angew. Chem., Int. Ed. Engl.*, 1995, **34**, 2328.
- <sup>75</sup> J. M. Clemente-Juan, E. Coronado and A. Gaita-Ariño, *Chem. Soc. Rev.*, 2012, **41**, 7464 and references cited therein.
- <sup>76</sup> (a) M. T. Pope, *Heteropoly and Isopoly Oxometalates*, Springer, Berlin, 1983. (b) See special issues on POMs: *Chem. Rev.*, 1998, **98**, 1; *Chem. Soc. Rev.*, 2012, **22**, 7325. (c) P. Day and E. Coronado, in *Magnetism: Molecules to Materials*, ed. J. S. Miller, M. Drillon, Wiley-VCH, Weinheim, 2005; Vol. V, p. 105. (d) D. Gatteschi, R. Sessoli and J. Villain, *Molecular Nanomagnets*, Oxford University Press, Oxford, 2006.
- <sup>77</sup> See e.g. S. L. Castro, Z. Sun, C. M. Grant, J. C. Bollinger, D. N. Hendrickson and G. Christou, *J. Am. Chem. Soc.*, 1998, **120**, 2365.
- <sup>78</sup> E. M. Zueva, S. A. Borshch, M. M. Petrova, H. Chermette and A. M. Kuznetsov, *Eur. J. Inorg. Chem.*, 2007, 4317.
- <sup>79</sup> C. J. Calzado, J. M. Clemente-Juan, E. Coronado, A. Gaita-Arino and N. Suaud, *Inorg. Chem.*, 2008, **47**, 5889.
- <sup>80</sup> W. L. Queen, J. P. West, J. Hudson and S.-J. Hwu, *Inorg. Chem.*, 2011, **50**, 11064.
- <sup>81</sup> (a) S.-J. Hwu, *Chem. Mater.*, 1998, **10**, 2846. (b) W. L. Queen, S.-J. Hwu and L. Wang, *Angew. Chem., Int. Ed.*, 2007, **46**, 5344. (c) J. P. West, W. L. Queen, S.-J. Hwu and K. E. Michaux, *Angew. Chem., Int. Ed.*, 2011, **50**, 3780.
- <sup>82</sup> F. Gao and R. Hua, *Catal. Commun.*, 2006, **7**, 391.
- <sup>83</sup> For the synthesis of  $K_7[NiV_{13}O_{38}] \cdot 16H_2O$  see: C. M. Flynn and M. T. Pope, *J. Am. Chem. Soc.*, 1970, **92**, 85.
- <sup>84</sup> M. I. Khan, S. Tabussum, C. L. Marshall and M. K. Neylon, *Catal. Lett.*, 2006, **112**, 1.

- <sup>85</sup> (a) M. I. Khan, S. Deb and C. L. Marshall, *Catal. Lett.*, 2009, **128**, 256. (b) M. I. Khan, S. Deb, K. Aydemir, A. A. Alwarthan, S. Chattopadhyay, J. T. Miller and C. L. Marshall, *Catal. Lett.*, 2010, **135**, 282. (c) M. I. Khan, K. Aydemir, M. R. H. Siddiqui, A. A. Alwarthan and C. L. Marshall, *Catal. Lett.*, 2011, **141**, 538. See also (d) S. Albonetti, F. Cavani and F. Trifiro, *Catal. Rev. Sci. Eng.*, 1996, **38**, 413. (e) M. D. Argyle, K. Chen, A. T. Bell and E. Iglesia, *J. Catal.*, 2002, **208**, 139. (f) M. A. Bañares and S. J. Khatib, *Catal. Today*, 2004, **96**, 251. (g) O. R. Evans, A. T. Bell and T. D. Tilley, *J. Catal.*, 2004, **226**, 292.
- <sup>86</sup> Q. Wu, X. Hao, X. Feng, Y. Wang, Y. Li, E. Wang, X. Zhu and X. Pan, *Inorg. Chem. Commun.*, 2012, **22**, 137.
- <sup>87</sup> S. Chakrabarty and R. Banerjee, *Catal. Sci. Technol.*, 2012, **2**, 2224.
- <sup>88</sup> N. Kato and Y. Hayashi, *Dalton Trans.*, 2013, **42**, 11804.
- <sup>89</sup> M.-P. Santoni, G. La Ganga, V. M. Nardo, M. Natali, F. Puntoriero, F. Scandola and S. Campagna, *J. Am. Chem. Soc.*, 2014, **136**, 8189.
- <sup>90</sup> Y. Gao, Y. Chi and C. Hu, *Polyhedron*, 2014, **83**, 242.
- <sup>91</sup> R. C. Wheland, *J. Am. Chem. Soc.*, 1976, **98**, 3926.
- <sup>92</sup> (a) D. Gatteschi, L. Pardi, A. L. Barra and A. Müller, *Mol. Eng.*, 1993, **3**, 157. (b) G. Chaboussant, S. T. Ochsenein, A. Sieber, H.-U. Güdel, H. Mutka, A. Müller and B. Barbara, *Europhys. Lett.*, 2004, **66**, 423. (c) P. Kögerler, B. Tsukerblat and A. Müller, *Dalton Trans.*, 2010, **39**, 21. (e) B. Tsukerblat and A. Tarantul, in *Molecular Cluster Magnets*, ed. R. Winpenny, World Scientific Publishers, Singapore, 2011, chapter 3.
- <sup>93</sup> K. Ariga, J. P. Hill and Q. Ji, in *Supramolecular Soft Matter: Applications in Materials and Organic Electronics*, ed. T. Nakanishi, John Wiley & Sons, Hoboken, NJ, 2011.
- <sup>94</sup> (a) B. Nohra, H. El Moll, L. M. Rodriguez Albelo, P. Mialane, J. Marrot, C. Mellot-Draznieks, M. O'Keeffe, R. Ngo Biboum, J. Lemaire, B. Keita, L. Nadjo and A. Dolbecq, *J. Am. Chem. Soc.*, 2011, **133**, 13363. (b) P. Van Der Voort, K. Leus, Y.-Y. Liu, M. Vandichel, V. Van Speybroeck, M. Waroquier and S. Biswas, *New J. Chem.*, 2014, **38**, 1853.
- <sup>95</sup> X. Wang, L. Liu, G. Zhang and A. J. Jacobson, *Chem. Commun.*, 2001, 2472.
- <sup>96</sup> Y. Gao, Y. Xu, Y. Cao and C. Hu, *Dalton Trans.*, 2012, **41**, 567.
- <sup>97</sup> A. Tripathi, T. Hughbanks and A. Clearfield, *J. Am. Chem. Soc.*, 2003, **125**, 10528.
- <sup>98</sup> Y. Gao, Y. Xu, S. Li, Z. Han, Y. Cao, F. Cui and C. Hu, *J. Coord. Chem.*, 2010, **63**, 3373.
- <sup>99</sup> D. Pitzschke, J. Wang, R.-D. Hoffmann, R. Pöttgen and W. Bensch, *Angew. Chem., Int. Ed.*, 2006, **45**, 1305.
- <sup>100</sup> T. Whitfield, X. Wang and A. J. Jacobson, *Inorg. Chem.*, 2003, **42**, 3728.
- <sup>101</sup> J. Wang, C. Näther, P. Kögerler and W. Bensch, *Inorg. Chim. Acta*, 2010, **363**, 4399.
- <sup>102</sup> J. Wang, C. Näther, P. Kögerler and W. Bensch, *Eur. J. Inorg. Chem.*, 2012, 1237.
- <sup>103</sup> Y.-M. Chen, E.-B. Wang, B.-Z. Lin and S.-T. Wang, *Dalton Trans.*, 2003, 519.
- <sup>104</sup> L.-H. Bi, U. Kortz, M. H. Dickman, S. Nellutla, N. S. Dalal, B. Keita, L. Nadjo, M. Prinz and M. Neumann, *J. Clust. Sci.*, 2006, **17**, 143.

- <sup>105</sup> H. T. Evans, Jr. and J. A. Konnert, *Am. Mineral.*, 1978, **63**, 863.
- <sup>106</sup> A. Müller, J. Döring, M. I. Khan and V. Wittneben, *Angew. Chem., Int. Ed.*, 1991, **30**, 210.
- <sup>107</sup> (a) N. Suaud, Y. Masaro, E. Coronado, J. M. Clemente-Juan and N. Guihéry, *Eur. J. Inorg. Chem.*, 2009, 5109. (b) S. Cardona-Serra, J. M. Clemente-Juan, A. Gaita-Ariño, N. Suaud, O. Svoboda and E. Coronado, *Chem. Commun.*, 2013, **49**, 9621.
- <sup>108</sup> (a) B. Keita, K. Essaadi, L. Nadjo, R. Contant and Y. Justum, *J. Electroanal. Chem.*, 1996, **404**, 271. (b) B. Keita, I.-M. Mbomekalle, L. Nadjo, P. de Oliveira, A. Ranjbari and R. Contant, *C. R. Chimie*, 2005, **8**, 1057.
- <sup>109</sup> L.-S. You, Q.-Y. Zhu, X. Zhang, Y.-Y. Pu, G.-Q. Bian and J. Dai, *CrystEngComm*, 2013, **15**, 2411.
- <sup>110</sup> J. Zhou, J. Zhang, W.-H. Fang and G.-Y. Yang, *Chem. Eur. J.*, 2010, **16**, 13253.
- <sup>111</sup> (a) B. Botar, P. Kögerler, A. Müller, R. Garcia-Serres and C. L. Hill, *Chem. Commun.*, 2005, 5621. (b) B. Botar, A. Ellern, M. T. Sougrati and P. Kögerler, *Eur. J. Inorg. Chem.*, 2009, 5071.
- <sup>112</sup> J. Zhou, J.-W. Zhao, Q. Wei, J. Zhang and G.-Y. Yang, *J. Am. Chem. Soc.*, 2014, **136**, 5065.
- <sup>113</sup> Y. Gao, Y. Xu, K. Huang, Z. Han and C. Hu, *Dalton Trans.*, 2012, **41**, 6122.
- <sup>114</sup> J. Wang, C. Näther, M. Speldrich, P. Kögerler and W. Bensch, *CrystEngComm*, 2013, **15**, 10238.
- <sup>115</sup> (a) A. Müller, M. Penk and J. Döring, *Inorg. Chem.*, 1991, **30**, 4935. (b) A. L. Barra, D. Gatteschi, B. S. Tsukerblatt, J. Döring, A. Müller and L. C. Brunel, *Inorg. Chem.*, 1992, **31**, 5132.
- <sup>116</sup> M. I. Khan, Q. Chen and J. Zubieta, *Inorg. Chim. Acta*, 1993, **212**, 199.
- <sup>117</sup> G.-Q. Huang, S.-W. Zhang, Y.-G. Wei and M.-C. Shao, *Polyhedron*, 1993, **12**, 1483.
- <sup>118</sup> (a) W.-M. Bu, L. Ye, G.-Y. Yang, M.-C. Shao, Y.-G. Fan and J.-Q. Xu, *Chem. Commun.*, 2000, 1279. (b) Y. Zhao, Q. Liu, Y. Li, X. Chen and Z. Mai, *J. Mater. Chem.*, 2001, **11**, 1553.
- <sup>119</sup> A. Müller, J. Döring and H. Bögge, *J. Chem. Soc., Chem. Commun.*, 1991, 273.
- <sup>120</sup> D. Gatteschi, B. Tsukerblatt, A. L. Barra, L. C. Brunel, A. Müller and J. Döring, *Inorg. Chem.*, 1993, **32**, 2114.
- <sup>121</sup> R. Basler, G. Chaboussant, A. Sieber, H. Andres, M. Murrie, P. Kögerler, H. Bögge, D. C. Crans, E. Krickemeyer, S. Janssen, H. Mutka, A. Müller and H.-U. Güdel, *Inorg. Chem.*, 2002, **41**, 5675.
- <sup>122</sup> A. Wutkowski, N. Evers and W. Bensch, *Z. Anorg. Allg. Chem.*, 2011, **637**, 2205.
- <sup>123</sup> S.-T. Zheng, J. Zhang and G.-Y. Yang, *Eur. J. Inorg. Chem.*, 2004, 2004.
- <sup>124</sup> S.-T. Zheng, M.-H. Wang and G.-Y. Yang, *Inorg. Chem.*, 2007, **46**, 9503.
- <sup>125</sup> Y. Qi, Y. Li, E. Wang, Z. Zhang and S. Chang, *Dalton Trans.*, 2008, 2335.
- <sup>126</sup> Y. Qi, Y. Li, C. Qin, E. Wang, H. Jin, D. Xiao, X. Wang and S. Chang, *Inorg. Chem.*, 2007, **46**, 3217.
- <sup>127</sup> S.-T. Zheng, J. Zhang and G.-Y. Yang, *Inorg. Chem.*, 2005, **44**, 2426.
- <sup>128</sup> D. Zhao, S.-T. Zheng and G.-Y. Yang, *J. Solid State Chem.*, 2008, **181**, 3071.
- <sup>129</sup> X.-B. Cui, J.-Q. Xu, H. Meng, S.-T. Zheng and G.-Y. Yang, *Inorg. Chem.*, 2004, **43**, 8005.
- <sup>130</sup> A. Müller and J. Döring, *Z. Anorg. Allg. Chem.*, 1991, **595**, 251.
- <sup>131</sup> G. Huan, M. A. Greaney and A. J. Jacobson, *J. Chem. Soc., Chem. Commun.*, 1991, 260.

- <sup>132</sup> S.-T. Zheng, J. Zhang and G.-Y. Yang, *Z. Anorg. Allg. Chem.*, 2005, **631**, 170.
- <sup>133</sup> S.-T. Zheng, J. Zhang and G.-Y. Yang, *J. Mol. Struct.*, 2004, **705**, 127.
- <sup>134</sup> G. Zhou, Y. Xu, C. Guo, Y. Liu and X. Zheng, *J. Clust. Sci.*, 2007, **18**, 388.
- <sup>135</sup> X.-B. Cui, J.-Q. Xu, Y. Li, Y.-H. Sun, L. Ye and G.-Y. Yang, *J. Mol. Struct.*, 2003, **657**, 397.
- <sup>136</sup> S.-Y. Shi, Y. Chen, J.-N. Xu, Y.-C. Zou, X.-B. Cui, Y. Wang, T.-G. Wang, J.-Q. Xu and Z.-M. Gao, *CrystEngComm*, 2010, **12**, 1949.
- <sup>137</sup> E. Dumas, C. Livage, S. Halut and G. Hervé, *Chem. Commun.*, 1996, 2437.
- <sup>138</sup> S.-T. Zheng, J. Zhang and G.-Y. Yang, *J. Mol. Struct.*, 2005, **752**, 25.
- <sup>139</sup> S.-T. Zheng, J.-Q. Xu and G.-Y. Yang, *J. Clust. Sci.*, 2005, **16**, 23.
- <sup>140</sup> (a) Y.-F. Qi, Y. Li, E. Wang, D. Xiao and J. Hua, *J. Coord. Chem.*, 2007, **60**, 1403; (b) G. Zhou, C. Guo, W. Liu, Y. Xu and X. Zheng, *J. Coord. Chem.*, 2008, **61**, 202.
- <sup>141</sup> C. Wang, G. Zhou, Z. Zhang, D. Zhu and Y. Xu, *J. Coord. Chem.*, 2011, **64**, 1198.
- <sup>142</sup> A. Kondinski, T. Heine and K. Yu. Monakhov, 2015, submitted.
- <sup>143</sup> Y. Qi, Y. Li, E. Wang, H. Jin, Z. Zhang, X. Wang and S. Chang, *Inorg. Chim. Acta*, 2007, **360**, 1841.
- <sup>144</sup> S.-T. Zheng, J. Zhang, J.-Q. Xu and G.-Y. Yang, *J. Solid State Chem.*, 2005, **178**, 3740.
- <sup>145</sup> X.-B. Cui, J.-Q. Xu, Y. Li, Y.-H. Sun and G.-Y. Yang, *Eur. J. Inorg. Chem.*, 2004, 1051.
- <sup>146</sup> Y. Qi, Y. Li, E. Wang, H. Jin, Z. Zhang, X. Wang and S. Chang, *J. Solid State Chem.*, 2007, **180**, 382.
- <sup>147</sup> C.-M. Wang, Q.-X. Zeng, J. Zhang and G.-Y. Yang, *J. Clust. Sci.*, 2005, **16**, 65.
- <sup>148</sup> B. Dong, J. Peng, C. J. Gómez-García, S. Benmansour, H. Jia and N. Hu, *Inorg. Chem.*, 2007, **46**, 5933.
- <sup>149</sup> X.-B. Cui, Y.-Q. Sun and G.-Y. Yang, *Inorg. Chem. Commun.*, 2003, **6**, 259.
- <sup>150</sup> T. Arumuganathan and S. K. Das, *Inorg. Chem.*, 2009, **48**, 496.
- <sup>151</sup> A. Müller and J. Döring, *Angew. Chem., Int. Ed. Engl.*, 1988, **27**, 1721.
- <sup>152</sup> G.-Y. Yang, L.-S. Chen, J.-Q. Xu, Y.-F. Li, H.-R. Sun, Z.-W. Pei, Q. Su, Y.-H. Lin and Y. Xing, *Acta. Cryst.*, 1998, **C54**, 1556.
- <sup>153</sup> X.-B. Cui, J.-Q. Xu, L. Ding, H. Ding, L. Ye and G.-Y. Yang, *J. Mol. Struct.*, 2003, **660**, 131.
- <sup>154</sup> S.-T. Zheng, Y.-M. Chen, J. Zhang and G.-Y. Yang, *Z. Anorg. Allg. Chem.*, 2006, **632**, 155.
- <sup>155</sup> S.-T. Zheng, J. Zhang and G.-Y. Yang, *Chem. Lett.*, 2003, **32**, 810.
- <sup>156</sup> S.-T. Zheng, Y.-M. Chen, J. Zhang, J.-Q. Xu and G.-Y. Yang, *Eur. J. Inorg. Chem.*, 2006, 397.
- <sup>157</sup> W.-M. Bu, G.-Y. Yang, L. Ye, J.-Q. Xu and Y.-G. Fan, *Chem. Lett.*, 2000, 462.
- <sup>158</sup> X.-B. Cui, J.-Q. Xu, Y.-H. Sun, Y. Li, L. Ye and G.-Y. Yang, *Inorg. Chem. Commun.*, 2004, **7**, 58.
- <sup>159</sup> S.-T. Zheng, J. Zhang, B. Li and G.-Y. Yang, *Dalton Trans.*, 2008, 5584.
- <sup>160</sup> G. Huan, J. W. Johnson, A. J. Jacobson and J. S. Merola, *Chem. Mater.*, 1990, **2**, 719.
- <sup>161</sup> M. I. Khan, Y. Chang, Q. Chen, H. Hope, S. Parkin, D. P. Goshorn and J. Zubieta, *Angew. Chem., Int. Ed. Engl.*, 1992, **31**, 1197.
- <sup>162</sup> M. I. Khan and J. Zubieta, *Angew. Chem., Int. Ed. Engl.*, 1994, **33**, 760.

- 
- <sup>163</sup> L. Zhang and W. Schmitt, *J. Am. Chem. Soc.*, 2011, **133**, 11240.
- <sup>164</sup> O. Delgado, A. Dress, A. Müller and M. T. Pope, *Mol. Engineer.*, 1993, **3**, 9.
- <sup>165</sup> J. M. Breen, L. Zhang, R. Clement and W. Schmitt, *Inorg. Chem.*, 2012, **51**, 19.
- <sup>166</sup> J. M. Breen and W. Schmitt, *Angew. Chem., Int. Ed.*, 2008, **47**, 6904.
- <sup>167</sup> (a) J. S. Anderson, *Nature*, 1937, **140**, 850. (b) H. T. Evans Jr., *J. Am. Chem. Soc.*, 1948, **70**, 1291. (c) A. Bridgeman and G. Cavigliasso, *Inorg. Chem.*, 2002, **41**, 1761. (d) A. Bridgeman and G. Cavigliasso, *J. Phys. Chem. A*, 2003, **107**, 6613.
- <sup>168</sup> (a) I. Lindqvist, *Acta Cryst.*, 1950, **3**, 159. (b) B. Courcot and A. J. Bridgeman, *J. Phys. Chem. A*, 2009, **113**, 10540.
- <sup>169</sup> K. Yu. Monakhov, C. Gourlaouen, R. Pattacini and P. Braunstein, *Inorg. Chem.*, 2012, **51**, 1562.
- <sup>170</sup> I. Chiorescu, W. Wernsdorfer, A. Müller, H. Bögge and B. Barbara, *J. Magn. Magn. Mater.*, 2000, **221**, 103.
- <sup>171</sup> G. Chaboussant, R. Basler, A. Sieber, S. T. Ochsenbein, A. Desmedt, R. E. Lechner, M. T. F. Telling, P. Kögerler, A. Müller and H.-U. Güdel, *Europhys. Lett.*, 2002, **59**, 291.
- <sup>172</sup> D. Procissi, A. Lascialfari, E. Micotti, M. Bertassi, P. Carretta, Y. Furukawa and P. Kögerler, *Phys. Rev. B*, 2006, **73**, 184417.
- <sup>173</sup> I. Chiorescu, W. Wernsdorfer, A. Müller, S. Miyashita and B. Barbara, *Phys. Rev. B.*, 2003, **67**, 020402.
- <sup>174</sup> G. Chaboussant, S. T. Ochsenbein, A. Sieber, H.-U. Güdel, H. Mutka, A. Müller and B. Barbara, *Europhys. Lett.*, 2004, **66**, 423.
- <sup>175</sup> Y. Furukawa, Y. Nishisaka, K. Kumagai, P. Kögerler and F. Borsa, *Phys. Rev. B*, 2007, **75**, 220402.
- <sup>176</sup> A. Tarantul, B. Tsukerblat and A. Müller, *Inorg. Chem.*, 2007, **46**, 161.
- <sup>177</sup> S. Bertaina, S. Gambarelli, T. Mitra, B. Tsukerblat, A. Müller and B. Barbara, *Nature*, 2008, **453**, 203.
- <sup>178</sup> A. Tarantul and B. Tsukerblat, *Inorg. Chim. Acta*, 2010, **363**, 4361.
- <sup>179</sup> D. Gatteschi, L. Pardi, A. L. Barra and A. Müller, *Mol. Engineer.*, 1993, **3**, 157.
- <sup>180</sup> (a) I. Chiorescu, W. Wernsdorfer, A. Müller, H. Bögge and B. Barbara, *Phys. Rev. Lett.*, 2000, **84**, 3454. (b) K. Kajiyoshi, T. Kambe, M. Mino, H. Nojiri, P. Kögerler and M. Luban, *J. Magn. Magn. Mater.*, 2007, **310**, 1203.
- <sup>181</sup> (a) D. W. Boukhvalov, V. V. Dobrovitski, M. I. Katsnelson, A. I. Lichtenstein, B. N. Harmon and P. Kögerler, *Phys. Rev. B*, 2004, **70**, 054417. (b) M. Machida and S. Miyashita, *Physica E*, 2005, **29**, 538.
- <sup>182</sup> D. Gatteschi, L. Pardi, A. L. Barra, A. Müller and J. Döring, *Nature*, 1991, **354**, 463.
- <sup>183</sup> D. W. Boukhvalov, V. V. Dobrovitski, M. I. Katsnelson, A. I. Lichtenstein, B. N. Harmon and P. Kögerler, *J. Appl. Phys.*, 2003, **93**, 7080.
- <sup>184</sup> X.-X. Hu, J.-Q. Xu, X.-B. Cui, J.-F. Song and T.-G. Wang, *Inorg. Chem. Commun.*, 2004, **7**, 264.
- <sup>185</sup> R. Kiebach, C. Näther and W. Bensch, *Solid State Sci.*, 2006, **8**, 964.

- <sup>186</sup> R. Kiebach, C. Näther, P. Kögerler and W. Bensch, *Dalton Trans.*, 2007, 3221.
- <sup>187</sup> A. Wutkowski, C. Näther, P. Kögerler and W. Bensch, *Inorg. Chem.*, 2008, **47**, 1916.
- <sup>188</sup> E. Antonova, C. Näther, P. Kögerler and W. Bensch, *Angew. Chem., Int. Ed.*, 2011, **50**, 764.
- <sup>189</sup> Y. Gao, Z. Han, Y. Xu and C. Hu, *J. Clust. Sci.*, 2010, **21**, 163.
- <sup>190</sup> E. Antonova, C. Näther, P. Kögerler and W. Bensch, *Dalton Trans.*, 2012, **41**, 6957.
- <sup>191</sup> L. Zhang, X. Zhao, J. Xu and T. Wang, *J. Chem. Soc., Dalton Trans.*, 2002, 3275.
- <sup>192</sup> E. Antonova, C. Näther and W. Bensch, *CrystEngComm*, 2012, **14**, 6853.
- <sup>193</sup> E. Antonova, A. Wutkowski, C. Näther and W. Bensch, *Solid State Sci.*, 2011, **13**, 2154.
- <sup>194</sup> E. Antonova, C. Näther, P. Kögerler and W. Bensch, *Inorg. Chem.*, 2012, **51**, 2311.
- <sup>195</sup> H. Lühmann, C. Näther, P. Kögerler and W. Bensch, *Inorg. Chim. Acta*, 2014, **421**, 549.
- <sup>196</sup> E. Antonova, C. Näther and W. Bensch, *Dalton Trans.*, 2012, **41**, 1338.
- <sup>197</sup> A. Wutkowski, C. Näther, P. Kögerler and W. Bensch, *Inorg. Chem.*, 2013, **52**, 3280.
- <sup>198</sup> (a) S. Albonetti, F. Cavani, F. Trifiro, M. Gazzano, F. C. Aissi, A. Aboukais and M. J. Guelton, *J. Catal.*, 1994, **146**, 491. (b) S. Albonetti, F. Cavani, M. Koutyrev and F. Trifiro, *Catal. Lett.*, 1995, **30**, 253. (c) F. Cavani, M. Koutyrev and F. Trifiro, *Catal. Today*, 1995, **24**, 365. (d) F. Cavani, M. Koutyrev and F. Trifiro, *Catal. Today*, 1996, **28**, 319. (e) F. Cavani, A. Tanguy, F. Trifiro and M. Koutyrev, *J. Catal.*, 1998, **174**, 231.
- <sup>199</sup> J. Spengler, F. Anderle, E. Bosch, R. K. Grasselli, B. Pillep, P. Behrens, O. B. Lapina, A. A. Shubin, H.-J. Eberle and H. Knözinger, *J. Phys. Chem. B*, 2001, **105**, 10772.
- <sup>200</sup> M. Schindler, F. C. Hawthorne and W. H. Baur, *Chem. Mater.*, 2000, **12**, 1248.
- <sup>201</sup> R. B. King, *J. Mol. Struct. (Theochem)*, 1995, **336**, 165.
- <sup>202</sup> (a) A. B. Bourlinos, K. Raman, R. Herrera, Q. Zhang, L. A. Archer and E. P. Giannelis, *J. Am. Chem. Soc.*, 2004, **126**, 15358. (b) P. G. Rickert, M. R. Antonio, M. A. Firestone, K.-A. Kubatko, T. Szreder, J. F. Wishart and M. L. Dietz, *J. Phys. Chem. B*, 2007, **111**, 4685. (c) P. G. Rickert, M. R. Antonio, M. A. Firestone, K.-A. Kubatko, T. Szreder, J. F. Wishart and M. L. Dietz, *Dalton Trans.*, 2007, 529. (d) S. Herrmann, M. Kostrzewa, A. Wierschem and C. Streb, *Angew. Chem., Int. Ed.*, 2014, 13596. (e) S. Herrmann, A. Seliverstov and C. Streb, *J. Mol. Eng. Mater.*, 2014, **2**, 1440001.
- <sup>203</sup> S. S. Mal, O. Tröppner, I. Ivanović-Burmazović and P. Burger, *Eur. J. Inorg. Chem.*, 2013, 1960.
- <sup>204</sup> A. Proust, R. Thouvenot and P. Gouzerh, *Chem. Commun.*, 2008, 1837.
- <sup>205</sup> Y. V. Geletii, B. Botar, P. Kögerler, D. A. Hillesheim, D. G. Musaev and C. L. Hill, *Angew. Chem., Int. Ed.*, 2008, **47**, 3896.
- <sup>206</sup> (a) J. Tucher, L. C. Nye, I. Ivanovic-Burmazovic, A. Notarnicola and C. Streb, *Chem. Eur. J.*, 2012, **18**, 10949. (b) J. Tucher and C. Streb, *Beilstein J. Nanotechnol.*, 2014, **5**, 711.
- <sup>207</sup> C. Aronica, G. Chastanet, E. Zueva, S. A. Borshch, J. M. Clemente-Juan and D. Luneau, *J. Am. Chem. Soc.*, 2008, **130**, 2365.
- <sup>208</sup> (a) M.-M. Rohmer and M. Bénard, *J. Am. Chem. Soc.*, 1994, **116**, 6959. (b) M.-M. Rohmer, J. Devemy, R. Wiest and M. Bénard, *J. Am. Chem. Soc.*, 1996, **118**, 13007. (c) C. Menke, E. Diemann and A. Müller, *J. Mol. Struct.*, 1997, **436–437**, 35. See also (d) J. M. Poble, X. López and C. Bo,

*Chem. Soc. Rev.*, 2003, **32**, 297. (e) X. López, J. J. Carbó, C. Bo and J. M. Poblet, *Chem. Soc. Rev.*, 2012, **41**, 7537.

<sup>209</sup> (a) M. R. S. A. Janjua, Z.-M. Su, W. Guan, A. Irfan, S. Muhammad and M. Iqbal, *Can. J. Chem.*, 2010, **88**, 434. (b) V. V. Maslyuk, I. Mertig, O. V. Farberovich, A. Tarantul and B. Tsukerblat, *Eur. J. Inorg. Chem.*, 2013, 1897.

<sup>210</sup> D. Rehder, *Dalton Trans.*, 2013, **42**, 11749.

<sup>211</sup> (a) D. Rehder, *Bioinorganic Vanadium Chemistry*, John Wiley & Sons, Hoboken, NJ, 2008, pp. 13–51. See, also: (b) B. D. Wladkowski, L. A. Svensson, L. Sjölin, J. E. Ladner and G. L. Gilliland, *J. Am. Chem. Soc.*, 1998, **120**, 5488.

<sup>212</sup> (a) E. G. DeMaster and R. A. Mitchell, *Biochem.*, 1973, **12**, 3616. (b) E. F. Pai, W. Sachsenheimer, R. H. Schirmer and G. E. Schulz, *J. Mol. Biol.*, 1977, **114**, 37. (c) G. Choate and T. E. Mansour, *J. Biol. Chem.*, 1979, **254**, 11457. (d) G. Soman, Y. C. Chang and D. J. Graves, *Biochem.*, 1983, **22**, 4994. (e) D. W. Boyd, K. Kustin and M. Niwa, *Biochim. Biophys. Acta*, 1985, **827**, 472. (f) D. C. Crans, K. Sudhakar and T. J. Zamborelli, *Biochem.*, 1992, **31**, 6812.

<sup>213</sup> N. Steens, A. M. Ramadan, G. Absillis and T. N. Parac-Vogt, *Dalton Trans.*, 2010, **39**, 585.

<sup>214</sup> S. S. Soares, C. Gutiérrez-Merino and M. Aureliano, *J. Inorg. Biochem.*, 2007, **101**, 789.

<sup>215</sup> H. Stephan, M. Kubeil, F. Emmerling and C. E. Müller, *Eur. J. Inorg. Chem.*, 2013, 1585.

<sup>216</sup> (a) N. D. Chasteen, *Struct. Bond.*, 1983, **53**, 105. (b) D. C. Crans, in *Polyoxometalates: From Platonic Solids to Anti-Retroviral Activity*, ed. A. Müller, M. T. Pope, Kluwer Academic Publishers, Dordrecht, 1993, pp. 399–406.

<sup>217</sup> *Vanadium Compounds, Chemistry, Biochemistry, and Therapeutic Applications*, ed. A. S. Tracey, D. C. Crans, American Chemical Society, Washington, DC, 1998, **711**.

<sup>218</sup> (a) D. C. Crans, R. L. Bunch and L. A. Theisen, *J. Am. Chem. Soc.*, 1989, **111**, 7597. (b) D. C. Crans, J. J. Smee, E. Gaidamauskas and L. Yang, *Chem. Rev.*, 2004, **104**, 849. (c) M. Aureliano, *World. J. Biol. Chem.*, 2011, **2**, 215 and references cited therein. (d) S. Ramos, J. J. G. Moura and M. Aureliano, *Metallomics*, 2012, **4**, 16.

<sup>219</sup> (a) J. Stankiewicz, A. S. Tracey and D. C. Crans, in *Vanadium and Its Role in Life: Metal Ions in Biological Systems Vol. 31*, ed. H. Sigel, A. Sigel, Marcel Dekker, New York, 1995, ed. H. Sigel, A. Sigel, Marcel Dekker, New York, 1995, pp. 287–324. (b) A. Bishayee, A. Waghray, M. A. Patel and M. Chatterjee, *Cancer Lett.*, 2010, **294**, 1.

<sup>220</sup> E. Antonova, B. Seidlhofer, J. Wang, M. Hinz and W. Bensch, *Chem. Eur. J.*, 2012, **18**, 15316.

<sup>221</sup> (a) J. Fielden, K. Quasdorf, L. Cronin and P. Kögerler, *Dalton Trans.*, 2012, **41**, 9876. (b) B. Botar, A. Ellern and P. Kögerler, *Dalton Trans.*, 2012, **41**, 8951. (c) B. Botar, A. Ellern, R. Hermann and P. Kögerler, *Angew. Chem., Int. Ed.*, 2009, **48**, 9080.